Diversity and Diversification Across the Global Radiation of Extant Bats

by

Jeff J. Shi

A dissertation submitted in partial fulfillment
of the requirements for the degree of
Doctor of Philosophy
(Ecology and Evolutionary Biology)
in the University of Michigan
2018

Doctoral Committee:

Professor Catherine Badgley, co-chair
Assistant Professor and Assistant Curator Daniel Rabosky, co-chair
Associate Professor Geoffrey Gerstner
Associate Research Scientist Miriam Zelditch

Kalong (Malay, traditional)
Pteropus vampyrus (Linnaeus, 1758)
Illustration by Gustav Mützel (Brehms Tierleben), 1927[1]

[1] Reproduced as a work in the public domain of the United States of America; accessible via the Wikimedia Commons repository.

EPIGRAPHS

"...one had to know the initial and final states to meet that goal;
one needed knowledge of the effects before the causes could be initiated."
Ted Chiang; *Story of Your Life* (1998)

"Dr. Eleven: What was it like for you, at the end?
Captain Lonagan: It was exactly like waking up from a dream."
Emily St. John Mandel; *Station Eleven* (2014)

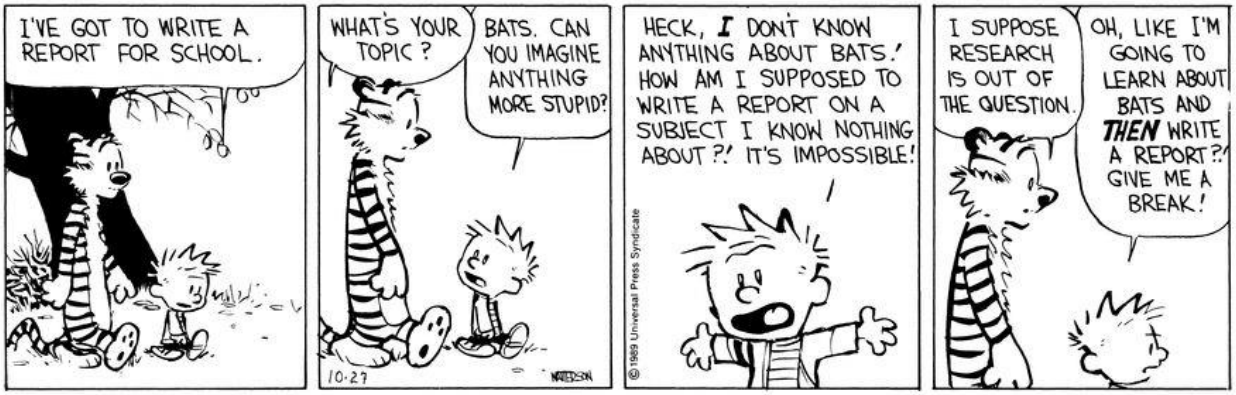

Bill Watterson; *Calvin & Hobbes* (October 27, 1989)[2]

[2] Reproduced according to the educational usage policies of,
and direct correspondence with Andrews McMeel Syndication.

2018
jeffjshi@umich.edu
ORCID: 0000-0002-8529-7100

DEDICATION

To the memory and life of Samantha Jade Wang.

ACKNOWLEDGMENTS

All of the research presented here was supported by a National Science Foundation (NSF) Graduate Research Fellowship, an Edwin H. Edwards Scholarship in Biology, and awards from the University of Michigan's Rackham Graduate School and the Department of Ecology & Evolutionary Biology (EEB). A significant amount of computational work was funded by a Michigan Institute for Computational Discovery and Engineering fellowship; specimen scanning, loans, and research assistants were funded by the Museum of Zoology's Hinsdale & Walker fund and an NSF Doctoral Dissertation Improvement Grant.

This research would not have been possible without the continued support of my co-advisors and committee chairs, Dan Rabosky and Catherine Badgley. I cannot thank either of them enough for humoring the various dead ends, seemingly fruitless explorations, and detours that have colored these last six years. I would also like to thank the other members of my committee, Geoffrey Gerstner and Miriam Zelditch, for their support, input, and advice. Finally, I want to highlight the truly heroic efforts of the EEB office staff through the years - particularly those of Cindy Carl and Jane Sullivan - which should truly earn them all places on each and every thesis and dissertation committee coming out of this department.

I would also like to acknowledge the many, many members of the Rabosky and Badgley labs over the past six years. Special thanks to Pascal Title, for being infallible in his assistance with visualization and spatial analyses, to Michael Grundler and Iris Holmes, for patiently listening to me argue and debate and ramble in the office, and to Erin Westeen, for the thankless and herculean feat of digitizing morphological data for this dissertation. Thanks as well to Sonal Singhal, Talia Moore, Katie Loughney, and Tara Smiley for inspiration and conversations they probably do not remember, but I very much do. More thanks go to Nathan Katlein and Heather Williams for also toiling away in the specimen collections. To everyone else in both labs: thank you for your support, especially through the times when I least appreciated it. I would also like to

thank Stephen Smith, Cody Hinchcliff, Aaron King, Cody Thompson, Michelle Lynch, and Caroline Parins-Fukuchi for support and assistance through the years.

My scientific inspirations and support extend well past EEB, UM, and the last six years. I must thank the Organization for Tropical Studies, SANParks, Laurence Kruger, and Corrie Schoeman for thinking it was a good idea to let me explore Kruger National Park at night, in search of bats, alongside my fellow amateur researchers, Matthew Minder and Amar Doshi. My deepest gratitude goes to Rytas Vilgalys, V. Louise Roth, Dan McShea, Kevin Wright, and Paul Manos at Duke University's Department of Biology for their patience and hand in shaping my entire foundation for evolution and ecology. And, of course, thank you to Anne Yoder and Lauren Chan for taking me under their wings, and treating me like a colleague from the beginning. Thanks to the rest of the Yoder Lab *c.* 2010-2012, including Meredith Barrett, Sheena Faherty, Amy Heilman, and Megan Morikawa, for everything I know about research. Outside of Science Drive, I want to thank Annie Boehling, Jessie Tang, Sean Hyberg, Greg Bachman, Kelly Adamski, Erica Duh, and Alena Reich for their support through many years in and out of North Carolina as I found my way and place in science. I am also indebted to a truly spectacular group of North American bat biologists for years of collaboration, conversation, and good company: Betsy Dumont, Sharlene Santana, Liliana Dávalos, Nancy Simmons, Kelly Speer, Christine Avena, Laurel Yohe, Abigail Curtis, Jasmin Camacho, Leith Miller, Amy Wray, and Aja Marcato. I look forward to the next time I work with you all. My deepest thanks go to the unnamed scientists whose efforts, specimens, maps, and sequences have built more dissertations and research projects than they could have ever imagined, including this one.

Though they may not realize it, this six-year journey would likely not have finished without the truly incredible staff, volunteers, and interns at 826michigan. Thank you Amanda Uhle, Frances Martin, Catherine Calabro, D'Real Graham, Kati Shanks, Megan Gilson, Lucy Huber, Matthew Beyersdorf, Hannah Rose Neuhauser, Tom Bianchi, Terra Reed, and so, so many more people through the years for their kindness, unyielding optimism, and invaluable support. In addition, thank you to the wonderful leadership and staff of the Center for Research on Learning and Teaching for lighting the way, especially Nicole Tuttle, Victoria Genetin,

Stephanie Moody, Michelle Majeed, Ronit Ajlen, Matt Kaplan, and Tazin Daniels. I cannot imagine how this dissertation and budding career could exist without all of you.

Finally, it sometimes felt like it took the city of Ann Arbor to drag and haul this dissertation to the finish line. Thank you to Kevin Bakker, Paul Glaum, Pascal Title (again), and Celia Miller for our hours of toiling and the (many more) hours of lounging. Thank you to Alison Gould, Tara Smiley (again), Micaela Martinez, Tommy Jenkinson for doing all of this first. Thank you to a long list of past and present friends both in and outside of Michigan that have been and will continue to be my entirely unearned support system: Ashleigh Bell, Kevin Boehnke, Mara Bollard, Sally Carson, Leslie Decker, Julie Deeke, Jason Dobkowski, Michelle Fearon, Tim Fortescue, Josh Gardner, Sarah Hoffman, Anneka Jankowiak, Lisa Jong, Peter Kirk, Leigh Korey, Jennifer Kron, Clifton Martin, Jeff May, Meghan Moynihan, Jillian Myers, Timothy Necamp, Elizabeth Pierce, Elizabeth Pringle, Kelly Riffer, Andrew Schwartz, Jay Smith, Alex Taylor, Paula Teichholtz, Lauren Trimble, Lizz Ultee, Annie Wang, and Isabelle Winer. I am eternally grateful to each and every one of you for the many person-years of time and energy. Thank you to the endless patience of my family in Los Angeles, Las Vegas, and Hong Kong, who I know are always there for me, even when I least deserve it.

Above all, my eternal gratitude and appreciation to Dori Cross, *sine qua non*.

TABLE OF CONTENTS

DEDICATION ii
ACKNOWLEDGMENTS iii
LIST OF TABLES vii
LIST OF FIGURES ix
ABSTRACT xi
CHAPTER 1 Introduction: global patterns of bat spatial diversity and richness 1
CHAPTER 2 Speciation dynamics across the global radiation of extant bats 52
CHAPTER 3 Ecomorphological and phylogenetic constraints on sympatry across extant bats 106
CHAPTER 4 Digitizing extant bat diversity: an open-access repository of 3D μCT-scanned skulls for research and education 145
CHAPTER 5 The omnivores' dilemma: decoupling of ecological and morphological evolution across New World bats 175
CHAPTER 6 Conclusion 231

LIST OF TABLES

Table 1.1 Metadata on bat diversity for major biogeographic realms 35
Table S1.1 Palearctic bat families and species with IUCN range data 42
Table S1.2a Afrotropical (mainland) bat families and species with IUCN range data..... 43
Table S1.2b Afrotropical (Indian Ocean islands) bat families and species with IUCN range data 44
Table S1.3 Indomalayan bat families and species with IUCN range data 45
Table S1.4 Oceanian & Australasian bat families and species with IUCN range data..... 47
Table S1.5 Nearctic bat families and species with IUCN range data 48
Table S1.6 Neotropical bat families and species with IUCN range data 49
Table 2.1 Genetic loci and phylogenetic coverage 83
Table 2.2 Fossil constraints..... 84
Table 2.3 Stem and crown age comparisons..... 86
Table 2.4 Crown age ranges across bootstrap replicates..... 87
Table S2.1 Pruned taxa..... 95
Table S2.2 Supermatrix genus-level sampling percentages..... 96
Table S2.3 Effects of incomplete sampling 98
Table 3.1 Age-sympatry relationships 130
Table 3.2 Ecomorphology-sympatry relationships 131
Table S3.1 Sympatry and range overlap data for all realms 136
Table S3.2 Maximum-likelihood model descriptions..... 137
Table S3.3 Likelihood-ratio tests for maximum-likelihood models 138
Table S3.4 Maximum-likelihood parameter estimates 139
Table S3.5 Furnariid ecomorphology-sympatry relationships..... 140
Table S3.6 Furnariid maximum-likelihood model descriptions..... 141
Table S3.7 Furnariid ΔAICc scores and likelihood-ratio tests..... 142

Table S3.8 Neotropical ecomorphology-sympatry relationships at finer scales 143
Table S4.1 Specimen details 161
Table S4.2 Percentage difference between physical and digital measurements 174
Table 5.1 Ecological trophic cohorts 203
Table 5.2 Morphological shape cohorts 204
Table S5.1 Phylogenetic, ecological, and morphological metadata 210
Table S5.2 Phylogenetic disparity 218
Table S5.3 Constraints on evolutionary rate 219
Table S5.4 Convergence of trophic guilds 220
Table S5.5 Convergence among vampires and other trophic guilds 221

LIST OF FIGURES

Figure 1.1 Palearctic bat richness 36
Figure 1.2 Afrotropical bat richness 37
Figure 1.3 Indomalayan bat richness 38
Figure 1.4 Oceanian & Australasian bat richness 39
Figure 1.5 Nearctic bat richness 40
Figure 1.6 Neotropical bat richness 41
Figure 2.1 Species richness patterns across bats 88
Figure 2.2 Maximum-likelihood phylogeny of bats 89
Figure 2.3 Marginal probabilities and Bayes factor evidence of regime shifts 90
Figure 2.4 Prior and quasi-posterior distributions of shifts 91
Figure 2.5 Macroevolutionary cohort matrices 92
Figure 2.6 Speciation rates through time across bats 93
Figure 2.7 Phylogenetic imbalance through time 94
Figure S2.1 Sample cohort matrix 99
Figure S2.2 Null expectation of imbalance through time 100
Figure S2.3 Fan phylogeny of bats 101
Figure S2.4 Credible shift configurations 102
Figure S2.5 Cohort matrix with halved sampling fractions 103
Figure S2.6 Crown family age vs. family level richness 104
Figure S2.7 Phylogenetic imbalance through time without stenodermatines 105
Figure 3.1 Global richness patterns of bats 132
Figure 3.2 Potential models of sympatry-divergence relationships 133
Figure 3.3 Range randomization approach 134
Figure 3.4 Negative Neotropical relationship between ecomorphology and sympatry 135
Figure S3.1 Null distributions of age-sympatry relationships across realms 144

Figure 4.1 Sampling of each extant bat family within this repository 158
Figure 4.2 Species and skull disparity included in this repository 159
Figure 4.3 Relationships between measurements taken from digital and physical specimens .. 160
Figure 5.1 Phylogeny of New World bats 205
Figure 5.2 Ecological cohort matrix 206
Figure 5.3 Disparity-age relationship 207
Figure 5.4 Principal component analysis of New World bat crania 208
Figure 5.5 Morphological shape cohort matrix 209
Figure S5.1 Cohort matrix illustration 222
Figure S5.2 Landmarking details 223
Figure S5.3 Results from all BMM models 224
Figure S5.4 Principal components in a phylogenetic context 225
Figure S5.5 PCA with all trophic guilds 226
Figure S5.6 Results from more conservative ecological state assignments 227
Figure S5.7 Ecological transition rates and cranial shape evolution rates 228
Figure S5.8 Cumulative Akaike weights 229
Figure S5.9 Diet states among phyllostomid species 230
Figure 6.1 *Kunstformen der Natur*, plate 67: Chiroptera (1904) 240
Figure 6.2 Insights from the tree of life 241

ABSTRACT

Diversity is not distributed equally across the tree of life. This fundamental observation is central to ecology and evolutionary biology, and spans both spatial and temporal scales. Species richness, for example, is unevenly distributed both within and across clades. Biodiversity is often spatially concentrated in the tropics, with lower richness in temperate biomes. Some clades are characterized by extremely high ecological and morphological diversity, while others remain static across geologic timescales. This dissertation highlights these patterns of diversity across extant bats, the Order Chiroptera, and seeks to understand the evolutionary processes of diversification that govern them.

Chapter 1 serves as both an introduction to the major questions of the dissertation and an overview of extant bat diversity, and how it varies spatially, phylogenetically, and ecologically across the globe. In this chapter, I primarily focus on spatial variation in regional richness patterns, and on the major differences between temperate and tropical bat diversity. In Chapter 2, I assemble a species-level molecular phylogeny of the order that is time-calibrated with fossil data. Using this phylogeny, I infer speciation dynamics across the order, and find that despite the imbalances in species richness, speciation rates are relatively homogeneous. I only infer strong evidence for more rapid rates within the subfamily Stenodermatinae, a clade of Neotropical phyllostomid bats.

In Chapter 3, I develop models to test whether bat species co-occurrence is constrained by relatedness or ecomorphological similarity. Contrary to theoretical predictions and results from other major clades, I find that neither of these metrics of divergence controls co-occurrence

in sympatry across most bats and realms. The only exception is the Neotropical realm, where bat species are most likely to co-occur when they are the most ecomorphologically similar to one another. This potentially indicates that Neotropical bat communities and species pools, at broad regional scales, are sorted by filtering processes that cluster bats with similar ecologies together in space.

For Chapters 4 and 5, I assess how ecology and morphology are linked in New World bats. Chapter 4 describes an open-access, X-ray computed microtomography database of bat skulls, and how this resource can be used by the broader scientific and educational community. Chapter 5 combines crania from that database with diet data across New World bats, and tests whether ecological and morphological evolution are correlated in this group. Surprisingly, I find that patterns of ecological, trophic evolution are largely decoupled from morphological evolution. There is considerable heterogeneity in how readily different clades transition among trophic guilds, yet cranial shape evolution is surprisingly homogeneous. This decoupled pattern is potentially driven by underestimated trophic plasticity and omnivory among noctilionoid bats, as well as high lability among bat crania. Finally, in Chapter 6, I conclude with a summary of our major findings, and some thoughts on ecological and macroevolutionary inference both within bats and across the tree of life.

CHAPTER 1

Introduction: Global patterns of bat spatial diversity and richness

INTRODUCTION

The spatial distribution of diversity, including how species ranges and regional richness varies across the globe, is fundamental to our understanding of ecological and evolutionary patterns and processes. Spatial patterns of diversity can reflect the dispersal of organisms (Holt 2003, Ree & Smith 2008), how local habitat suitability and resource availability structure metapopulations (Brown 1984), and how organisms interact with each other and their environments (Sexton *et al.* 2009, Louthan *et al.* 2015). These patterns can also inform our understanding of the geography of speciation (Fitzpatrick & Turelli 2006) and how ecological interactions change through time (Connell 1980, Jackson 1981). Understanding the spatial structure of diversity unites macroecology and macroevolution with population and community ecology, population genetics, and biogeography.

Patterns and predictors of richness often vary by scale; these scales can be spatial, temporal, and phylogenetic. Studies of community and local richness are likely to focus on factors like microhabitat variation and resource abundance, based on individual species requirements for shelter and food (Kolb *et al.* 2006, Sexton *et al.* 2009). Regional turnover and beta diversity are linked to the sorting and composition of regional species pools, and may largely be governed by source-sink dynamics and dispersal (Mouquet & Loreau 2003, Leibold *et*

al. 2004). At even larger continental scales, richness patterns of entire clades can reflect glacial and climatic history and present energy availability (Currie 1991, Oberdoff *et al.* 1995, Francis & Currie 2003, Montoya *et al.* 2007).

Bats (Order Chiroptera) are one of the most diverse clades of modern mammals, with more than 1300 species across roughly 20 ecologically and morphologically distinct families (Shi & Rabosky 2015, Simmons 2005). The order is cosmopolitan, with species on all continents except Antarctica. However, bat diversity is not equally distributed according to multiple metrics. Bat species richness varies across extant families, and regional richness is negatively associated with latitude. Furthermore, the high ecological and morphological diversity (Nowak 1994, Simmons & Conway 2003, Simmons 2005) of some clades make it possible to test whether spatial richness patterns are linked to ecological species interactions. Dispersal via powered flight also makes them an intriguing system for evaluating how regional species pools are sorted into local communities.

In this chapter, I review spatial patterns of bat species richness, and how these vary both within and across clades and biogeographic realms. For example, I explore whether or not regional richness patterns can be predicted by abiotic and biotic factors, and whether this differs among clades and realms. I then discuss how the phylogenetic and ecological diversity of bats within each realm may contribute to overall patterns of spatial diversity. Finally, I discuss major differences between tropical and temperate bat species pools. As is true across many branches of the tree of life, there is a strong latitudinal diversity gradient among bats. In fact, it has been suggested that the overall gradient across mammals is largely driven by bats (Willig *et al.* 2003). The tropical realms of the world - the Neotropics, Afrotropics, Indomalaya, and Oceania - are generally characterized by higher levels of taxonomic, morphological, and ecological diversity

among bats. Through reviewing patterns of bat richness across the globe, I highlight some of the factors that distinguish tropical and temperate bat diversity.

MATERIALS AND METHODS

To evaluate how regional richness varies within biogeographic realms, I downloaded all accessible range polygons of bat species from the IUCN's Red List of Threatened Species (IUCN 2017). Of these polygons, 696 are associated with the species included in the molecular phylogeny of Shi & Rabosky (2015). These range polygons are considered maximum extent approximations of actual species distributions (Gaston & Fuller 2008). However, they remain some of our best estimates on species occurrences across many branches of the tree of life.

For the rest of this study, I refer to the WWF biogeographic realms as described by Olson *et al.* (2001): the temperate Nearctic and Palearctic, and the tropical Afrotropics, Neotropics, Indomalaya, Australasia, and Oceania. A previous clustering analysis of bat distributions inferred that these major biogeographic divisions are generally well-supported by species pools and range overlap; in other words, these realms are known to have distinct bat fauna (Procheş 2005).

With the IUCN range polygons, I classified bat species by their presence and absence in each biogeographic realm. To do so, I used a threshold of 20% overlap - that is, a bat is considered to be part of a realm's species pool if more than 20% of its maximum range-extent polygon occurs within it. Species present at overlap percentages below this threshold were considered opportunistic visitors, and not permanent residents of that realm. Using smaller thresholds generally changed the number of species present in a realm by less than 10%. Other downstream effects of varying this threshold are discussed in Shi *et al.* (2018); this is meant as an initial, and conservative approach to assessing realm-level diversity. I then built regional

richness maps for each realm, based on these species pools, using the *rangeBuilder* R package (Davis Rabosky *et al.* 2016). I describe some more detailed aspects of each realm's diversity, including family and species pools, in Table 1.1 and Tables S1.1-S1.6.

OLD WORLD BATS

The Old World Realms

There are five WWF biogeographic realms (Olson *et al.* 2001) within the Old World, as it is typically known to European biologists. Beyond these realms, I also discuss differences in patterns between the temperate regions - the Palearctic and most of continental Australasia - and the Old World tropics, which span much of the Afrotropics and Indomalaya, and parts of Oceania and Australasia. The bat faunas of the five Old World realms are distinctively different (Table 1.1).

The Palearctic

Despite being the largest of the WWF biogeographic realms, the Palearctic is extremely low in bat species diversity, second only to the smaller Nearctic realm (Table 1.1). Only about 10% of extant bat species occur in this realm, and regional richness is generally low (Figure 1.1). Most Palearctic bats belong to the family Vespertilionidae, the most speciose family of bats (Simmons 2005, Shi & Rabosky 2015). Nearly 80% of Palearctic bats are vespertilionids; furthermore, nearly half of the vespertilionids in the realm are species of *Myotis* (Table S1.1), the most speciose and widely distributed of all bat genera (Ruedi & Mayer 2001). Palearctic bats are almost all obligate insectivores, though this does not mean they are behaviorally uniform. For example, bats of the family Molossidae are generally high-flying aerial hawkers (Jung *et al.*

2014). On the the other hand, the Old World leaf-nosed bats (Rhinolophoidea: Rhinolophidae and Hipposideridae) include both gleaners and hawkers, often in close sympatry (Jones & Rayner 1989, Siemers & Ivanova 2004).

The western Palearctic has higher regional richness than the rest of the realm (Figure 1.1), and richness is well-predicted by abiotic variables like climate and precipitation (Ulrich *et al.* 2007, Bilgin *et al.* 2008, Rebelo *et al.* 2009). Among European bats, especially at northern latitudes, it appears that environmental temperature range is a primary control of regional richness (Ulrich *et al.* 2007, Rebelo *et al.* 2010). This may be linked to the local availability of suitable bat hibernacula and roosts; many taxa have narrow tolerances for temperatures at roosting sites (Kerth *et al.* 2001, Lourenço & Palmeirim 2004). Palearctic bat distributions also clearly reflect elevational gradients in the availability of suitable roosts, though it is difficult to tease apart the individual contributions of temperature and elevation (Georgiakakis *et al.* 2010, Piksa *et al.* 2013). Along the Mediterranean, it has been suggested that precipitation and humidity are disproportionately important climatic variables that govern regional richness patterns (Russo & Jones 2003, Sachonowicz *et al.* 2006). Moisture and water availability, in general, often control regional richness patterns in bats (McCain 2007). However, a more proximate factor could be that insect abundances are highest near water sources.

Less is known about the factors that govern regional richness across the Mediterranean Sea, in North Africa and the Middle East (Figure 1.1). The sea itself is a barrier between Europe and these two regions for many bats, even across the Strait of Gibraltar (Castella *et al.* 2000, Juste *et al.* 2004). There is some evidence that bat richness in the Middle East reflects glacial refugia, as in continental Europe (Furman *et al.* 2008). Regional richness is also highest near water, including along the Nile River and the Mediterranean Sea (Figure 1.1). Many of the

riparian species here are wide-ranging species that also exist in parts of Europe, and are primarily generalist insectivores (Herkt *et al.* 2016). However, much of the research in both Africa and the Middle East focuses on the distinct, more ecologically diverse Afrotropical bat fauna.

The species pool of bats in the eastern Palearctic is similar in composition to that of Europe. Regional richness is highest in southeast Asia, where *Myotis* species are extremely common and wide-ranging. Southeast Asia may, in fact, be the origin of the global myotine radiation (Ruedi *et al.* 2013). Many modern distributions of Asian bats reflect the glacial history of the region (Flanders *et al.* 2010, Kruskop *et al.* 2012). For example, the broadly distributed species of the genus *Rhinolophus* display strong population-level differentiation in western and central Asia that reflect glacial refugia (Rossiter *et al.* 2007). While most analyses seem to indicate that abiotic factors, like the climatic history of the realm, are the most predictive for Palearctic bat distributions, large regions of the realm remain unstudied. These analyses should be replicated across other bat clades common in all regions of the Palearctic to fully evaluate the factors that govern richness patterns of the realm.

The Afrotropics

Afrotropical bats can be subdivided into those bats that are endemic to mainland Africa, and those that are endemic to Madagascar, Comoros, Seychelles, and other major islands in the Indian Ocean. Both the familial and species pools present in each region are clearly distinct from each other, and are each more balanced (at the family level) than the Palearctic (Table 1.1, Table S1.2). Afrotropical bats span a wide range of trophic diversity, including insectivory, carnivory, frugivory, and nectarivory. Regional richness is highest throughout the wettest, tropical rainforests and savannahs of sub-Saharan Africa (Figure 1.2). Richness is also positively

associated with rugged and complex terrain, potentially indicating that topographic complexity influences diversity patterns within this realm (Herkt *et al.* 2016, *sensu* Badgley *et al.* 2017).

A large percentage of Afrotropical bats are insectivores of the superfamily Vespertilionoidea (~45% of species are in the families Vespertilionidae and Molossidae), though with relatively few *Myotis*. A significant percentage of mainland Afrotropical diversity is comprised of Old World flying foxes (Family Pteropodidae) (Table 1.1). Most pteropodids are obligate frugivores, and the clade diverged from vespertilionoids in the early Eocene (Shi & Rabosky 2015). Fruits are generally present in many parts of Africa throughout the year, whereas insect abundance can be highly seasonal (Schoeman *et al.* 2013). Across the mainland Afrotropics, regional turnover in bat species is better predicted by habitat type than by geographic distance, regardless of clade or feeding guild (Fahr & Kalko 2011). Environmental filtering, especially by vegetation, may thus be a strong sorting mechanism of bat diversity on the mainland.

At local scales, the pteropodid diversity of the Afrotropical mainland is vertically stratified within tropical forests, given species preferences for different fruits and tree species (Henry *et al.* 2004). If stratification were widespread, we might observe relatively low horizontal turnover in community composition, even though there is actually strong local sorting based on resource availability. Afrotropical pteropodids appear to follow this trend, as they are characterized by extremely broad distributions and strong partitioning within communities. There is also evidence that pteropodid ranges fluctuate to reflect temporal and seasonal variation driven by factors like plant phenology. For example, the ubiquitous species *Eidolon helvum* is known to be very wide-ranging, but migrates to track preferred fruits and trees, and thus fluctuates in density across its range and through the seasons (Richter & Cumming 2005, Ossa *et*

al. 2012, Shi *et al.* 2014). Other widely distributed pteropodid genera, such as *Epomophorus* and *Rousettus*, appear sympatric but do not interact in syntopy, as they forage at different times within the same canopy (Thomas & Fenton 1978). Seasonal and temporal partitioning appears common across the Afrotropics, and may also be prevalent other tropical regions of the world with high diversity and wide-ranging species.

The large Indian Ocean islands of Madagascar, Seychelles, and Comoros, among others in the region, are known for their species of locally abundant pteropodids, many of which are endemic with highly fragmented local ranges (Nicoll & Racey 1981, Sewall *et al.* 2003, Jenkins *et al.* 2007, Picot *et al.* 2007). As on the mainland, these species of frugivores are often very broadly distributed, with high connectivity among populations and low within-island genetic structure (Goodman *et al.* 2010, Chan *et al.* 2011), reflecting regional migration to track plant phenology (Goodman & Ganzhorn 1997, Andriafidison *et al.* 2006, Shi *et al.* 2014). However, there is clear between-island population structure across many species, with evidence that oceanic distances promote isolation followed by radiations within islands (Goodman *et al.* 2010).

Wide-ranging molossids are also diverse among these islands, with many species shared with the African mainland or with the southern Arabian Peninsula. Even across wide ocean expanses, many molossid species display low levels of population differentiation (Ratrimomanarivo *et al.* 2009a, Ratrimomanarivo *et al.* 2009b, Goodman *et al.* 2010). Perhaps the most persistent trait across clades and both regions of the Afrotropics, then, is high levels of dispersal - sometimes even across oceanic divides. The more localized partitioning that readily occurs, especially among frugivores, may also be related to higher mobility and dispersal among Afrotropical bats, as they track preferred resources through time and space. Overall, these factors

imply that biotic factors, like vegetation type and plant phenology, are strong predictors of Afrotropical bat richness patterns.

Indomalaya

The Indomalayan species pool of bats is one of the richest in the world, second only to that of the Neotropics (Table 1.1). Nearly half of all extant bat families occur in the realm. Within the Indian subcontinent, bat species are generally shared among the Afrotropical, Palearctic, and Indomalayan realms (Procheş 2005), with overall low regional richness. Indomalayan richness is much higher in southeastern Asia, and across the various island archipelagos of the Indian Ocean between Asia and Australia (Figure 1.3). Across the Malay Peninsula and these archipelagos, bats depend upon and are adapted to a rich variety of roosting habitats throughout forests and rocky outcrops among the montane landscapes (Kingston 2010). Rugged physiography may contribute to the much higher regional diversity of this part of the realm by providing more diverse, suitable habitats for these species.

Most of the insectivorous bats in Indomalaya are vespertilionoids, and as in the neighboring Palearctic, *Myotis* diversity is notably high (Table S1.3). The putative origin of the genus is on the border of the two realms (Ruedi *et al.* 2013), and new myotine species are continually discovered and described in this region (Bates *et al.* 2005, Kruskop & Borisenko 2013, Ruedi *et al.* 2018). Indomalayan vespertilionoids also readily coexist with rhinolophoid insectivores, as both clades are adapted to the cluttered forest environments throughout southeast Asia (Kingston *et al.* 2003). Rhinolophoid bats (Hipposideridae and Rhinolophidae) are notably speciose in this realm (Table 1.1, Table S1.3). Within the dense forests of the region, the Indomalayan rhinolophoid radiation is characterized by acoustic divergence, where individual

species differ by echolocation frequency (Hughes *et al.* 2010). This is coupled with high degrees of prey specificity that distinguish these insectivores from the generalists of the temperate Palearctic. Specialization may be key to high insectivore diversity here, but competition for resources may also have driven trait divergence. As in much of the Old World, however, small insectivorous bats are disproportionately understudied compared to frugivorous pteropodids (Bumrungsri *et al.* 2005). As loss of their dense primary forest habitat is one of the most severe threats facing biodiversity in Indomalaya (Zubaid 1993, Struebig *et al.* 2010), we must continue to highlight the factors that affect insectivorous bats in these forests.

Frugivorous pteropodids are also abundant and diverse in Indomalaya. Flying fox (Family Pteropodidae) distributions in the realm are highly fragmented, especially among the Indonesian islands along Wallace's Line. Biogeographic patterns among Indomalayan pteropodids reflect cycles of vicariance and re-connectivity from the opening and flooding of isthmuses and straits, and fluctuating sea levels over geologic time (Heaney *et al.* 2006, Almeida *et al.* 2009). At the finest scales, sympatric pteropodid species are vertically and temporally stratified by tree roost and resource availability (Francis 1994, Hodgkison *et al.* 2004a, Hodgkison *et al.* 2004b, Campbell *et al.* 2006, Maryanto *et al.* 2010). Many Indomalayan pteropodids have strong preferences for particular fruits; the distribution and seasonality of fruit abundance may thus be primary controls on pteropodid richness patterns in this realm (Hodgkison *et al.* 2003). Considering the similar patterns found among Afrotropical pteropodids, fine-scale local partitioning based on plant diversity may be a distinctive feature of the entire family across the Old World tropics.

Oceania & Australasia

Though traditionally considered separate biogeographic realms, Oceania and Australasia share similar bat faunas. Regional richness is highest among the largest Indonesian islands just east of Wallace's Line, and along the forests and savannas on the northern and eastern coasts of the Australian continent (Figure 1.4). Many of these bats have extremely broad distributions, extending even to some of the most isolated islands in the Pacific, highlighting the potential for dispersal across oceanic divides in these realms (*e.g.*, Daniel 1975).

Sulawesi and New Guinea have the highest regional richness of bats among the major islands of these two realms (Figure 1.4). Many species in this region are shared with both Indomalaya and the rest of Oceania and Australasia, with no clear division in faunas across Wallace's Line (Procheş 2005). This is perhaps unsurprising, as small, cosmopolitan mammals like bats and rodents were long considered exceptions to Wallace's original biogeographic division (Mayr 1944). Furthermore, based on the ranges of many organisms (Simpson 1977, Kitchener *et al.* 1993), it seems that a Wallacean region straddling Indomalaya and Oceania & Australasia encompasses a bat fauna (Kingston & Rossiter 2004) that is distinct from mainland Asia and Australia. As in Indomalaya, the rhinolophoids of Sulawesi and neighboring islands are highly diverse, and are characterized by divergent echolocation calls specialized for different prey in dense primary forest (Kingston & Rossiter 2004). The pteropodids of these islands also partition local habitats like their Indomalayan counterparts, with evidence for strong species-level associations with plant phenology and distributions (Giannini *et al.* 2006, Maryanto *et al.* 2010).

The exceptionally high diversity of pteropodid bats is perhaps the most distinguishing feature of the bats of both realms (Table 1.1, Table S1.4). This region is the most likely origin of

most pteropodid subfamilies, and perhaps the entire clade (Almeida *et al.* 2011, 2014). Many Australian and Oceanic pteropodids are clearly ecologically and morphologically specialized for fruit at the genus and species level (Dumont & O'Neal 2004). On the Australian continent, pteropodid richness is highest along the northern and eastern coasts, where fruit abundances and precipitation are highest year-round (Figure 1.4, Olson *et al.* 2001). Many of the largest, charismatic flying foxes along the coasts, especially across Queensland and New South Wales, have very broad ranges. These ranges reflect long-range dispersal and seasonal variation, and follow the highest abundances of preferred fruits, blossoms, and nectar, as well as suitable maternity roost habitats (Nelson 1965, Eby 1991, Palmer *et al.* 2000, Parry-Jones & Augee 2001).

In the more arid regions of Australia, such as the interior and the southwest, regional bat species richness is lower, and comparable with the temperate Palearctic. The bats here are generally smaller insectivorous and carnivorous bats (Lumsden & Bennet 1995, Young & Ford 2000). As in other arid regions of the world, the small bats of Australian arid zones survive and even flourish despite patchy water and prey availability. Bat abundance in Australian deserts seems to be predominantly predicted by the abiotic variables influencing availability of suitable large, stable roosts and hibernacula like rocky caves, tunnels, and crevasses. Torpor and hibernation in these roosts may be key to survival during the driest months with few arthropods (Geiser 2004, Williams & Dickman 2004, Bondarenco *et al.* 2016). While the various clades of insectivorous and carnivorous (Family Megadermatidae) bats often share foraging sites and roosts, there is evidence for fine-scale roost partitioning based on species-level preferences for microclimates within roosts (Baudinette *et al.* 2000). Throughout Oceania and Australasia, it seems that both faunivorous and frugivorous bats are more plastic in local habitat use than may

be expected from large-scale regional distribution patterns. However, spatial partitioning amongst tropical bats seems to be driven by biotic conditions, like resource availability, for both frugivores and insectivores. In the deserts, abiotic conditions that affect roost availability may be the primary controls on largely insectivorous bat communities.

NEW WORLD BATS

The New World Realms

The two biogeographic realms - the Nearctic and the Neotropics - of the New World have distinct bat faunas (Table 1.1, Table S1.5, Table S1.6; Wilson 1973). There is a clear delineation between the vespertilionoid-dominated, low-richness Nearctic, and the noctilionoid-dominated, high-richness Neotropics. The superfamily Noctilionoidea - especially its largest family Phyllostomidae, the New World leaf-nosed bats - alone accounts for the majority of ecological, morphological, and behavioral diversity in extant bats (Dumont *et al.* 2012, Santana *et al.* 2012). Though the fossil record of bats is quite poor, this Nearctic-Neotropical dichotomy is likely ancient, and existed prior to the interchange of fauna between North and South America (Morgan 2005, Rojas *et al.* 2016).

The Nearctic

The Nearctic realm has the fewest bat species of all biogeographic realms, despite being comparable in size with both the Afrotropics and the Neotropics (Table 1.1). Nearly all Nearctic bats are obligate insectivores, and are predominantly vespertilionoids of the families Vespertilionidae and Molossidae (Rodríguez & Arita 2004). Only a few noctilionoid phyllostomids and mormoopids are present in the southernmost parts of the realm. Nearctic

regional richness is highest in the most arid and topographically complex parts of the realm, including the Great Basin and the Mojave and Sonoran Deserts, and peaks in the dry, thorny scrublands of central Mexico (Figure 1.5). This strong latitudinal diversity gradient of Nearctic bats anchors the overall gradient for all mammals in the realm (Wilson 1974).

The link between topographic complexity and richness in the Nearctic is not unique to bats. It is documented for many Nearctic mammals (Kerr & Packer 1997, Badgley & Fox 2000, Qian *et al.* 2013), and has repeatedly occurred through geologic history (Badgley & Finarelli 2013). Topographic complexity can promote speciation and extinction by fragmenting and isolating populations, and can also drive adaptation and specialization along local microhabitat gradients that naturally arise across mountains and valleys. For Nearctic bats, an important predictor of regional bat diversity may be the availability of summer and nursery roosts, with species-specific affinities for abiotic factors like roost microclimates and temperatures along topographic gradients (Humphrey 1975, Perkins 1996). Microhabitat variation in vegetation cover and climate also strongly predicts bat distributions in the southernmost parts of the Nearctic where regional richness is highest, though these communities contain many Neotropical bats (López-González *et al.* 2015).

By contrast, Nearctic vespertilionoid richness does not closely track arthropod abundance, and species do not seem to partition foraging sites based on prey availability (Bell 1980). However, at finer scales, broadly co-occurring vespertilionoids are temporally partitioned, and there is some degree of prey specialization (Black 1974). Insectivorous bat species are generally constrained to a particular size class of prey, based on maneuverability and echolocation frequency (Black 1974, Barclay & Brigham 1991). Within these constraints, however, most Nearctic insectivorous bats are opportunistic and flexible, as insect communities

fluctuate seasonally and temporally. Individual Nearctic bat species will readily consume a wide variety of arthropods, even if those prey require very divergent hunting and foraging strategies (Fenton & Morris 1976, Anthony & Kunz 1977, Whitaker 1995, Whitaker *et al.* 1996, Agosta 2002). It may thus be unsurprising that Nearctic bat distributions do not appear to closely track insect distributions. A more important predictor of bat richness in the Nearctic, as in arid Australia and the temperate Palearctic, is the availability of drinking water. The regions of highest bat abundance and richness in Nearctic deserts are generally also those with the highest water availability and transpiration (Wilson 1974, McCain 2007). Seasonal water availability may even govern regional and continental patterns of Nearctic richness, such as along the Rocky Mountains in the west (Figure 1.5).

Unlike in the tropics, food in the temperate Nearctic is not consistently plentiful. It has been suggested that one reason diversity and regional richness are particularly low in both the Nearctic and Palearctic is that insectivorous bats need to either hibernate or migrate to warmer and wetter regions during winter months when insects are rare (Wilson 1974). Indeed, the majority of Nearctic (and Palearctic) bats hibernate (*e.g., Myotis* and tree bats such as *Eptesicus*), with fewer migratory species (*e.g., Tadarida*) (Table S1.5). Hibernacula in North America are highly species-specific, with individual species having different microclimatic tolerances of temperature and humidity even within one large roost like a cave system (Agosta 2002, Humphries *et al.* 2002, Neubam *et al.* 2006). Widespread hibernation may thus also contribute to an overall Nearctic pattern of abiotic characteristics being more important for governing spatial richness patterns than biotic influences, including prey distributions.

Among non-hibernating Nearctic bats, migration is often opportunistic, limited to some populations, and/or driven by seasonal fluctuations in availability of both plant and arthropod

resources (Rojas-Martínez *et al.* 1999, Russell *et al.* 2005, McCracken *et al.* 2008). This pattern of resource tracking makes migrating bats more similar to the Neotropical species pool, as discussed in the following section. As the data used for this chapter are maximum-extent polygons that do not partition ranges by wintering and breeding grounds, there are clear avenues for future studies to test if richness patterns in migrating bats are better predicted by biotic variables, like resource distributions, unlike in hibernating bats.

The Neotropics

The Neotropics are home to the highest diversity of bats in the world, by any nearly any metric: described species, ecological diversity, morphological disparity, and behavioral diversity. While nearly half of extant bat families are present in the Neotropics, most Neotropical bats belong to the superfamily Noctilionoidea - in particular, to its largest family Phyllostomidae (Table 1.1; Dumont *et al.* 2012). Noctilionoids are not only the most diverse bats in the Neotropics, but are among the most common and diverse mammals in the realm (Fleming & Kress 2013). Noctilionoids likely colonized South America by the Eocene, and then radiated during its subsequent isolation (Rojas *et al.* 2016). While regional richness is extremely high throughout the Neotropics, it is highest at low latitudes within the western Amazon Basin and along the Andes (Figure 1.6). Beta diversity among Neotropical bats, especially in the wettest, equatorial regions of maximal richness, is also high wherever it has been estimated (Stevens & Willig 2002, Bergallo *et al.* 2003, Bernard *et al.* 2010, Sampaio *et al.* 2010).

As in the Old World tropics, high Neotropical bat diversity and regional richness has been explained by the year-around availability of diverse food resources, particularly plants. Frugivores, nectarivores, and generalist herbivores are ubiquitous among phyllostomids

(Monteiro & Nogueira 2011, Rojas *et al.* 2011). At the local and community level, noctilionoids and vespertilionoids readily co-occur in extremely diverse bat assemblages throughout the realm (Villalobos & Arita 2010). It is still unclear, however, how generalizable the mechanisms are for the sorting of Neotropical bats from regional species pools into these diverse, local communities. Community assembly processes involving niche partitioning and habitat filtering can potentially be tested using a combination of spatial, ecological, morphological, and phylogenetic data to test whether divergence can predict co-occurrence.

Many bat species in this realm are characterized by morphological specialization for preferred resources. However, many species are also opportunistically and facultatively omnivorous, depending on seasonality and plant phenology. Arthropods and plants can be locally and seasonally limited, despite being more diverse than in temperate realms. Yet there is little evidence for competitive structuring of Neotropical bat assemblages at the broadest scales (Meyer & Kalko 2008). Combined, these factors likely drive the overall impression that Neotropical bat distributions - particularly among noctilionoids - can be highly fragmented and fluid, yet closely track the distributions and abundances of food resources (Medellín *et al.* 2000, Schulze *et al.* 2000, Patterson *et al.* 2003). Maximum extent ranges like IUCN distributions, then, may not accurately reflect bat distributions throughout the year, as they likely encompass dispersal, migration, and seasonal variation. Actual patterns of spatial diversity in Neotropical bats would thus reflect filtering by available resources. These filtering mechanisms likely change seasonally with precipitation and plant phenology, with omnivorous species even switching preferred diets to compensate for any resource scarcity.

At the finest scales within Neotropical forests, bat assemblages are vertically stratified (Bernard 2001, Kalko & Handley 2001, Rex *et al.* 2008), though there is less evidence for

temporal partitioning of local habitats (Presley *et al.* 2009). This vertical stratification is driven by species preferences for available resources, as individual bat species forage for plants and prey that occur at different levels of the forest. These overall characteristics further illustrate a general pattern of Neotropical bat abundances and ranges being closely associated with resource availability, unlike temperate bats. Given the accelerated fragmentation of Neotropical forests, it is especially important for conservationists to take into account just how reliant many Neotropical bat species are for patchy and fragmented resources (Medellín *et al.* 2000, Schulze *et al.* 2000, Meyer *et al.* 2007).

The majority of Neotropical bat research focuses on frugivores, nectarivores, and omnivores. However, many species of obligate insectivores also occur in the Neotropics, including vespertilionids, molossids, and emballonurids (Table 1.1). Accurate sampling for insectivorous bats is notoriously more difficult than for herbivorous bats, and insectivorous bat diversity and richness is likely underestimated (MacSwiney G *et al.* 2008). Insectivores may also be vertically stratified, making them especially difficult to sample and detect using traditional methods that focus on the lower canopy, including mist nets and acoustic detection (João *et al.* 2010, Pereira *et al.* 2010). The Neotropics are also home to perhaps the most derived trophic specialists, the vampire bats (Phyllostomidae: Desmodontinae). Vampire bat distributions are closely studied in relation to agriculture and livestock, especially when it comes to the most common species, *Desmodus rotundus*. The three species of vampire bats are specialized for different hosts and feeding strategies (Voigt & Kelm 2006). Their distribution patterns and population structure often reflect these close host associations, though in the case of *Desmodus*, it appears that introduced livestock is preferred over endemic species (Lee *et al.* 2012). As is the

case in many parts of the world, the effects of development and agriculture on endemic diversity can be unpredictable.

BAT DIVERSITY ACROSS THE GLOBE

Temperate and tropical bat diversity are fundamentally different in many respects, especially with regards to how regional richness patterns reflect the availability of resources and habitats. In both parts of the globe, bats are often characterized by high plasticity and flexibility when it comes to their diets. Most temperate bats are generalist insectivores (or faunivores, *sensu* Fenton 1990), and will readily shift their diets to whatever is available across both individual nights and seasons. Many tropical bats are partially and facultatively omnivorous, switching among plant resources or even between plant and animal diets depending on scarcity.

However, we find different spatial patterns of diversity between the two types of realms. Temperate bats have broad ranges, and we generally find low turnover among relatively similar bat communities. For example, Nearctic bat communities are relatively homogeneous, with low beta diversity and turnover even at continental scales (Rodríguez & Arita 2004). Prey distributions also do not seem to predict regional richness patterns among temperate bats. Overall patterns of spatial diversity in temperate bats are most strongly predicted by both the availability of water and roosting habitats, including hibernacula. Many temperate bats rely on torpor and hibernation to persist through dry and cold months with few insects. Hibernacula availability is a key limiting factor of regional richness in temperate bats, which may further erase any relationships between bat and insect distributions. As a whole, we may expect that temperate bat distributions are more seasonally static because of these strong *abiotic* predictors, with individual species consuming whatever arthropods are available within those limits.

The species-rich tropical realms of the world are characterized by a much broader suite of trophic ecology and behavior. Richness is highest in the wettest parts of the tropics along the equator, where there is generally less variability in arthropod abundance. Furthermore, there are also year-round, readily available plant resources for frugivores, nectarivores, and omnivores due to decreased seasonality (Stevens 2011). Tropical bats appear to more closely track the ranges of their diet items despite this stability. These species can have highly seasonal distributions that reflect plant phenology and vertical stratification within forest canopies, and they are not evenly dispersed across ranges based on resource variation. True tropical bat distributions may thus be relatively fluid based on resource availability. Furthermore, many species opportunistically and seasonally shift their diets in times of scarcity, with hibernation being a generally rare strategy. This functional versatility despite ecomorphological specialization can potentially explain the high bat species richness of the Neotropics (Robinson & Wilson 1998, Bellwood *et al.* 2006). Considering how many species appear to be at least partially omnivorous, tropical bat distributions may also be particularly hard to map and predict, as they reflect many different fluctuating *biotic* predictors.

Predictors of spatial diversity may be difficult to fully tease apart for all bat species. For example, water and elevation predict abundance, turnover, and richness across numerous realms (McCain 2007). However, in temperate realms, this appears most related to other abiotic factors, like roost suitability. In the tropics, water and elevation may be more linked to the biotic factors like the ranges and tolerances of available arthropods and plants. Another limitation is that for many species of temperate insectivorous bats, detailed diet descriptions are unavailable. Our data may simply be too coarse to detect when temperate bat ranges are limited by prey availability. The continued application of stable isotope methods (Herrera M *et al.* 2009) and increased,

diversified methods of field sampling may reveal clearer trends in local factors that scale to structure spatial diversity.

As is true for countless other clades, bat populations are heavily impacted by habitat destruction, ecosystem disturbance, and global climate change. Bat ranges have both expanded and contracted in response to rapidly changing conditions across the globe. In the Nearctic, the migratory molossid *Tadarida brasiliensis*, is expanding its large range even farther into northern latitudes as winters become more mild (McCracken *et al.* 2018). Other temperate bats are declining in abundance and contracting their ranges as available hibernacula and water sources disappear with warming climates (Adams 2010, Sherwin *et al.* 2012). Habitat destruction from urbanization, agriculture, and deforestation affects bats worldwide, and tropical bats may disproportionately be impacted given their higher degrees of specialization to resources. In areas of heavy deforestation, generalist insectivores like vespertilionids and molossids appear to have more stable ranges and populations than those of specialized herbivores (Fenton *et al.* 1998). The most specialized frugivores and nectarivores across the tropics have experienced considerable declines associated with habitat destruction (Quesada *et al.* 2003, Meyer & Kalko 2008).

Dynamics of global change may also affect the relationships among species, local environmental variables, and broader, regional richness patterns. Generalists with high dispersal abilities may in fact flourish in heavily fragmented tropical forests, potentially replacing the most specialized species that are adapted to patchy or threatened resources (Gorresen & Willig 2003, Bernard & Fenton 2006, Meyer & Kalko 2008). The relationships between species' dispersal abilities and their ranges, or between biotic interactions and range limits, may also change in response to external stimuli (Kokko & López-Sepulcre 2006, Brooker *et al.* 2007), with unpredictable results that can reshape regional species pools and communities.

While it is difficult to accurately predict the composition of future bat assemblages in the face of overwhelming global change, we know that bat species are critically interwoven into ecosystems and human economies worldwide as seed dispersers, pollinators, and predators (Williams-Guillén *et al.* 2008, Kunz *et al.* 2011). Sometimes, the effects of continued development have had surprising effects on bats, providing opportunities to study and understand their resilience to disturbance. In temperate realms where bats are most limited by roost availability, some bat species have readily adapted to using man-made structures as both temporary and permanent roosts (Fenton 1997, McAney 1999). By improving our understanding of bat richness patterns, we can better understand how they will respond to global change, and how we can best preserve the order's rich biodiversity.

DISSERTATION CHAPTER OVERVIEW

In the following chapters, I discuss major patterns of diversity and diversification across extant bats. Chapter 2 (Shi & Rabosky 2015) focuses on the observation of unequal species richness within the order. A common explanation for the variation in species diversity across clades is that rates of diversification are also not constant. To test this hypothesis, we constructed a species-level, molecular phylogeny that included the majority of described bat species. We then extended a recently-developed paradigm for inferring rates of diversification on phylogenies, and clustering species into shared macroevolutionary regimes.

We found that, contrary to expectations, there is little rate heterogeneity across the tree. Most bats are united into a single, macroevolutionary cohort of speciation rates, with only one exception - the phyllostomid subfamily Stenodermatinae. We also developed a method for testing phylogenetic imbalance across trees, and confirmed that species richness across the order

is indeed more unequally distributed than expected under null expectations. Because there is a positive relationship between clade age and richness, we also suggest that bat diversity may still be expanding (Shi & Rabosky 2015).

In Chapter 3 (Shi *et al.* 2018), we return to spatial patterns of diversity across the order, specifically focusing on how patterns of sympatry vary across the globe. We tested for how divergence among bat species may be related to co-occurrence in sympatry across biogeographic realms. Theory predicts that, among other possibilities, ecological similarity may preclude sympatry due to interspecific competition for resources. Phylogenetic relatedness may thus also negatively predict sympatry, given the correlation between ecological divergence and time since divergence. We may also predict that closely related species are less likely to be sympatric if speciation generally occurs in allopatry, and because sympatric incipient species complexes are more likely to collapse due to hybridization.

We tested these hypotheses across bats using a combination of IUCN range data and linear measurements from bat skulls that are closely linked to trophic ecology and feeding performance. Using simulations, linear mixed modeling, and other model-fitting approaches, we found that in most cases, neither phylogenetic nor ecomorphological divergence predicts co-occurrence between pairs of bat taxa. The sole exception is in the Neotropics, where we found that bats are most likely to co-occur when they are morphologically similar. These findings suggested that sympatry may occur readily across the order, with little signal of competitive controls or phylogenetic constraints. Among Neotropical bats, we found evidence that suggests filtering by habitat and resources is the predominant mechanism structuring co-occurrence across the realm (Shi *et al.* 2018).

Chapter 4 outlines the collection and digitization of a high-resolution morphological database of bat skulls. In this chapter, we outlined how X-ray computed microtomography (μCT) scanning of specimens can both highlight patterns of morphological disparity and make specimen-based research more accessible and collaborative. We μCT-scanned a large set of bat skulls that spanned both the ecological and phylogenetic breadth of the order. We made these scans available to the public for both research and education, and also described how they can be reliably used within a traditional framework that relies on museum specimens.

Chapter 5 tests for the relationship between skull shape evolution, as inferred from these 3D digital specimens, and ecological evolution in New World bats. These analyses combined our 3D data with a species-level diet database compiled from previous studies and the wider literature. We developed a likelihood-based approach, analogous to the clustering of cohorts in Chapter 2, for identifying groups of New World species that are most likely to share regimes of ecological and morphological evolution. Surprisingly, we find that dynamics of cranial shape evolution appear decoupled from those of ecological evolution. Ecological evolution across New World bats is strikingly heterogeneous, and is closely aligned with the distribution of trophic categories we see among extant species. By contrast, cranial shape evolution is characterized by largely homogeneous dynamics, even across distant relatives and ecological guilds. We suggest that this may be caused by high cranial lability among New World bats, as well as the possibility that more Neotropical bats are ecologically plastic and omnivorous than is typically assumed.

Finally, in Chapter 6, I discuss the major findings of the dissertation in the broader context of both bat research and the fields of ecology and evolutionary biology. Many of the results presented here imply that extant bat diversity is not saturated, and may still be expanding across the globe. I emphasize many unique attributes of the bat radiation that make them an

excellent study system. With our findings in mind, I conclude the dissertation with thoughts on ecology and macroevolution, and our overall goal to understand the distribution of biodiversity across time and space.

REFERENCES

Adams, R.A. (2010) Bat reproduction declines when conditions mimic climate change projections for western North America. *Ecology*, **91**, 2437–2445.

Agosta, S.J. (2002) Habitat use, diet and roost selection by the Big Brown Bat (*Eptesicus fuscus*) in North America: a case for conserving an abundant species. *Mammal Review*, **32**, 179–198.

Almeida, F.C., Giannini, N.P., DeSalle, R., & Simmons, N.B. (2009) The phylogenetic relationships of cynopterine fruit bats (Chiroptera: Pteropodidae: Cynopterinae). *Molecular Phylogenetics and Evolution*, **53**, 772–783.

Almeida, F.C., Giannini, N.P., DeSalle, R., & Simmons, N.B. (2011) Evolutionary relationships of the Old World fruit bats (Chiroptera, Pteropodidae): another star phylogeny? *BMC Evolutionary Biology*, **11**, 281.

Almeida, F.C., Giannini, N.P., Simmons, N.B., & Helgen, K.M. (2014) Each flying fox on its own branch: a phylogenetic tree for *Pteropus* and related genera (Chiroptera: Pteropodidae). *Molecular Phylogenetics and Evolution*, **77**, 83–95.

Andriafidison, D., Andrianaivoarivelo, R.A., Ramilijaona, O.R., Razanahoera, M.R., MacKinnon, J., Jenkins, R.K.B., & Racey, P.A. (2006) Nectarivory by endemic Malagasy fruit bats during the dry season. *Biotropica*, **38**, 85–90.

Anthony, E.L.P. & Kunz, T.H. (1977) Feeding strategies of the little brown bat, *Myotis lucifugus*, in southern New Hampshire. *Ecology*, **58**, 775–786.

Badgley, C. & Finarelli, J.A. (2013) Diversity dynamics of mammals in relation to tectonic and climatic history: comparison of three Neogene records from North America. *Paleobiology*, **39**, 373–399.

Badgley, C. & Fox, D.L. (2000) Ecological biogeography of North American mammals: species density and ecological structure in relation to environmental gradients. *Journal of Biogeography*, **27**, 1437–1467.

Badgley, C., Smiley, T.M., Terry, R., Davis, E.B., DeSantis, L.R.G., Fox, D.L., Hopkins, S.S.B., Jezkova, T., Matocq, M.D., Matzke, N., McGuire, J.L., Mulch, A., Riddle, B.R., Roth, V.L., Samuels, J.X., Strömberg, C.A.E., & Yanites, B.J. (2017) Biodiversity and topographic complexity: modern and geohistorical perspectives. *Trends in Ecology & Evolution*, **32**, 211–226.

Barclay, R.M.R. & Brigham, R.M. (1991) Prey detection, dietary niche breadth, and body size in bats: why are aerial insectivorous bats so small? *The American Naturalist*, **137**, 693–703.

Bates, P.J.J., Nwe, T., Bu, S.S.H., Mie, K.M., Swe, K.M., Nyo, N., Khaing, A.A., Aye, N.N., Toke, Y.Y., Aung, N.N., Thi, M.M., & Mackie, I. (2005) A review of the genera *Myotis, Ia, Pipistrellus, Hypsugo*, and *Arielulus* (Chiroptera: Vespertilionidae) from Myanmar (Burma), including three species new to the country. *Acta Chiropterologica*, **7**, 205–236.

Baudinette, R. V., Churchill, S.K., Christian, K.A., Nelson, J.E., & Hudson, P.J. (2000) Energy, water balance and the roost microenvironment in three Australian cave-dwelling bats (Microchiroptera). *Journal of Comparative Physiology B: Biochemical, Systemic, and Environmental Physiology*, **170**, 439–446.

Bell, G.P. (1980) Habitat use and response to patches of prey by desert insectivorous bats. *Canadian Journal of Zoology*, **58**, 1876–1883.

Bellwood, D.R., Wainwright, P.C., Fulton, C.J., & Hoey, A.S. (2006) Functional versatility supports coral reef biodiversity. *Proceedings of the Royal Society B: Biological Sciences*, **273**, 101-107.

Bergallo, H.G., Esbérard, C.E.L., Mello, M.A.R., Lins, V., Mangolin, R., Melo, G.G.S., & Baptista, M. (2003) Bat species richness in Atlantic forest: what is the minimum sampling effort? *Biotropica*, **35**, 278–288.

Bernard, E. (2001) Vertical stratification of bat communities in primary forests of Central Amazon, Brazil. *Journal of Tropical Ecology*, **17**, 115–126.

Bernard, E., Albernaz, A.L.K.M., & Magnusson, W.E. (2001) Bat species composition in three localities in the Amazon Basin. *Studies on Neotropical Fauna and Environment*, **36**, 177–184.

Bernard, E. & Fenton, M.B. (2007) Bats in a fragmented landscape: species composition, diversity and habitat interactions in savannas of Santarém, Central Amazonia, Brazil. *Biological Conservation*, **134**, 332–343.

Bilgin, R., Karataş, A., Çoraman, E., Disotell, T., & Morales, J. (2008) Regionally and climatically restricted patterns of distribution of genetic diversity in a migratory bat species, *Miniopterus schreibersii* (Chiroptera: Vespertilionidae). *BMC Evolutionary Biology*, **8**, 209.

Black, H.L. (1974) A north temperate bat community: structure and prey populations. *Journal of Mammalogy*, **55**, 138–157.

Bondarenco, A., Körtner, G., & Geiser, F. (2016) How to keep cool in a hot desert: torpor in two species of free-ranging bats in summer. *Temperature*, **3**, 476–483.

Brooker, R.W., Travis, J.M.J., Clark, E.J., & Dytham, C. (2007) Modelling species' range shifts in a changing climate: The impacts of biotic interactions, dispersal distance and the rate of climate change. *Journal of Theoretical Biology*, **245**, 59–65.

Brown, J.H. (1984) On the relationship between abundance and distribution of species. *The American Naturalist*, **124**, 255–279.

Bumrungsri, S., Harrison, D.L., Satasook, C., Prajukjitr, A., Thong-Aree, S., & Bates, P.J.J. (2006) A review of bat research in Thailand with eight new species records for the country. *Acta Chiropterologica*, **8**, 325–359.

Campbell, P., Reid, N.M., Zubaid, A., Adnan, A.M., & Kunz, T.H. (2006) Comparative roosting ecology of *Cynopterus* (Chiroptera: Pteropodidae) fruit bats in peninsular Malaysia. *Biotropica*, **38**, 725–734.

Castella, V., Ruedi, M., Excoffier, L., Ibáñez, C., Arlettaz, R., & Hausser, J. (2000) Is the Gibraltar Strait a barrier to gene flow for the bat *Myotis myotis* (Chiroptera: Vespertilionidae)? *Molecular Ecology*, **9**, 1761–1772.

Chan, L.M., Goodman, S.M., Nowak, M.D., Weisrock, D.W., & Yoder, A.D. (2011) Increased population sampling confirms low genetic divergence among *Pteropus* (Chiroptera: Pteropodidae) fruit bats of Madagascar and other western Indian Ocean islands. *PLoS Currents*, **3**, RRN1226.

Connell, J.H. (1980) Diversity and the coevolution of competitors, or the ghost of competition past. *Oikos*, **35**, 131–138.
Currie, D.J. (1991) Energy and large-scale patterns of animal- and plant-species richness. *The American Naturalist*, **137**, 27–49.
Daniel, M.J. (1975) First record of an Australian fruit bat (Megachiroptera: Pteropodidae) reaching New Zealand. *New Zealand Journal of Zoology*, **2**, 227–231.
Davis Rabosky, A.R., Cox, C.L., Rabosky, D.L., Title, P.O., Holmes, I.A., Feldman, A., & McGuire, J.A. (2016) Coral snakes predict the evolution of mimicry across New World snakes. *Nature Communications*, **7**, 11484.
Dumont, E.R. & O'Neal, R. (2004) Food hardness and feeding behavior in Old World fruit bats (Pteropodidae). *Journal of Mammalogy*, **85**, 8–14.
Dumont, E.R., Dávalos, L.M., Goldberg, A., Santana, S.E., Rex, K., & Voigt, C.C. (2012) Morphological innovation, diversification and invasion of a new adaptive zone. *Proceedings of the Royal Society B: Biological Sciences*, **279**, 1797–1805.
Eby, P. (1991) Seasonal movements of grey-headed flying-foxes, *Pteropus poliocephalus* (Chiroptera: Pteropodidae), from two maternity camps in northern New South Wales. *Wildlife Research*, **18**, 547–559.
Fahr, J. & Kalko, E.K. V. (2011) Biome transitions as centres of diversity: habitat heterogeneity and diversity patterns of West African bat assemblages across spatial scales. *Ecography*, **34**, 177–195.
Fenton, M.B. (1997) Science and the conservation of bats. *Journal of Mammalogy*, **78**, 1–14.
Fenton, M.B. & Morris, G.K. (1976) Opportunistic feeding by desert bats (*Myotis* spp.). *Canadian Journal of Zoology*, **54**, 526–530.
Fenton, M.B. (1990) The foraging behaviour and ecology of animal-eating bats. *Canadian Journal of Zoology*, **68**, 411–422.
Fenton, M.B., Cumming, D.H.M., Rautenbach, I.L., Cumming, G.S., Cumming, M.S., Ford, G., Taylor, R.D., Dunlop, J., Hovorka, M.D., Johnston, D.S., Portfors, C. V., Kalcounis, M.C., & Mahlanga, Z. (2008) Bats and the loss of tree canopy in African woodlands. *Conservation Biology*, **12**, 399–407.
Fitzpatrick, B.M. & Turelli, M. (2006) The geography of mammalian speciation: mixed signals from phylogenies and range maps. *Evolution*, **60**, 601–615.
Flanders, J., Wei, L., Rossiter, S.J., & Zhang, S. (2011) Identifying the effects of the Pleistocene on the greater horseshoe bat, *Rhinolophus ferrumequinum*, in East Asia using ecological niche modelling and phylogenetic analyses. *Journal of Biogeography*, **38**, 439–452.
Fleming, T. & Kress, W. (2013) *The ornaments of life: coevolution and conservation in the tropics.* University of Chicago Press, Chicago.
Francis, A.P. & Currie, D.J. (2003) A globally consistent richness-climate relationship for angiosperms. *The American Naturalist*, **161**, 523–536.
Francis, C.M. (1994) Vertical stratification of fruit bats (Pteropodidae) in lowland dipterocarp rainforest in Malaysia. *Journal of Tropical Ecology*, **10**, 523–530.
Furman, A., Çoraman, E., Bilgin, R., & Karataş, A. (2009) Molecular ecology and phylogeography of the bent-wing bat complex (*Miniopterus schreibersii*) (Chiroptera: Vespertilionidae) in Asia Minor and adjacent regions. *Zoologica Scripta*, **38**, 129–141.
Gaston, K.J. & Fuller, R.A. (2009) The sizes of species' geographic ranges. *Journal of Applied Ecology*, **46**, 1–9.

Geiser, F. (2004) The role of torpor in the life of Australian arid zone mammals. *Australian Mammalogy*, **26**, 125–134.
Georgiakakis, P., Vasilakopoulos, P., Mylonas, M., & Russo, D. (2010) Bat species richness and activity over an elevation gradient in mediterranean shrublands of Crete. *Hystrix*, **21**.
Giannini, N.P., Almeida, F.C., Simmons, N.B., & DeSalle, R. (2006) Phylogenetic relationships of the enigmatic harpy fruit bat, *Harpyionycteris* (Mammalia: Chiroptera: Pteropodidae). *American Museum Novitates*, **3533**, 1–12.
Goodman, S.M., Buccas, W., Naidoo, T., Ratrimomanarivo, F., Taylor, P.J., Lamb, J., & Lamb, J. (2010) Patterns of morphological and genetic variation in western Indian Ocean members of the *Chaerephon "pumilus"* complex (Chiroptera: Molossidae), with the description of a new species from Madagascar. *Zootaxa*, **2551**, 1–36.
Goodman, S.M. & Ganzhorn, J.U. (1997) Rarity of figs (Ficus) on Madagascar and its relationship to a depauperate frugivore community. *Revue d'Ecologie*, **52**, 321–329.
Goodman, S.M., Chan, L.M., Nowak, M.D., & Yoder, A.D. (2010) Phylogeny and biogeography of western Indian Ocean *Rousettus* (Chiroptera: Pteropodidae). *Journal of Mammalogy*, **91**, 593–606.
Gorresen, P.M. & Willig, M.R. (2004) Landscape responses of bats to habitat fragmentation in Atlantic forest of Paraguay. *Journal of Mammalogy*, **85**, 688–697.
Heaney, L.R., Tabaranza Jr., B.R., Balete, D.S., & Rigertas, N. (2006) Synopsis and biogeography of the mammals of Camiguin Island, Philippines. *Fieldiana Zoology*, **106**, 28–48.
Henry, M., Barrière, P., Gautier-Hion, A., & Colyn, M. (2004) Species composition, abundance and vertical stratification of a bat community (Megachiroptera: Pteropodidae) in a West African rain forest. *Journal of Tropical Ecology*, **20**, 21–29.
Herkt, K.M.B., Barnikel, G., Skidmore, A.K., & Fahr, J. (2016) A high-resolution model of bat diversity and endemism for continental Africa. *Ecological Modelling*, **320**, 9–28.
Herrera M., L.G., Hobson, K.A., Manzo A., A., Estrada B., D., Sánchez-Cordero, V., & Méndez C, G. (2009) The role of fruits and insects in the nutrition of frugivorous bats: evaluating the use of stable isotope models. *Biotropica*, **33**, 520–528.
Hodgkison, R., Balding, S.T., Zubaid, A., & Kunz, T.H. (2003) Fruit bats (Chiroptera: Pteropodidae) as seed dispersers and pollinators in a lowland Malaysian rain forest. *Biotropica*, **35**, 491–502.
Hodgkison, R., Balding, S.T., Zubaid, A., & Kunz, T.H. (2004) Temporal variation in the relative abundance of fruit bats (Megachiroptera: Pteropodidae) in relation to the availability of food in a lowland Malaysian rain forest. *Biotropica*, **36**, 522–533.
Hodgkison, R., Balding, S.T., Zubaid, A., & Kunz, T.H. (2004) Habitat structure, wing morphology, and the vertical stratification of Malaysian fruit bats (Megachiroptera: Pteropodidae). *Journal of Tropical Ecology*, **20**, 667–673.
Holt, R.D. (2003) On the evolutionary ecology of species' ranges. *Evolutionary Ecology Research*, **5**, 159–178.
Hughes, A.C., Satasook, C., Bates, P.J.J., Soisook, P., Sritongchuay, T., Jones, G., & Bumrungsri, S. (2010) Echolocation call analysis and presence-only modelling as conservation monitoring tools for rhinolophoid bats in Thailand. *Acta Chiropterologica*, **12**, 311–327.
Humphrey, S.R. (1975) Nursery roosts and community diversity of Nearctic bats. *Journal of Mammalogy*, **56**, 321–346.

Humphries, M.M., Thomas, D.W., & Speakman, J.R. (2002) Climate-mediated energetic constraints on the distribution of hibernating mammals. *Nature*, **418**, 313–316.
IUCN. (2017) *The IUCN Red List of threatened species.* **Version 2017-3**.
Jackson, J.B.C. (1981) Interspecific competition and species' distributions: the ghosts of theories and data past. *American Zoologist*, **21**, 889–901.
Jenkins, R.K.B., Racey, P.A., Andriafidison, D., Razafindrakoto, N., Razafimahatratra, E., Rabearivelo, A., Ratsimandresy, Z., Andrianandrasana, R.H., & Razafimanahaka, H.J. (2007) Not rare, but threatened: the endemic Madagascar flying fox *Pteropus rufus* in a fragmented landscape. *Oryx*, **41**, 263–271.
João, M., Pereira, R., Marques, J.T., & Palmeirim, J.M. (2010) Vertical stratification of bat assemblages in flooded and unflooded Amazonian forests. *Current Zoology*, **56**, 469–478.
Jones, G. & Rayner, J.M. V. (1989) Foraging behavior and echolocation of wild horseshoe bats *Rhinolophus ferrumequinum* and *R. hipposideros* (Chiroptera, Rhinolophidae). *Behavioral Ecology and Sociobiology*, **25**, 183–191.
Jung, K., Molinari, J., & Kalko, E.K. V. (2014) Driving factors for the evolution of species-specific echolocation call design in New World free-tailed bats (Molossidae). *PLoS ONE*, **9**, e85279.
Juste, J., Ibáñez, C., Muñoz, J., Trujillo, D., Benda, P., Karataş, A., & Ruedi, M. (2004) Mitochondrial phylogeography of the long-eared bats (*Plecotus*) in the Mediterranean Palaearctic and Atlantic Islands. *Molecular Phylogenetics and Evolution*, **31**, 1114–1126.
Kalko, E.K.V. & Handley Jr., C.O. (2001) Neotropical bats in the canopy: diversity, community structure, and implications for conservation. *Plant Ecology*, **153**, 319–333.
Kerr, J.T. & Packer, L. (1997) Habitat heterogeneity as a determinant of mammal species richness in high-energy regions. *Nature*, **385**, 252–254.
Kerth, G., Weissmann, K., & König, B. (2001) Day roost selection in female Bechstein's bats (*Myotis bechsteinii*): a field experiment to determine the influence of roost temperature. *Oecologia*, **126**, 1–9.
Kingston, T. (2010) Research priorities for bat conservation in Southeast Asia: a consensus approach. *Biodiversity and Conservation*, **19**, 471–484.
Kingston, T., Francis, C.M., Akbar, Z., & Kunz, T.H. (2003) Species richness in an insectivorous bat assemblage from Malaysia. *Journal of Tropical Ecology*, **19**, 67–79.
Kingston, T. & Rossiter, S.J. (2004) Harmonic-hopping in Wallacea's bats. *Nature*, **429**, 654–657.
Kitchener, D.J., Packer, W.C., & Maryanto, I. (1993) Taxonomic status of *Nyctimene* (Chiroptera: Pteropodidae) from the Banda, Kai, and Aru islands, Maluku, Indonesia - implications for biogeography. *Records of the Western Australian Museum*, **16**, 399–417.
Kokko, H. & López-Sepulcre, A. (2006) From individual dispersal to species ranges: perspectives for a changing world. *Science*, **313**, 789–791.
Kolb, A., Barsch, F., & Diekmann, M. (2006) Determinants of local abundance and range size in forest vascular plants. *Global Ecology and Biogeography*, **15**, 237–247.
Kruskop, S. V., Borisenko, A. V., Ivanova, N. V., Lim, B.K., & Eger, J.L. (2012) Genetic diversity of northeastern Palaearctic bats as revealed by DNA barcodes. *Acta Chiropterologica*, **14**, 1–14.

Kruskop, S. V. & Borisenko, A. V. (2013) A new species of south-east Asian *Myotis* (Chiroptera: Vespertilionidae), with comments on Vietnamese "whiskered bats." *Acta Chiropterologica*, **15**, 293–305.

Kunz, T.H., de Torrez, E.B., Bauer, D., Lobova, T., & Fleming, T.H. (2011) Ecosystem services provided by bats. *Annals of the New York Academy of Sciences*, **1223**, 1–38.

Lee, D.N., Papeş, M., & Van Den Bussche, R.A. (2012) Present and potential future distribution of common vampire bats in the Americas and the associated risk to cattle. *PLoS ONE*, **7**, e42466.

Leibold, M.A., Holyoak, M., Mouquet, N., Amarasekare, P., Chase, J.M., Hoopes, M.F., Holt, R.D., Shurin, J.B., Law, R., Tilman, D., Loreau, M., & Gonzalez, A. (2004) The metacommunity concept: a framework for multi-scale community ecology. *Ecology Letters*, **7**, 601–613.

López-González, C., Presley, S.J., Lozano, A., Stevens, R.D., & Higgins, C.L. (2015) Ecological biogeography of Mexican bats: the relative contributions of habitat heterogeneity, beta diversity, and environmental gradients to species richness and composition patterns. *Ecography*, **38**, 261–272.

Lourenço, S.I. & Palmeirim, J.M. (2004) Influence of temperature in roost selection by *Pipistrellus pygmaeus* (Chiroptera): relevance for the design of bat boxes. *Biological Conservation*, **119**, 237–243.

Louthan, A.M., Doak, D.F., & Angert, A.L. (2015) Where and when do species interactions set range limits? *Trends in Ecology and Evolution*, **30**, 780–792.

Lumsden, I. & Bennet, A. (1995) Bats of a semi-arid environment in south-eastern Australia: biogeography, ecology and conservation. *Wildlife Research*, **22**, 217–239.

MacSwiney G., M.C., Clarke, F.M., & Racey, P.A. (2008) What you see is not what you get: the role of ultrasonic detectors in increasing inventory completeness in Neotropical bat assemblages. *Journal of Applied Ecology*, **45**, 1364–1371.

Maryanto, I., Yani, M., Prijono, S.N., & Wiantoro, S. (2010) Altitudinal distribution of fruit bats (Pteropodidae) in Lore Lindu National Park, Central Sulawesi, Indonesia. *Hystrix*, **22**.

Mayr, E. (1944) Wallace's Line in the light of recent zoogeographic studies. *The Quarterly Review of Biology*, **19**, 1–14.

McAney, K. (1999) Mines as roosting sites for bats: their potential and protection. *Biology and Environment: Proceedings of the Royal Irish Academy*, **99**, 63–65.

McCain, C.M. (2007) Could temperature and water availability drive elevational species richness patterns? A global case study for bats. *Global Ecology and Biogeography*, **16**, 1–13.

McCracken, G.F., Gillam, E.H., Westbrook, J.K., Lee, Y.-F., Jensen, M.L., & Balsley, B.B. (2007) Brazilian free-tailed bats (*Tadarida brasiliensis*: Molossidae, Chiroptera) at high altitude: links to migratory insect populations. *Integrative and Comparative Biology*, **48**, 107–118.

McCracken, G.F., Bernard, R.F., Gamba-Rios, M., Wolfe, R., Krauel, J.J., Jones, D.N., Russell, A.L., & Brown, V.A. (2018) Rapid range expansion of the Brazilian free-tailed bat in the southeastern United States, 2008–2016. *Journal of Mammalogy*.

Medellín, R.A., Equihua, M., & Amin, M.A. (2008) Bat diversity and abundance as indicators of disturbance in Neotropical rainforests. *Conservation Biology*, **14**, 1666–1675.

Meyer, C.F.J., Fründ, J., Lizano, W.P., & Kalko, E.K.V. (2007) Ecological correlates of vulnerability to fragmentation in Neotropical bats. *Journal of Applied Ecology*, **45**, 381–391.

Meyer, C.F.J. & Kalko, E.K. V. (2008) Bat assemblages on Neotropical land-bridge islands: nested subsets and null model analyses of species co-occurrence patterns. *Diversity and Distributions*, **14**, 644–654.
Monteiro, L.R. & Nogueira, M.R. (2011) Evolutionary patterns and processes in the radiation of phyllostomid bats. *BMC Evolutionary Biology*, **11**, 137.
Montoya, D., Rodríguez, M.A., Zavala, M.A., & Hawkins, B.A. (2007) Contemporary richness of holarctic trees and the historical pattern of glacial retreat. *Ecography*, **30**, 173–182.
Morgan, G.S. (2005) The great American biotic interchange in Florida. *Bulletin of the Florida Museum of Natural History*, **45**, 271–311.
Mouquet, N. & Loreau, M. (2003) Community patterns in source-sink metacommunities. *The American Naturalist*, **162**, 544–557.
Nelson, J. (1965) Movements of Australian flying foxes (Pteropodidae: Megachiroptera). *Australian Journal of Zoology*, **13**, 53–74.
Neubaum, D.J., O'Shea, T.J., & Wilson, K.R. (2006) Autumn migration and selection of rock crevices as hibernacula by big brown bats in Colorado. *Journal of Mammalogy*, **87**, 470–479.
Nicoll, M.E. & Racey, P.A. (1981) The Seychelles Fruit Bat, *Pteropus seychellensis seychellensis*. *African Journal of Ecology*, **19**, 361–364.
Nowak, M.D. (1994) *Walker's bats of the world.* Johns Hopkins University Press, Baltimore.
Oberdoff, T., Guegan, J.-F., & Hugueny, B. (1995) Global scale patterns of fish species richness in rivers. *Ecography*, **18**, 345–352.
Olson, D.M., Dinerstein, E., Wikramanayake, E.D., Burgess, N.D., Powell, G.V.N., Underwood, E.C., D'amico, J. A., Itoua, I., Strand, H.E., Morrison, J.C., Loucks, C.J., Allnutt, T.F., Ricketts, T.H., Kura, Y., Lamoreux, J.F., Wettengel, W.W., Hedao, P., & Kassem, K.R. (2001) Terrestrial ecoregions of the world: a new map of life on Earth. *BioScience*, **51**, 933–938.
Ossa, G., Kramer-Schadt, S., Peel, A.J., Scharf, A.K., & Voigt, C.C. (2012) The movement ecology of the straw-colored fruit bat, *Eidolon helvum*, in sub-Saharan Africa assessed by stable isotope ratios. *PLoS ONE*, **7**, e45729.
Palmer, C., Price, O., & Bach, C. (2000) Foraging ecology of the black flying fox (*Pteropus alecto*) in the seasonal tropics of the Northern Territory, Australia. *Wildlife Research*, **27**, 169–178.
Parry-Jones, K.A. & Augee, M.L. (2001) Factors affecting the occupation of a colony site in Sydney, New South Wales by the Grey-headed Flying-fox *Pteropus poliocephalus* (Pteropodidae). *Austral Ecology*, **26**, 47–55.
Patterson, B.D., Willig, M.R., & Stevens, R.D. (2003) Trophic strategies, niche partitioning, and patterns of ecological organization. *Bat Ecology* (ed. by T.H. Kunz and M.B. Fenton), pp. 536–557. University of Chicago Press, Chicago.
Perkins, J.M. (1996) Does competition for roosts influence bat distribution in a managed forest? 164–172.
Picot, M., Jenkins, R.K.B., Ramilijaona, O., Racey, P.A., & Carrière, S.M. (2007) The feeding ecology of *Eidolon dupreanum* (Pteropodidae) in eastern Madagascar. *African Journal of Ecology*, **45**, 645–650.
Piksa, K., Nowak, J., Żmihorski, M., & Bogdanowicz, W. (2013) Nonlinear distribution pattern of hibernating bats in caves along an elevational gradient in mountain (Carpathians, southern Poland). *PLoS ONE*, **8**, e68066.

Presley, S.J., Willig, M.R., Castro-Arellano, I., & Weaver, S.C. (2009) Effects of habitat conversion on temporal activity patterns of phyllostomid bats in lowland Amazonian rain forest. *Journal of Mammalogy*, **90**, 210–221.

Procheş, Ş. (2005) The world's biogeographical regions: cluster analyses based on bat distributions. *Journal of Biogeography*, **32**, 607–614.

Qian, H., Badgley, C., & Fox, D.L. (2009) The latitudinal gradient of beta diversity in relation to climate and topography for mammals in North America. *Global Ecology and Biogeography*, **18**, 111–122.

Quesada, M., Stoner, K.E., Rosas-Guerrero, V., Palacios-Guevara, C., & Lobo, J.A. (2003) Effects of habitat disruption on the activity of nectarivorous bats (Chiroptera: Phyllostomidae) in a dry tropical forest: implications for the reproductive success of the neotropical tree Ceiba grandiflora. *Oecologia*, **135**, 400–406.

Ratrimomanarivo, F.H., Goodman, S.M., Stanley, W.T., Naidoo, T., Taylor, P.J., & Lamb, J. (2009) Geographic and phylogeographic variation in *Chaerephon leucogaster* (Chiroptera: Molossidae) of Madagascar and the western Indian Ocean Islands of Mayotte and Pemba. *Acta Chiropterologica*, **11**, 25–52.

Ratrimomanarivo, F.H., Goodman, S.M., Taylor, P.J., Melson, B., & Lamb, J. (2009) Morphological and genetic variation in *Mormopterus jugularis* (Chiroptera: Molossidae) in different bioclimatic regions of Madagascar with natural history notes. *Mammalia*, **73**, 110–129.

Rebelo, H., Tarroso, P., & Jones, G. (2010) Predicted impact of climate change on European bats in relation to their biogeographic patterns. *Global Change Biology*, **16**, 561–576.

Ree, R.H. & Smith, S.A. (2008) Maximum likelihood inference of geographic range evolution by dispersal, local extinction, and cladogenesis. *Systematic Biology*, **57**, 4–14.

Rex, K., Helm, D.H., Wiesner, K., Kunz, T.H., & Voigt, C.C. (2008) Species richness and structure of three Neotropical bat assemblages. *Biological Journal of the Linnean Society*, **94**, 617–629.

Richter, H.V. & Cumming, G.S. (2005) Food availability and annual migration of the straw-colored fruit bat (*Eidolon helvum*). *Journal of Zoology*, **268**, 35–44.

Robinson, B.W. & Wilson, D.S. (1998) Optimal foraging, specialization, and a solution to Liem's paradox. *The American Naturalist*, **151**, 223-235.

Rodríguez, P. & Arita, H.T. (2004) Beta diversity and latitude in North American mammals: testing the hypothesis of covariation. *Ecography*, **27**, 547–556.

Rojas-Martínez, A., Valiente-Banuet, A., del Coro Arizmendi, M., Alcántara-Eguren, A., & Arita, H.T. (1999) Seasonal distribution of the long-nosed bat (*Leptonycteris curasoae*) in North America: does a generalized migration pattern really exist? *Journal of Biogeography*, **26**, 1065–1077.

Rojas, D., Vale, Á., Ferrero, V., & Navarro, L. (2011) When did plants become important to leaf-nosed bats? Diversification of feeding habits in the family Phyllostomidae. *Molecular Ecology*, **20**, 2217–2228.

Rojas, D., Warsi, O.M., & Dávalos, L.M. (2016) Bats (Chiroptera: Noctilionoidea) challenge a recent origin of extant Neotropical diversity. *Systematic Biology*, **65**, 432–448.

Rossiter, S.J., Benda, P., Dietz, C., Zhang, S., & Jones, G. (2007) Rangewide phylogeography in the greater horseshoe bat inferred from microsatellites: implications for population history, taxonomy and conservation. *Molecular Ecology*, **16**, 4699–4714.

Ruedi, M., Eger, J.L., Lim, B.K., & Csorba, G. (2018) A new genus and species of vespertilionid bat from the Indomalayan Region. *Journal of Mammalogy*, **99**, 209–222.
Ruedi, M. & Mayer, F. (2001) Molecular systematics of bats of the genus *Myotis* (Vespertilionidae) suggests deterministic ecomorphological convergences. *Molecular Phylogenetics and Evolution*, **21**, 436–448.
Ruedi, M., Stadelmann, B., Gager, Y., Douzery, E.J.P., Francis, C.M., Lin, L.-K., Guillén-Servent, A., & Cibois, A. (2013) Molecular phylogenetic reconstructions identify East Asia as the cradle for the evolution of the cosmopolitan genus *Myotis* (Mammalia, Chiroptera). *Molecular Phylogenetics and Evolution*, **69**, 437–449.
Russo, D. & Jones, G. (2003) Use of foraging habitats by bats in a Mediterranean area determined by acoustic surveys: conservation implications. *Ecography*, **26**, 197–209.
Sachanowicz, K., Wower, A., & Bashta, A.-T. (2006) Further range extension of *Pipistrellus kuhlii* (Kuhl, 1817) in central and eastern Europe. *Acta Chiropterologica*, **8**, 543–548.
Sampaio, E.M., Kalko, E.K. V., Bernard, E., Rodríguez-Herrera, B., & Handley, C.O. (2003) A biodiversity assessment of bats (Chiroptera) in a tropical lowland rainforest of central Amazonia, including methodological and conservation considerations. *Studies on Neotropical Fauna and Environment*, **38**, 17–31.
Santana, S.E., Grosse, I.R., & Dumont, E.R. (2012) Dietary hardness, loading behavior, and the evolution of skull form in bats. *Evolution*, **66**, 2587–2598.
Schoeman, M.C., Cotterill, F.P.D., Taylor, P.J., & Monadjem, A. (2013) Using potential distributions to explore environmental correlates of bat species richness in southern Africa: effects of model selection and taxonomy. *Current Zoology*, **59**, 279–293.
Schulze, M.D., Seavy, N.E., & Whitacre, D.F. (2000) A comparison of the phyllostomid bat assemblages in undisturbed Neotropical forest and in forest fragments of a slash-and-burn farming mosaic in Petén, Guatemala. *Biotropica*, **32**, 174–184.
Sewall, B.J., Granek, E.F., & Trewhella, W.J. (2003) The endemic Comoros Islands fruit bat *Rousettus obliviosus*: ecology, conservation, and Red List status. *Oryx*, **37**, 344–352.
Sexton, J.P., McIntyre, P.J., Angert, A.L., & Rice, K.J. (2009) Evolution and ecology of species range limits. *Annual Review of Ecology, Evolution, and Systematics*, **40**, 415–436.
Sherwin, H.A., Montgomery, W.I., & Lundy, M.G. (2013) The impact and implications of climate change for bats. *Mammal Review*, **43**, 171–182.
Shi, J.J., Chan, L.M., Peel, A.J., Lai, R., Yoder, A.D., & Goodman, S.M. (2014) A deep divergence time between sister species of *Eidolon* (Family Pteropodidae), with evidence for widespread panmixia. *Acta Chiropterologica*, **16**, 279–292.
Shi, J.J. & Rabosky, D.L. (2015) Speciation dynamics during the global radiation of extant bats. *Evolution*, **69**, 1528–1545.
Shi, J.J., Westeen, E.P., Katlein, N.T., Dumont, E.R., & Rabosky, D.L. (2018) Ecomorphological and phylogenetic controls on sympatry across extant bats. *Journal of Biogeography*.
Siemers, B.M. & Ivanova, T. (2004) Ground gleaning in horseshoe bats: comparative evidence from *Rhinolophus blasii*, *R. euryale* and *R. mehelyi*. *Behavioral Ecology and Sociobiology*, **56**, 464–471.
Simmons, N.B. & Conway, T.M. (2003) Evolution of ecological diversity in bats. *Bat ecology* (ed. by T.H. Kunz and M.B. Fenton), pp. 493–535. University of Chicago Press, Chicago.
Simmons, N.B. (2005) Order Chiroptera. *Mammal species of the world: a taxonomic and geographic reference* (ed. by D.E. Wilson and D.M. Reeder), pp. 312–529. Johns Hopkins University Press, Baltimore.

Simpson, G.G. (1977) Too many lines; the limits of the Oriental and Australian zoogeographic regions. *Proceedings of the American Philosophical Society*, **121**, 107–120.
Stevens, R.D. (2011) Relative effects of time for speciation and tropical niche conservatism on the latitudinal diversity gradient of phyllostomid bats. *Proceedings of the Royal Society B: Biological Sciences*, **278**, 2528–2536.
Stevens, R.D. & Willig, M.R. (2002) Geographical ecology at the community level: perspectives on the diversity of New World bats. *Ecology*, **83**, 545–560.
Struebig, M.J., Christy, L., Pio, D., & Meijaard, E. (2010) Bats of Borneo: diversity, distributions and representation in protected areas. *Biodiversity and Conservation*, **19**, 449–469.
Thomas, D.W. & Fenton, M.B. (2009) Notes on the dry season roosting and foraging behaviour of *Epomophorus gambianus* and *Rousettus aegyptiacus* (Chiroptera: Pteropodidae). *Journal of Zoology*, **186**, 403–406.
Ulrich, W., Sachanowicz, K., & Michalak, M. (2007) Environmental correlates of species richness of European bats (Mammalia: Chiroptera). *Acta Chiropterologica*, **9**, 347–360.
Voigt, C.C. & Kelm, D.H. (2006) Host preference of the common vampire bat (*Desmodus rotundus*; Chiroptera) assessed by stable isotopes. *Journal of Mammalogy*, **87**, 1–6.
Whitaker Jr., J.O. (1995) Food of the big brown bat *Eptesicus fuscus* from maternity colonies in Indiana and Illinois. *American Midland Naturalist*, **134**, 346-360.
Whitaker Jr., J.O., Neefus, C., & Kunz, T.H. (1996) Dietary variation in the Mexican free-tailed bat (*Tadarida brasiliensis mexicana*). *Journal of Mammalogy*, **77**, 716-724.
Williams-Guillén, K., Perfecto, I., & Vandermeer, J. (2008) Bats limit insects in a neotropical agroforestry system. *Science*, **320**, 70.
Williams, A. & Dickman, C. (2004) The ecology of insectivorous bats in the Simpson Desert central Australia: habitat use. *Australian Mammalogy*, **26**, 205–214.
Willig, M.R., Kaufman, D.M., & Stevens, R.D. (2003) Latitudinal gradients of biodiversity: pattern, process, scale, and synthesis. *Annual Review of Ecology, Evolution, and Systematics*, **34**, 273–309.
Wilson, D.E. (1973) Bat faunas: a trophic comparison. *Systematic Zoology*, **22**, 14–29.
Wilson, J.W. (1974) Analytical zoogeography of North American mammals. *Evolution*, **28**, 124–140.
Young, R.A. & Ford, G.I. (2000) Bat fauna of a semi-arid environment in central western Queensland, Australia. *Wildlife Research*, **27**, 203–215.
Zubaid, A. (1993) A comparison of the bat fauna between a primary and fragmented secondary forest in Peninsular Malaysia. *Mammalia*, **57**, 201–206.

Table 1.1 Metadata on bat diversity for major biogeographic realms

All biogeographic realms referred to in this review, its estimated range size, the number of species that are present in each realm, and the extant bat families they represent. For each bat family, the percentage of that realm's species-level diversity is calculated. Families are thus presented in rank-order of abundance.

realm	realm size (km^2)	species	extant families (% of species-level realm diversity)								
Palearctic	52849857	70	Vespertilionidae (79%)	Rhinolophidae (13%)	Hipposideridae (4%)	Molossidae (3%)	Rhino-pomatidae (1%)				
Afrotropics (mainland)	21060290	78	Vespertilionidae (29%)	Pteropodidae (19%)	Molossidae (14%)	Rhino-lophidae (14%)	Hippo-sideridae (12%)	Nycteridae (6%)	Emballo-nuridae (4%)	Mega-dermatidae (1%)	NA
Afrotropics (Indian Ocean islands)	596949	31	Pteropodidae (26%)	Molossidae (26%)	Vespertilionidae (16%)	Emballo-nuridae (13%)	Hippo-sideridae (13%)	Myzo-podidae (6%)			
Indomalaya	8499096	175	Vespertilionidae (36%)	Pteropodidae (21%)	Hipposideridae (17%)	Rhino-lophidae (17%)	Molossidae (4%)	Emballo-nuridae (3%)	Craseo-nycteridae (1%)	Mega-dermatidae (1%)	Nycteridae (1%)
Oceania & Australasia	9274414	82	Pteropodidae (54%)	Vespertilionidae (13%)	Hipposideridae (11%)	Emballo-nuridae (10%)	Molossidae (5%)	Rhino-lophidae (5%)	Mega-dermatidae (1%)	Mysta-cinidae (1%)	
Nearctic	20491302	40	Vespertilionidae (80%)	Phyllostomidae (10%)	Molossidae (8%)	Mormo-opidae (2%)					
Neotropics	19308843	235	Phyllostomidae (59%)	Vespertilionidae (15%)	Molossidae (10%)	Emballo-nuridae (9%)	Natalidae (3%)	Mormo-opidae (2%)	Noctilionidae (1%)	Thyro-pteridae (1%)	Furipteridae (0.4%)

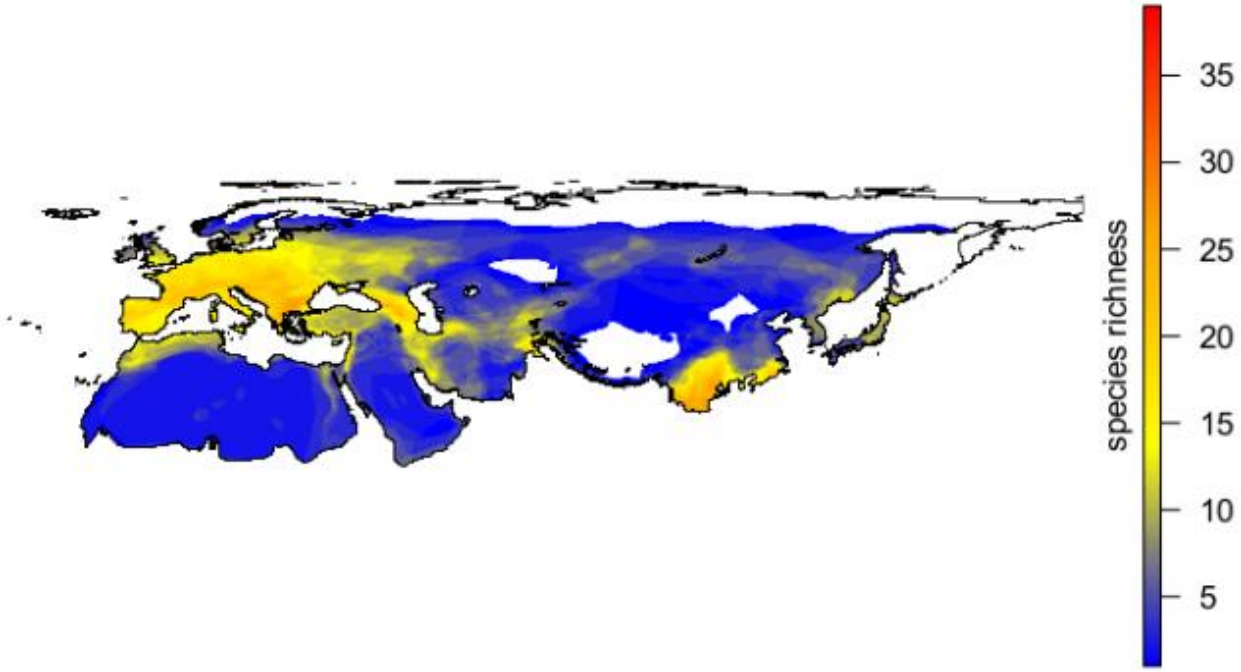

Figure 1.1 Palearctic bat richness
Bat species richness across the Palearctic. Richness is relatively low through most of the realm. It is highest in the relatively temperate forests of continental Europe and eastern Asia, and in the Caucasus region. Scale of this plot is restricted to the range of regional diversity in this realm, to highlight within-realm patterns.

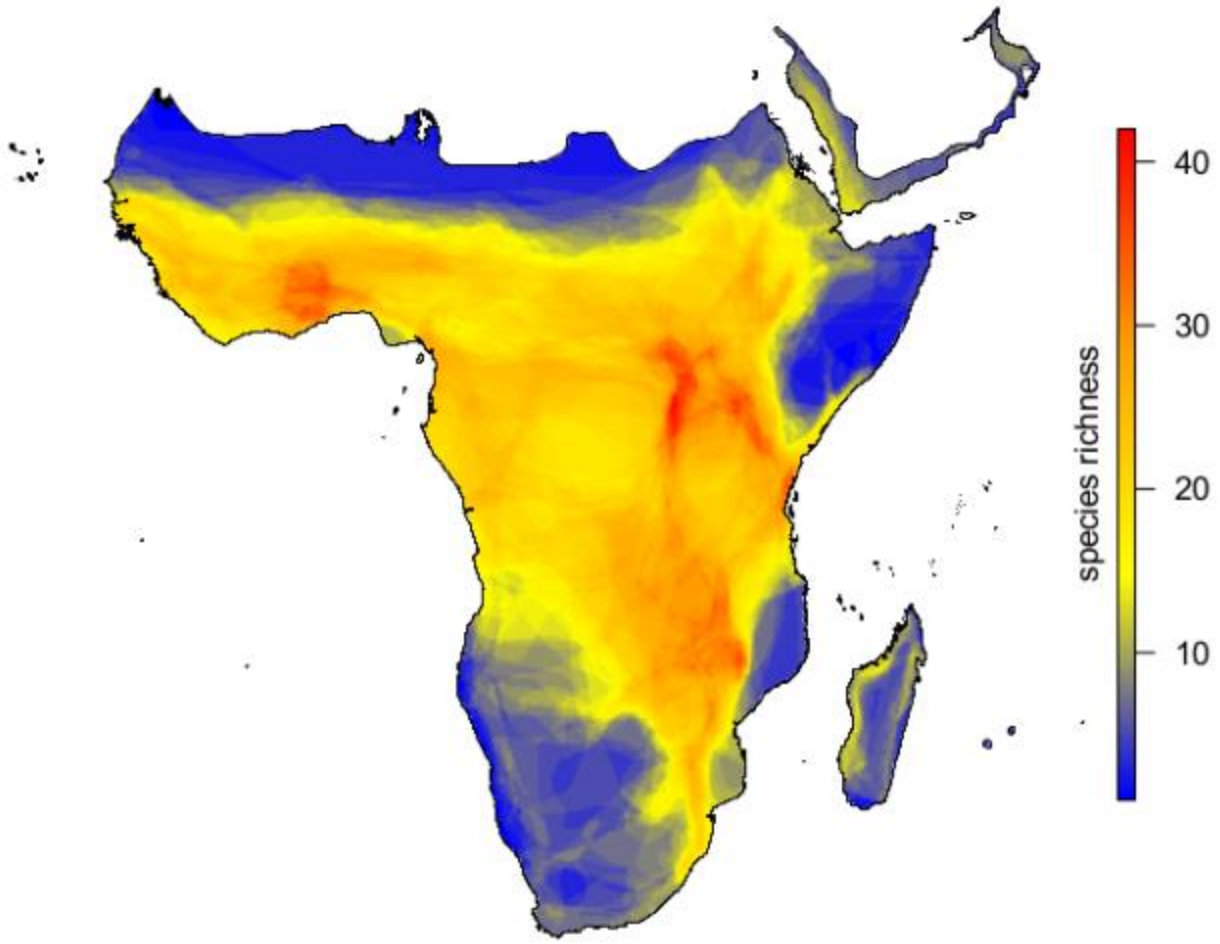

Figure 1.2 Afrotropical bat richness
Bat species richness across the Afrotropics. Richness is highest across the tropical rainforests and savannahs of sub-Saharan Africa, and peaks close to the equator. Scale of this plot is restricted to the range of regional diversity in this realm, to highlight within-realm patterns.

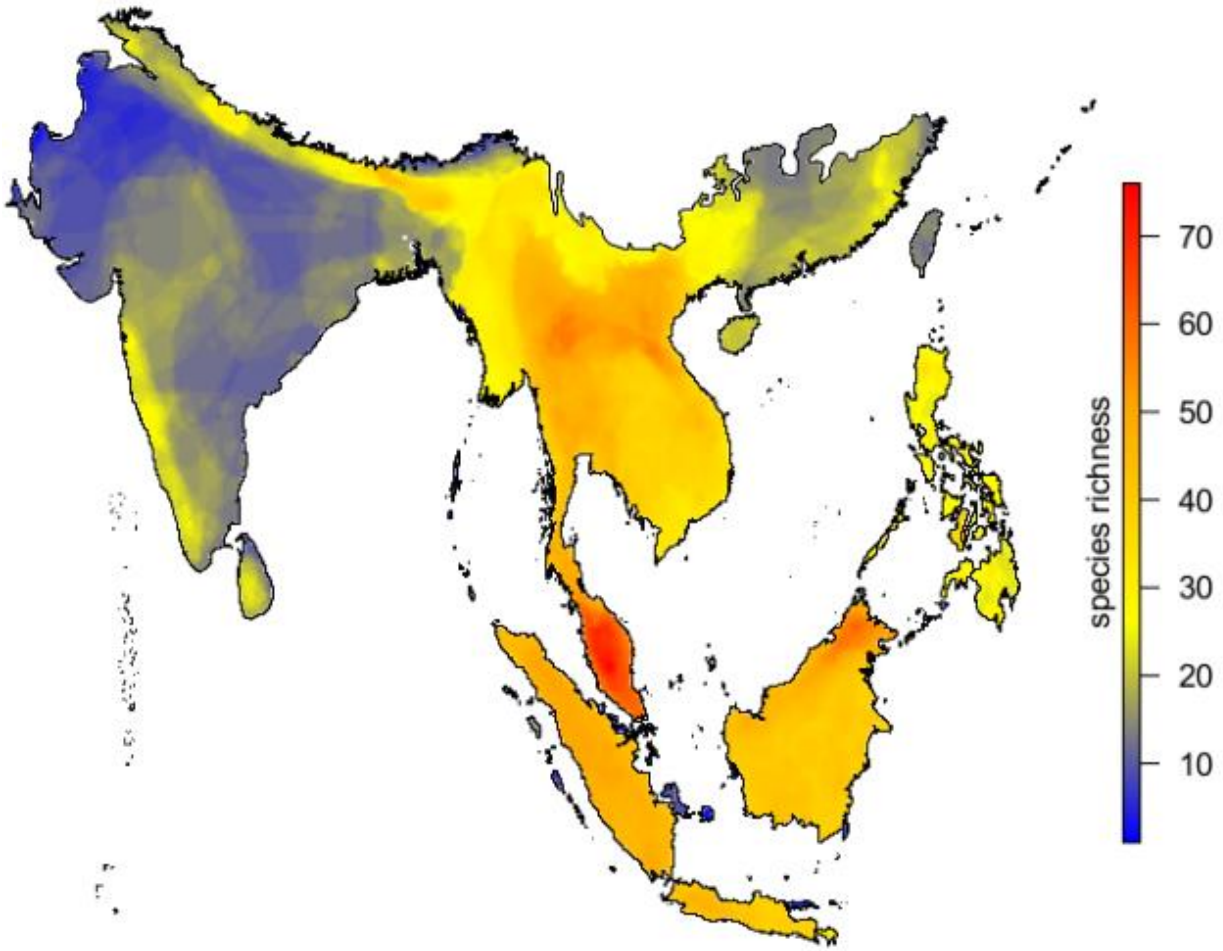

Figure 1.3 Indomalayan bat richness
Bat species richness across Indomalaya. While richness is relatively low on the Indian subcontinent, it is high across much of southeast Asia, and increases along the Malay Peninsula and across the Indonesian islands. Scale of this plot is restricted to the range of regional diversity in this realm, to highlight within-realm patterns.

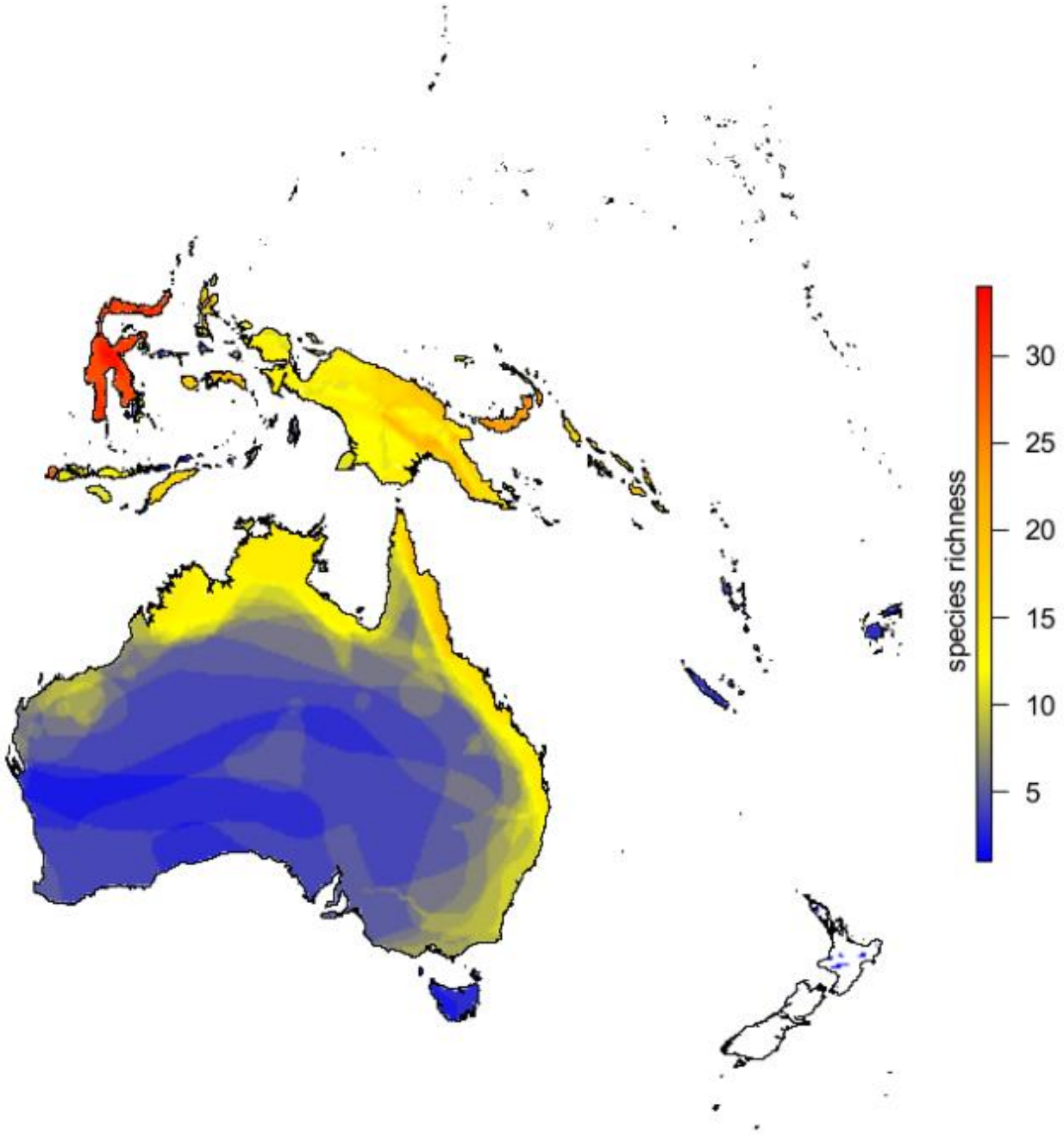

Figure 1.4 Oceanian & Australasian bat richness
Bat species richness across Oceania and Australasia combined. Regional richness is highest just east of Wallace's Line, on the islands of Sulawesi and New Guinea. On Australia, richness is highest along a narrow strip of forest and savannah along the northern and eastern coastal mountains. Note that bats are present even on very isolated islands across Australasia. Scale of this plot is restricted to the range of regional diversity in this realm, to highlight within-realm patterns. Also note that while New Zealand has two endemic species of bats (Family Mystacinidae), their ranges are poorly known.

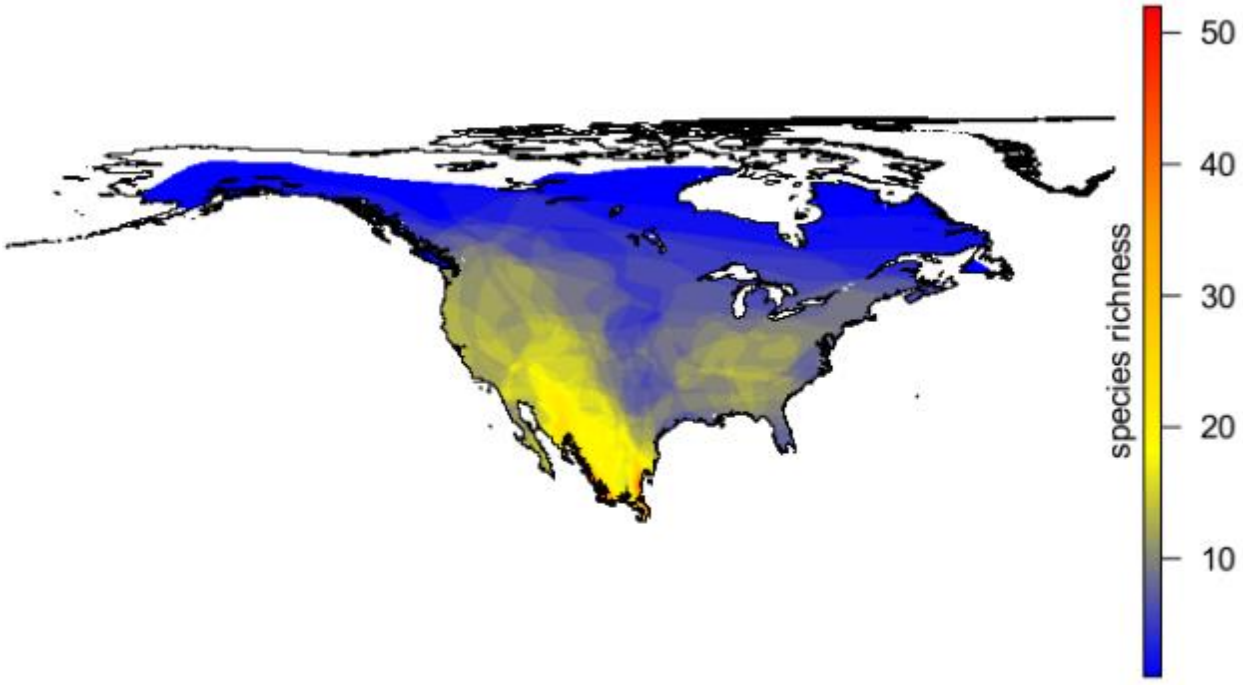

Figure 1.5 Nearctic bat richness
Bat species richness across the Nearctic. Richness is extremely low through most of temperate North America, but is higher along the Rocky and Appalachian mountain ranges. It is also notably high in the Mojave and Sonoran deserts, extending into central Mexico, where it reaches a peak at the border with the Neotropics. Scale of this plot is restricted to the range of regional diversity in this realm, to highlight within-realm patterns.

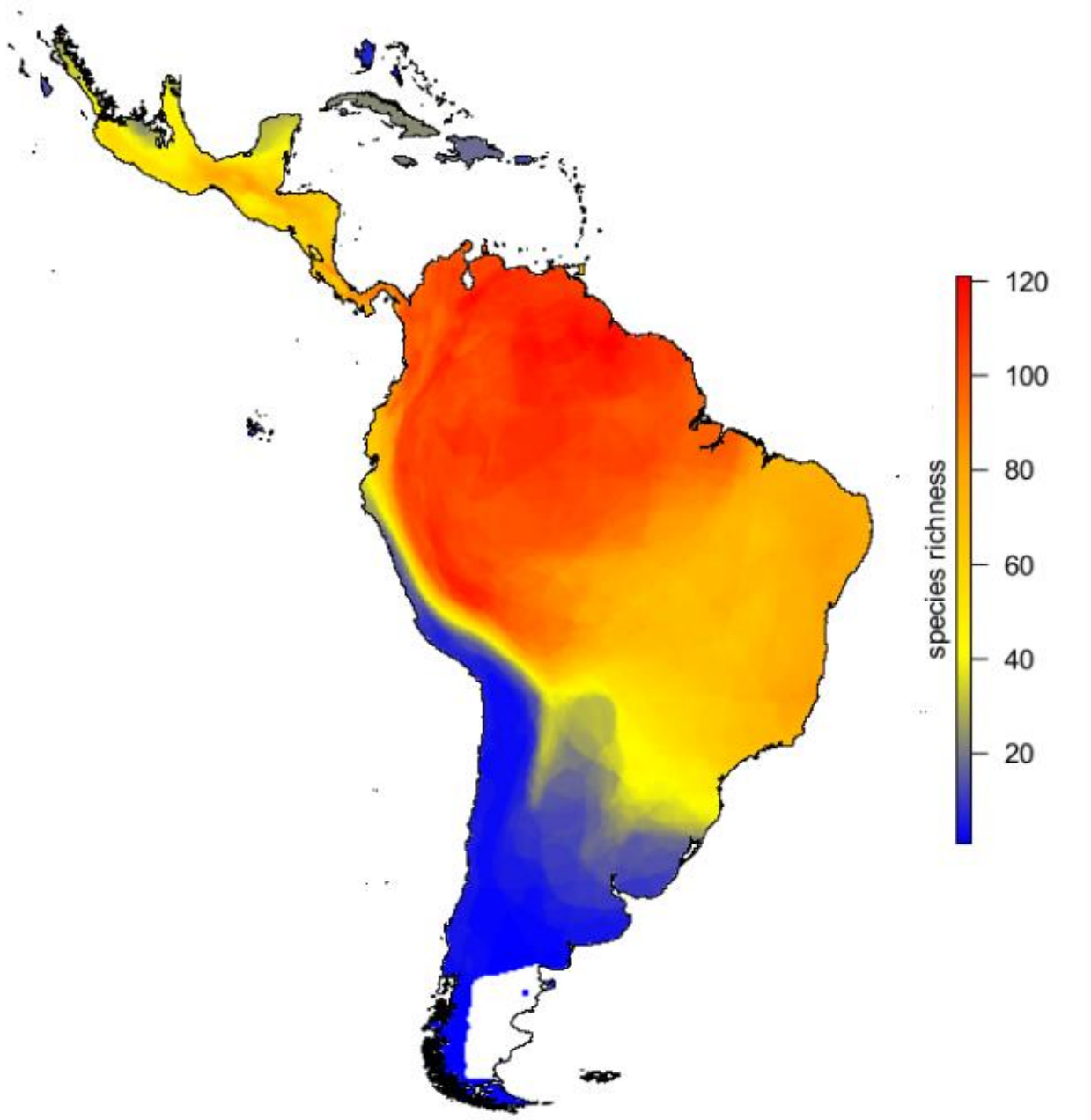

Figure 1.6 Neotropical bat richness
Bat species richness across the Neotropics. While richness is extremely high throughout all of Central America and the tropical rainforests of South America, it is the highest in the Amazon Basin and along the Andes. Scale of this plot is restricted to the range of regional diversity in this realm, to highlight within-realm patterns.

Table S1.1 Palearctic bat families and species with IUCN range data

species	area (sq km)
Family Hipposideridae	
Asellia tridens	16920012
Aselliscus stoliczkanus	1362301
Hipposideros pratti	2242890
Family Molossidae	
Tadarida insignis	308643
Tadarida teniotis	3743688
Family Rhinolophidae	
Rhinolophus affinis	5506447
Rhinolophus blasii	3410352
Rhinolophus hipposideros	6256436
Rhinolophus macrotis	2338732
Rhinolophus mehelyi	1978078
Rhinolophus pearsonii	3176369
Rhinolophus rex	52963
Rhinolophus sinicus	2168789
Rhinolophus thomasi	1407413
Family Rhinopomatidae	
Rhinopoma muscatellum	446979
Family Vespertilionidae	
Barbastella barbastellus	3802955
Barbastella leucomelas	3926553
Eptesicus bobrinskoi	643807
Eptesicus bottae	3885001
Eptesicus gobiensis	3884753
Eptesicus nasutus	1865268
Eptesicus serotinus	12116736
Ia io	1506456
Murina aurata	313348
Murina hilgendorfi	3618860
Murina huttoni	415999
Murina leucogaster	616121
Murina ussuriensis	311431
Myotis altarium	1575031
Myotis aurascens	2616237
Myotis blythii	6194563
Myotis bombinus	1653296
Myotis capaccinii	1228797
Myotis chinensis	2263086
Myotis dasycneme	5423865
Myotis daubentonii	14655028
Myotis emarginatus	4473541
Myotis fimbriatus	271079
Myotis formosus	2064180
Myotis frater	1329121
Myotis hajastanicus	826
Myotis laniger	2138475
Myotis longipes	61479
Myotis macrodactylus	682508
Myotis myotis	3874482
Myotis mystacinus	4972250
Myotis nipalensis	4948354
Myotis pequinius	564695
Myotis pruinosus	2084
Myotis punicus	648329
Myotis schaubi	119115
Nyctalus aviator	695946
Nyctalus azoreum	2237
Nyctalus lasiopterus	2905796
Nyctalus noctula	8033639
Otonycteris hemprichii	1283184
Pipistrellus hanaki	40223
Pipistrellus maderensis	4798
Pipistrellus nathusii	5885996
Pipistrellus pipistrellus	11496855
Pipistrellus pygmaeus	1954270
Plecotus auritus	6532388
Plecotus austriacus	3049172
Plecotus christii	130184
Plecotus ognevi	5952795
Plecotus sardus	23981
Plecotus teneriffae	3405
Scotomanes ornatus	2690024
Vespertilio murinus	15709417
Vespertilio sinensis	1565758

Table S1.2a Afrotropical (mainland) bat families and species with IUCN range data

species	area (sq km)
Family Emballonuridae	
Coleura afra	2795076
Taphozous hildegardeae	44749
Taphozous nudiventris	1207395
Family Hipposideridae	
Asellia tridens	16920012
Cloeotis percivali	528519
Hipposideros abae	2324174
Hipposideros beatus	1635925
Hipposideros cyclops	2331295
Hipposideros fuliginosus	1334533
Hipposideros gigas	3575481
Hipposideros ruber	9059982
Triaenops persicus	1163359
Family Megadermatidae	
Cardioderma cor	2247887
Family Molossidae	
Chaerephon ansorgei	5630017
Chaerephon chapini	4295184
Chaerephon nigeriae	4801532
Chaerephon pumilus	7239484
Mops condylurus	9120936
Mops midas	415308
Myopterus daubentonii	1597089
Otomops martiensseni	7309458
Sauromys petrophilus	728166
Tadarida aegyptiaca	4176029
Tadarida fulminans	295437
Family Nycteridae	
Nycteris arge	3979107
Nycteris grandis	4403938
Nycteris hispida	11505156
Nycteris macrotis	12089038
Nycteris thebaica	14396321
Family Pteropodidae	
Casinycteris argynnis	1707516
Epomophorus gambianus	3790881
Epomophorus labiatus	2158825
Epomophorus wahlbergi	5001006
Epomops franqueti	4538760
Hypsignathus monstrosus	2860316
Megaloglossus woermanni	3430047
Micropteropus pusillus	5380417
Myonycteris brachycephala	691
Myonycteris relicta	141883
Myonycteris torquata	4522691
Nanonycteris veldkampii	1711287
Pteropus voeltzkowi	909
Rousettus aegyptiacus	3888247
Scotonycteris zenkeri	2023486
Family Rhinolophidae	
Rhinolophus alcyone	2858819
Rhinolophus capensis	242700
Rhinolophus darlingi	1359988
Rhinolophus denti	1703171
Rhinolophus eloquens	711894
Rhinolophus fumigatus	8361571
Rhinolophus landeri	12117530
Rhinolophus maclaudi	8188
Rhinolophus ruwenzorii	24862
Rhinolophus simulator	1911035
Rhinolophus swinnyi	1347743
Family Vespertilionidae	
Eptesicus hottentotus	2853298
Eptesicus nasutus	1865268
Glauconycteris argentata	3995878
Glauconycteris egeria	386592
Glauconycteris variegata	8693358
Laephotis botswanae	330931
Laephotis namibensis	27769
Laephotis wintoni	1918120
Myotis anjouanensis	426
Myotis bocagii	1819116
Myotis scotti	94416
Myotis tricolor	4237828
Myotis welwitschii	4310948
Neoromicia capensis	13742711
Neoromicia rendalli	8370257
Neoromicia tenuipinnis	4246822
Plecotus balensis	1229
Scotoecus hirundo	4915713
Scotophilus dinganii	10952062
Scotophilus leucogaster	5428078
Scotophilus nigrita	2194568
Scotophilus nux	951022
Scotophilus viridis	4659936

Table S1.2b Afrotropical (Indian Ocean islands) bat families and species with IUCN range data

species	area (sq km)
Family Emballonuridae	
Coleura afra	2795076
Coleura seychellensis	228
Emballonura atrata	105701
Emballonura tiavato	149404
Family Hipposideridae	
Hipposideros commersoni	513053
Triaenops auritus	5254
Triaenops furculus	57132
Triaenops rufus	284129
Family Molossidae	
Chaerephon jobimena	186280
Chaerephon pumilus	7239484
Mops leucostigma	211464
Mops midas	415308
Mormopterus acetabulosus	4998
Mormopterus jugularis	235451
Otomops madagascariensis	3539
Tadarida fulminans	295437
Family Myzopodidae	
Myzopoda aurita	107298
Myzopoda schliemanni	36334
Family Pteropodidae	
Pteropus aldabrensis	158
Pteropus livingstonii	636
Pteropus niger	4414
Pteropus rodricensis	111
Pteropus rufus	185399
Pteropus seychellensis	2731
Rousettus madagascariensis	292755
Rousettus obliviosus	1667
Family Vespertilionidae	
Myotis goudoti	504523
Scotophilus borbonicus	2541
Scotophilus marovaza	75582
Scotophilus robustus	398670
Scotophilus tandrefana	46267

Table S1.3 Indomalayan bat families and species with IUCN range data

species	area (sq km)
Family Craseonycteridae	
Craseonycteris thonglongyai	7954
Family Emballonuridae	
Emballonura alecto	1212059
Emballonura monticola	1690478
Taphozous longimanus	4790747
Taphozous melanopogon	5623327
Taphozous nudiventris	1207395
Family Hipposideridae	
Aselliscus stoliczkanus	1362301
Coelops frithii	2490979
Coelops robinsoni	137744
Hipposideros ater	3677391
Hipposideros bicolor	1584431
Hipposideros cervinus	1964903
Hipposideros cineraceus	2203657
Hipposideros coronatus	236
Hipposideros coxi	2202
Hipposideros diadema	3318702
Hipposideros doriae	1251661
Hipposideros dyacorum	764979
Hipposideros fulvus	2263617
Hipposideros galeritus	2343755
Hipposideros grandis	185992
Hipposideros halophyllus	9355
Hipposideros khaokhouayensis	17746
Hipposideros larvatus	3287819
Hipposideros lekaguli	95993
Hipposideros lylei	1013381
Hipposideros obscurus	150982
Hipposideros pomona	2840866
Hipposideros pratti	2242890
Hipposideros pygmaeus	47480
Hipposideros ridleyi	219043
Hipposideros rotalis	29359
Hipposideros scutinares	23765
Hipposideros speoris	1224570
Hipposideros turpis	48777
Family Megadermatidae	
Megaderma lyra	6041336
Megaderma spasma	4058730
Family Molossidae	
Chaerephon plicatus	2462175
Cheiromeles parvidens	443817
Cheiromeles torquatus	1329658
Mops mops	611981
Otomops wroughtoni	13431
Tadarida aegyptiaca	4176029
Tadarida insignis	308643
Family Nycteridae	
Nycteris javanica	135481
Nycteris tragata	1394635
Family Pteropodidae	
Acerodon jubatus	155342
Aethalops alecto	682352
Alionycteris paucidentata	6418
Balionycteris maculata	570366
Chironax melanocephalus	177749
Cynopterus brachyotis	2699375
Cynopterus horsfieldii	1485601
Cynopterus sphinx	6455957
Cynopterus titthaecheilus	598087
Dyacopterus spadiceus	445040
Eonycteris major	732628
Eonycteris robusta	114506
Eonycteris spelaea	3525480
Haplonycteris fischeri	264779
Harpyionycteris whiteheadi	171865
Latidens salimalii	15078
Macroglossus minimus	3590169
Macroglossus sobrinus	2435587
Megaerops ecaudatus	1274129
Megaerops kusnotoi	14104
Megaerops niphanae	1321397
Megaerops wetmorei	165912
Otopteropus cartilagonodus	105071
Penthetor lucasi	1288201
Ptenochirus jagori	271017
Ptenochirus minor	118794
Pteropus giganteus	4002209
Pteropus hypomelanus	524208
Pteropus lylei	106823
Pteropus pumilus	57994
Pteropus speciosus	3657
Pteropus vampyrus	1940598
Rousettus amplexicaudatus	4281494
Rousettus leschenaultii	6764169
Rousettus spinalatus	71651
Sphaerias blanfordi	471485
Styloctenium mindorensis	11
Family Rhinolophidae	
Rhinolophus acuminatus	1077158
Rhinolophus affinis	5506447

Rhinolophus arcuatus	352721
Rhinolophus beddomei	185973
Rhinolophus borneensis	743699
Rhinolophus celebensis	308234
Rhinolophus coelophyllus	426069
Rhinolophus creaghi	161695
Rhinolophus formosae	30584
Rhinolophus inops	137806
Rhinolophus lepidus	3508936
Rhinolophus macrotis	2338732
Rhinolophus malayanus	1538882
Rhinolophus marshalli	652658
Rhinolophus paradoxolophus	421900
Rhinolophus pearsonii	3176369
Rhinolophus philippinensis	247489
Rhinolophus robinsoni	47299
Rhinolophus rouxii	863568
Rhinolophus rufus	34730
Rhinolophus sedulus	805437
Rhinolophus shameli	766363
Rhinolophus siamensis	310607
Rhinolophus sinicus	2168789
Rhinolophus stheno	2203369
Rhinolophus subrufus	45305
Rhinolophus thomasi	1407413
Rhinolophus trifoliatus	1344635
Rhinolophus virgo	281699
Family Vespertilionidae	
Arielulus aureocollaris	2503
Arielulus circumdatus	170206
Eptesicus dimissus	4071
Eudiscopus denticulus	1659
Falsistrellus petersi	28176
Glischropus tylopus	2451362
Harpiocephalus harpia	904078
Harpiocephalus mordax	194502
Harpiola isodon	11833
Hesperoptenus blanfordi	460424
Hesperoptenus tickelli	1051806
Ia io	1506456
Kerivoula hardwickii	4047218
Kerivoula intermedia	867950
Kerivoula kachinensis	570580
Kerivoula lenis	129194
Kerivoula minuta	143466
Kerivoula papillosa	789930
Kerivoula pellucida	1213324
Kerivoula picta	2925015
Kerivoula titania	562124
Kerivoula whiteheadi	214657
Murina aenea	92937
Murina aurata	313348
Murina cyclotis	2021097
Murina huttoni	415999
Murina leucogaster	616121
Murina puta	35903
Murina rozendaali	16208
Murina suilla	1441579
Murina tubinaris	964782
Myotis adversus	242651
Myotis altarium	1575031
Myotis annamiticus	110
Myotis annectans	244313
Myotis ater	125969
Myotis chinensis	2263086
Myotis formosus	2064180
Myotis frater	1329121
Myotis gomantongensis	732494
Myotis hasseltii	947129
Myotis horsfieldii	2561877
Myotis laniger	2138475
Myotis longipes	61479
Myotis macrotarsus	281869
Myotis montivagus	766979
Myotis muricola	4642851
Myotis ridleyi	864276
Myotis rosseti	467833
Myotis sicarius	69837
Myotis siligorensis	1309734
Myotis yanbarensis	32
Philetor brachypterus	1317156
Phoniscus jagorii	347539
Pipistrellus coromandra	3656018
Pipistrellus javanicus	3707748
Pipistrellus paterculus	782241
Pipistrellus stenopterus	640600
Pipistrellus tenuis	7848096
Scotomanes ornatus	2690024
Scotophilus heathii	5739538
Tylonycteris pachypus	4169956
Tylonycteris robustula	2706501

Table S1.4 Oceanian and Australasian bat families and species with IUCN range data

species	area (sq km)
Family Emballonuridae	
Emballonura beccarii	91116
Emballonura dianae	90454
Emballonura raffrayana	216475
Emballonura semicaudata	16542
Emballonura serii	9326
Mosia nigrescens	1090668
Saccolaimus flaviventris	6051826
Taphozous australis	38335
Family Hipposideridae	
Aselliscus tricuspidatus	274647
Hipposideros ater	3677391
Hipposideros boeadii	381
Hipposideros calcaratus	217478
Hipposideros cervinus	1964903
Hipposideros diadema	3318702
Hipposideros dinops	24099
Hipposideros pelingensis	177328
Rhinonicteris aurantia	747434
Family Megadermatidae	
Macroderma gigas	1078804
Family Molossidae	
Chaerephon jobensis	2337028
Cheiromeles parvidens	443817
Mormopterus beccarii	3946921
Mormopterus planiceps	3439145
Family Mystacinidae	
Mystacina tuberculata	12604
Family Pteropodidae	
Acerodon celebensis	177574
Dobsonia inermis	34750
Dobsonia minor	614805
Dobsonia moluccensis	878250
Dobsonia pannietensis	5415
Dobsonia praedatrix	44746
Dobsonia viridis	27753
Harpyionycteris celebensis	169411
Macroglossus minimus	3590169
Megaerops kusnotoi	14104
Melonycteris fardoulisi	16830
Melonycteris melanops	45240
Melonycteris woodfordi	16783
Nyctimene aello	621338
Nyctimene albiventer	748030
Nyctimene cephalotes	239455
Nyctimene certans	212404
Nyctimene major	70315
Nyctimene robinsoni	351651
Nyctimene vizcaccia	70177
Paranyctimene raptor	781866
Pteralopex atrata	5154
Pteropus admiralitatum	75835
Pteropus alecto	1353681
Pteropus anetianus	11334
Pteropus capistratus	44171
Pteropus conspicillatus	219521
Pteropus hypomelanus	524208
Pteropus mariannus	1026
Pteropus molossinus	346
Pteropus neohibernicus	672547
Pteropus ornatus	18361
Pteropus poliocephalus	249369
Pteropus rayneri	29500
Pteropus samoensis	20148
Pteropus scapulatus	3037832
Pteropus speciosus	3657
Pteropus temminckii	26749
Pteropus tonganus	57841
Pteropus vetulus	16533
Pteropus woodfordi	13703
Rousettus amplexicaudatus	4281494
Syconycteris australis	1053909
Thoopterus nigrescens	182867
Family Rhinolophidae	
Rhinolophus celebensis	308234
Rhinolophus euryotis	771261
Rhinolophus megaphyllus	876288
Rhinolophus philippinensis	247489
Family Vespertilionidae	
Chalinolobus gouldii	7369440
Chalinolobus morio	2316997
Chalinolobus nigrogriseus	1476703
Falsistrellus petersi	28176
Murina florium	158996
Myotis ater	125969
Myotis macropus	1326574
Nyctophilus arnhemensis	703912
Nyctophilus geoffroyi	7272629
Nyctophilus gouldi	959019
Philetor brachypterus	1317156

Table S1.5 Nearctic bat families and species with IUCN range data

species	area (sq km)
Family Molossidae	
Eumops underwoodi	955533
Nyctinomops femorosaccus	1251449
Tadarida brasiliensis	13833670
Family Mormoopidae	
Mormoops megalophylla	3738452
Family Phyllostomidae	
Artibeus hirsutus	396913
Choeronycteris mexicana	1777464
Leptonycteris yerbabuenae	1233477
Macrotus californicus	642862
Family Vespertilionidae	
Antrozous pallidus	4366863
Corynorhinus mexicanus	514929
Corynorhinus townsendii	4596733
Eptesicus fuscus	13168295
Euderma maculatum	2104576
Idionycteris phyllotis	1390580
Lasionycteris noctivagans	10110373
Lasiurus blossevillii	19044624
Lasiurus borealis	4882261
Lasiurus cinereus	21079570
Lasiurus intermedius	1748582
Lasiurus seminolus	1193281
Myotis auriculus	791609
Myotis austroriparius	832811
Myotis californicus	3984267
Myotis ciliolabrum	1387940
Myotis evotis	3163275
Myotis fortidens	474062
Myotis grisescens	852990
Myotis keenii	109268
Myotis leibii	1422938
Myotis lucifugus	12040436
Myotis planiceps	12291
Myotis septentrionalis	4946759
Myotis sodalis	1565208
Myotis thysanodes	3472025
Myotis velifer	1954188
Myotis volans	4711730
Myotis yumanensis	4063101
Nycticeius humeralis	2883010
Pipistrellus subflavus	4263808
Rhogeessa parvula	448874

Table S1.6 Neotropical bat families and species with IUCN range data

species	area (sq km)
Family Emballonuridae	
Balantiopteryx infusca	2842
Balantiopteryx io	170582
Balantiopteryx plicata	833094
Centronycteris centralis	2377736
Centronycteris maximiliani	5647042
Cormura brevirostris	7825195
Cyttarops alecto	1353175
Diclidurus albus	12496308
Diclidurus ingens	2088132
Diclidurus isabellus	1061772
Diclidurus scutatus	2894838
Peropteryx kappleri	11922961
Peropteryx leucoptera	5088912
Peropteryx macrotis	12696825
Peropteryx trinitatis	6619
Rhynchonycteris naso	11506838
Saccopteryx bilineata	12631739
Saccopteryx canescens	6383176
Saccopteryx gymnura	782108
Saccopteryx leptura	12288468
Family Furipteridae	
Furipterus horrens	9445800
Family Molossidae	
Cynomops abrasus	10670598
Cynomops paranus	12228466
Cynomops planirostris	11449114
Eumops auripendulus	14106380
Eumops bonariensis	14760710
Eumops dabbenei	2407793
Eumops glaucinus	11387259
Eumops hansae	6415795
Eumops maurus	267600
Eumops patagonicus	1535914
Eumops perotis	11694941
Eumops underwoodi	955533
Molossops mattogrossensis	6688675
Molossops neglectus	6514249
Molossops temminckii	11604213
Molossus coibensis	3476575
Molossus molossus	15766204
Molossus rufus	14799495
Nyctinomops aurispinosus	2633034
Nyctinomops laticaudatus	13100597
Nyctinomops macrotis	15742455
Promops centralis	4618248
Tadarida brasiliensis	13833670
Family Mormoopidae	
Mormoops megalophylla	3738452
Pteronotus gymnonotus	3202584
Pteronotus macleayii	119897
Pteronotus parnellii	117654
Pteronotus quadridens	200546
Family Natalidae	
Chilonatalus micropus	191794
Chilonatalus tumidifrons	6412
Natalus jamaicensis	11025
Natalus major	74328
Natalus stramineus	4473
Natalus tumidirostris	1593615
Nyctiellus lepidus	110184
Family Noctilionidae	
Noctilio albiventris	12853879
Noctilio leporinus	14625255
Family Phyllostomidae	
Ametrida centurio	6857128
Anoura caudifer	8856455
Anoura cultrata	757489
Anoura geoffroyi	7791747
Anoura latidens	710043
Ardops nichollsi	4743
Ariteus flavescens	11021
Artibeus amplus	595512
Artibeus anderseni	4071846
Artibeus aztecus	590449
Artibeus concolor	3060880
Artibeus fimbriatus	1000998
Artibeus fraterculus	181401
Artibeus hirsutus	396913
Artibeus inopinatus	43492
Artibeus intermedius	1118187
Artibeus jamaicensis	1428771
Artibeus lituratus	13462565
Artibeus obscurus	9091536
Artibeus planirostris	12216589
Artibeus schwartzi	1428533
Artibeus toltecus	849474

Brachyphylla cavernarum	14908
Brachyphylla nana	269970
Carollia benkeithi	2310703
Carollia brevicauda	10748131
Carollia manu	31953
Carollia perspicillata	13795815
Carollia sowelli	790231
Carollia subrufa	212247
Centurio senex	2085278
Chiroderma doriae	2631154
Chiroderma improvisum	1571
Chiroderma salvini	3419281
Chiroderma trinitatum	9383888
Chiroderma villosum	10416177
Choeroniscus godmani	2679284
Choeroniscus minor	6415546
Choeronycteris mexicana	1777464
Chrotopterus auritus	13126034
Dermanura bogotensis	2306231
Dermanura rosenbergi	113667
Desmodus rotundus	17726359
Diaemus youngi	13058206
Ectophylla alba	124369
Erophylla bombifrons	82892
Erophylla sezekorni	122945
Glossophaga commissarisi	3716043
Glossophaga leachii	480779
Glossophaga longirostris	1570788
Glossophaga morenoi	327052
Glossophaga soricina	14858261
Glyphonycteris daviesi	4659668
Glyphonycteris sylvestris	6013551
Hylonycteris underwoodi	445922
Leptonycteris curasoae	840760
Leptonycteris yerbabuenae	1233477
Lichonycteris obscura	7336874
Lonchophylla chocoana	1934
Lonchophylla handleyi	124132
Lonchophylla mordax	2258607
Lonchophylla robusta	1116230
Lonchophylla thomasi	8383004
Lonchorhina aurita	11574471
Lonchorhina inusitata	2855463
Lonchorhina orinocensis	386538
Lophostoma brasiliense	8222183
Lophostoma evotis	176607
Lophostoma schulzi	564363
Lophostoma silvicolum	12148534
Macrophyllum macrophyllum	13066261
Macrotus waterhousii	1406921
Mesophylla macconnelli	8815935
Micronycteris brosseti	3671823
Micronycteris buriri	350
Micronycteris giovanniae	2889
Micronycteris hirsuta	9073480
Micronycteris matses	2878
Micronycteris megalotis	12093440
Micronycteris microtis	4406787
Micronycteris minuta	12092468
Micronycteris schmidtorum	6511506
Mimon bennettii	4371300
Mimon crenulatum	11135046
Monophyllus plethodon	5400
Monophyllus redmani	202239
Musonycteris harrisoni	54477
Phylloderma stenops	10971022
Phyllonycteris aphylla	215
Phyllonycteris poeyi	257110
Phyllops falcatus	181363
Phyllostomus discolor	12503835
Phyllostomus elongatus	10668335
Phyllostomus hastatus	12629190
Phyllostomus latifolius	1634615
Platalina genovensium	323688
Platyrrhinus albericoi	607979
Platyrrhinus aurarius	349878
Platyrrhinus brachycephalus	6158638
Platyrrhinus dorsalis	770794
Platyrrhinus infuscus	1466940
Platyrrhinus ismaeli	181685
Platyrrhinus lineatus	5807781
Platyrrhinus masu	172399
Platyrrhinus matapalensis	80807
Platyrrhinus recifinus	2015113
Platyrrhinus vittatus	769777
Pygoderma bilabiatum	2957239
Rhinophylla alethina	125703
Rhinophylla fischerae	4564253
Rhinophylla pumilio	8332336
Sphaeronycteris toxophyllum	4539289

Stenoderma rufum	9281
Sturnira aratathomasi	72662
Sturnira bidens	713969
Sturnira bogotensis	525981
Sturnira erythromos	2534602
Sturnira hondurensis	549138
Sturnira lilium	6252144
Sturnira ludovici	2234357
Sturnira luisi	451266
Sturnira magna	1568130
Sturnira mordax	26176
Sturnira nana	134163
Sturnira oporaphilum	1045756
Sturnira parvidens	2273465
Sturnira perla	2282
Sturnira tildae	10660604
Tonatia bidens	3599852
Trachops cirrhosus	12642577
Uroderma bilobatum	12793922
Uroderma magnirostrum	10830757
Vampyressa bidens	6730256
Vampyressa melissa	445311
Vampyressa nymphaea	248097
Vampyressa pusilla	1111685
Vampyressa thyone	4543655
Vampyrodes caraccioli	7345906
Vampyrum spectrum	6127240
Family Thyropteridae	
Thyroptera discifera	6236351
Thyroptera tricolor	8565603
Family Vespertilionidae	
Corynorhinus mexicanus	514929
Eptesicus brasiliensis	12912583
Eptesicus chiriquinus	187154
Eptesicus diminutus	2385987
Eptesicus furinalis	16292635
Histiotus macrotus	1804780
Histiotus magellanicus	364796
Lasiurus atratus	399784
Lasiurus blossevillii	19044624
Lasiurus cinereus	21079570
Lasiurus ega	15725975
Lasiurus egregius	1322647
Lasiurus intermedius	1748582
Myotis albescens	14594617
Myotis atacamensis	253598
Myotis chiloensis	445536
Myotis dominicensis	2235
Myotis elegans	587270
Myotis fortidens	474062
Myotis keaysi	3204224
Myotis levis	1394485
Myotis martiniquensis	3813
Myotis nesopolus	54645
Myotis nigricans	14379997
Myotis oxyotus	2601591
Myotis riparius	14109869
Myotis ruber	1795840
Myotis simus	4709799
Rhogeessa aeneus	144233
Rhogeessa alleni	261936
Rhogeessa genowaysi	913
Rhogeessa gracilis	178190
Rhogeessa io	7196015
Rhogeessa mira	3346
Rhogeessa parvula	448874
Rhogeessa tumida	565651

CHAPTER 2

Speciation dynamics during the global radiation of extant bats[3]

ABSTRACT

Species richness varies widely across extant clades, but the causes of this variation remain poorly understood. We investigate the role of diversification rate heterogeneity in shaping patterns of diversity across families of extant bats. To provide a robust framework for macroevolutionary inference, we assemble a time-calibrated, species-level phylogeny using a supermatrix of mitochondrial and nuclear sequence data. We analyze the phylogeny using a Bayesian method for modeling complex evolutionary dynamics. Surprisingly, we find that variation in family richness can largely be explained without invoking heterogeneous diversification dynamics. We document only a single well-supported shift in diversification dynamics across bats, occurring at the base of the subfamily Stenodermatinae. Bat diversity is phylogenetically imbalanced, but - contrary to previous hypotheses - this pattern is unexplained by any simple patterns of diversification rate heterogeneity. This discordance may indicate that diversification dynamics are more complex than can be captured using the statistical tools available for modeling data at this scale. We infer that bats as a whole are almost entirely united into one macroevolutionary cohort, with decelerating speciation through time. There is also a

[3] Shi, J.J. & Rabosky, D.L. (2015) Speciation dynamics during the global radiation of extant bats. *Evolution*, **69**, 1528–1545.

significant relationship between clade age and richness, suggesting that global bat diversity may still be expanding.

INTRODUCTION

One of the most striking trends across the tree of life is the unequal distribution of diversity across extant clades (Raup *et al.* 1973, Gould *et al.* 1987, McPeek & Brown 2007, Alfaro *et al.* 2009). While many groups of organisms have dramatically radiated over evolutionary timescales, others have stagnated or failed to diversify, and remain species-poor. Evolutionary extremes at both ends of the spectrum, across the tree of life, have long captivated evolutionary biologists and ecologists. For example, angiosperms and beetles are famously species-rich, while groups ranging from tuataras to coelacanths have persisted at low diversity (Farrell 1998, Magallón & Sanderson 2001, Harmon 2012). What has driven this pervasive pattern of unequal species richness throughout the tree of life?

A long-standing hypothesis is that unequal diversity stems from diversification rate variation across clades (Stanley 1979, Strathmann & Slatkin 1983, Kirkpatrick & Slatkin 1993, Barraclough & Nee 2001, Chan & Moore 2002, Wiens 2011). Proposed factors that control diversification rate heterogeneity invoke both biotic interactions among organisms as well as the external influences of environment and geography (Vrba 1992, Barnosky 2001, Benton 2009, Badgley & Finarelli 2013). Diversification rates may vary based on ecological and geographic opportunity, as in the presence or absence of competitors, depopulated niche spaces, or the opening of niche space following the evolution of a key innovation (Simpson 1953, Benton 1987, Erwin *et al.* 1987, Rosenzweig & McCord 1991, Schluter 2000, Yoder *et al.* 2010, Rabosky 2013). Quantifying diversification rate variation is the first step to potentially

uncovering ecological and geographical drivers of extant diversity patterns.

In this study, we investigate macroevolutionary patterns across extant bats (Order Chiroptera). Bats are the second most species-rich order of extant mammals and are distributed across nearly all terrestrial biomes (Nowak 1994, Simmons 2005b). Their taxonomic diversity is complemented by considerable morphological and ecological diversity. Bat trophic ecology includes insectivory, vertebrate carnivory, frugivory, nectarivory, and sanguivory (Nowak 1994, Simmons & Conway 2003). Bat diversity is also not equally distributed across the order: some clades of bats have radiated into a variety of species, ecological niches, and biogeographic zones, while others remain restricted or conserved (Jones *et al.* 2005, Simmons 2005b). For example, New World leaf-nosed bats are known for both high species richness and morphological disparity, while the closely-related New Zealand short-tailed and Neotropical bulldog bats are species-poor with highly specialized morphologies.

The more than 1300 species of extant bats are partitioned into 20 ecologically and geographically heterogeneous families (Simmons 2005b). Six families of extant bats are more species-rich than all others: Pteropodidae, Rhinolophidae, Hipposideridae, Phyllostomidae, Molossidae, and Vespertilionidae encompass roughly 75% of extant species diversity (Figure 2.1). This apparent imbalance of diversity may be driven by clade-specific differences in diversification rate (Jones *et al.* 2005). For example, the Neotropical phyllostomids are thought to have shifted to higher diversification rates in association with their ecological diversification (Monteiro & Nogueira 2011, Dumont *et al.* 2012, Santana *et al.* 2012). The evolution of the leaf-nose in both phyllostomids and the Old World rhinolophoids has been considered a key innovation that precipitated rapid diversification and high species richness (Teeling *et al.* 2002, Fenton 2010). Other researchers have inferred accelerated diversification in the cosmopolitan

vespertilionids, perhaps due to increased substitution rates or heightened transposon activity (Lack and Van Den Bussche 2010, Platt II *et al.* 2014). Frugivory in both phyllostomids and pteropodids has been considered a key innovation that may have driven accelerated diversification within both families (Almeida *et al.* 2011, Rojas *et al.* 2012). Overall, many potential macroevolutionary processes can be evaluated in this highly diverse clade of animals.

While it is possible that unequal bat clade diversity is driven by diversification rate shifts, it is also possible that imbalance reflects clade ages. The radiation of crown Chiroptera likely dates to the early Cenozoic, as with other major mammalian lineages (Simmons 2005a, Simmons *et al.* 2008, Meredith *et al.* 2011, Raia *et al.* 2012). Identifying significant diversification rate shifts is only possible with accurate time-calibration. However, phylogenetic resolution and time calibration across the order has historically been difficult, given the notoriously poor bat fossil record and numerous systematic revisions (Eiting & Gunnell 2009, Teeling *et al.* 2012). Though the backbone of bat families is well-resolved (Teeling *et al.* 2005), a robust time-calibrated, species-level phylogeny encompassing the majority of extant bat diversity has remained elusive. Recent efforts have focused on higher levels, such as genus, or are limited to one or few genetic loci (Agnarsson *et al.* 2011, Yu *et al.* 2014).

We present an analysis of macroevolutionary dynamics across extant bats. We first assembled a time-calibrated, species-level phylogeny of bats by aggregating multilocus genetic data and incorporating fossil dating across extant families. We then quantified diversification rates to test whether the variation in species richness across bats (Figure 2.1) is a product of diversification rate heterogeneity, or whether it largely reflects other factors, such as the amount of time available for diversity to accumulate.

METHODS

Sequence alignment

We mined GenBank for all available bat mitochondrial and nuclear sequences, utilizing scripts that automated sequence identification, cleaning, and alignment, and generally followed the supermatrix approaches of Hinchcliff and Roalson (2013) and Zanne *et al.* (2014).

We first used the PhyLoTa Browser (Sanderson *et al.* 2008) to identify all loci sequenced for at least 20 unique bat species within GenBank release 194. We then downloaded the entire NCBI SQLite 3 database of Chiroptera nucleotide data using the program PHLAWD (Smith *et al.* 2009). Within this set, we identified "guide sequences" for each of the aforementioned candidate loci from PhyLoTa. Guide sequences aided in identification of homologous loci, and were selected to maximize family-level coverage. We chose the longest sequence for each of the monotypic bat families. For all other families, we chose either the two genera with the longest sequences, or for the highly diverse families Vespertilionidae and Phyllostomidae, the four genera with the longest sequences. Based on these guide sequences, we used PHLAWD to parse the NCBI database and identify sequences for each locus. We plotted BLAST scores of coverage against identity for these sequences, and excluded outliers. Finally, we assembled alignments for each locus, with one representative sequence per taxon. We also included sequences for three mammalian outgroups: *Canis lupus* and *Sorex araneus* from the same superorder (Laurasiatheria), and *Mus musculus* from an earlier diverging superorder (Euarchontoglires).

Each alignment was cleaned in the program Gblocks (Castresana 2000, Talavera & Castresana 2007), which identified conserved regions while allowing at most 50% gaps at any site. Finally, we concatenated all loci into a supermatrix with the program Phyutility (Smith & Dunn 2008). Each locus was specified as an independent partition for all subsequent

phylogenetic analyses. Using the taxonomy of Simmons (2005b), we collapsed all subspecies to the longest species-level sequence, and removed ambiguous species. For genera described since 2005, we collapsed to species-level sequences using the NCBI taxonomy.

Our final alignment included all 20 extant families. The 7 families represented by the most individual loci were the 6 largest families - Vespertilionidae, Phyllostomidae, Pteropodidae, Molossidae, Rhinolophidae, Hipposideridae - and Nycteridae (Figure 2.1), which together comprised 87% of species in our dataset. The concatenated and cleaned dataset included 29 loci, and totaled 20376 bp (Table 2.1). All alignments and PHLAWD output, with Genbank annotations for included sequences, have been archived in the Dryad repository.

Phylogeny construction

We estimated the maximum-likelihood (ML) phylogeny and bootstrap support using RAxML v8 (Stamatakis 2014). We parameterized RAxML by assigning a separate GTR+Γ model of rate heterogeneity to each locus, and initiated runs with maximum parsimony trees. To improve likelihood calculation, we constrained topologies to an established backbone, as in other large-scale phylogenies (*e.g.* Zanne *et al.* 2014). This backbone included the Yangochiroptera and Yinpterochiroptera suborders, and within those, the Rhinolophoidea, Emballonuroidea, Noctilionoidea, and Vespertilionoidea superfamilies of Teeling *et al.* (2005). For calibration purposes, we additionally enforced the monophyly of the large vespertilionid subfamily Myotinae.

After an initial ML search, we used the program RogueNaRok to identify “rogue taxa” (Aberer *et al.* 2013). Rogue taxa can bias phylogenetic inference, with low phylogenetic signal or even sequence misidentification within GenBank (Hinchcliff & Roalson 2013). We also

pruned two extremely long branch lengths to avoid biases of long branch attraction. We performed one final ML tree search after pruning (see Table S2.1), and also 100 rapid bootstrap analyses to assess support.

Using fossils, we time-calibrated the ML phylogeny using penalized likelihood as implemented in the program treePL (Sanderson 2002, Smith and O'Meara 2012). treePL explicitly allowed for rate variation across branches, but penalized rate differences after cross-validating initial analyses. We used 24 fossil calibration points (Table 2.2) as described by Jones *et al.* (2002, 2005), Teeling *et al.* (2003, 2005), and/or that were described and validated in the Paleobiology Database (PaleobDB). We followed PaleobDB taxonomy for consistency. An upper bound was also set for the divergence between crown Chiroptera and carnivores at the K-Pg boundary (65.5 million years ago [mya]; though see Springer *et al.* 2003, Teeling *et al.* 2003, Bininda-Emonds *et al.* 2007, Meredith *et al.* 2011 for debate).

Our fossils generally defined minimum dates for crown families, subfamilies, and genera, and were placed upon our ML phylogeny as such in treePL. We tested the correlation of our inferred ML family ages with the phylogenies of Jones *et al.* (2005) and Teeling *et al.* (2005) to compare our results with previous publications. Because crown ages are likely not normally distributed, we performed pairwise Spearman's rank correlation tests for these comparisons. For these correlations, the families Cistugidae and Miniopteridae were nested within the closely related Vespertilionidae, as was the case in Jones *et al.* (2005) and Teeling *et al.* (2005). The placement of Miniopteridae, which was elevated to family based on molecular data (Miller-Butterworth *et al.* 2007), has implications for bat systematics that should be kept in mind when considering these previous publications. We did not perform crown age tests on monotypic families.

Macroevolutionary modeling

We modeled macroevolutionary dynamics of diversification across bat phylogenies with the program BAMM v2.0 (Bayesian Analysis of Macroevolutionary Mixtures: Rabosky *et al.* 2013, Rabosky 2014; latest version available from http://bamm-project.org/). We used BAMM to quantify diversification rates throughout the bat clade, and to identify different macroevolutionary regimes. In the BAMM framework, regimes refer to a shared, potentially dynamic diversification process shared by all lineages downstream from the location of a rate shift. The posterior probability of a particular configuration of shifts can be estimated by the frequency at which it is sampled during the analysis. The number of shifts in any given shift configuration is one more than the number of regimes, given a starting "background" regime at the root.

For our ML phylogeny, we ran 10 million generations of reversible-jump Markov chain Monte Carlo (MCMC) sampling, with samples drawn from the posterior every 1000 generations. BAMM v2.0 (released June 2014) implements Metropolis-coupled Markov chain Monte Carlo (MCMCMC; MC3) to improve the efficiency of simulating the posterior probability distribution (Altekar *et al*. 2004). MC3 is a variant of MCMC sampling where multiple chains are run simultaneously. Inference about the posterior distribution is based on a single chain - the so-called "cold chain" - while the remaining chains ("heated chains") are used to more thoroughly explore parameter space. Heating a chain involves flattening the posterior probability distribution such that the chain is more free to wander through parameter space. Relative to the cold chain, heated chains are more likely to accept proposed states that move the chain into regions of lower posterior probability. As a consequence, heated chains are less likely to become stuck on local

optima than are cold chains. The implementation of MC3 in BAMM v2.0 follows the algorithm for chain swaps described in Altekar *et al.* (2004) and follows an incremental heating scheme.

To flatten a posterior probability distribution, chains are heated by modifying the acceptance probabilities of proposed states. Letting $f(\theta, M)$ denote the posterior probability of the current model (M) and parameters (θ), the probability of accepting a new state with model M' and parameters θ' is given by:

$$min\left[1, \left(\frac{f(\theta', M')}{f(\theta, M)}\right)^{\beta} Q\right],$$

where β is the "heat" that is applied to the chain and Q is the ratio of transition probabilities between current and proposed states. If $\beta = 1$, this equation reduces to standard MCMC. However, if $\beta < 1$, the algorithm will accept proportionately more proposals, thus enabling the chain to wander around a seemingly flattened probability landscape. The cold chain alone is used to approximate the true posterior distribution, but MC3 periodically proposes state swaps between the cold chain and the heated chains, which improves the overall efficiency of the algorithm (Altekar *et al.* 2004). In BAMM, two randomly chosen chains j and k with respective heating parameters β_j and β_k are selected to exchange states with a predetermined swap frequency, and the state swap is accepted with probability:

$$\min\left[1, \frac{f(M_k, \theta_k)^{\beta_j}}{f(M_j, \theta_j)^{\beta_j}} \frac{f(M_j, \theta_j)^{\beta_k}}{f(M_k, \theta_k)^{\beta_k}}\right].$$

The heat parameter β is determined by an incremental heating scheme (Altekar e*t al.* 2004), where a set of n chains $i \in (1, 2, ... n)$, combined with a temperature parameter ΔT, allows for the computation of the heat for the i'th chain as:

$$\beta_i = \frac{1}{1 + (i - 1)\,\Delta T}\ .$$

This equation reduces to $\beta = 1$ (standard MCMC) when $n = 1$. For our analyses of the bat phylogeny, we performed MC3 sampling with $n = 8$ chains, $\Delta T = 0.1$, and swaps between chains were proposed every 1000 generations.

We estimated speciation and extinction priors with the R package BAMMtools v2.0 (Rabosky *et al.* 2014b), and specified a value of 1.0 for the exponential hyperprior governing the number of distinct rate shift regimes. This hyperprior was chosen to be conservative and to minimize type I errors (Rabosky 2014). We ran all analyses on the University of Michigan's Flux high performance computing cluster.

We also accounted for incomplete sampling of bat diversity, which can bias inferences of diversification rates (Nee *et al.* 1994, Pybus & Harvey 2000, Heath *et al.* 2008, Rabosky & Lovette 2008), by estimating the sampling percentage of each bat genus as described by Simmons (2005b) (Table S2.2). BAMM incorporates analytical corrections for incomplete taxon sampling (FitzJohn *et al.* 2009), under the assumption of random taxon sampling at some level of taxonomic hierarchy. In our case, we assumed that species were randomly sampled within genera, which allowed us to apply separate genus sampling fractions. For those genera with higher current species counts than are described in Simmons (2005b), we specified complete sampling. If estimated diversities of bat clades are inaccurate, due to crypsis or taxonomic artifacts, diversification results may change alongside sampling fractions. To test sensitivity to incorrect estimates of clade sizes and incomplete sampling, we ran an additional analysis where we assumed that the true genus-level diversity was twice that of current estimates. Practically, this entailed running an additional analysis with all sampling fractions halved.

To investigate the effect of topological uncertainty on our macroevolutionary inferences, we also ran BAMM on the 100 bootstrap replicate phylogenies from RAxML. We first time-

calibrated all bootstrap replicates using a subset of our fossil constraints that were either topologically constrained in the tree search or were monophyletic across all replicates (Table 2.2). We ran 10 million generations of MCMC sampling for each individually time-calibrated bootstrap phylogeny, with replicate-specific priors on speciation and extinction estimated using BAMMtools. All other priors and parameters were identical to our ML analysis.

We checked for convergence of the MCMC algorithm by plotting likelihood scores against sampled generations, ensuring adequate mixing of the chains, and checking for effective sample sizes above at least 10% of our 10 million generations. To be conservative, we then discarded the first 20% of samples as burn-in.

Branch-specific diversification rate shifts

BAMM enables researchers to estimate the marginal probability of a rate shift along a single branch of a phylogeny (Rabosky 2014, Rabosky *et al.* 2014a). The marginal probability of a rate shift is simply the frequency with which a rate shift is observed on a particular branch across the full posterior distribution of macroevolutionary rate shift configurations simulated using BAMM. Here, we develop an alternative approach that uses Bayes factors (Kass & Raftery 1995) to evaluate branch-specific evidence for a rate shift. A branch-specific Bayes factor is a measure of the evidence for a rate shift along a particular branch relative to the evidence for an alternative model without a rate shift on the branch, and takes branch length into account. Generally, the Bayes factor associated with two models M_j and M_k can be computed as:

$$\frac{\frac{\Pr(M_j)}{\pi(M_j)}}{\frac{\Pr(M_k)}{\pi(M_k)}},$$

where $Pr(M_j)$ and $Pr(M_k)$ are the posterior probabilities of models *j* and *k*, and $\pi(M_j)$ and $\pi(M_k)$ are the prior probabilities of models *j* and *k*.

In our case, for a given branch *x*, the marginal shift probability P_x is an estimate of the posterior probability of a model with a shift, and $(1 - P_x)$ is the posterior probability of no shift. BAMM assumes that diversification rate shifts occur on phylogenetic trees under a compound Poisson process and provides an estimate of the prior probability of a rate shift on each branch in the tree. Thus, if π_x is the prior probability of a rate shift on branch *x*, $(1 - \pi_x)$ is the prior probability of no shift on that branch. It is then straightforward to compute a branch-specific Bayes factor for branch *x* as:

$$\frac{\frac{P_x}{\pi_x}}{\frac{1-P_x}{1-\pi_x}} \cdot$$

We refer to this as a "marginal" Bayes factor, because it is computed across the posterior distribution while ignoring the degree to which shift probabilities on specific branches may covary with one another. Shift probabilities along branches are not independent of those on other branches (Rabosky *et al.* 2014a) and cannot be interpreted as such; this also applies to the Bayes factors computed here. For example, adjacent branches often have strong negative covariances in shift occurrences (Rabosky *et al.* 2014a). Because the prior probability of a rate shift on a particular branch is a strict function of branch length, we interpret marginal Bayes factors as the evidence favoring rate shifts after controlling for branch length. For example, we expect to observe more shifts on long branches than on short branches, even if shifts are randomly distributed across the tree. We computed branch-specific Bayes factors for each branch in the bat phylogeny. These methods have been implemented in the current versions of BAMM and BAMMtools.

Cohorts, age-richness, and phylogenetic imbalance

We established different macroevolutionary cohorts across bats (Rabosky *et al.* 2014a). A "macroevolutionary cohort" is a set of taxa that share a common set of macroevolutionary rate parameters. For example, if a given sample from the posterior has zero rate shifts, it is necessarily true that all lineages are assigned to the same evolutionary process that began at the root of the tree. All lineages would thus be considered part of the same macroevolutionary cohort when we infer elevated pairwise probabilities of originating under the same diversification process. With this analysis, we could easily visualize any heterogeneity in macroevolutionary regimes across all bats, and identify the unique cohorts most likely to be decoupled from the rest of the order (Figure S2.1).

Our cohort analysis was also performed across all bootstrap replicates, in case phylogenetic uncertainty affected cohort membership. We then calculated the posterior probabilities of different configurations of rate shifts across our ML phylogeny and bootstrap replicates. To also assess the effect of topological uncertainty upon rate shifts, we estimated a pooled distribution of macroevolutionary regime shifts across the 100 bootstrap replicates. It was most appropriate to refer to this distribution as a "quasi-posterior," as phylogenetic tree topologies were sampled by bootstrapping; a true posterior would sample them in proportion to their posterior probability. We computed Bayes factor evidence in favor of the model with the highest quasi-posterior probability over a model with no shifts.

We tested for a relationship between crown age and species richnesses of extant families, using both Spearman's rank correlation tests and phylogenetic generalized least squares (PGLS) with a Brownian correlation structure to correct for evolutionary non-independence (Martins & Hansen 1997). We only assessed the effect of crown age on diversity, as the use of stem ages is

known to strongly bias age-richness relationships (Stadler *et al.* 2014). We also used BAMMtools to calculate instantaneous rates of diversification across our ML phylogeny, for both our main run and the BAMM run with halved sampling fractions. To test for significance of non-constant rates of diversification, we calculated the γ-statistic (Pybus & Harvey 2000) for our ML phylogeny and all bootstrap phylogenies using the R package *phytools* (Revell 2012). We investigated the effect of incomplete sampling on the γ-statistic by simulating pure-birth phylogenies with varying levels of sampling using the R package *geiger* (Harmon *et al.* 2008).

To further explore the extent to which species richness in major bat clades can largely be explained by a single global diversification process, we quantified temporal patterns of bat phylogeny imbalance and compared them to a constant rate birth-death process as a corresponding null expectation of imbalance. We operationally defined imbalance as the variance in species richness among descendant clades of all lineages present at some time *t* in the phylogeny. To calculate this metric, we sampled the ML phylogeny in 100 "slices" evenly spaced from the root to the present. We then recorded the number of ancestral lineages *n* present at each slice *t*, and the number of extant descendants from each of these *n* lineages. We then calculated the empirical variance in log(species richness) among the *n* descendant clades, for each of the 100 time slices across the phylogeny. Each point produced by this method corresponded to the variance among realized evolutionary outcomes for each of the *n* ancestral lineages at each time *t*.

We then generated a null distribution of expected variances from the *n* ancestral lineages present at each time *t*. For each slice, we randomly assigned the estimated 1300 extant species of bats into *n* clades, then simulated our incomplete sampling by arbitrarily selecting 812 (the number of species in the ML phylogeny) of these 1300. This procedure simulated expected clade

diversities descended from *n* ancestral lineages, if the descendant diversity of a clade is random with respect to its ancestral lineage. On average, the distribution of clade diversities at any time approximated a geometric rank-abundance curve (Nee *et al.* 1992, Rabosky 2009b). We replicated this simulation 100 times to calculate the variance among log(richnesses) of the *n* simulated clades at each time slice *t*. In this framework, high empirical values imply a more imbalanced phylogeny, while low values imply more evenness distributed across clades. The null expectation of imbalance is the variance under a constant birth-death process, which we confirmed with a phylogeny simulated under this assumption using *geiger* (Harmon *et al.* 2008, Figure S2.2). Imbalance may vary through time to reflect changes in macroevolutionary conditions, such as diversification rate shifts or differential diversity limits.

RESULTS

Phylogeny construction

Our time-calibrated phylogeny (Figure 2.2) includes 812 species of bats, or about 62.5% of current diversity estimates (assuming ~1300 total species). Overall, 62% of nodes are recovered with at least 70% bootstrap support. This increases to 76% of nodes with at least 50% bootstrap support, and 82% of nodes with at least 40% bootstrap support. These percentages are robust across taxonomic groupings, with two notable exceptions. The superfamily Noctilionoidea (Teeling *et al.* 2005: families Myzopodidae, Furipteridae, Thyropteridae, Mystacinidae, Noctilionidae, Mormoopidae, Phyllostomidae) is extremely well-supported, with 75% of nodes supported by at least 70% of bootstrap replicates, and nearly 90% of nodes supported by at least 50% of bootstrap replicates. Conversely, the family Molossidae is the least well-supported, with only 62% of nodes supported by even 50% of bootstrap replicates. One systematic revision with

relatively high support (70% bootstrap support) is proposed here, with the superfamily Emballonuroidea (families Emballonuridae and Nycteridae) recovered sister to Noctilionoidea. As this was not part of the established systematic constraints used to parameterize our tree search (Teeling *et al.* 2005), we suggest it merits continued investigation.

We infer generally early-to-mid Eocene divergence times for the extant families of bats, ranging from ~40 mya to ~55 mya, with a crown Chiroptera age inferred around 58 mya. Correlation tests of our ML times with those of Jones *et al.* (2005) and Teeling *et al.* (2005) confirm that stem ages are generally comparable with previous research (Table 2.3). Spearman's rank correlation tests are highly significant, revealing a positive linear correlation between our phylogeny and that of Jones *et al.* (2005; $p = 0.04$, Spearman's $\rho = 0.488$) and a much stronger linear correlation between our phylogeny and that of Teeling *et al.* (2005; $p < 0.001$, Spearman's $\rho = 0.795$). Our results notably suggest that the "Eocene big bang" of chiropteran diversification was even earlier than previously suggested (Simmons 2005a).

Crown ages among the three compared phylogenies vary the most for the families Natalidae, Noctilionidae, Rhinolophidae, and Myzopodidae. The family Natalidae, in particular, may be calibrated with fossils of uncertain placement within Nataloidea, and we include an alternate crown date that does not affect downstream analyses (Tables 2.2, 2.3). If we exclude all of these crown ages, both pairwise tests are highly significant, with a strong, positive linear correlations between our ML crown ages and those of Jones *et al.* (2005; $p = 0.025$, Spearman's $\rho = 0.682$) and those of Teeling *et al.* (2005; $p = 0.012$, Spearman's $\rho = 0.745$). Overall, these discrepancies should be taken into consideration for our findings, and as such we caution that the phylogeny we present is not meant to be a systematic revision of the order. Inferences for the species-rich family Rhinolophidae are the most likely to be affected, as the other families

represent an extremely small percentage of extant bat diversity. Because the relative relationships among crown ages are fairly constant across our phylogeny and previous studies, we present our macroevolutionary results with the caveat that absolute dates are subject to further calibration and inference. Across our bootstrap replicates, the crown ages of extant bats vary as reported in Table 2.4.

Macroevolutionary regimes and rate shifts

Though BAMM returns overall diversification rates from individual estimates of speciation and extinction rates, we report only speciation data for this study unless otherwise specified. The linear correlation between net diversification and speciation rates in our analyses is extremely positive (Pearson's $r = 0.996$, $p < 0.001$; PGLS $t = 90.087$, $p < 0.001$), and macroevolutionary inferences with diversification rates are highly similar, so we feel our results are robust to this consideration. Actual estimates of extinction rates are not reported considering our phylogeny is composed entirely of molecular data (Rabosky 2010).

BAMM results from our ML tree support a single rate shift and two macroevolutionary regimes, with the majority of extant bat diversity being governed by a common background regime. The post-burnin posterior distribution of the number of rate shifts is right-skewed (with a mean of 1.35 shifts and a median of 1 shift). In this distribution, a single shift occurs with a posterior probability (*pp*) of 70.5%, 2 shifts occur with *pp* = 23.8%. A configuration of 0 shifts only occurs with *pp* = 3%.

We use both branch-specific Bayes factors and marginal shift probabilities to localize regime shift information on the ML phylogeny. Both metrics strongly favor a model that includes a shift at the base of Stenodermatinae over a model without a shift in this tree (Figure

2.3). Importantly, it is conceptually possible for these two metrics to be in conflict, depending on the phylogeny. The compound Poisson process used in BAMM assumes a uniform probability density of rate shifts across phylogenies, leading to a positive correlation between branch length and the prior probability of a rate shift along a branch. As such, the branch-specific Bayes factors are essentially marginal probabilities weighted by the phylogenetic branch length. Theoretically, one could observe a low marginal probability of a rate shift along a very short branch, yet - if the prior probability of a shift along the branch is sufficiently small - the Bayes factor associated with a shift on the branch may be extremely high. This would imply that the "density" of rate shifts per unit branch length is high. In the case of extant bats, we infer that the concordance between both metrics is strong evidence for a stenodermatine diversification rate shift, even after taking into account the prior distribution of rate shifts expected based on topology.

The low number of inferred shifts is not likely a product of topological uncertainty, given results from our bootstraps. Across the post-burnin BAMM results of all bootstrap replicates combined (the quasi-posterior), there is a different distribution of shifts than the prior (Figure 2.4). Notably, there is extremely low quasi-posterior probability of zero shifts (3.15%), and the highest quasi-posterior probability is for one shift. The Bayes factor evidence in favor of this model over a model with 0 shifts is 120.6, indicating very strong support.

The 95% credible set of shift configurations comprises the set of distinct, sampled configurations that sum to 95% of the posterior probability. In the ML tree, all of the configurations within this credible set contain shifts either at the base of Stenodermatinae or at an ancestral noctilionoid node. The different shift configurations in the credible set allow us to quantify uncertainty in placement of a stenodermatine shift or a more broadly-encompassing shift. The shift configuration sampled at the highest frequency, 64%, contains only a

stenodermatine shift, with all other configurations sampled at a frequency of 12% or lower (Figure S2.4).

Macroevolutionary cohort analysis

We can use our results to calculate the probability of clades being independent macroevolutionary cohorts. Our cohort analysis also supports the decoupling of stenodermatines and the rest of bats (Rabosky *et al.* 2014a). In our ML phylogeny, we reveal striking homogeneity that unites almost all extant bats in one cohort, except the stenodermatines (Figure 2.5A). It is clear that there is essentially a 0% probability of stenodermatines being part of the same cohort as all non-phyllostomids. There is weaker support for other phyllostomids also being part of a distinct cohort apart from other bats. A distinct stenodermatine cohort appears to be somewhat robust to topological uncertainty, though this pattern becomes more equivocal (Figure 2.5B). Interestingly, these bootstrap topology analyses highlight a decoupled *Pteropus* cohort. It is unclear what drives this pattern, as there is no *Pteropus* signal in the ML phylogeny, but it is possible this is a product of low genus-level sampling (Table S2.2).

Our BAMM analysis with all sampling fractions halved, which tests sensitivity to incomplete sampling, is extremely similar with respect to our findings about macroevolutionary homogeneity, diversification rate, and the uniqueness of Stenodermatinae (Figure S2.5).

Age-richness relationships

We explore the effect of age on diversity using age-richness correlations. A Spearman's rank-correlation test for a relationship between crown ages and species richnesses is highly significant, revealing a positive and linear correlation (Spearman's $\rho = 0.766$, $p < 0.001$). The

PGLS test for a relationship between crown family ages and log(species richnesses) is also highly significant ($t = 4.677$, $p = 0.0003$), with a clear positive and linear relationship between age and log(richness) (Figure S2.6).

Speciation rates through time

Our BAMM results for the ML topology are evidence for decreasing speciation rates through time, both across bats as a whole and within the stenodermatine macroevolutionary cohort (Figure 2.6). These results are corroborated by the γ-statistic, which tests for significance of temporal decelerations in the rate of speciation (Pybus & Harvey 2000). The γ-statistic of our ML phylogeny is -10.675 ($p < 0.001$), and the distribution of γ-statistics across all 100 bootstrap replicates ranges from -12.649 to -1.982 (mean = -7.840, median = -6.572, with all $p < 0.05$). We infer from negative values that the internal nodes are significantly closer to the root than expected under a pure-birth model (Pybus & Harvey 2000). Our results are unlikely to be explained by incomplete taxon sampling, assuming sampling is nonrandomly biased. True bat diversity would need to be near 3000 species (compared to current estimates around 1300) to produce an artifactual γ-statistic as negative as in our ML phylogeny, or would need to be near 2000 to match the bootstraps' mean (Rabosky & Lovette 2008, Table S2.3).

Phylogenetic imbalance

Empirical estimates of clade diversity variance, conditioned upon the number of descendants of ancestral lineages at any point in time, are higher than expected under a constant rate birth-death process for the majority of the order's history (Figure 2.7). Bats thus appear to have partitioned diversity into clades more unevenly than expected by chance alone, and that this

pattern has been fairly consistent throughout their history. We only include results between roughly 50 and 15 million years ago. This excludes the early history of the clade, when variances are extremely volatile due to the low number of ancestral lineages, and the last 15 million years, when the effects of incomplete sampling are most dramatic. Results are nearly identical even after excluding the subfamily Stenodermatinae, indicating that this radiation alone does not drive the imbalance (Figure S2.7).

DISCUSSION

Bat diversification dynamics

Our macroevolutionary analyses suggest that the global radiation of bats is characterized by a remarkably homogeneous diversification process. Most extant bat species can be united into a single, paraphyletic macroevolutionary cohort (Figure 2.5A), with only the subfamily Stenodermatinae having an extremely high probability of being defined by a shift in diversification rate (Figure 2.3, Figure S2.4). Bat speciation dynamics can be characterized by a single global deceleration in the rate of speciation, combined with a recent burst of speciation at the base of the stenodermatines (Figure 2.6). We infer stenodermatine diversification rates more than twice that of the rest of the bat radiation, which falls in line with previous studies on this subfamily (Dumont *et al.* 2012).

Stenodermatinae is a well-studied Neotropical radiation, and diversification rate shifts have previously been inferred at the base of this subfamily. The stenodermatine radiation may be coupled with morphological and behavioral specializations for frugivory (Monteiro & Noguiera 2011, Dumont *et al.* 2012, Santana *et al.* 2012). In this framework, stenodermatines are an adaptive radiation nested within the radiation of Chiroptera as a whole, potentially spurred by the

key innovation of frugivory (Rojas *et al.* 2012). Stenodermatine skulls are known to have unique biomechanical properties for processing hard fruit, affording their expansion into unexplored niche space and potentially elevating speciation rates (Dumont *et al.* 2012, 2014).

The relative homogeneity of bat diversification is surprising, especially in the context of past macroevolutionary research. Jones *et al.* (2005) inferred multiple diversification rate shifts across bats: though the authors found the strongest evidence for rate shifts within Molossidae and Phyllostomidae, they also suggested shifts in the rhinolophoids, vespertilionids, and pteropodids. We do not find strong evidence for this amount of heterogeneity, using a method that explicitly allows for rate heterogeneity and infers probabilities of entire shift configurations. It is unknown how common an overall pattern of relative homogeneity is among other animals. Diversification studies in other metazoans often find considerable rate heterogeneity, perhaps making bats curiously unique given their high diversity (Chan & Moore 2002, Purvis & Agapow 2002, Alfaro *et al.* 2009, Barker *et al.* 2013, Rabosky *et al.* 2013, Rabosky *et al.* 2014a). However, previous studies on rate heterogeneity may not be directly comparable to our methods. As the second-most species-rich order of extant mammals, we suggest that bats as a whole may have high diversification rates. This hypothesis can be tested with diversification studies across a time-calibrated, species-level phylogeny of all mammals.

Unresolved or uncertain phylogenetics can compromise accurate macroevolutionary inference. We caution that the phylogeny we present here (Figure 2.2) is not meant to be a systematic reworking of the order, and note some issues that bear future consideration. Finer-scale fossil calibration, especially with methods that explicitly take into account molecular clock variation, can improve our absolute inferences of crown ages. Topologically, groups within Molossidae are not well-supported by our bootstrap replicates. This does not appear to reflect

low sequence coverage, as we have molossid data for every included locus. A previous phylogenetic study of Molossidae also raised taxonomic issues regarding genus-level paraphyly that cannot simply be explained by gene tree conflicts (Lamb *et al.* 2011). Discordances among bootstrap replicates may also reflect incongruence among the concatenated loci, taxonomic uncertainty, extremely rapid divergences, or other evolutionary processes (Knowles 2009, Dávalos *et al.* 2012, Salichos & Rokas 2013).

Possibly due to these issues, some well-studied genera are paraphyletic in our ML phylogeny. General findings of paraphyly and polyphyly in studies of this scale may be more common than expected (Funk & Omland 2003). Complete resolution of species-level relationships will require careful integration of morphological characters and fossils, as well as more widely-available genomic data (Harrison & Kidner 2011, Dávalos *et al.* 2012, Slater *et al.* 2012). Even with these caveats, we continue to find signal for a decoupled stenodermatine cohort with respect to phylogenetic uncertainty (Figure 2.5B). Because the cohort probabilities are lowered, however, the stenodermatine shift should continue to be revisited as we further resolve bat phylogenetics.

Notably, the flying fox genus *Pteropus* also appears as a decoupled cohort when accounting for uncertainty, despite being absent from the 95% credibility set of shift configurations in the ML phylogeny (Figure S2.4). This genus, and its family Pteropodidae, may be responsible for the inflated numbers of shifts in the quasi-posterior distribution across all bootstrap topologies, as well (Figure 2.4). These Old World fruit bats are known for their species-richness and potentially rapid diversification (Almeida *et al.* 2011), but are also quite undersampled (Table S2.2). In addition, the family Pteropodidae as a whole is notoriously lacking in fossils (Eiting & Gunnell 2009; Table 2.2), leading to highly variable node dates

(Table 2.4) across bootstrap replicates and the possibility that this signal is an artifact of both sampling and dating. We suggest that future research pursues the phylogenetics of this group more deeply, with careful analysis of genomic data.

Macroevolution of Chiroptera

As we do not find evidence for widespread diversification rate heterogeneity, the possibility remains that patterns of diversity are mostly driven by the effect of clade age (McPeek & Brown 2007). We explore this hypothesis using the crown ages of extant families (Stadler *et al.* 2014). We find a positive linear relationship between crown family age and richness (Figure S2.6), and early family divergences overall. What caused bat families to diverge early in the Eocene, followed by radiations within these families (Figure 2.2, Simmons 2005a)? Many large clades are characterized by major ecological and geographic divisions preceding taxonomic, local differentiation (Simpson 1953, Foote 1993, Glor 2010, Sahney *et al.* 2010, Raia *et al.* 2012). Declining rates of diversification through time may be one phylogenetic signal of this process: clades switch from early and rapid ecological divergence, to a diversity-dependent slowing of diversification as ecological niches become saturated (Gould *et al.* 1977, Nee *et al.* 1992, Rabosky & Lovette 2008, Etienne & Haegeman 2012, Rabosky 2013). We find support for slowdown across the order, with strong evidence for temporal declines in diversification rates throughout bats (Figure 2.6) coupled with a significant negative γ-statistic that is robust to topological uncertainty (Pybus & Harvey 2000).

Specifically, bat diversification appears to be governed by two conflicting macroevolutionary models. The inferred strong slowdown in diversification (Figure 2.7) suggests diversity-dependent diversification, yet the significant age-richness relationship (Figure S2.6)

can be interpreted to contradict this inference (Rabosky 2009a, Wiens 2011). However, diversity-dependence does not preclude increasing diversity through time (Cornell 2013). Support for damped but increasing diversification has been found when investigating other large-scale diversity patterns (Kisel *et al.* 2011, Cornell 2013). In addition, diversification slowdowns can be caused by other factors, including the mode of speciation or external, abiotic factors (Moen & Morlon 2014), potentially reconciling our findings.

Despite the striking homogeneity of bat diversification, we detect phylogenetic imbalance across bat clades. This imbalance is not explained by the explosive radiation of stenodermatines (Figure 2.7, Figure S2.7). BAMM may not have enough power to detect certain types of diversification rate heterogeneity that can produce imbalanced phylogenies. In addition, clades at smaller scales (*e.g.* a single family within one biome) may be more prone to saturation. If these diversity limits are specific to local ecology and biogeography, diversity may be unequally distributed (Rabosky 2009b, Weir & Price 2011). These hypotheses can be tested in the future with phylogenies at the suborder and superfamily scale, where similar diversification regimes may be teased apart, and by explicitly assessing support for damped diversification versus unbounded diversification at different geographic scales.

Many aspects of bat macroevolution remain unknown, but we are beginning to overcome their poor fossil record with widely available genomic data and careful analysis of the available historical data. Van Valen (1979) once mused that, “one may hypothesize that bats did originate, but it is harder to go beyond this.” Not only have we moved quite far beyond this initial hypothesis, but our results suggest that bat evolution may be simultaneously more simple and puzzling that even Van Valen could have predicted.

ACKNOWLEDGEMENTS

The authors thank C. Badgley and E.R. Dumont for general research advice, S.A. Smith and C.E. Hinchcliff for computational and methodological assistance, P.O. Title and M.C. Grundler for input on graphics, and two anonymous reviewers for their comments. We also thank C.J. Anderson for developing the MC3 implementation of BAMM. J.J.S. thanks K.M. Bakker, L.E. Decker, P.R. Glaum, A.L. Gould, M.E. Martinez-Bakker, C.J.H. Miller, A.B. Taylor, and O. Whent for their invaluable support. This research was supported in part by NSF DEB-1256330.

DATA ARCHIVING

All data for this study are archived on and freely available from TreeBASE (Study 17613) and Dryad (https://doi.org/10.5061/dryad.2451q).

REFERENCES

Aberer, A.J., Krompass, D., & Stamatakis, A. (2013) Pruning rogue taxa improves phylogenetic accuracy: an efficient algorithm and webservice. *Systematic Biology*, **62**, 162–166.

Agnarsson, I., Zambrana-Torrelio, C.M., Flores-Saldana, N.P., & May-Collado, L.J. (2011) A time-calibrated species-level phylogeny of bats (Chiroptera, Mammalia). *PLoS Currents*, **3**.

Alfaro, M.E., Santini, F., Brock, C., Alamillo, H., Dornburg, A., Rabosky, D.L., Carnevale, G., & Harmon, L.J. (2009) Nine exceptional radiations plus high turnover explain species diversity in jawed vertebrates. *Proceedings of the National Academy of Sciences of the United States of America*, **106**, 13410–13414.

Almeida, F.C., Giannini, N.P., DeSalle, R., & Simmons, N.B. (2011) Evolutionary relationships of the Old World fruit bats (Chiroptera, Pteropodidae): another star phylogeny? *BMC Evolutionary Biology*, **11**, 281.

Altekar, G., Dwarkadas, S., Huelsenbeck, J.P., & Ronquist, F. (2004) Parallel Metropolis coupled Markov chain Monte Carlo for Bayesian phylogenetic inference. *Bioinformatics*, **20**, 407–415.

Badgley, C. & Finarelli, J.A. (2013) Diversity dynamics of mammals in relation to tectonic and climatic history: comparison of three Neogene records from North America. *Paleobiology*, **39**, 373–399.

Barker, F.K., Burns, K.J., Klicka, J., Lanyon, S.M., & Lovette, I.J. (2013) Going to extremes: contrasting rates of diversification in a recent radiation of new world passerine birds. *Systematic Biology*, **62**, 298–320.

Barnosky, A.D. (2001) Distinguishing the effects of the Red Queen and Court Jester on Miocene mammal evolution in the northern Rocky Mountains. *Journal of Vertebrate Paleontology*, **21**, 172–185.

Barraclough, T.G. & Nee, S. (2001) Phylogenetics and speciation. *Trends in Ecology & Evolution*, **16**, 391–399.

Benton, M.J. (1987) Progress and competition in macroevolution. *Biological Reviews*, **62**, 305–338.

Benton, M.J. (2009) The Red Queen and the Court Jester: species diversity and the role of biotic and abiotic factors through time. *Science*, **323**, 728–732.

Bininda-Emonds, O.R.P., Cardillo, M., Jones, K.E., MacPhee, R.D.E., Beck, R.M.D., Grenyer, R., Price, S.A., Vos, R.A., Gittleman, J.L., & Purvis, A. (2007) The delayed rise of present-day mammals. *Nature*, **446**, 507–512.

Castresana, J. (2000) Selection of conserved blocks from multiple alignments for their use in phylogenetic analysis. *Molecular Biology and Evolution*, **17**, 540–552.

Chan, K.M.A. & Moore, B.R. (2002) Whole-tree methods for detecting differential diversification rates. *Systematic Biology*, **51**, 855–865.

Cornell, H. V (2013) Is regional species diversity bounded or unbounded? *Biological Reviews*, **88**, 140–165.

Dávalos, L.M., Cirranello, A.L., Geisler, J.H., & Simmons, N.B. (2012) Understanding phylogenetic incongruence: lessons from phyllostomid bats. *Biological Reviews*, **87**, 991–1024.

Dumont, E.R., Dávalos, L.M., Goldberg, A., Santana, S.E., Rex, K., & Voigt, C.C. (2012) Morphological innovation, diversification and invasion of a new adaptive zone. *Proceedings of the Royal Society B: Biological Sciences*, **279**, 1797–1805.

Dumont, E. R., Samadevam, L., Grosse, I., Warsi, O.M., Baird, B., & Dávalos, L.M. (2014) Selection for mechanical advantage underlies multiple cranial optima in New World leaf-nosed bats. *Evolution*, **68**, 1436–1449.

Eiting, T.P. & Gunnell, G.F. (2009) Global completeness of the bat fossil record. *Journal of Mammalian Evolution*, **16**, 151–173.

Erwin, D.H., Valentine, J.W., & Sepkoski Jr., J.J. (1987) A comparative study of diversification events: the early Paleozoic versus the Mesozoic. *Evolution*, **41**, 1177–1186.

Etienne, R.S. & Haegeman, B. (2012) A conceptual and statistical framework for adaptive radiations with a key role for diversity dependence. *The American Naturalist*, **180**, E75–E89.

Farrell, B.D. (1998) "Inordinate fondness" explained: why are there so many beetles? *Science*, **281**, 555–559.

Fenton, M.B. (2010) Convergences in the diversification of bats. *Current Zoology*, **56**, 454–468.

FitzJohn, R.G., Maddison, W.P., & Otto, S.P. (2009) Estimating trait-dependent speciation and extinction rates from incompletely resolved phylogenies. *Systematic Biology*, **58**, 595–611.

Foote, M. (1993) Contributions of individual taxa to overall morphological disparity. *Paleobiology*, **19**, 403–419.

Funk, D.J. & Omland, K.E. (2003) Species-level paraphyly and polyphyly: frequency, causes, and consequences, with insights from animal mitochondrial DNA. *Annual Review of Ecology, Evolution, and Systematics*, **34**, 397–423.
Glor, R.E. (2010) Phylogenetic insights on adaptive radiation. *Annual Review of Ecology, Evolution, and Systematics*, **41**, 251–270.
Gould, S.J., Raup, D.M., & Sepkoski Jr., J.J. (1977) The shape of evolution: a comparison of real and random clades. *Paleobiology*, **3**, 23–40.
Gould, S.J., Gilinsky, N.L., & German, R.Z. (1987) Asymmetry of lineages and the direction of evolutionary time. *Science*, **236**, 1437–1441.
Harmon, L.J. (2012) An inordinate fondness for eukaryotic diversity. *PLoS Biology*, **10**, e1001382.
Harmon, L.J., Weir, J.T., Brock, C.D., Glor, R.E., & Challenger, W. (2008) GEIGER: investigating evolutionary radiations. *Bioinformatics*, **24**, 129–131.
Harrison, N. & Kidner, C.A. (2011) Next-generation sequencing and systematics: what can a billion base pairs of DNA sequence data do for you? *Taxon*, **60**, 1552–1566.
Heath, T.A., Zwickl, D.J., Kim, J., & Hillis, D.M. (2008) Taxon sampling affects inferences of macroevolutionary processes from phylogenetic trees. *Systematic Biology*, **57**, 160–166.
Hinchliff, C.E. & Roalson, E.H. (2013) Using supermatrices for phylogenetic inquiry: an example using the sedges. *Systematic Biology*, **62**, 205–219.
Jones, K.E., Bininda-Emonds, O.R.P., & Gittleman, J.L. (2005) Bats, clocks, and rocks: diversification patterns in Chiroptera. *Evolution*, **59**, 2243–2255.
Jones, K.E., Purvis, A., MacLarnon, A., Bininda-Emonds, O.R.P., & Simmons, N.B. (2002) A phylogenetic supertree of the bats (Mammalia: Chiroptera). *Biological Reviews*, **77**, 223–259.
Kass, R.E. & Raftery, A.E. (1995) Bayes factors. *Journal of the American Statistical Association*, **90**, 773–795.
Kirkpatrick, M. & Slatkin, M. (1993) Searching for evolutionary patterns in the shape of a phylogenetic tree. *Evolution*, **47**, 1171–1181.
Kisel, Y., McInnes, L., Toomey, N.H., & Orme, C.D.L. (2011) How diversification rates and diversity limits combine to create large-scale species-area relationships. *Philosophical Transactions of the Royal Society B: Biological Sciences*, **366**, 2514–2525.
Knowles, L.L. (2009) Estimating species trees: methods of phylogenetic analysis when there is incongruence across genes. *Systematic Biology*, **58**, 463–467.
Lack, J.B. & Van Den Bussche, R.A. (2010) Identifying the confounding factors in resolving phylogenetic relationships in Vespertilionidae. *Journal of Mammalogy*, **91**, 1435–1448.
Lamb, J.M., Ralph, T.M.C., Naidoo, T., Taylor, P.J., Ratrimomanarivo, F., Stanley, W.T., & Goodman, S.M. (2011) Toward a molecular phylogeny for the Molossidae (Chiroptera) of the Afro-Malagasy region. *Acta Chiropterologica*, **13**, 1–16.
Magallón, S. & Sanderson, M.J. (2001) Absolute diversification rates in angiosperm clades. *Evolution*, **55**, 1762–1780.
Martins, E.P. & Hansen, T.F. (1997) Phylogenies and the comparative method: a general approach to incorporating phylogenetic information into the analysis of interspecific data. *The American Naturalist*, **149**, 646–667.
McPeek, M.A. & Brown, J.M. (2007) Clade age and not diversification rate explains species richness among animal taxa. *The American Naturalist*, **169**, E97-106.

Meredith, R.W., Janečka, J.E., Gatesy, J., et al. (2011) Impacts of the Cretaceous terrestrial revolution and KPg extinction on mammal diversification. *Science*, **334**, 521–524.
Miller-Butterworth, C.M., Murphy, W.J., O'Brien, S.J., Jacobs, D.S., Springer, M.S., & Teeling, E.C. (2007) A family matter: conclusive resolution of the taxonomic position of the long-fingered bats, Miniopterus. *Molecular Biology and Evolution*, **24**, 1553–1561.
Moen, D. & Morlon, H. (2014) Why does diversification slow down? *Trends in Ecology & Evolution*, **29**, 190–197.
Monteiro, L.R. & Nogueira, M.R. (2011) Evolutionary patterns and processes in the radiation of phyllostomid bats. *BMC Evolutionary Biology*, **11**, 137.
Nee, S., Holmes, E.C., May, R.M., & Harvey, P.H. (1994) Extinction rates can be estimated from molecular phylogenies. *Philosophical Transactions of the Royal Society B: Biological Sciences*, **344**, 77–82.
Nee, S., Mooers, A.O., & Harvey, P.H. (1992) Tempo and mode of evolution revealed from molecular phylogenies. *Proceedings of the National Academy of Sciences of the United States of America*, **89**, 8322–8326.
Nowak, M.D. (1994) *Walker's bats of the world.* Johns Hopkins University Press, Baltimore.
Platt II, R.N., Vandewege, M.W., Kern, C., Schmidt, C.J., Hoffmann, F.G., & Ray, D.A. (2014) Large numbers of novel miRNAs originate from DNA transposons and are coincident with a large species radiation in bats. *Molecular Biology and Evolution*, **31**, 1536–1545.
Purvis, A. & Agapow, P.M. (2002) Phylogeny imbalance: taxonomic level matters. *Systematic Biology*, **51**, 844–854.
Pybus, O.G. & Harvey, P.H. (2000) Testing macro-evolutionary models using incomplete molecular phylogenies. *Proceedings of the Royal Society B: Biological Sciences*, **267**, 2267–2272.
Rabosky, D.L., Donellan, S.C., Grundler, M.C., & Lovette, I.J. (2014) Analysis and visualization of complex macroevolutionary dynamics: an example from Australian scincid lizards. *Systematic Biology*, **63**, 610–627.
Rabosky, D.L., Grundler, M.C., Anderson, C.J.R., Title, P.O., Shi, J.J., Brown, J.W., Huang, H., & Larson, J.G. (2014) BAMMtools: an R package for the analysis of evolutionary dynamics on phylogenetic trees. *Methods in Ecology and Evolution*, **5**, 701–707.
Rabosky, D.L., Santini, F., Eastman, J., Smith, S.A., Sidlauskas, B., Chang, J., & Alfaro, M.E. (2013) Rates of speciation and morphological evolution are correlated across the largest vertebrate radiation. *Nature Communications*, **4**, 1958.
Rabosky, D.L. (2009a) Ecological limits and diversification rate: alternative paradigms to explain the variation in species richness among clades and regions. *Ecology Letters*, **12**, 735–743.
Rabosky, D.L. (2009b) Ecological limits on clade diversification in higher taxa. *The American Naturalist*, **173**, 662–674.
Rabosky, D.L. (2010) Extinction rates should not be estimated from molecular phylogenies. *Evolution*, **64**, 1816–1824.
Rabosky, D.L. & Lovette, I.J. (2008) Explosive evolutionary radiations: decreasing speciation or increasing extinction through time? *Evolution*, **62**, 1866–1875.
Rabosky, D.L. (2013) Diversity-dependence, ecological speciation, and the role of competition in macroevolution. *Annual Review of Ecology, Evolution, and Systematics*, **44**, 481–502.
Rabosky, D.L. (2014) Automatic detection of key innovations, rate shifts, and diversity-dependence on phylogenetic trees. *PLoS One*, **9**, e89543.

Raia, P., Carotenuto, F., Passaro, F., Piras, P., Fulgione, D., Werdelin, L., Saarinen, J., & Fortelius, M. (2012) Rapid action in the Palaeogene, the relationship between phenotypic and taxonomic diversification in Coenozoic mammals. *Proceedings of the Royal Society B: Biological Sciences*, **280**, 20122244.

Raup, D.M., Gould, S.J., Schopf, T.J.M., & Simberloff, D.S. (1973) Stochastic models of phylogeny and the evolution of diversity. *The Journal of Geology*, **81**, 525–542.

Revell, L.J. (2012) Phytools: an R package for phylogenetic comparative biology (and other things). *Methods in Ecology and Evolution*, **3**, 217–223.

Rojas, D., Vale, Á., Ferrero, V., & Navarro, L. (2012) The role of frugivory in the diversification of bats in the Neotropics. *Journal of Biogeography*, **39**, 1948–1960.

Rosenzweig, M.L. & McCord, R.D. (1991) Incumbent replacement: evidence for long-term evolutionary progress. *Paleobiology*, **17**, 202–213.

Sahney, S., Benton, M.J., & Ferry, P.A. (2010) Links between global taxonomic diversity, ecological diversity and the expansion of vertebrates on land. *Biology Letters*, **6**, 544–547.

Salichos, L. & Rokas, A. (2013) Inferring ancient divergences requires genes with strong phylogenetic signals. *Nature*, **497**, 327–331.

Sanderson, M.J. (2002) Estimating absolute rates of molecular evolution and divergence times: a penalized likelihood approach. *Molecular Biology and Evolution*, **19**, 101–109.

Sanderson, M.J., Boss, D., Chen, D., Cranston, K.A., & Wehe, A. (2008) The PhyLoTA Browser: processing GenBank for molecular phylogenetics research. *Systematic Biology*, **57**, 335–346.

Santana, S.E., Grosse, I.R., & Dumont, E.R. (2012) Dietary hardness, loading behavior, and the evolution of skull form in bats. *Evolution*, **66**, 2587–2598.

Schluter, D. (2000) *The ecology of adaptive radiation.* Oxford University Press, Oxford.

Simmons, N.B. & Conway, T.M. (2003) Evolution of ecological diversity in bats. *Bat ecology* (ed. by T.H. Kunz and M.B. Fenton), pp. 493–535. University of Chicago Press, Chicago.

Simmons, N.B. (2005a) An Eocene big bang for bats. *Science*, **307**, 527–528.

Simmons, N.B. (2005b) Order Chiroptera. *Mammal species of the world: a taxonomic and geographic reference* (ed. by D.E. Wilson and D.M. Reeder), pp. 312–529. Johns Hopkins University Press, Baltimore.

Simmons, N.B., Seymour, K.L., Habersetzer, J., & Gunnell, G.F. (2008) Primitive early Eocene bat from Wyoming and the evolution of flight and echolocation. *Nature*, **451**, 818–821.

Simpson, G.G. (1953) *The major features of evolution.* Columbia City Press, New York.

Slater, G.J., Harmon, L.J., Wegmann, D., Joyce, P., Revell, L.J., & Alfaro, M.E. (2012) Fitting models of continuous trait evolution to incompletely sampled comparative data using approximate Bayesian computation. *Evolution*, **66**, 752–762.

Smith, S.A., Beaulieu, J.M., & Donoghue, M.J. (2009) Mega-phylogeny approach for comparative biology: an alternative to supertree and supermatrix approaches. *BMC Evolutionary Biology*, **9**, 37.

Smith, S.A. & Dunn, C.W. (2008) Phyutility: a phyloinformatics tool for trees, alignments and molecular data. *Bioinformatics*, **24**, 715–716.

Smith, S.A. & O'Meara, B.C. (2012) treePL: divergence time estimation using penalized likelihood for large phylogenies. *Bioinformatics*, **28**, 2689–2690.

Springer, M.S., Murphy, W.J., Eizirik, E., & O'Brien, S.J. (2003) Placental mammal diversification and the Cretaceous-Tertiary boundary. *Proceedings of the National Academy of Sciences of the United States of America*, **100**, 1056–1061.
Stadler, T., Rabosky, D.L., Ricklefs, R.E., & Bokma, F. (2014) On age and species richness of higher taxa. *The American Naturalist*, **184**, 447–455.
Stamatakis, A. (2014) RAxML version 8: a tool for phylogenetic analysis and post-analysis of large phylogenies. *Bioinformatics*, **30**, 1312–1313.
Stanley, S.M. (1979) *Macroevolution: pattern and process.* W.H. Freeman, San Francisco.
Strathmann, R.R. & Slatkin, M. (1983) The improbability of animal phyla with few species. *Paleobiology*, **9**, 97–106.
Talavera, G. & Castresana, J. (2007) Improvement of phylogenies after removing divergent and ambiguously aligned blocks from protein sequence alignments. *Systematic Biology*, **56**, 564–577.
Teeling, E.C., Madsen, O., Van den Bussche, R.A., de Jong, W.W., Stanhope, M.J., & Springer, M.S. (2002) Microbat paraphyly and the convergent evolution of a key innovation in Old World rhinolophoid microbats. *Proceedings of the National Academy of Sciences of the United States of America*, **99**, 1431–1436.
Teeling, E.C., Madsen, O., Murphy, W.J., Springer, M.S., & O'Brien, S.J. (2003) Nuclear gene sequences confirm an ancient link between New Zealand's short-tailed bat and South American noctilionoid bats. *Molecular Phylogenetics and Evolution*, **28**, 308–319.
Teeling, E.C., Springer, M.S., Madsen, O., Bates, P., O'Brien, S.J., & Murphy, W.J. (2005) A molecular phylogeny for bats illuminates biogeography and the fossil record. *Science*, **307**, 580–584.
Teeling, E.C., Dool, S., & Springer, M.S. (2012) Phylogenies, fossils, and functional genes: the evolution of echolocation in bats. *Evolutionary history of bats: fossils, molecules, and morphology* (ed. by G.F. Gunnell and N.B. Simmons), pp. 1–22. Cambridge University Press, Cambridge.
Van Valen, L. (1979) The evolution of bats. *Evolutionary Theory*, **4**, 103–121.
Vrba, E.S. (1992) Mammals as a key to evolutionary theory. *Journal of Mammalogy*, **73**, 1–28.
Weir, J.T. & Price, T.D. (2011) Limits to speciation inferred from times to secondary sympatry and ages of hybridizing species along a latitudinal gradient. *The American Naturalist*, **177**, 462–469.
Wiens, J.J. (2011) The causes of species richness patterns across space, time, and clades and the role of "ecological limits." *The Quarterly Review of Biology*, **86**, 75–96.
Yoder, J.B., Clancey, E., Des Roches, S., Eastman, J.M., Gentry, L., Godsoe, W., Hagey, T.J., Jochimsen, D., Oswald, B.P., Robertson, J., Sarver, B.A.J., Schenk, J.J., Spear, S.F., & Harmon, L.J. (2010) Ecological opportunity and the origin of adaptive radiations. *Journal of Evolutionary Biology*, **23**, 1581–1596.
Yu, W., Wu, Y., & Yang, G. (2014) Early diversification trend and Asian origin for extent bat lineages. *Journal of Evolutionary Biology*, **27**, 2204–2218.
Zanne, A.E., Tank, D.C., Cornwell, W.K., *et al*. (2014) Three keys to the radiation of angiosperms into freezing environments. *Nature*, **506**, 89–92.

Table 2.1. **Genetic loci and phylogenetic coverage**
Loci included in this study, as well as relevant information on location, length, phylogenetic coverage, and the GenBank coverage/identity scores used to parameterize PHLAWD searches and alignments. This table is abbreviated; see published study for full metadata.

Locus	Abbreviation	Genome	Base pairs	Taxa	Families
12S, tRNA-Valine, and/or 16S	12S-tRNAVal-16S	mitochondrion	2306	269	15
adenosine A3 receptor	ADORA3	nucleus	320	33	7
beta-2 adrenergic receptor	ADRB2	nucleus	700	32	7
apolipoprotein B	apoB	nucleus	277	135	7
amyloid precursor protein	APP	nucleus	612	28	7
copper-transporting ATPase 1	ATP7A	nucleus	628	35	7
brain-derived neurotrophic factor	BDNF	nucleus	533	33	7
beta fibrinogen	BFIB	nucleus	624	57	7
breast cancer type 1 susceptibility protein	BRCA1	nucleus	1316	85	7
c-mos oocyte maturation protooncogene	C-MOS	nucleus	463	41	7
cytochrome oxidase subunit 1	COI	mitochondrion	651	489	16
cytochrome *b*	CYTB	mitochondrion	706	743	18
endothelial differentiation gene 1	EDG1	nucleus	370	30	7
potassium voltage-gated channel subfamily KQT member 4	KCNQ4	nucleus	160	22	6
NADH dehydrogenase subunit 1	ND1	mitochondrion	798	236	11
NADH dehydrogenase subunit 2	ND2	mitochondrion	1043	163	7
blue-sensitive opsin	OPN1SW	nucleus	1895	35	7
prepronociceptin	PNOC	nucleus	269	32	7
protein kinase C iota	PRKC1	nucleus	369	174	10
recombination activating protein 1	RAG1	nucleus	768	129	7
recombination activating protein 2	RAG2	nucleus	752	335	15
spectrin non-erythroid beta chain 1	SPTBN	nucleus	574	44	7
signal transducer and activator of transcription 5A	STAT5A	nucleus	461	146	7
taste receptor type 1 member 2	TAS1R2	nucleus	711	42	7
thyroid stimulating hormone beta	TSHB	nucleus	407	109	7
titin	TTN	nucleus	1155	33	7
tyrosinase	TYR	nucleus	325	31	7
von Willenbrand factor	VWF	nucleus	1005	132	7
zinc finger protein X-linked	ZFX	nucleus	178	25	6

Table 2.2. Fossil constraints
Fossil taxa used to time-calibrate the phylogenies in this study, along with relevant citations and defined clades. Unless otherwise indicated, dates were considered minimum constraints for the specified group(s). Constraints marked with an asterisk were also used to time-calibrate our bootstrap replicates, as they were either included in the backbone during tree searching or were always recovered as monophyletic. Full citation information can be found in the Supplementary Materials of the published paper.

Fossil constraint	**Clade**	**Approximate Fossil Date**	**Citation(s)**
*Onychonycteris finneyi**	Chiroptera	55.8 mya	Simmons *et al.* 2008
Rhinolophoidea*	Rhinolophoidea	55 mya (maximum)	Teeling *et al.* 2005
*Rhinolophus**	crown *Rhinolophus*	37.2 mya	Crochet *et al.* 1981, Teeling *et al.* 2005
*Hipposideros**	crown *Hipposideros*, internal Hipposideridae	40.4 mya	Crochet *et al.* 1981, Sigé 1988
Rhinolophidae, Hipposideridae split	Rhinolophidae, Hipposideridae divergence time	37 mya	Teeling *et al.* 2003, Almeida *et al.* 2009
*Macroderma**	crown *Macroderma*, internal Megadermatidae	23.03 mya	Hand & Archer 2005
Megadermatidae, Rhinopomatidae split	Rhinopomatidae divergence time	34 mya	McKenna & Bell 1997, Teeling *et al.* 2003, 2005, Almeida *et al.* 2009
*Tachypteron**	Emballonuridae	44 mya	Storch *et al.* 2002
Diclidurus	crown *Diclidurus*, internal Emballonuridae	13 mya	Carlini *et al.* 1997, Czaplewski 1997
*Nycteris**	Nycteridae	5.332 mya	Black & Krishtalka 1986
Mystacinidae	Mystacinidae	20.1 mya	Hand et al. 2013
*Thyroptera lavali**	Thyropteridae	13 mya	Czaplewski 1997, Czaplewski *et al.* 2003
Mormoopidae*	Mormoopidae	30 mya	Morgan & Czaplewski 2003, Teeling *et al.* 2005
*Noctilio albiventris**	Noctilionidae	13 mya	Czaplewski 1997, Czaplewski *et al.* 2003
Phyllostomidae*	Phyllostomidae	34 mya (maximum)	Teeling *et al.* 2005

*Palynephyllum**	crown Lonchophyllinae, internal Phyllostomidae	13 mya	Dávalos *et al.* 2014
Desmodus archaeodaptes	crown Desmodontinae, internal Phyllostomidae	4.9 mya	Morgan 1991
Nataloidea*	Natalidae	43 mya	McKenna & Bell 1997, but see Simmons & Geisler 1998, Morgan & Czaplewski 2003
Molossidae*	Molossidae	37.2 mya	Arroyo-Cabrales *et al.* 2002, Teeling *et al.* 2005
Eumops	crown Eumops, internal Molossidae	13 mya	Czaplewski *et al.* 2003
*Miniopterus fossilis**	Miniopteridae	13.65 mya	Sabol & Holec 2002
*Stehlinia**	Vespertilionidae	42.7 mya	Gunnell & Simmons 2012, Gunnell (pers. comm.)
*Myotis**	crown Myotinae, internal Vespertilionidae	27 mya	Gunnell & Simmons 2012, Gunnell (pers. comm.)

Table 2.3. Stem and crown age comparisons
Comparisons of family-level stem ages / crown ages (for families with more than one representative), in millions of years, for our ML phylogeny, and for the previous studies of Jones *et al.* (2005) and Teeling *et al.* (2005). For this table, Vespertilionidae includes the now-separate families of Vespertilionidae, Miniopteridae, and Cistugidae. For Natalidae and Rhinolophidae, alternate crown dates are also provided by excluding their fossils (see Table 2.2 and Supplementary Materials of published paper for Natalidae discussion), but usage of these dates do not affect any results.

Family	**this study**	**Jones *et al*. (2005)**	**Teeling *et al.* (2005)**
Vespertilionidae	52.1 / 51.1	47.1 / 47.0	49.3 / 49.2
Molossidae	53.8 / 45.2	47.1 / 35.7	49.3 / 38.2
Natalidae	54.8 / 43.0 (22.2)	50.1 / 15.1	51.4 / 17.3
Phyllostomidae	43.3 / 34.0	37.1 / 27.4	38.8 / 28.1
Mormoopidae	43.3 / 39.2	37.1 / 33,7	38.8 / 34.2
Thyropteridae	46.8 / 13.8	50.2 / 12.9	42.1 / 15.0
Noctilionidae	42.9 / 13.0	42.7 / 3.0	36.2 / 2.6
Furipteridae	42.9 / NA	50.1 / 0.1	36.2 / 0.1
Mystacinidae	50.3 / NA	42.8 / 42.8	46.1 / 46.1
Myzopodidae	54.1 / 1.1	51.8 / 51.8	51.6 / 51.6
Emballonuridae	52.8 / 47.7	53.7 / 45.0	52.1 / 46.1
Nycteridae	52.8 / 17.9	43.4 / 26.2	52.1 / 26.1
Rhinolophidae	49.9 / 49.8 (37.2)	28.7 / 6.5	34.9 / 8.7
Hipposideridae	49.9 / 49.3	28.7 / 26.5	34.9 / 34.8
Rhinopomatidae	51.9 / 26.9	12.0 / 9.5	39.0 / 19.4
Craseonycteridae	51.9 / NA	12.0 / 12.0	38.9 / 38.9
Megadermatidae	53.4 / 27.2	43.5 / 39.2	38.9 / 38.9
Pteropodidae	56.6 / 40.2	61.7 / 36.1	55.8 / 24.6

Table 2.4. Crown age ranges across bootstrap replicates
Variation in family-level (non-monotypic) crown ages (in millions of years) across all bootstrap replicate phylogenies. For this table, Vespertilionidae includes the now-separate families of Vespertilionidae, Miniopteridae, and Cistugidae. We report the mean and median inferences, and the full range, in millions of years. Other unreported families (Natalidae, Noctilionidae, Myzopodidae, Phyllostomidae, Megadermatidae) do not vary at this precision across bootstrap replicates, and match the inferences found in Table 2.3.

Family	mean	median	range
Vespertilionidae	51.1	51.1	46.0 - 54.1
Molossidae	40.4	39.4	37.2 - 46.8
Mormoopidae	38.1	38.2	30.6 - 41.3
Thyropteridae	14.1	14	13.0 - 16.5
Emballonuridae	46.8	46.9	44.0 - 48.5
Nycteridae	18.1	18.1	15.0 - 19.8
Rhinolophidae	47.6	47.5	45.9 - 54.3
Hipposideridae	46.5	46.6	40.4 - 51.9
Rhinopomatidae	27	26.5	17.5 - 34.2
Pteropodidae	32.6	30	22.0 - 41.0

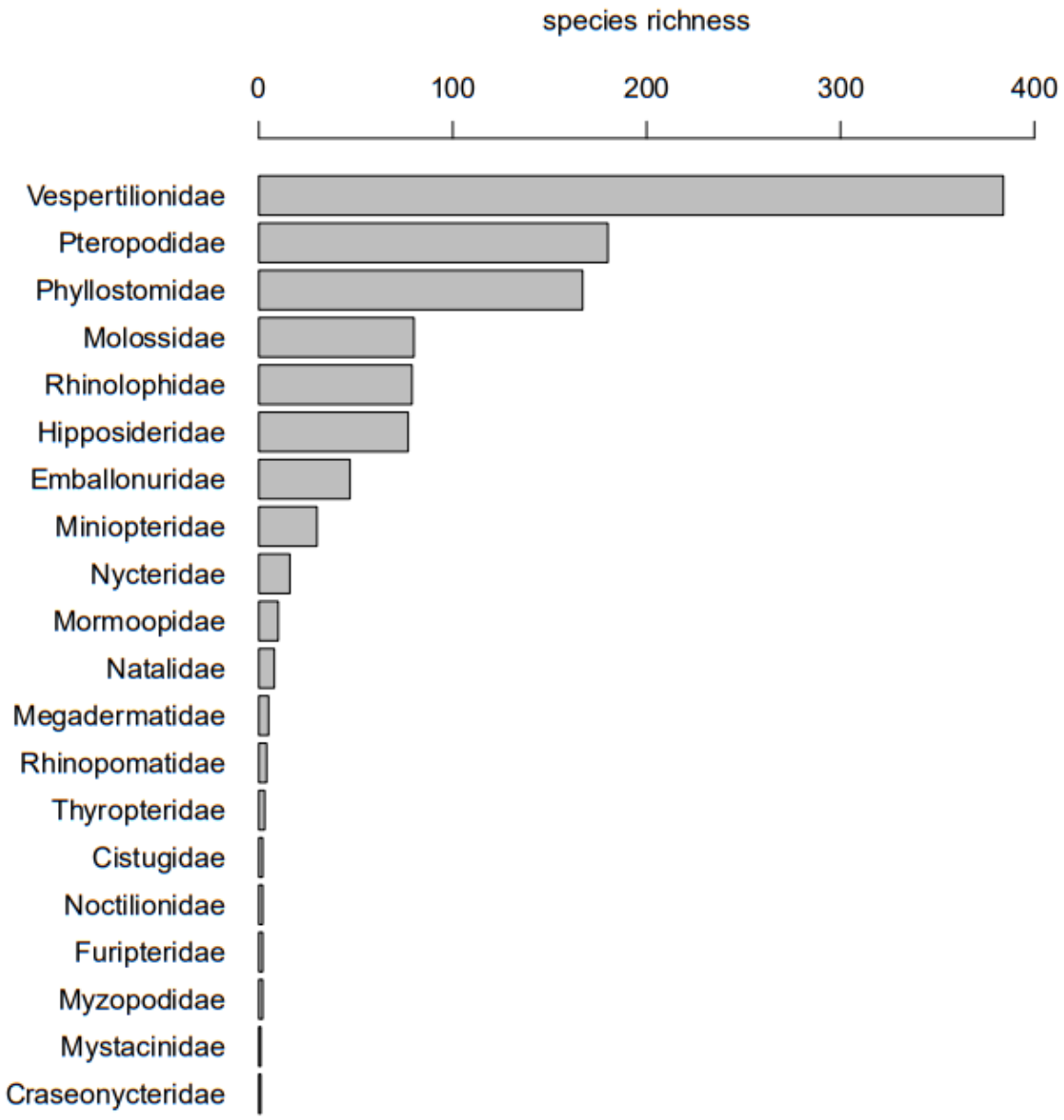

Figure 2.1 Species richness patterns across bats
Species richnesses of all extant bat families in rank-order, taken from Simmons (2005b).

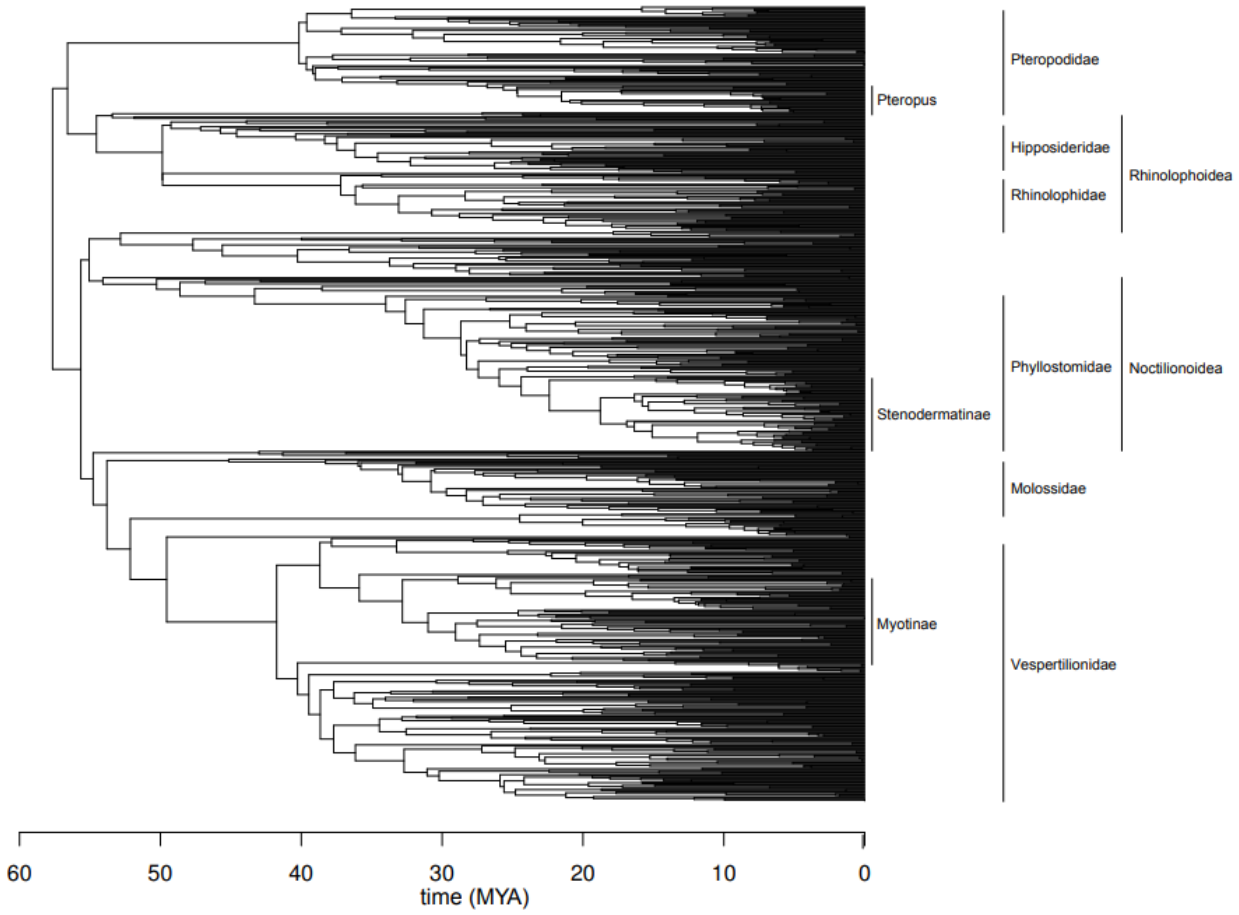

Figure 2.2 Maximum-likelihood phylogeny of bats
Time-calibrated (axis in millions of years), maximum-likelihood phylogeny of 812 extant species of bats. The six largest families (see Figure 2.1) of bats are labeled, as well as relevant genera, subfamilies, and superfamilies for this study.

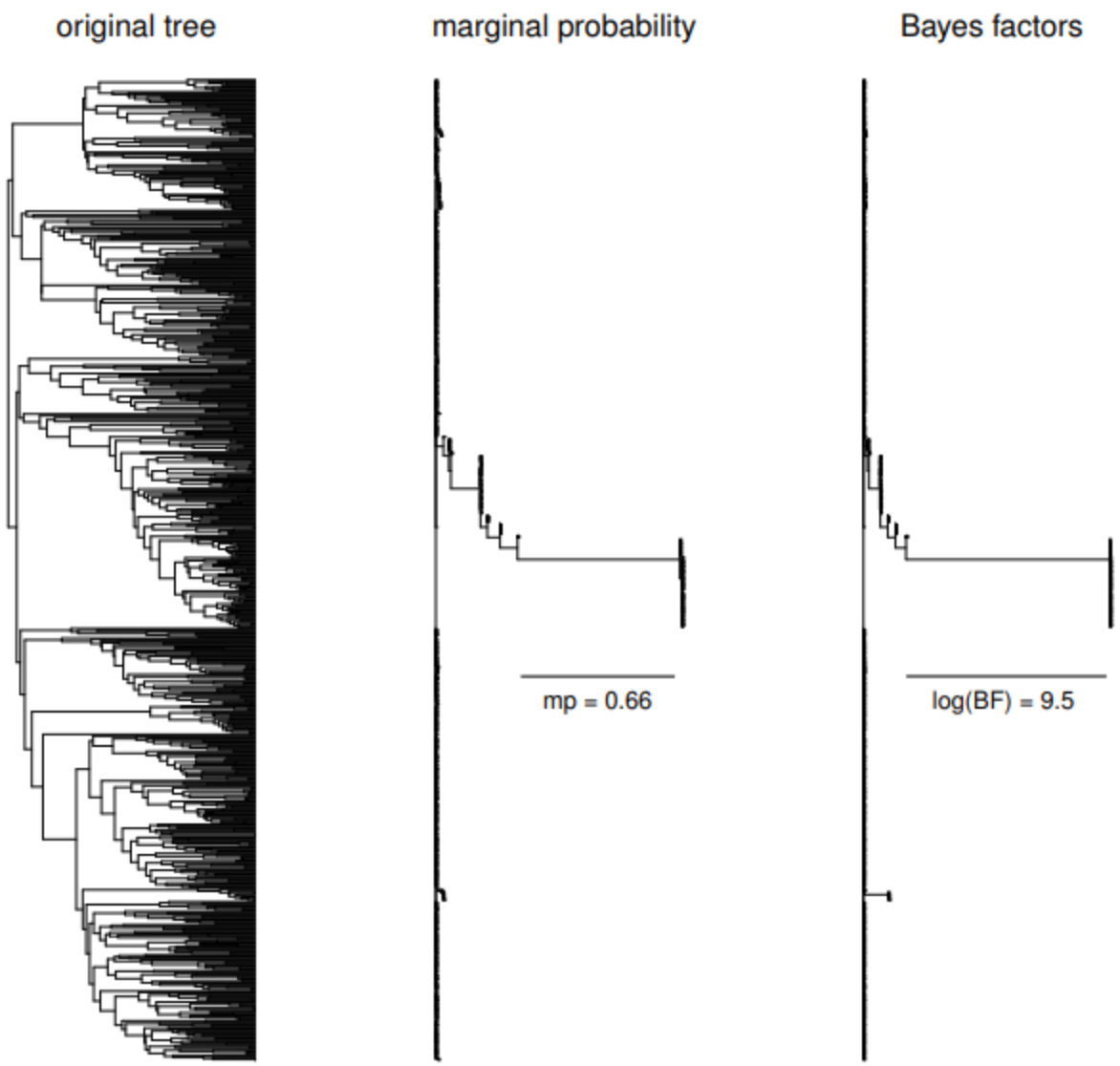

Figure 2.3 Marginal probabilities and Bayes factor evidence of regime shifts
Two different methods of weighing the relative evidence of a regime shift occurring along any individual branch. In the marginal probability (mp) tree, each individual branch length corresponds to the mp of a shift occurring along that branch across the posterior distribution of BAMM results. In the marginal Bayes factor (BF) tree, each individual branch length represents relative shift density in relation to the prior distribution. The ML tree topology from Figure 2.2 is included for reference. The longest branch length, in both mp or log(BF), is labeled for reference. In both cases, the longest branch is at the base of the subfamily Stenodermatinae.

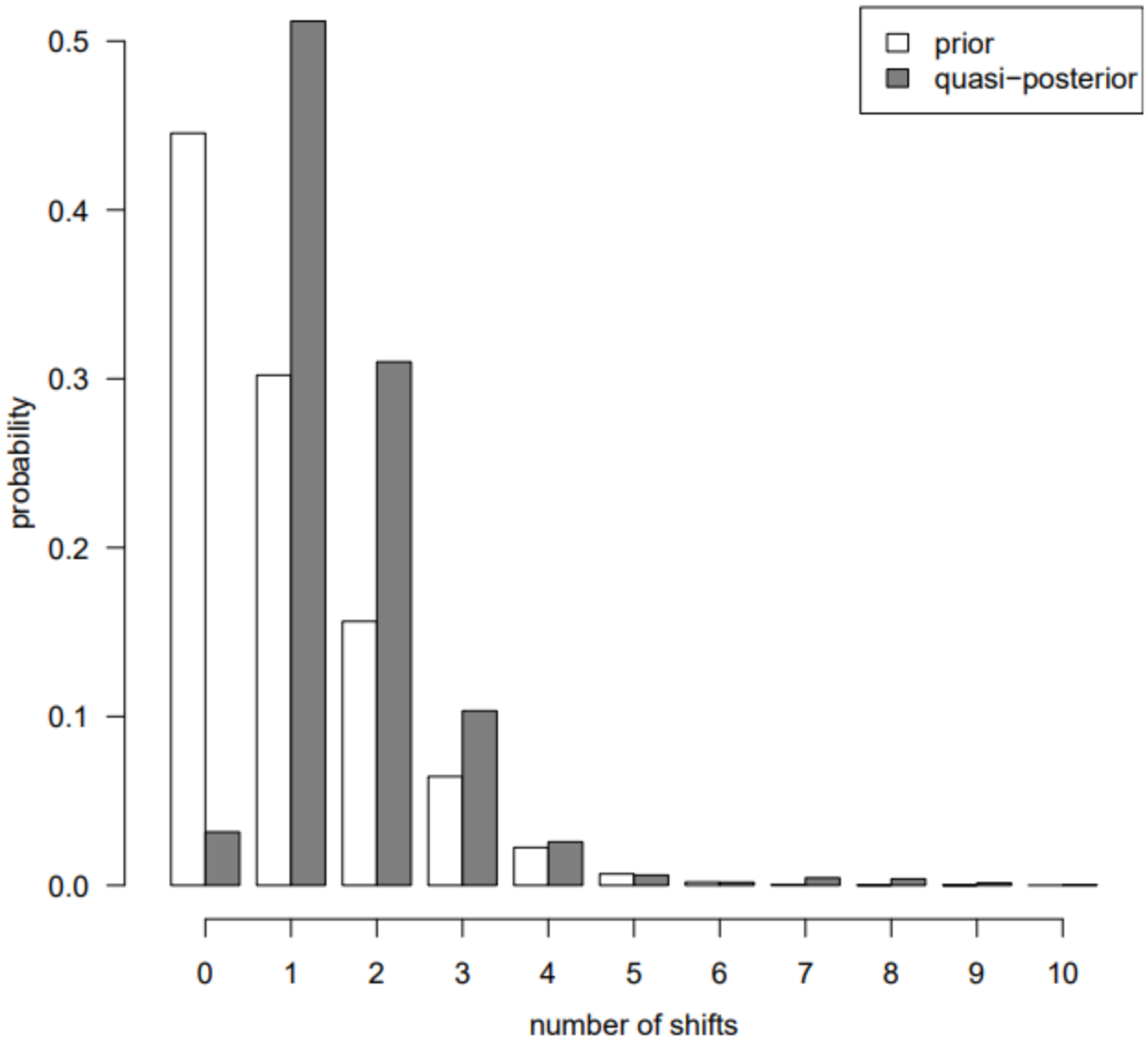

Figure 2.4 Prior and quasi-posterior distributions of shifts
The prior distribution (white) of shifts across the bat phylogeny and the quasi-posterior distribution (gray) of shifts pooled from all the BAMM results on bootstrap replicates. Note that there is nearly zero quasi-posterior probability of zero shifts, and that the highest quasi-posterior probability is for a single shift.

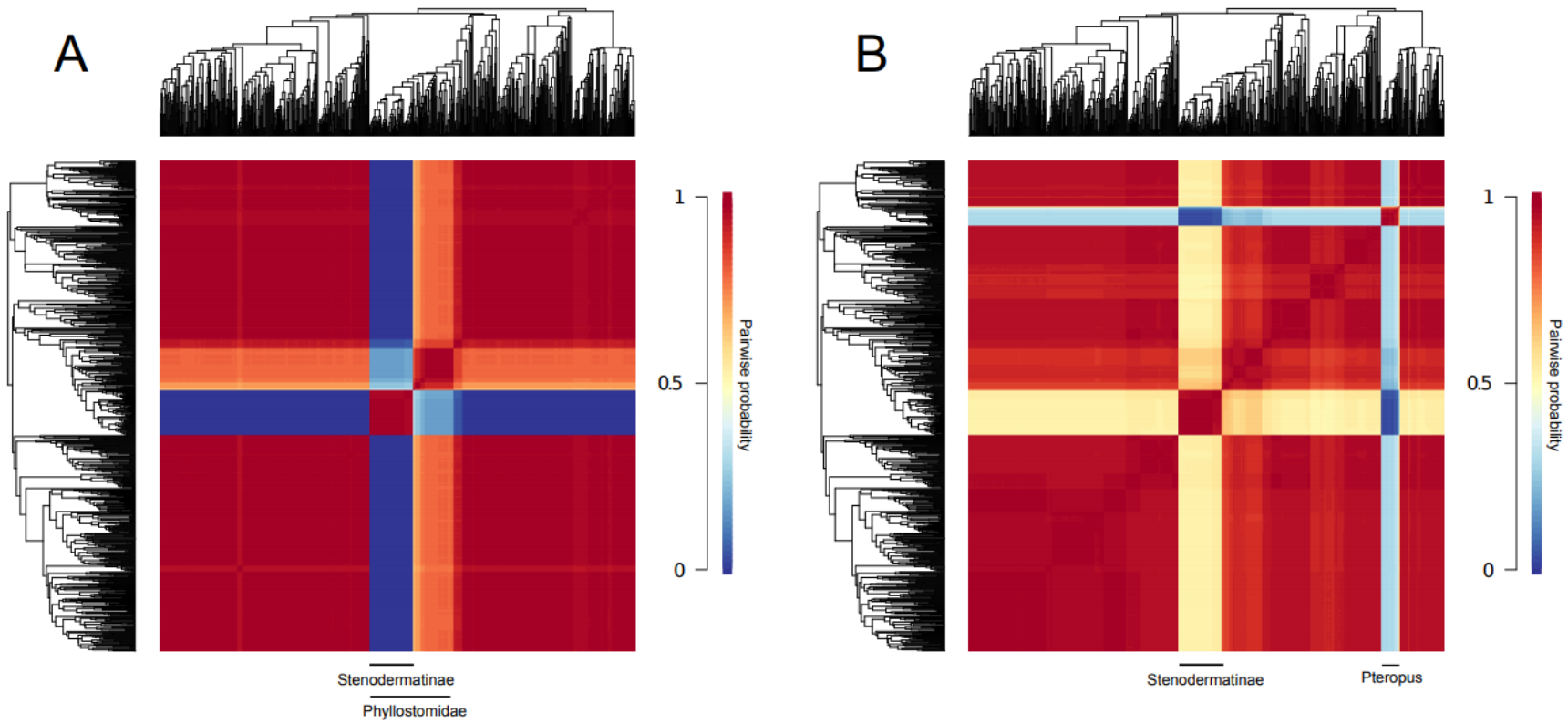

Figure 2.5 Macroevolutionary cohort matrices
(A) A macroevolutionary cohort matrix for our maximum-likelihood phylogeny of bats. There is only strong evidence for stenodermatines being part of a decoupled diversification regime from other bats. (B) A cohort matrix averaged across all bootstrap replicates to investigate the effect of topological uncertainty. Each point on the main plot represents the average probability across all bootstrap replicates that the two specified branches ever share a macroevolutionary regime. Hence, each individual bootstrap replicate was reshuffled to match the order of branches. We still find evidence for a stenodermatine cohort, but also a *Pteropus* cohort.

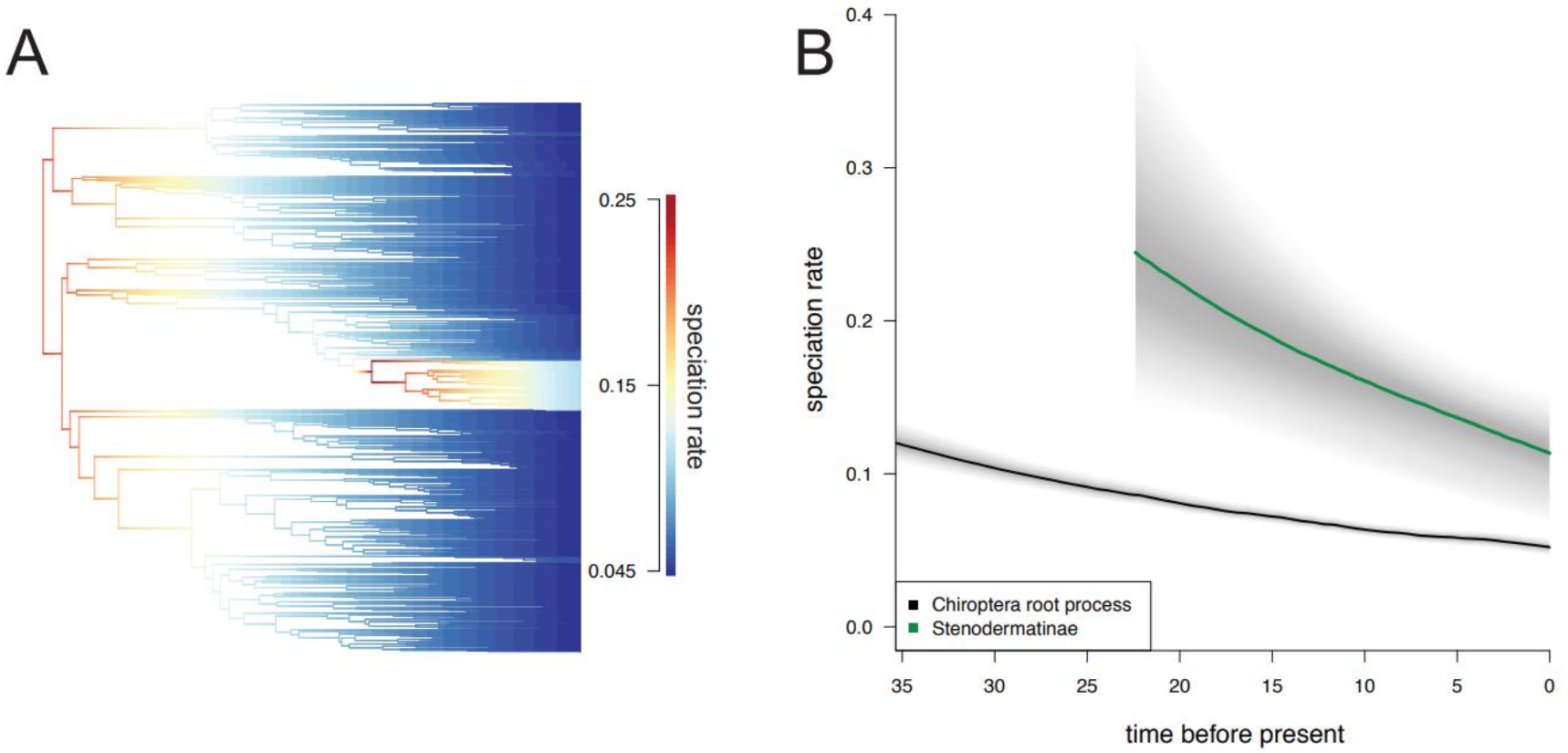

Figure 2.6 Speciation rates through time across bats
(A) Maximum-likelihood phylogeny of bats, with BAMM estimates of instantaneous speciation rate represented by colors along individual branches. (B) Instantaneous speciation rates through time for both stenodermatines (top curve) and non-stenodermatine bats (bottom curve). Around each curve, 90% credibility intervals from the posterior distribution of BAMM results. Speciation rates are the lambda rate parameters of exponential distributions.

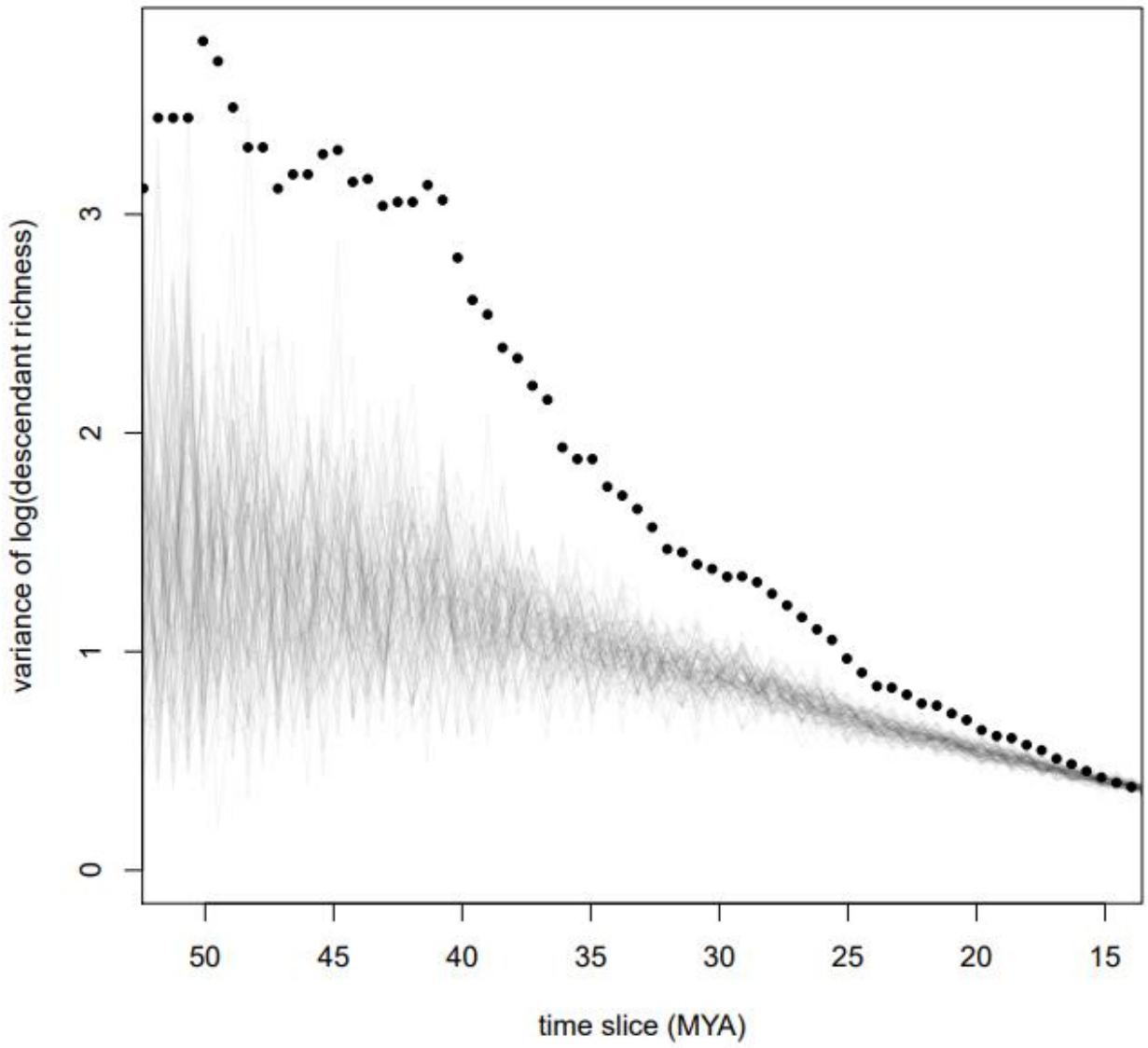

Figure 2.7 Phylogenetic imbalance through time
Changes in species richness variance across clades as lineages accumulate through time. Transparent grey lines represent 100 simulations of among-clade variance in species richness as expected under a constant rate birth-death process. Black circles represent empirical variances among clades descended from the lineages that exist at time *t*, in the maximum-likelihood phylogeny of extant bats. For most of bat history, there has been more variance in diversity among bat clades than expected under a constant rate birth-death process.

Table S2.1 Pruned taxa
List of taxa removed from the dataset following an initial RAxML search. Improvement refers to RogueNaRok criteria for pruning rogue taxa.

Taxon	Method	Improvement
Anthops ornatus	RogueNaRok	3.318
Hipposideros jonesi	RogueNaRok	3.318
Myotis davidii	RogueNaRok	1.258
Aproteles bulmerae	RogueNaRok	1.19
Arielulus cuprosus	RogueNaRok	1.014
Pipistrellus ceylonicus	RogueNaRok	0.976
Pteropus personatus	RogueNaRok	0.966
Myotis vivesi	RogueNaRok	0.804
Notopteris macdonaldi	RogueNaRok	0.77
Myotis moluccarum	RogueNaRok	0.738
Kerivoula krauensis	RogueNaRok	0.726
Hesperoptenus tomesi	RogueNaRok	0.7
Pipistrellus nanulus	RogueNaRok	0.636
Artibeus cinereus	RogueNaRok	0.624
Myotis alcathoe	RogueNaRok	0.604
Pteralopex acrodonta	RogueNaRok	0.574
Hipposideros lankadiva	RogueNaRok	0.548
Pipistrellus rueppellii	RogueNaRok	0.506
Chaerephon atsinanana	Long branch length	NA
Aethalops aequalis	Long branch length	NA

Table S2.2 Supermatrix genus-level sampling percentages

Approximate supermatrix sampling percentages (*i.e.* at least one locus was included per species) for all extant genera of bats included in this study; these percentages were used to parameterize BAMM analysis and account for incomplete sampling. Total richness estimates are from Simmons (2005b).

Genus	Approximate sampling fraction
Acerodon	40%
Aethalops	50%
Alionycteris	100%
Ametrida	100%
Anoura	80%
Antrozous	100%
Ardops	100%
Arielulus	40%
Ariteus	100%
Artibeus	100%
Asellia	50%
Aselliscus	100%
Balantiopteryx	100%
Balionycteris	100%
Barbastella	100%
Boneia	100%
Brachyphylla	100%
Cardioderma	100%
Carollia	100%
Casinycteris	100%
Centronycteris	100%
Centurio	100%
Chaerephon	50%
Chalinolobus	100%
Cheiromeles	100%
Chilonatalus	100%
Chiroderma	100%
Chironax	100%
Choeroniscus	66.70%
Choeronycteris	100%
Chrotopterus	100%
Cistugo	100%
Cloeotis	100%
Coelops	100%
Coleura	100%
Cormura	100%
Corynorhinus	66.70%
Craseonycteris	100%
Cynomops	60%
Cynopterus	57.10%
Cyttarops	100%
Dermanura	44.40%
Desmalopex	100%
Desmodus	100%
Diaemus	100%
Diclidurus	100%
Diphylla	100%
Dobsonia	42.90%
Dyacopterus	50%
Ectophylla	100%
Eidolon	50%
Emballonura	100%
Eonycteris	100%
Epomophorus	50%
Epomops	33.30%
Eptesicus	78.30%
Erophylla	100%
Euderma	100%
Eudiscopus	100%
Eumops	100%
Falsistrellus	20%
Furipterus	100%
Glauconycteris	25%
Glischropus	50%
Glossophaga	100%
Glyphonycteris	66.70%
Haplonycteris	100%
Harpiocephalus	100%
Harpiola	100%
Harpyionycteris	100%
Hesperoptenus	40%
Hipposideros	62.70%
Histiotus	28.60%
Hylonycteris	100%
Hypsignathus	100%
Hypsugo	38.90%
Ia	100%
Idionycteris	100%
Kerivoula	52.60%
Laephotis	75%
Lasionycteris	100%
Lasiurus	47.10%
Latidens	100%
Leptonycteris	66.70%
Lichonycteris	100%
Lionycteris	100%
Lonchophylla	71.40%
Lonchorhina	60%
Lophostoma	100%

Macroderma	100%
Macroglossus	100%
Macrophyllum	100%
Macrotus	100%
Megaderma	100%
Megaerops	100%
Megaloglossus	100%
Melonycteris	100%
Mesophylla	100%
Micronycteris	100%
Micropteropus	50%
Mimon	75%
Miniopterus	100%
Molossops	75%
Molossus	50%
Monophyllus	100%
Mops	33.30%
Mormoops	66.70%
Mormopterus	40%
Mosia	100%
Murina	100%
Musonycteris	100%
Myonycteris	100%
Myopterus	50%
Myotis	86.40%
Mystacina	50%
Myzopoda	100%
Nanonycteris	100%
Natalus	100%
Neoromicia	63.60%
Noctilio	100%
Nyctalus	87.50%
Nycteris	43.80%
Nycticeinops	100%
Nycticeius	33.30%
Nyctiellus	100%
Nyctimene	46.70%
Nyctinomops	100%
Nyctophilus	27.30%
Otomops	42.90%
Otonycteris	100%
Otopteropus	100%
Paranyctimene	50%
Parastrellus	100%
Penthetor	100%
Peropteryx	100%
Philetor	100%
Phoniscus	25%

Phylloderma	100%
Phyllonycteris	100%
Phyllops	100%
Phyllostomus	100%
Pipistrellus	48.40%
Platalina	100%
Platyrrhinus	100%
Plecotus	100%
Promops	50%
Ptenochirus	100%
Pteralopex	20%
Pteronotus	100%
Pteropus	46.20%
Pygoderma	100%
Rhinolophus	76.60%
Rhinonicteris	100%
Rhinophylla	100%
Rhinopoma	75%
Rhogeessa	90%
Rhynchonycteris	100%
Rousettus	60%
Saccolaimus	50%
Saccopteryx	80%
Sauromys	100%
Scotoecus	20%
Scotomanes	100%
Scotonycteris	50%
Scotophilus	91.70%
Sphaerias	100%
Sphaeronycteris	100%
Stenoderma	100%
Stenonycteris	50%
Sturnira	100%
Styloctenium	100%
Syconycteris	33.30%
Tadarida	50%
Taphozous	42.90%
Thoopterus	100%
Thyroptera	100%
Tonatia	100%
Trachops	100%
Triaenops	100%
Tylonycteris	100%
Uroderma	100%
Vampyressa	100%
Vampyrodes	100%
Vampyrum	100%
Vespertilio	100%

Table S2.3 Effects of incomplete sampling
Phylogenies simulated under a pure birth model with differing levels of incomplete sampling, and the resulting γ-statistic (Pybus & Harvey 2000) for each level of sampling. Each phylogeny has 812 tips following random sampling from a larger simulated phylogeny, simulating the effect of having more bat diversity than assumed. Each percentage was simulated 10 times, with the statistics averaged. For reference, our phylogeny assumes we sample 812 out of all ~1300 (62.5%) bat species, and we empirically infer γ-statistics on the order of -10.3 (see Results).

total taxa	sampling percentage	average γ-statistic
1353	60%	-4.08
1476	55%	-4.93
1624	50%	-5.67
1804	45%	-6.63
2030	40%	-7.69
2320	35%	-8.89
2707	30%	-9.96
3248	25%	-11.06
4060	20%	-12.24
5413	15%	-14.95
8120	10%	-17.47

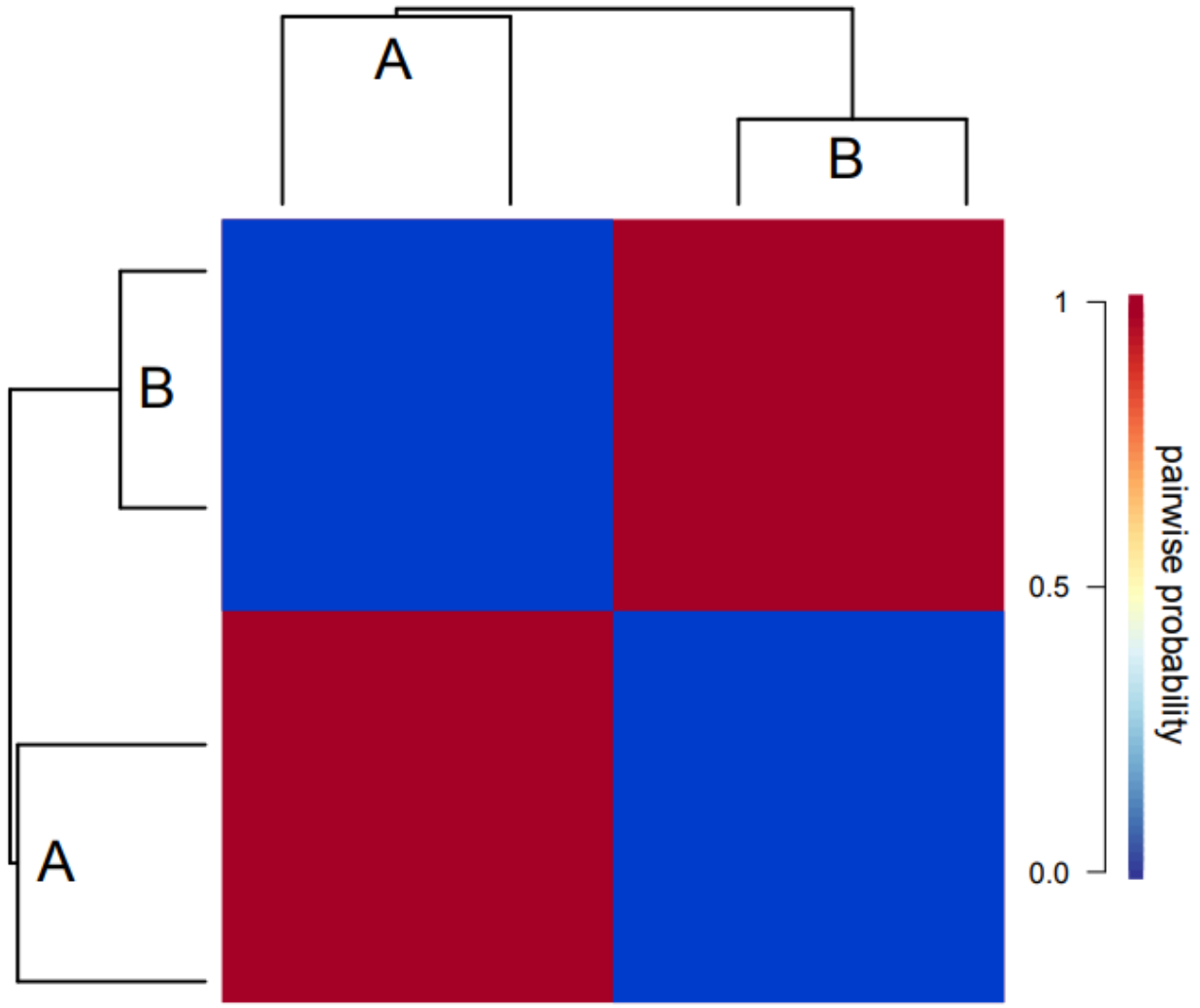

Figure S2.1 Sample cohort matrix
An example cohort matrix constructed using a simulated phylogeny of 4 taxa, separated into two clades A and B. The same phylogeny is mirrored on the left and top of the matrix. The matrix itself depicts two macroevolutionary cohorts, or groups of tips with elevated probabilities (colored according to the legend) of sharing the same macroevolutionary regime. In this example, both clades have a high probability of being their own, independent cohorts, with very low probabilities that they belong to the same cohort and evolved under the same diversification dynamic.

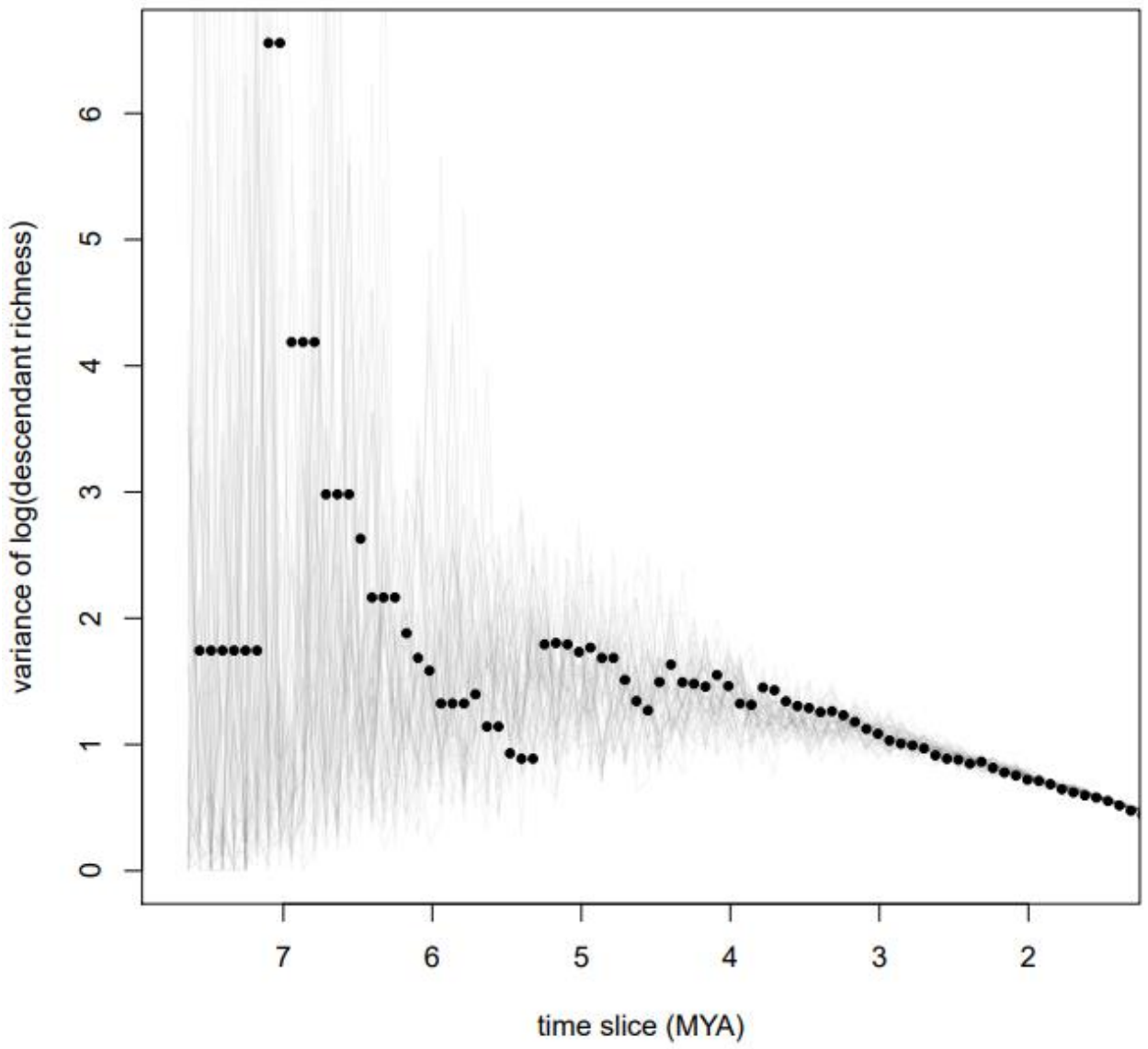

Figure S2.2 Null expectation of imbalance through time
The null expectation of a constant rate birth-death process for our operational definition of imbalance and its change through time. This simulated phylogeny contains 3125 taxa randomly sampled from 5000 taxa, to match the sampling percentage in our bat phylogeny. As expected, the simulated estimates of imbalance fall entirely within the null distribution of imbalance.

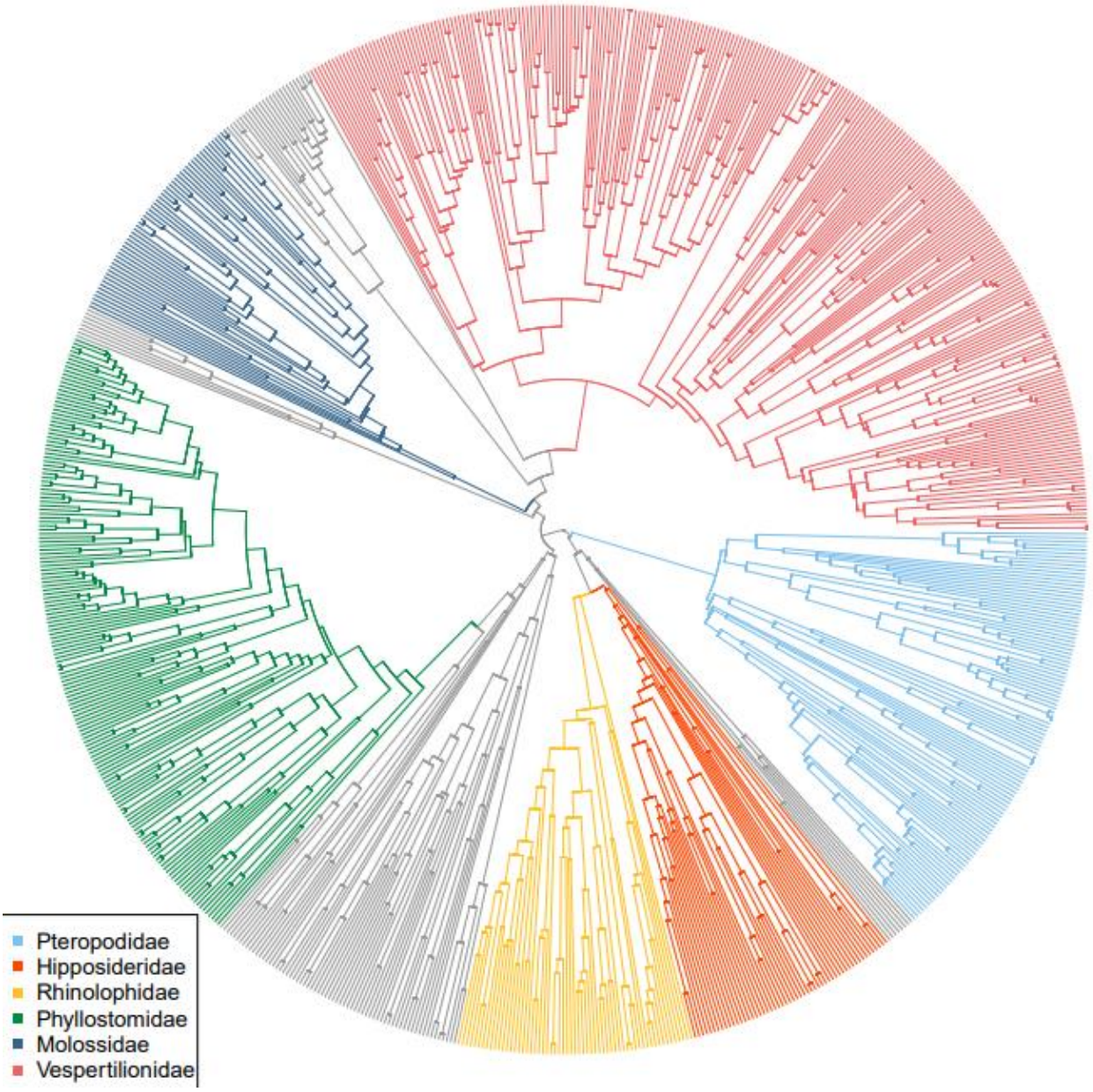

Figure S2.3 Fan phylogeny of bats
The maximum-likelihood phylogeny of 812 extant species of bats based on 29 genetic loci (Table 2.1), with the most species-rich families labeled.

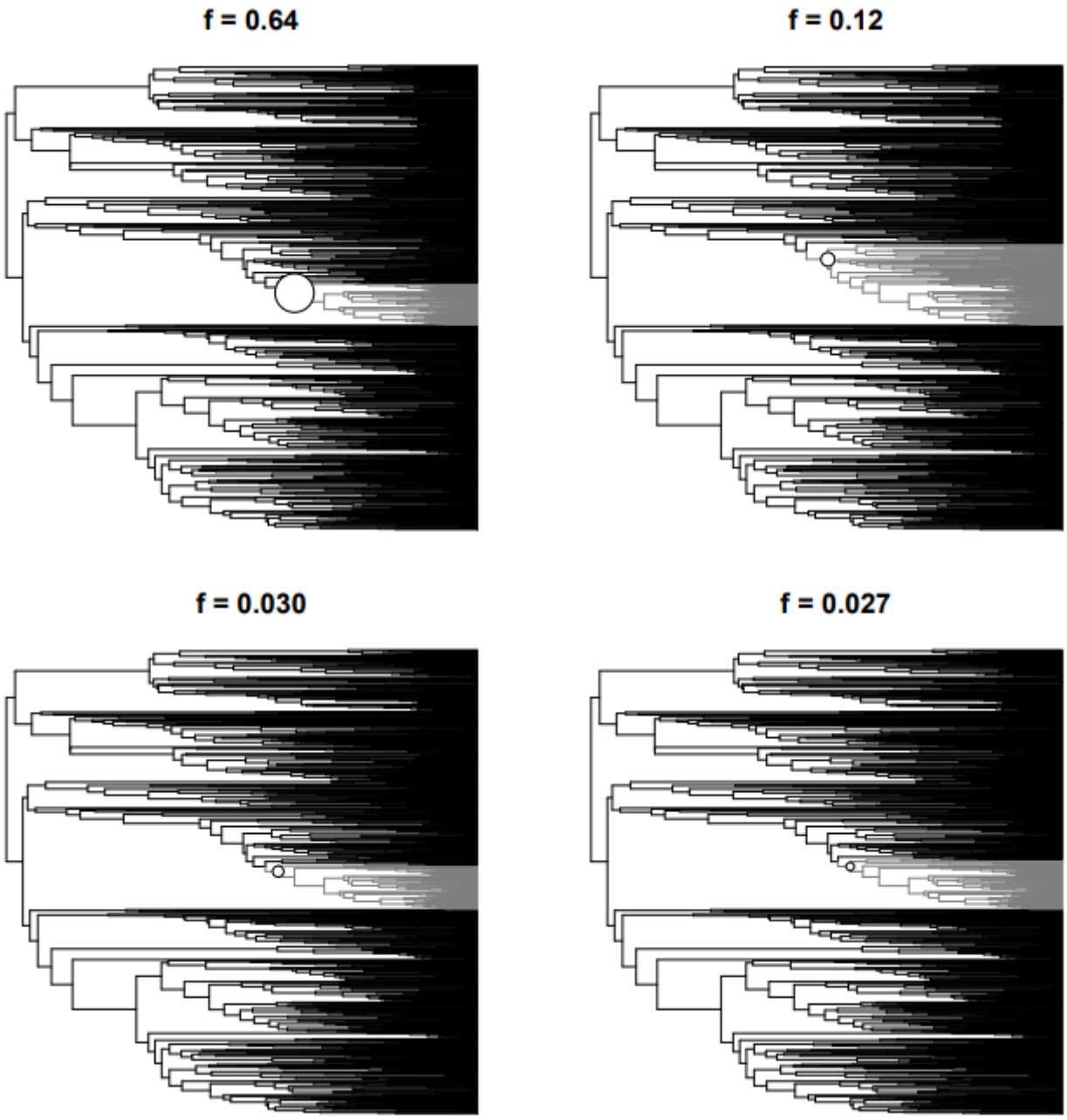

Figure S2.4 Credible shift configurations
A set of shift configurations comprising the four most credible of all possible shift configurations from our BAMM analysis on the ML phylogeny. Branch shades represent different macroevolutionary regimes. Shift locations are denoted by circles on each phylogeny. The marginal probability of an individual shift location is depicted as the size of the circle. The subfamily Stenodermatinae is either the location of a shift or nested within a shift for every configuration here. This is also true for the rest of the 95% credibility interval, which is not included for ease of interpretation. The frequency of each shift configuration is labeled above the phylogeny.

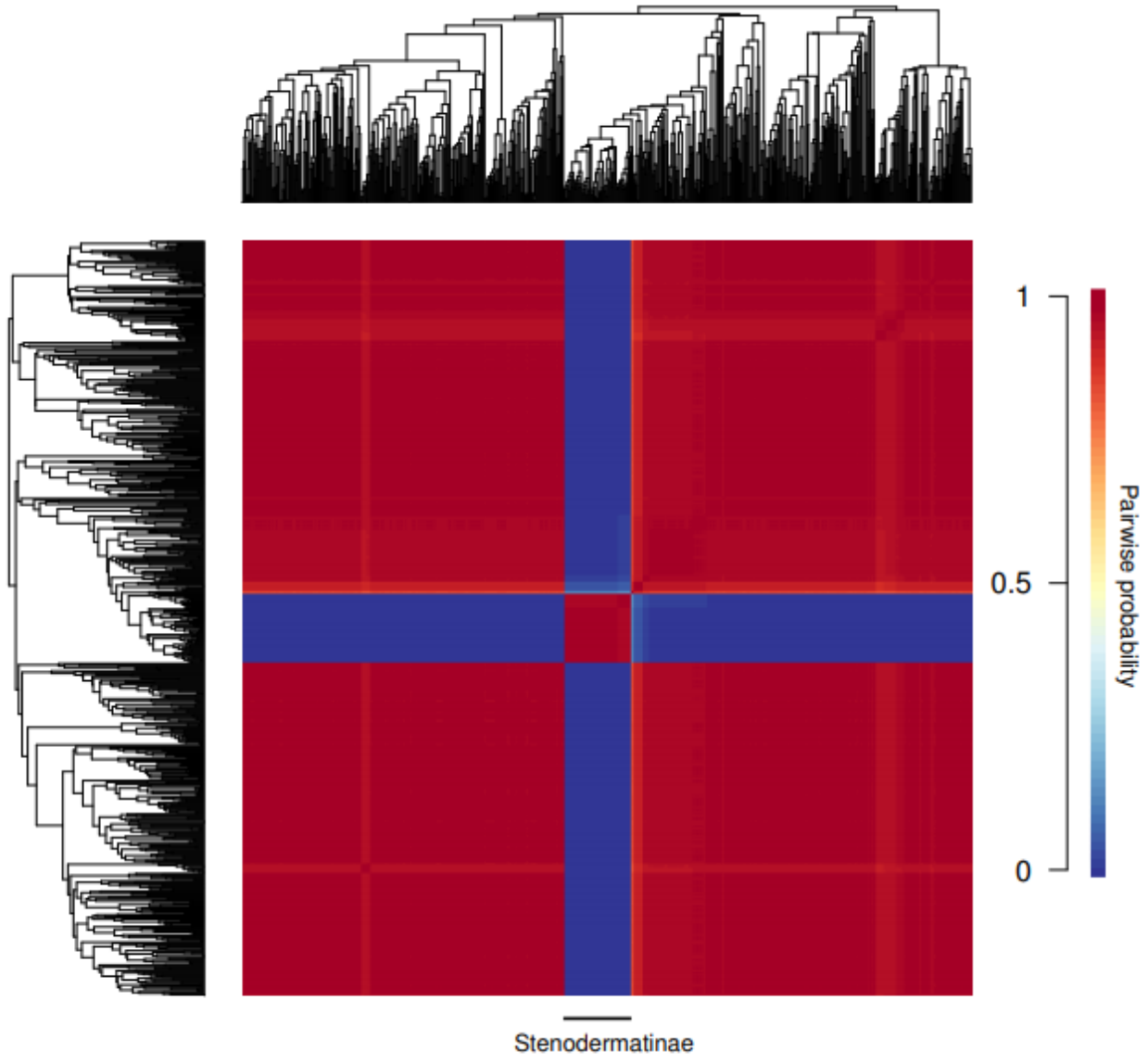

Figure S2.5 Cohort matrix with halved sampling fractions
A cohort matrix (see Figure 2.5, Figure S2.1) for the variant of our BAMM analysis with halved sampling fractions. Our overall inferences regarding the uniqueness of the subfamily Stenodermatinae are robust to this different sampling.

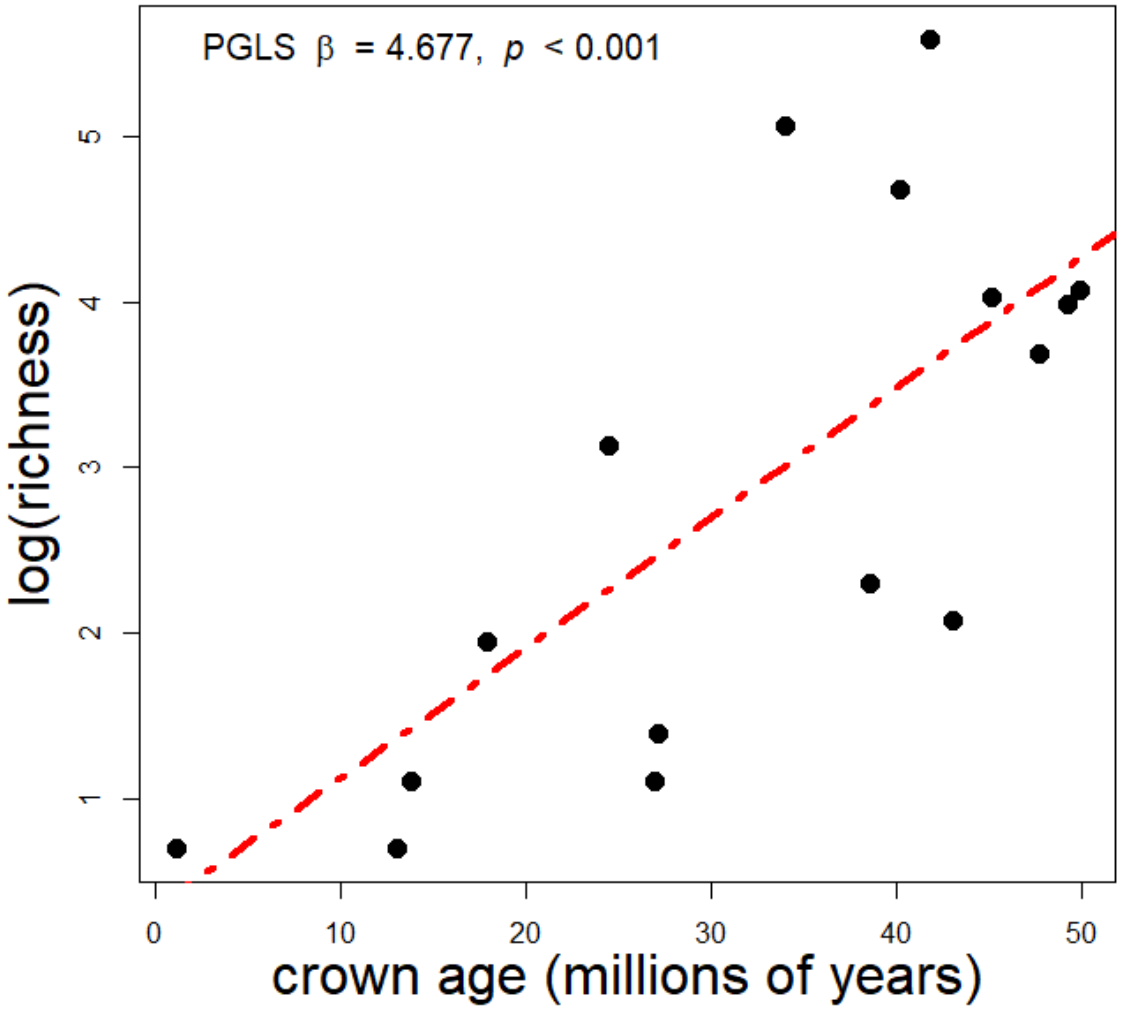

Figure S2.6 Crown family age vs. family level richness
A plot depicting the relationship between crown family age, in millions of years, and log(richness) for each non-monotypic family. A linear regression line is included.

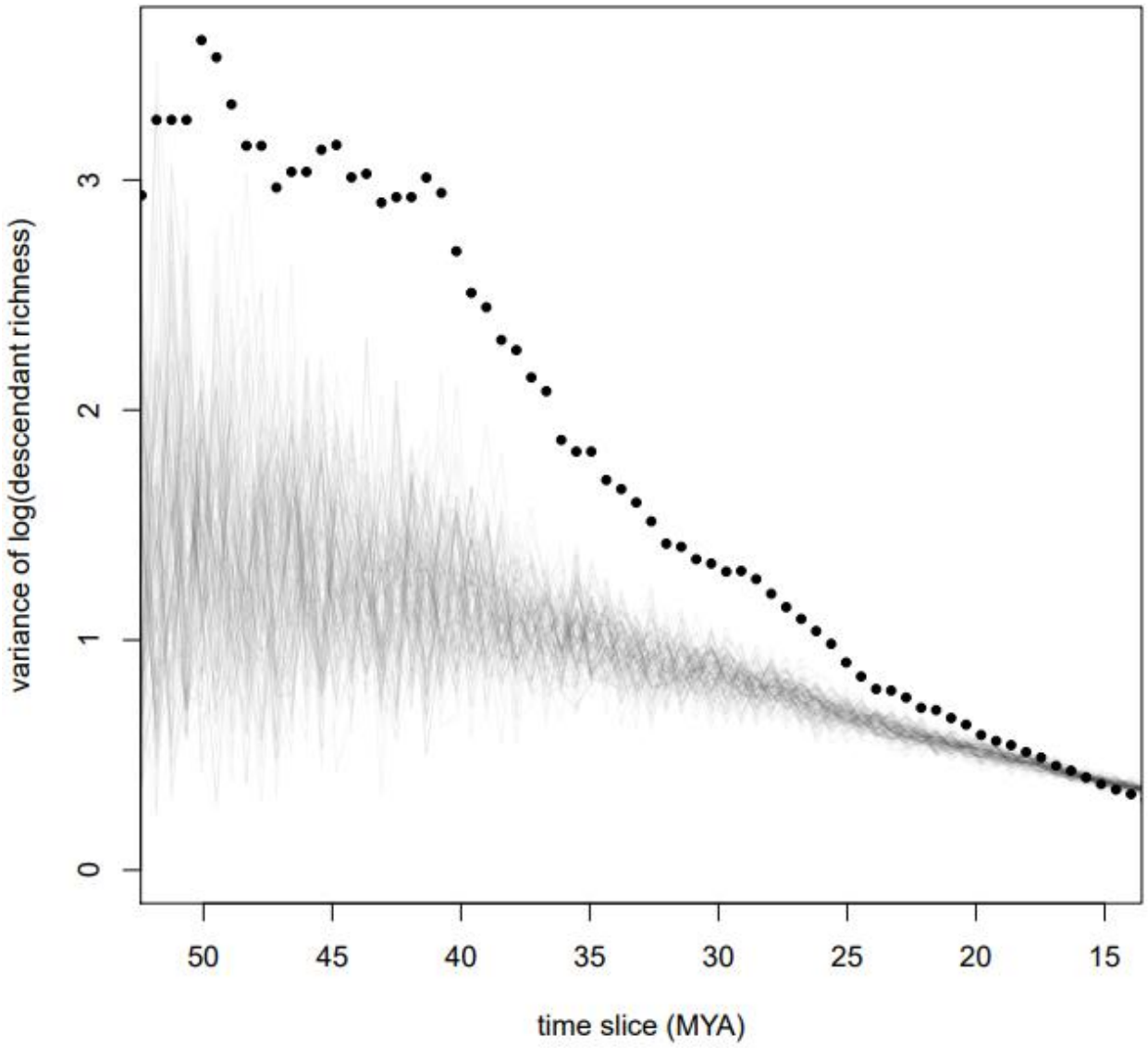

Figure S2.7 Phylogenetic imbalance through time without stenodermatines
An analysis of phylogenetic imbalance through time, without the exceptional subfamily Stenodermatinae. Interpretation of the figure matches that of Figure 2.7.

CHAPTER 3

Ecomorphological and phylogenetic controls on sympatry across extant bats[4]

ABSTRACT

Macroecological patterns of sympatry can inform our understanding of how ecological and evolutionary processes govern species distributions. Following speciation, both intrinsic and extrinsic factors may determine how readily sympatry occurs. One possibility is that sympatry most readily occurs with ecological divergence, especially if broad-scale co-occurrence is mediated by niche differentiation. Time since divergence may also predict sympatry if hybridization and gene flow lead to the collapse of species boundaries between closely-related taxa. Here, we test for ecological and phylogenetic predictors of sympatry across the global radiation of extant bats. We used a combination of linear mixed modeling, simulations, and maximum-likelihood modeling to test whether phylogenetic and ecomorphological divergence between species predict sympatry. We further assess how these relationships vary based on biogeographic realm. We find that time since divergence does not predict sympatry in any biogeographic realm. Morphological divergence is negatively related to sympatry in the Neotropics, but shows no relationship with sympatry elsewhere. To the extent that pairwise phylogenetic and morphological divergence reflect ecological differentiation, our results suggest

[4] Shi, J.J., Westeen, E.P., Katlein, N.T., Dumont, E.R., & Rabosky, D.L. (2018) Ecomorphological and phylogenetic controls on sympatry across extant bats. *Journal of Biogeography*.

that abiotic and environmental factors may be more important than species interactions in determining patterns of sympatry across bats.

INTRODUCTION

Species' geographic distributions and their ranges reflect the interplay between ecological processes and evolutionary patterns (Ricklefs 2007; Grossenbacher *et al.* 2015). In many ways, geographic distributions are unifying units of macroecology and macroevolution, as they are determined by interactions with other species and the environment, and can govern both speciation and extinction. The extent and spatial configuration of species ranges can be controlled by ecological factors, including species interactions (Sexton *et al.* 2009; Louthan *et al.* 2015), abiotic characteristics of the environment (Terribile *et al.* 2009), and dispersal (Jønsson *et al.* 2016). Teasing apart these factors is central to macroecological and macroevolutionary research, especially as researchers strive to understand how ecological processes like competition may change distributions and community compositions over macroevolutionary time (Pigot & Tobias 2013, 2014).

The configuration of species ranges can reflect patterns of sympatry across species, where "sympatry" refers to broad-scale spatial overlap between species regardless of whether they co-occur in local syntopy. Sympatry at this scale can have multiple controlling factors. The probability of broad-scale sympatry could be dependent on competitive interactions that lead to character displacement and niche divergence (Brown & Wilson 1956, Stuart & Losos 2013, Cardillo & Warren 2016), or even to local extinction due to competitive exclusion (Connell 1972, Bengtsson 1989, Silvestro *et al.* 2015). These general hypotheses invoke stabilizing mechanisms (*sensu* Chesson 2000) as a link between divergence and sympatry. Broad-scale

sympatry could also be unrelated to resource competition, and instead occurs only in the absence of hybridization, which collapses incipient species (Grant & Grant 1997, Taylor *et al.* 2006). If divergence and reproductive isolation generally increase with time, and if those factors are important controls on sympatry, then we should expect to find a positive correlation between phylogenetic divergence and the probability of sympatry (Barraclough & Vogler 2000).

Other models also raise the possibility that greater ecological divergence does not predict extant sympatry. Instead, sympatry can reflect the sorting of regional species pools into communities based on habitat. Species may be more likely to co-occur at low levels of divergence if environmental filtering selects for species with phylogenetically-conserved traits (Webb 2000, Graham & Fine 2008, Cavender-Bares *et al.* 2009) and are thus not structured by present-day competitive interactions (McPeek & Brown 2000). Some traits may also reflect equalizing mechanisms that reduce fitness differences among organisms (Chesson 2000, Adler *et al*. 2007), and thus would promote sympatry among more similar taxa.

The relationships among sympatry and phylogenetic or phenotypic divergence are unknown across much of the tree of life. Sympatry and divergence are positively related in birds, suggesting a link between local species interactions and broad-scale distributions (Weir & Price 2011, Pigot & Tobias 2013). Many non-volant mammalian clades, however, exhibit no relationship between sympatry and phylogenetic divergence (Fitzpatrick & Turelli 2006). Such a pattern could indicate that ecological divergence accumulates rapidly in these groups, or that in many cases, sympatric species are not syntopic and do not interact ecologically.

Extant bats (Order Chiroptera) are particularly tractable for exploring the influences of species interactions, phylogeny, and patterns of sympatry at a macroecological scale because of their cosmopolitan distribution and the breadth of their diversity (Jones *et al.* 2005, Simmons

2005, Shi & Rabosky 2015). Their potential for high dispersal via flight may mean that species interactions are more important than landscape or edaphic features for predicting spatial patterns. As regional dispersal can also erode any local signals of species interactions, bats may be a system where sorting patterns play a disproportionate role.

Bats feed on a wide variety of resources, including arthropods, vertebrates, fruits, and nectar (Nowak 1994, Simmons & Conway 2003). Competition for these resources structures many bat communities at local scales, such as within Neotropical savannahs (Aguirre *et al.* 2002, Estrada-Villegas *et al.* 2012). There is also evidence that some bat communities are structured by echolocation frequency and trophic ecology (Findley & Black 1983, Siemers & Schnitzler 2004, Moreno *et al.* 2006). However, we do not know the extent to which competitive interactions for resources among bats are important controls on sympatry, or how these controls may vary across global bat diversity (Figure 3.1).

Bat ecology is tightly coupled with morphology; this is especially well-studied with trophic ecology and skull morphology. The shape and size of bat skulls reflect the link between physiological performance and the ability to capture and process foods with highly variable mechanical properties (Saunders & Barclay 1992, Dumont 2004, Nogueira *et al.* 2009, Santana *et al.* 2010, Santana & Cheung 2016), and thus are often used as proxies for ecological metrics in the absence of observational and experimental data. In some families, skull morphology is also closely tied with echolocation ability, another dimension of trophic ecology (Santana & Lofgren 2013, Curtis & Simmons 2017). While relative feeding performance data among coexisting bat species are rare, morphological divergence is often considered to be at least one predictor of ecological divergence.

In this study, we test whether overall, broad patterns of sympatry can be predicted by phylogenetic and/or morphological divergence across extant bats. With range data and museum specimens, we use phylogenetic linear mixed-modeling to test predictors of sympatry, and a maximum-likelihood framework to model the probability of sympatry as a function of age and morphological distance. We explore the influence of phylogenetic dependence on our range data, and propose a general framework for testing if sympatry can be related to various metrics of divergence.

MATERIALS & METHODS

Overall framework and scope

We explored how sympatry varies with two pairwise metrics of divergence: time to the most recent common ancestor, and ecomorphological divergence as represented by Euclidean distances between skulls in morphospace. We focused on the binary *presence* (0/1) of broad-scale sympatry, given a threshold of continuous *range overlap* (a percentage) in a species pair. Our framework involved three approaches: (1) pairwise linear mixed-models to test divergence predictors of sympatry, accounting for random effects of phylogeny and species identity; (2) maximum-likelihood modeling of how multiple parameters of sympatry may vary with pairwise divergence among sister taxa (*sensu* Pigot & Tobias 2013); (3) randomizations that infer the null distributions of sympatry across species pairs given no relationship with divergence. For the pairwise linear mixed models (approach 1), we integrated data from all species pairs. In the maximum-likelihood models (approach 2), we focused on a subset of sister species, where we might expect species interactions to be strongest. All analyses used the species-level Chiroptera

phylogeny of Shi & Rabosky (2015), which contains 812 of the roughly 1300 extant species of bats.

All analyses were divided into biogeographic realms, representing regional pools of species that could reasonably co-occur in the absence of constraints on sympatry. We used World Wildlife Fund (WWF) realms (Olson *et al.* 2001), though we combined the small Oceanic and Australasian realms and excluded bats endemic to Madagascar, Seychelles, and Comoros from the Afrotropics. We divided our analyses to infer how predictors of sympatry vary by region, to capture species pools that sort into communities (Lessard *et al.* 2012), and to minimize one potential source of biogeographic bias. To illustrate this, consider the different species pools between the Indian Ocean islands and the mainland Afrotropics. Even if taxa in these two regions are rarely found in sympatry due to ancient vicariance, pairwise allopatry states would be repeatedly counted in all comparisons between descendant species of the two regions, regardless of the time since divergence. This would artificially bias relationships between divergence and sympatry in a negative direction (*e.g.* greater divergence being correlated with lower probabilities of sympatry).

Morphological data

We took 9 linear measurements (see appendix of published paper) from bat skulls at the University of Michigan Museum of Zoology (UMMZ) and the American Museum of Natural History (AMNH). These measurements followed Dumont (2004) and Dumont *et al.* (2012), who linked ecomorphology and diversification in the family Pteropodidae and the superfamily Noctilionoidea. From species-level averaged measurements, we calculated pairwise Euclidean

distances in 9-dimensional trait space between all pairs as our metric of pairwise ecomorphological divergence.

We targeted 241 species across fourteen of the twenty extant families of bats based on available specimens, representing roughly 30% of the phylogeny.

Spatial data and sympatry

We used species ranges from the IUCN's Red List of Threatened Species (IUCN 2016), though with modifications to the superfamily Noctilionoidea (see published paper). We targeted available range polygons based on our phylogeny.

With these polygons, we used the *rgeos* and *maptools* R packages to code sympatry state for all pairs of extant bat species in the spatial dataset. We first calculated geographic range overlap with the Szymkiewicz-Simpson coefficient, or the sum area of overlap divided by the range size of the species with the smaller range, for each species pair. We then designated each pair of bat species as sympatric or allopatric based on a threshold of 20% range overlap (as in Pigot & Tobias 2013; more conservative thresholds reported in the published paper). We decomposed our data into binary states, as opposed to continuous overlap, as the latter metric is more sensitive to assumptions of speciation mode (Phillimore *et al.* 2008).

Phylogenetic linear mixed-modeling

To test if overall pairwise sympatry within biogeographic realms is predicted by divergence, we used phylogenetic linear mixed-models (PLMMs). PLMMs are particularly flexible for their ease of interpretation and implementation in a standard mixed-modeling

framework, and the ability to test for distinct fixed and random predictor(s) on response variable(s). Furthermore, they can easily incorporate paired, continuous, and categorical data.

We used Markov chain Monte Carlo to simulate posterior distributions of model parameters using the *MCMCglmm* R package (Hadfield 2010). Our PLMMs took the general form: $S_{i,j} = \beta X_{i,j} + Z_1 u_{i,j} + Z_{2,i} + Z_{2,j}$. Our response variable *S* corresponded with the probability of sympatry for a given species pair *i* and *j* and was related to the observed data (sympatry/allopatry) using a probit ("threshold") link function. We tested for a vector of fixed effects β, given a matrix *X* of divergence metric(s) between species *i* and *j*. We then incorporated two distinct classes of random effects *Z* into our PLMMs: the hierarchical effect of phylogenetic structure (Z_1), and species identity (Z_2) (Hadfield & Nakagawa 2010, Tobias *et al.* 2014). Z_1 accounted for the possibility that fixed effects depend on phylogenetic node structure ($u_{i,j}$) and thus subclade identity, while Z_2 accounted for the multiple times each unique species *i* and *j* was represented in our datasets. We ran all models with a standard inverse-gamma prior on the variance structure of our random effects (Hadfield 2010). We checked all MCMC output for autocorrelation at different levels of sample thinning, while also confirming high (variance > 1000) effective sample sizes.

As we did not have representative morphological data for every species, we ran two groups of PLMMs with varying β and *X* vectors. The first set of PLMMs only tested for β_1, the effect of phylogenetic divergence (in mya) on pairwise sympatry, with separate models for each realm. For each model, we simulated the posterior distributions of model parameters using 20 million generations of MCMC simulation, sampling every 10,000 generations, with 10% discarded as a burnin.

The second set of PLMMs tested for three fixed effects: (1) β_1, (2) β_2: the effect of ecomorphological divergence, and (3) β_3: the interaction of both divergence metrics. β_3 accounted for the possibility that the strength of ecomorphological control depends on time since divergence. Given the limited sampling of our morphological data, this second set was divided into just the Nearctic and Neotropical realms, as well as the combined New World. We simulated this second set of posterior distributions of model parameters using 10 million generations of MCMC simulation, sampled every 5,000 generations, with 10% discarded as burnin, as these were much smaller datasets.

Modeling the probability of sympatry

We further used a maximum-likelihood (ML) framework to compare models where multiple parameters that govern the relationship between sympatry and divergence can be estimated. We fit models in which the probability of sympatry explicitly varies with phylogenetic (*t*, time in mya) and/or morphological (*d*, pairwise Euclidean distance) divergence (Figure 3.2). We tested covariates independently, and also in interaction (*td*), to account for scenarios where morphological divergence has the most dramatic effect in close relatives. We restricted these analyses to sister taxa represented in the tree, as we may expect to find the strongest signal of divergence among young pairs. Although these pairs may not be true sisters, this restriction accounted for phylogenetic nonindependence of data; this general approach was analogous to that of Pigot & Tobias (2013). We performed the following analyses for all measured sister species pairs, and for the subset composed of New World pairs, where the bulk of our morphological data are represented.

For these analyses, we treated the probability of sympatry as a binomially distributed random variable with a single parameter θ. The likelihood L of observing any combination of allopatry (0) and sympatry (1) states across pairs of species i and j, in a set of n species Y, was thus denoted by $L = \prod_{i,j=1}^{n} Pr(Y_{i,j}|\ \theta)$, where $Pr(Y_{i,j}\ |\ \theta) \sim binom(\theta)$. θ, in turn, was governed by three potential models of sympatry (Figure 3.2). For M1, θ was treated as a constant. This model served as our null hypothesis: under this model, the ML estimate for the probability of sympatry is simply the percentage of sympatric pairs in a given set Y.

In M2, θ varied as an exponential decay function with t, d, or td as follows (written for t alone): $\theta = \alpha\left(1 - e^{-\mathrm{kt}}\right)$. M2 reflected scenarios in which pairwise sympatry varied with divergence. Because θ approaches an unfixed asymptote α, which is a parameter estimated from the data, the model also accounted for the biological reality that some species pairs will simply never become sympatric due to geographic or historical constraints (Figure 3.2). The rate parameter k, which reflects how rapidly θ approaches α, was also estimated from the data, where M2 reduces to M1 as k approaches infinity.

In our final model (M3), θ varied logistically with t, d, or td as follows (written for t alone): $\theta = \frac{\alpha}{1+e^{-k(t-w)}}$. M3 represented a scenario analogous to one proposed by Pigot & Tobias (2013, 2014), where θ is correlated with time and/or ecomorphology, but includes a lag or delay parameter (w) before sympatry is readily attained (Figure 3.2). This w parameter may represent a minimum threshold of morphological divergence to avoid competition, or a minimum age threshold to avoid hybridization, among other possibilities. In this case, α, w, and the rate parameter k were all estimated from the data, where M3 will also reduce to M1 when $w = 0$ and k approaches infinity.

We fitted all seven potential models to sister species data using the *bbmle* R package. We tested overall model fit using the corrected Akaike Information Criterion (AICc). Our model setup also allowed us to explicitly test hypotheses using likelihood-ratio tests within the three groups of related models (one group for each metric of divergence *t*, *d*, or *td*, where M1 was always the null hypothesis of no relationship between divergence and θ).

PLMM and ML model validation

We applied both our PLMM and ML model-fitting approaches to the phylogenetic, morphological, and spatial data of sister species pairs of Neotropical ovenbirds (Family Furnariidae) from Pigot & Tobias (2013), who concluded that ecomorphological and phylogenetic divergence affected the rate at which species pairs became sympatric. By using the same data as Pigot & Tobias (2013), we tested whether our analytical framework could recover similar relationships between divergence and sympatry as reported in their study.

Sympatry-age relationships

Finally, we inferred a null distribution of the relationship between pairwise sympatry state and time since divergence by using a set of randomizations (Figure 3.3). We randomly assigned species (and thus ages) to ranges, for each extant bat, and then fit a logistic model for sympatry as a function of age. This randomization process, representing a model where the pattern of sympatry across bats is random with respect to divergence time, was repeated 500 times. These randomizations established a distribution of randomized log-odds from logistic models, and we compared this to the empirical age-overlap relationship. We performed these randomization tests for each of the 6 WWF biogeographic realms.

RESULTS

Data summary

Overall, we report results for 696 bats with spatial data that are included in our phylogenetic tree. We measured 1073 adult specimens at the UMMZ and combined these data with the previously published AMNH data of Dumont *et al.* (2012) (mean specimens/species = 3.86, *sd* = 3.53).

Regional pairwise sympatry among bats is consistently high, given a 20% threshold of overlap (Table S3.1; weighted average: 42.2% of pairs are sympatric). This does not appear to be correlated with regional species diversity or realm size, as even the relatively low diversity but large Nearctic realm has over 50% of its species pairs in sympatry. In both New World realms (the Neotropics and the Nearctic), 50% or more of species pairs are sympatric, with average overlap percentages near 40%. We note that in all realms but the Palearctic, average overlap is above our base threshold for sympatry.

PLMM results

MCMCglmm returns pMCMC-values, which are two-tailed calculations of the proportion of simulations where fixed effects differ from zero. We use these to assess the significance of fixed effects in PLMMs, and find that time since divergence does not significantly predict sympatry in any realm (Table 3.1). We can also use highest posterior density intervals and credibility intervals to evaluate our posterior distribution, but in our analyses all these methods are concordant.

In the New World bats, when we incorporate ecomorphological divergence, we find that there are notable differences between Nearctic and Neotropical bats. There are no significant

effects of divergence in the Nearctic. However, we recover significant evidence for a negative relationship between ecomorphological divergence and binary sympatry state in the Neotropics (Table 3.2; Figure 3.4). While there is some uncertainty in the specific relationship - particularly in a threshold of ecomorphological divergence that makes sympatry less likely - there is extremely strong support for a negative signal in the data (Figure 3.4b). This negative relationship does not appear to be driven by divergent outliers, as we recover concordant results with an analysis on a smaller subset of our data (Figure 3.4c; Table S3.8). Across the entire New World (Nearctic + Neotropics), the interaction of phylogeny with ecomorphology has a negative effect on sympatry, though the two variables are not significant predictors independently (Table 3.2). These negative relationships imply that sympatry is actually less likely as divergence increases.

If we subsample by varying the threshold overlap percentage for sympatry, we generally recover concordant results in our PLMMs, implying that our main analyses are conservative in estimating predictors of sympatry (see appendix of published paper).

ML models of the probability of sympatry

We fit our ML models of sympatry to 67 sister species pairs, as well as 53 New World sister species pairs. A simple, null model where all species pairs share a common probability of sympatry, regardless of any type of divergence, was the best-fitting model (Table S3.3).

PLMM and ML model validation

We recover, as do Pigot & Tobias (2013), positive effects of both divergence time and ecomorphology on sympatry in furnariid sister species with both PLMMs and our ML models.

We specifically find strong evidence for models with a lagtime, further suggesting that species interactions mediate sympatry (Tables S3.5-S3.7).

Sympatry-age relationships

In each WWF biogeographic realm, the null distributions of age-sympatry relationships (calculated from range randomizations as log-odds from logistic regressions between sympatry state and time since divergence, as described in Figure 3.3) are centered around 0, as expected. The empirical age-sympatry relationship does not appear to significantly deviate from the null distribution in any realm, though it skews slightly negative in the Afrotropics (Figure S3.1).

DISCUSSION

Divergence time and sympatry

We find no significant effects of age on pairwise patterns of sympatry (Table 3.1). We also find that there is no significant difference between a process-neutral null model and any ML model where the probability of sympatry varies with age. Age is often intrinsic to any explanation for patterns of sympatry, especially given correlations of divergence with time. However, our finding is consistent across all biogeographic realms. Therefore, even though one explanation for this null pattern is that divergence and time are simply not well-correlated in bats, it is unlikely this is true across all families and realms.

Ecomorphology and sympatry in the New World

We find no evidence for ecomorphological controls on sympatry among the measured Nearctic bat species, but find that there is a negative relationship between ecomorphological

divergence and sympatry among Neotropical bats (Figure 3.4b, c). We also find a negative interaction effect of age and ecomorphology on sympatry across New World bats as a whole in our PLMMs (Table 3.2). As noctilionoids are characterized by strong relationships between ecology and highly specialized morphology (Dumont *et al.* 2012), we may have expected to see the strongest link between divergence and sympatry in this realm. Nevertheless, Neotropical species pairs are more likely to co-occur when they are morphologically similar. Multiple hypotheses could explain this pattern, including community assembly via environmental filtering, or within-realm sorting that biases where similar species are most likely to be found (Webb 2000, Leibold & McPeek 2006, Graham & Fine 2008, Cavender-Bares *et al.* 2009). Within noctilionoids, there are numerous examples both of clades that are filtered by resource availability, leading to sympatry among the most similar pairs, and those that assemble into communities based on stabilizing mechanisms (Villalobos & Arita 2010). As our morphological data are partial proxies for ecological divergence, a deeper dataset that addresses feeding mechanics and performance may yield a fine-grained picture of how functional divergence relates to co-occurrence within communities.

Despite the significant negative effect of ecomorphology in our PLMMs, our best-fitting ML model is a simple one in which all pairs share a common probability of sympatry regardless of phylogenetic or morphological divergence. This discrepancy likely reflects a fundamental difference between the two datasets. It is possible that the shorter timescales associated with sister taxa are insufficient for accumulating enough ecomorphological divergence to influence the processes governing sympatry. Our sister species dataset is also relatively small, and it thus possible that statistical power was lower for these analyses.

The significant New World interaction effect of divergence metrics on sympatry in our PLMMs (Table 3.2) likely reflects scale and differences between Nearctic and Neotropical bats. Nearctic bats are predominantly insectivorous vespertilionoids, while the Neotropics are dominated by their high richness of noctilionoid bats, which span the full breadth of bat feeding diversity (Nowak 1994, Simmons 2005). We can interpret this significant effect as evidence that, at the scale of the entire New World, we are most likely to find morphologically similar and closely-related bats in sympatry. This is likely compounded by the fact that morphological divergence among many Neotropical species can be relatively large, and is recent compared with the relatively ancient (~50 mya) divergence of noctilionoids from Nearctic vespertilionoids (Shi & Rabosky 2015).

Sympatry-divergence relationships across extant bats and potential causes

Multiple interactions beyond resource competition can drive patterns of sympatry. Mutualistic interactions with plants, or predation and parasitism (McIntire & Farjado 2014, Spiesman & Inouye 2014) can govern spatial patterns. Some bat communities, their distributions, and abundances are non-randomly structured with respect to other phenotypic traits, including flight ability and echolocation (Norberg & Rayner 1987, Schoeman & Jacobs 2003, Siemers & Schnitzler 2004, Santana & Lofgren 2013, Corcoran & Conner 2014), as well as available foraging and roosting habitats (Schoeman & Jacobs 2011, Voss *et al.* 2016). These multiple pressures existing in conjunction could mask relationships between skull morphology and sympatry. The framework we develop here is flexible to the integration of other metrics of divergence, including measures of ecological performance that more directly test for competition.

Low competition for resources among bats may also decouple divergence from sympatry, especially if resources like aerial insects are ubiquitous and plentiful at night (Fenton & Thomas 1980, Fleming 1986). Studies that test for resource competition among bats are uncommon, and there is mixed evidence depending on guild, body size, and seasonality (Heithaus *et al.* 1975, Swift & Racey 1983, Kingston *et al.* 2000). Divergence may also occur in situations when species historically co-occurred, but exist presently in allopatry, thereby masking the signature of the sympatry-divergence relationship (Anacker & Strauss 2014). Furthermore, we must also acknowledge that ranges themselves are inherited and non-independent properties of species. While we partially account for this in the random effects of our PLMMs, there is considerable room for the integration of models that simulate range heritability and evolution.

Divergence may also be unrelated to sympatry if abiotic filtering is the dominant process shaping species assemblages at the spatial scales considered here. For example, elevation and water availability (Henry *et al.* 2004, McCain 2007a, 2007b) control syntopy at local scales, but this fine-grained spatial structuring might not translate to regional range overlap. Bat diversity in the Afrotropics, for instance, appears to be highest in the wettest and most humid regions (Figure 3.1); this pattern may underlie co-occurrence in sympatry. Bat distributions can also vary with temporal and seasonal variation in resource use (Kronfeld-Schor & Dayan 2003, Adams & Thibault 2006). Abiotic, environmental conditions can also mediate ecological interactions, eroding clear relationships between divergence and sympatry (Chesson 1986, Dunson & Travis 1991). If traits actually underlie fitness differences as opposed to niche differences, then equalizing mechanisms may be the most important promoters of coexistence, which can also result in null or negative relationships between divergence and sympatry (Chesson 2000, Adler *et*

al. 2006). This seems less likely in bats, where morphological differences are linked to major trophic categories, but is a possibility for other taxa characterized by generally low divergence.

It is also possible that there are trade-offs between mechanisms of divergence and habitat filtering that scale with community and range sizes (Kneitel & Chase 2004). Local communities can be overdispersed without this pattern manifesting at the regional scale (*e.g.* Rabosky *et al.* 2011). Local and regional scales are also not consistent across organisms and biomes, given differences in dispersal ability (Warren *et al.* 2014). Finally, processes that control the degree of overlap may be distinct from those that preclude co-occurrence altogether. Even given no relationship between divergence and the *presence* of sympatry, there may still be a relationship between divergence and the *degree* of overlap in a subset of sympatric pairs, indicating that once requirements for sympatry are met, range overlap is readily increased.

Our results indicating weak or null effects of phylogenetic distance on regional co-occurrence could also be evidence for alternative modes of speciation, including speciation in sympatry. While speciation in allopatry is often assumed to be the most prevalent mode, sympatric speciation could cloud any signals of divergence upon sympatry (Fitzpatrick & Turelli 2006), especially if extant ranges largely reflect the geography of speciation. Reproductive sorting by echolocation frequency has been suggested as a driver of sympatric speciation in some clades of bats (Kingston & Rossiter 2004). Considering the generally coarse nature of available range data, allopatric pairs may even appear sympatric, as in cases where isolation depends on microhabitat availability like roosts (Voss *et al.* 2016). Spatial patterns of bat diversity may also be unrelated to divergence if larger ranges are simply more likely to overlap when constrained by continental geography, analogous to the mid-domain explanation for the latitudinal diversity gradient (Colwell & Lees 2000). This would also be evidence for dispersal ability as a driver of

sympatry across bats, though testing would require higher-resolution data on range limits. Dispersal could even erode signals of local competitive exclusion, leading to the appearance of widespread sympatry.

One of the biggest limiting factors to macroecological studies is the quality and accuracy of data. Uncertainty in divergence time estimation can impede efforts to infer the effects of age on extant diversity. The presence of cryptic species may make identification of syntopic species difficult. Furthermore, all studies that use spatial data are sensitive to the accuracy of range maps, which have not been systematically reviewed across Chiroptera, to our knowledge. Ultimately, it is unlikely that ecological interactions scale to macroecological patterns and macroevolutionary dynamics equally across the tree of life. The negative relationship between divergence and co-occurrence across bats is potentially evidence that their diversity is unsaturated (Shi & Rabosky 2015), and that they are continuing to radiate into a diversity of ecological niches and biomes.

ACKNOWLEDGEMENTS

The authors would like to acknowledge M.C. Grundler and P.O. Title for their invaluable assistance and advice regarding statistical and spatial analyses, and three anonymous reviewers for improving the quality of this paper. J.J.S. would also like to thank L.M. Dávalos, J.P. Drury, J. Hadfield, K. Langstrom, A.L. Pigot, D. Rojas, S. Singhal, and H.L. Williams for methodological advice and data collection.

DATA ARCHIVING

All data for this study are archived on and freely available from the Dryad database (https://doi.org/10.5061/dryad.ph715dd).

REFERENCES

Adams, R.A. & Thibault, K.M. (2006) Temporal resource partitioning by bats at water holes. *Journal of Zoology*, **270**, 466–472.

Adler, P.B., HilleRisLambers, J. & Levine, J.M. (2007) A niche for neutrality. *Ecology Letters*, **10**, 95–104.

Aguirre, L.F., Herrel, A., van Damme, R. & Matthysen, E. (2002) Ecomorphological analysis of trophic niche partitioning in a tropical savannah bat community. *Proceedings of the Royal Society B: Biological Sciences*, **269**, 1271–1278.

Anacker, B.L. & Strauss, S.Y. (2014) The geography and ecology of plant speciation: range overlap and niche divergence in sister species. *Proceedings of the Royal Society B: Biological Sciences*, **281**, 20132980.

Barraclough, T.G. & Vogler, A.P. (2000) Detecting the geographical pattern of speciation from species-level phylogenies. *The American Naturalist*, **155**, 419–434.

Bengtsson, J. (1989) Interspecific competition increases local extinction rate in a metapopulation system. *Nature*, **340**, 713–715.

Brown Jr., W.L. & Wilson, E.O. (1956) Character displacement. *Systematic Zoology*, **5**, 49–64.

Cardillo, M. & Warren, D.L. (2016) Analysing patterns of spatial and niche overlap among species at multiple resolutions. *Global Ecology and Biogeography*, **25**, 951–963.

Cavender-Bares, J., Kozak, K.H., Fine, P.V.A. & Kembel, S.W. (2009) The merging of community ecology and phylogenetic biology. *Ecology Letters*, **12**, 693–715.

Chesson, P.L. (1986) Environmental variation and the coexistence of species. *Community ecology* (ed. by Diamond, J. & Case, T.J.), Harper and Row, New York, New York, USA, 240-256.

Chesson, P. (2000) Mechanisms of maintenance of species diversity. *Annual Review of Ecology and Systematics*, **31**, 343-366.

Colwell, R.K. & Lees, D.C. (2000) The mid-domain effect: geometric constraints on the geography of species richness. *Trends in Ecology and Evolution*, **15**, 70-76.

Connell, J.H. (1972) Interactions on marine rocky intertidal shores. *Annual Review of Ecology and Systematics*, **3**, 169–192.

Corcoran, A.J. & Conner, W.E. (2014) Bats jamming bats: Food competition through sonar interference. *Science*, **346**, 745–747.

Curtis, A.A. & Simmons, N.B. (2017) Unique turbinal morphology in horseshoe bats (Chiroptera: Rhinolophidae) *The Anatomical Record*, **300**, 309–325.

Dumont, E.R., Dávalos, L.M., Goldberg, A., Santana, S.E., Rex, K. & Voigt, C.C. (2012) Morphological innovation, diversification and invasion of a new adaptive zone. *Proceedings of the Royal Society B: Biological Sciences*, **279**, 1797–1805.

Dumont, E.R. (2004) Patterns of diversity in cranial shape among plant-visiting bats. *Acta*

Chiropterologica, **6**, 59–74.
Dunson, W. & Travis, J. (1991) The role of abiotic factors in community organization. *The American Naturalist,* **138**, 1067–1091.
Estrada-Villegas, S., McGill, B.J. & Kalko E.K.V. (2012) Climate, habitat & species interactions at different scales determine the structure of a Neotropical bat community. *Ecology,* **93**, 1183–1193.
Fenton, M.B. & Thomas, D.W. (1980) Dry-season overlap in activity patterns, habitat use & prey selection by sympatric African insectivorous bats. *Biotropica,* **12**, 81–90.
Findley, J.S. & Black, H.A.L. 1983. Morphological and dietary structuring of a Zambian insectivorous bat community. *Ecology*, **64**, 625–630.
Fitzpatrick, B.M. & Turelli, M. (2006) The geography of mammalian speciation: mixed signals from phylogenies and range maps. *Evolution*, **60**, 601–615.
Fleming, T.H. (1986) Opportunism versus specialization: the evolution of feeding strategies in frugivorous bats. *Frugivores and seed dispersal* (ed. by Estrada, A. & Fleming, T.H.), Dr W. Junk Publishers, Dordrecht, South Holland, Netherlands, 105-118.
Graham, C.H. & Fine, P.V.A. (2008) Phylogenetic beta diversity: linking ecological and evolutionary processes across space in time. *Ecology Letters,* **11**, 1265–1277.
Grant, P.R. & Grant, B.R. (1997) Genetics and the origin of bird species. *Proceedings of the National Academy of Sciences of the United States of America,* **94**, 7768–7775.
Grossenbacher, D., Briscoe Runquist, R., Goldberg, E.E. & Brandvain, Y. (2015) Geographic range size is predicted by plant mating system. *Ecology Letters*, **18**, 706–713.
Hadfield, J.D. (2010) MCMC methods for multi-response generalized linear mixed models: the MCMCglmm R package. *Journal of Statistical Software,* **33**, 1–22.
Hadfield, J.D. & Nakagawa, S. (2010) General quantitative genetic methods for comparative biology: phylogenies, taxonomies and multi-trait models for continuous and categorical characters. *Journal of Evolutionary Biology*, **23**, 494–508.
Heithaus, E.R., Fleming, T. H. & Opler, P. A. (1975) Foraging patterns and resource utilization in seven species of bats in a seasonal tropical forest. *Ecology*, **56**, 841–854.
Henry, M., Barrière, P., Gautier-Hion, A. & Colyn, M. (2004) Species composition, abundance and vertical stratification of a bat community (Megachiroptera: Pteropodidae) in a West African rain forest. *Journal of Tropical Ecology*, **20**, 21–29.
IUCN. (2016) *The IUCN red list of threatened species.* **Version 2016-2.**
Jones, K.E., Bininda-Emonds, O.R.P. & Gittleman, J.L. (2005) Bats, clocks & rocks: diversification patterns in Chiroptera. *Evolution*, **59**, 2243–2255.
Jønsson, K.A., Tøttrup, A.P., Borregaard, M.K., Keith, S.A., Rahbek, C. & Thorup, K. (2016) Tracking animal dispersal: from individual movement to community assembly and global range dynamics. *Trends in Ecology and Evolution*, **31**, 204-214.
Kingston, T., Jones, G., Zubaid, A. & Kunz, T.H. (2000) Resource partitioning in rhinolophoid bats revisited. *Oecologia,* **124**, 332-342.
Kingston, T., & Rossiter, S.J. (2004) Harmonic-hopping in Wallacea's bats. *Nature*, **429**, 654-657.
Kneitel, J.M. & Chase, J.M. (2004) Trade-offs in community ecology: Linking spatial scales and species coexistence. *Ecology Letters,* **7**, 69–80.
Kronfeld-Schor, N. & Dayan, T. (2003) Partitioning of time as an ecological resource. *Annual Review of Ecology, Evolution & Systematics,* **34**, 153–181.
Leibold, M.A. & McPeek, M.A. (2006) Coexistence of the niche and neutral perspectives in

community ecology. *Ecology*, **87**, 1399–1410.
Lessard, J.P., Belmaker, J., Myers, J.A., Chase, J.M., & Rahbek, C. (2012) Inferring local ecological processes amid species pool influences. *Trends in Ecology and Evolution*, **27**, 600–607.
Louthan, A.M., Doak, D.F., & Angert, A.L. (2015) Where and when do species interactions set range limits? *Trends in Ecology and Evolution*, **30**, 780-792.
McCain, C.M. (2007a) Area and mammalian elevational diversity. *Ecology*. **88**, 76–86.
McCain, C.M. (2007b) Could temperature and water availability drive elevational species richness patterns? A global case study for bats. *Global Ecology and Biogeography*, **16**, 1–13.
Mcintire, E.J.B. & Fajardo, A. (2014) Facilitation as a ubiquitous driver of biodiversity. *New Phytologist*, **201**, 403–416.
McPeek, M.A. & Brown, J.M. (2000) Building a regional species pool: diversification of the Enallagma damselflies in eastern North America. *Ecology*, **81**, 904–920.
Moreno, C., Arita, H. & Solis, L. (2006) Morphological assembly mechanisms in Neotropical bat assemblages and ensembles within a landscape. *Oecologia*, **149**, 133–140.
Nogueira, M.R., Peracchi, A.L. & Monteiro, L.R. (2009) Morphological correlates of bite force and diet in the skull and mandible of phyllostomid bats. *Functional Ecology*, **23**, 715–723.
Norberg, U.M. & Rayner, J.M.V. (1987) Ecological morphology and flight in bats (Mammalia; Chiroptera): wing adaptations, flight performance, foraging strategy and echolocation. *Philosophical Transactions of the Royal Society B: Biological Sciences*, **316**, 335–427.
Nowak, M.D. (1994) *Walker's bats of the world*. Johns Hopkins University Press, Baltimore, Maryland, USA.
Olson, D.M., Dinerstein, E., Wikramanayake, E.D., Burgess, N.D., Powell, G.V.N., Underwood, E.C., D'amico, J.A., *et al.* (2001) Terrestrial ecoregions of the world: a new map of life on Earth. *BioScience*, **51**, 933-938.
Phillimore, A.B., Orme, C.D.L., Thomas, G.H., Blackburn, T.M., Bennett, P.M., Gaston, K.J. & Owens, I.P.F. (2008) Sympatric speciation in birds is rare: insights from range data and simulations. *The American Naturalist*, **171**, 646–657.
Pigot, A.L. & Tobias, J.A. (2014) Dispersal and the transition to sympatry in vertebrates. *Proceedings of the Royal Society B: Biological Sciences*, **282**, 20141929.
Pigot, A.L. & Tobias, J.A. (2013) Species interactions constrain geographic range expansion over evolutionary time. *Ecology Letters*, **16**, 330–338.
Rabosky, D.L., Cowan, M.A., Talaba, A.L. & Lovette, I.J. (2011) Species interactions mediate phylogenetic community structure in a hyperdiverse lizard assemblage from arid Australia. *The American Naturalist*, **178**, 579–595.
Ricklefs, R.E. (2007) History and diversity: explorations at the intersection of ecology and evolution. *The American Naturalist*, **170 Suppl**, S56-70.
Santana, S.E. & Lofgren, S.E. (2013) Does nasal echolocation influence the modularity of the mammal skull? *Journal of Evolutionary Biology*, **26**, 2520–2526.
Santana, S.E. & Cheung, E. (2016) Go big or go fish: morphological specializations in carnivorous bats. *Proceedings of the Royal Society B: Biological Sciences*, **283**, 20160615.
Santana, S.E., Dumont, E.R. & Davis, J.L. (2010) Mechanics of bite force production and its

relationship to diet in bats. *Functional Ecology*, **24**, 776–784.
Saunders, M.B. & Barclay, R.M.R. (1992) Ecomorphology of insectivorous bats: a test of predictions using two morphologically similar species. *Ecology*, **73**, 1335–1345.
Schoeman, M.C. & Jacobs, D.S. (2011) The relative influence of competition and prey defences on the trophic structure of animalivorous bat ensembles. *Oecologia*, **1**, 493–506.
Schoeman, M.C. & Jacobs, D.S. (2003) Support for the allotonic frequency hypothesis in an insectivorous bat community. *Oecologia*, **134**, 154–162.
Sexton, J.P., McIntyre, P.J., Angert, A.L. & Rice, K.J. (2009) Evolution and ecology of species range limits. *Annual Review of Ecology, Evolution, and Systematics*, **40**, 415–436.
Shi, J.J. & Rabosky, D.L. (2015) Speciation dynamics during the global radiation of extant bats. *Evolution*, **69**, 1528–1545.
Siemers, B.M. & Schnitzler, H.-U. (2004) Echolocation signals reflect niche differentiation in five sympatric congeneric bat species. *Nature*, **429**, 657–661.
Silvestro, D., Antonelli, A., Salamin, N. & Quental, T.B. (2015) The role of clade competition in the diversification of North American canids. *Proceedings of the National Academy of Sciences of the United States of America*, **112**, 8684–8689.
Simmons, N.B. & Conway, T.M. (2003) Evolution of ecological diversity in bats. *Bat ecology* (ed. by Kunz, T.H. & Fenton, M.B.), University of Chicago Press, Chicago, Illinois, USA, 493-535.
Simmons, N.B. (2005) Order Chiroptera. *Mammal species of the world: a taxonomic and geographic reference, 3rd edition* (ed. by Wilson, D.E. & Reeder, D.M.) Johns Hopkins University Press, Baltimore, Maryland, USA, 312-529.
Spiesman, B.J. & Inouye, B.D. (2014) The consequences of multiple indirect pathways of interaction for species coexistence. *Theoretical Ecology*, **8**, 225–232.
Stuart, Y.E. & Losos, J.B. (2013) Ecological character displacement: glass half full or half empty? *Trends in Ecology and Evolution*, **28**, 402–408.
Swift, S.M. & Racey, P.A. (1983) Resource partitioning in two species of vespertilionid bats (Chiroptera) occupying the same roost. *Journal of Zoology*, **200**, 249–259.
Taylor, E.B., Boughman, J.W., Groenenboom, M., Sniatynski, M., Schluter, D. & Gow, J.L. (2006) Speciation in reverse: morphological and genetic evidence of the collapse of a three-spined stickleback (Gasterosteus aculeatus) species pair. *Molecular Ecology*, **15**, 343–355.
Terribile, L.C., Diniz-Filho, J.A.F., Rodríguez, M.Á. & Rangel, T.F.L.V.B. (2009) Richness patterns, species distributions and the principle of extreme deconstruction. *Global Ecology and Biogeography*, **18**, 123–136.
Tobias, J.A., Cornwallis, C.K., Derryberry, E.P., Claramunt, S., Brumfield, R.T. & Seddon, N. (2014) Species coexistence and the dynamics of phenotypic evolution in adaptive radiation. *Nature*, **506**, 359–363.
Villalobos, F. & Arita, H.T. (2010) The diversity field of New World leaf-nosed bats (Phyllostomidae) *Global Ecology and Biogeography*, **19**, 200-211.
Voss, R.S., Fleck, D.W., Strauss, R.E., Velazco, P.M. & Simmons, N.B. (2016) Roosting ecology of Amazonian bats: evidence for guild structure in hyperdiverse mammalian communities. *American Museum Novitates*, **3870**, 1–43.
Warren, D.L., Cardillo, M., Rosauer, D.F., & Bolnick, D.I. (2014) Mistaking geography for biology: inferring processes from species distributions. *Trends in Ecology and Evolution*, **29**, 572–580.

Webb, C.O. (2000) Exploring the phylogenetic structure of ecological communities: an example for rain forest trees. *The American Naturalist*, **156**, 145–155.
Weir, J.T. & Price, T.D. (2011) Limits to speciation inferred from times to secondary sympatry and ages of hybridizing species along a latitudinal gradient. *The American Naturalist*, **177**, 462–469.

Table 3.1 Age-sympatry relationships
PLMM results for the effect of age (β_1) alone on pairwise patterns of sympatry (at a 20% overlap threshold) for all pairs of bat species with spatial data, divided into WWF biogeographic realms. Posterior means and pMCMC values (see Results) are included.

Realm (*N*)	**β_1 posterior mean**	**β_1 pMCMC**
Afrotropics (78 species)	-0.016	0.060
Indomalaya (175 species)	-0.008	0.083
Nearctic (40 species)	-0.018	0.182
Neotropics (235 species)	-0.012	0.336
Oceania & Australasia (82 species)	-0.008	0.481
Palearctic (70 species)	-0.009	0.209

Table 3.2 Ecomorphology-sympatry relationships
PLMM results for the effects of age (β_1), ecomorphological divergence (β_2), and combined age and ecomorphological divergence (β_3) on pairwise patterns of sympatry (at a 20% overlap threshold) for all pairs of bat species with both types of divergence data. These pairs are divided according to realm. Posterior means and pMCMC values are included, and bolded when pMCMC < 0.05. Note that some species are part of the species pools of both realms.

Realm (*N*)	**β_1 posterior mean**	**β_1 pMCMC**	**β_2 posterior mean**	**β_2 pMCMC**	**β_3 posterior mean**	**β_3 pMCMC**
Nearctic (34 species)	-0.029	0.380	-0.015	0.958	-0.002	0.800
Neotropics (135 species)	-0.018	0.203	**-0.091**	**0.009***	< 0.001	0.621
New World (161 species)	-0.026	0.330	-0.029	0.360	**-0.002**	**0.004***

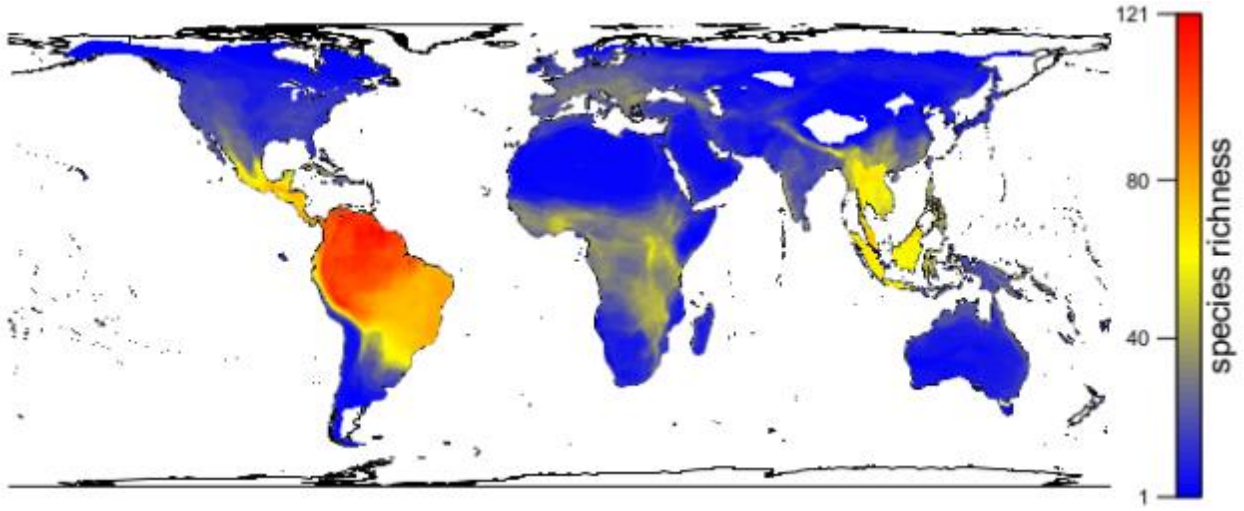

Figure 3.1 Global richness patterns of bats
Global richness of extant bats, based on 696 range polygons used for this study. Warmer colors represent higher species richness. Regional diversity of bats is highest in the tropics and peaks in the western Amazon basin and eastern slopes of the Andes.

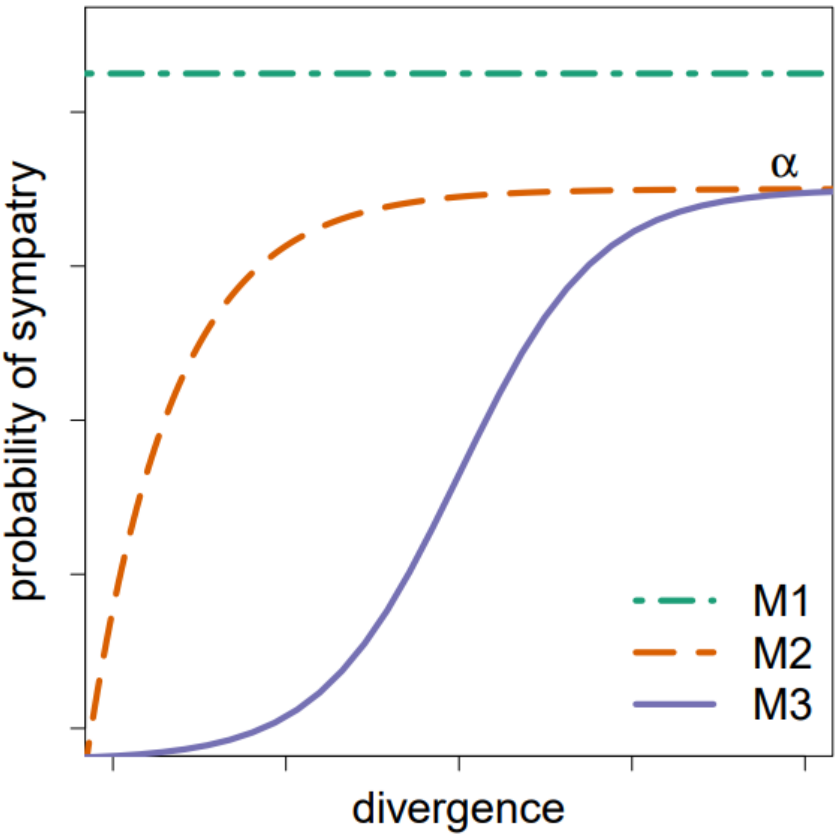

Figure 3.2 Potential models of sympatry-divergence relationships
Three models for how the probability of sympatry (θ) can vary as a function of either phylogenetic or morphological divergence. From top to bottom: M1, a model where θ is independent of the evolutionary or morphological divergence between taxa; M2, where θ approaches a limiting value α; M3, where θ logistically varies with divergence and also asymptotically approaches a limiting value α.

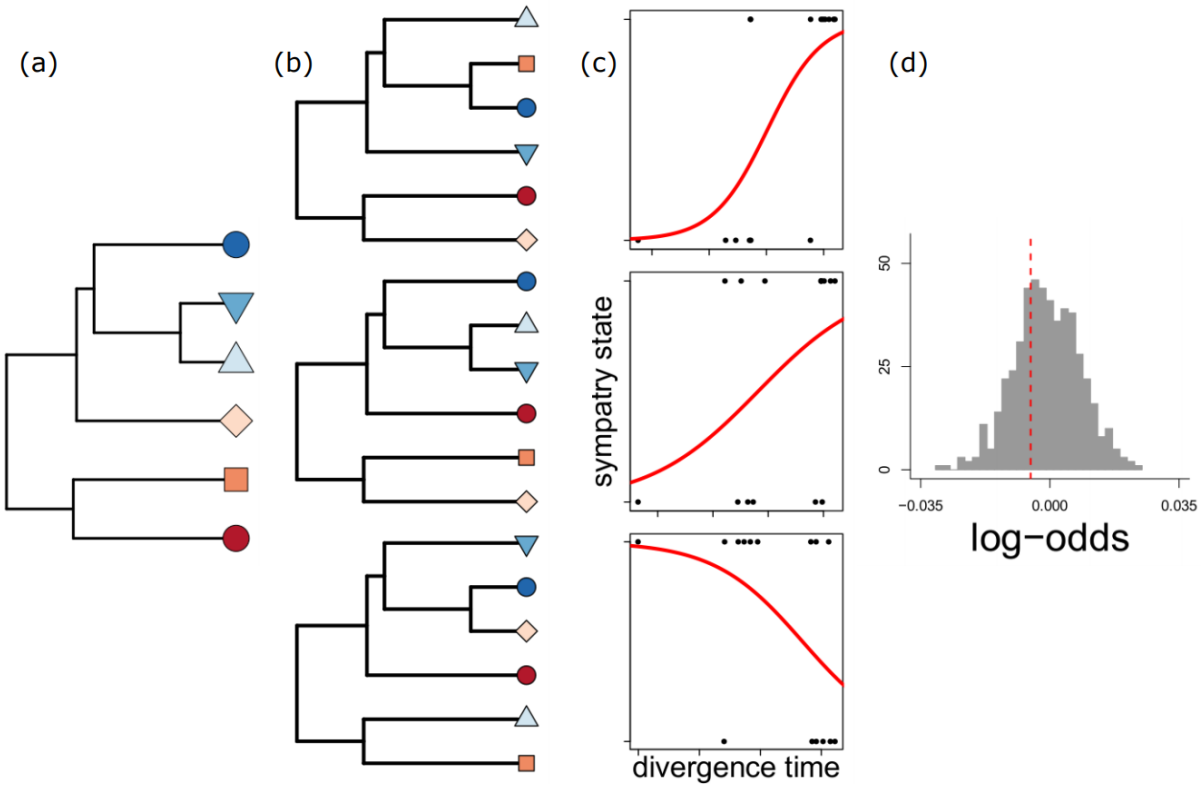

Figure 3.3 Range randomization approach
A schematic of our range randomization approach used to test the relationship between sympatry and the time since divergence. For each realm, we took the (a) phylogeny of all bat species endemic to that realm, and (b) randomized species and range identity while holding the tree constant. For each of these randomizations, we calculated (c) the logistic regression and associated log-odds between divergence time and sympatry state. Repeating (b) and (c) 500 times created (d) a null distribution of relationships, shown here as the logarithm of the odds-ratio between divergence time and sympatry state. This null distribution was then compared to the empirical value for that realm, indicated by the dashed line.

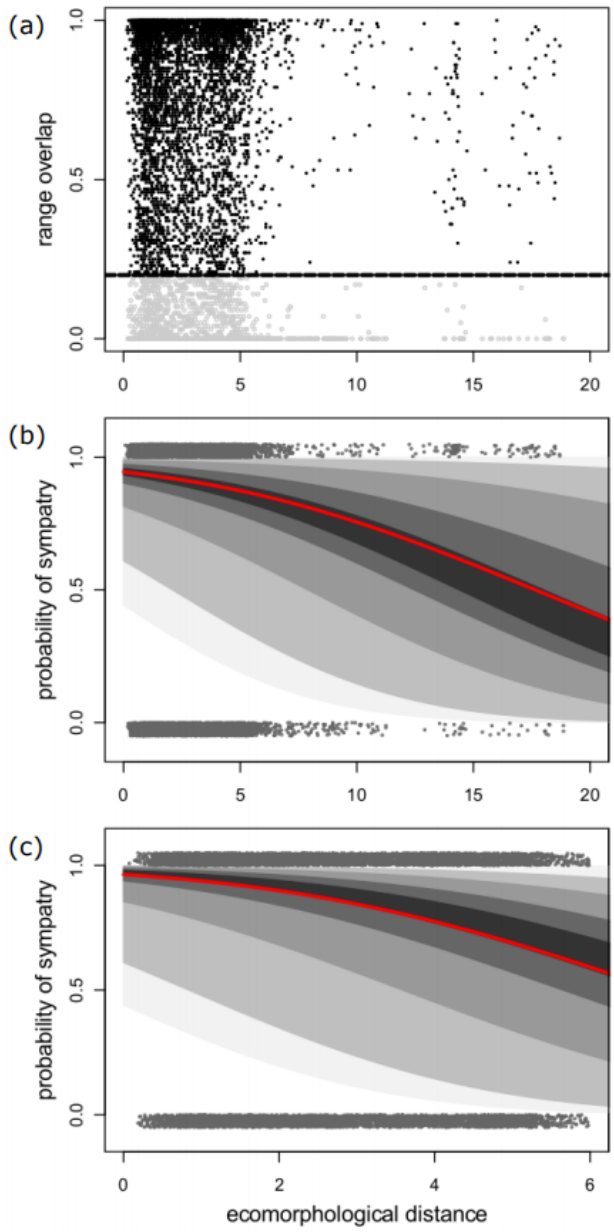

Figure 3.4 Negative Neotropical relationship between ecomorphology and sympatry
(a) Pairwise Euclidean distances (ecomorphology) versus percentage range overlap for all pairs of Neotropical bat species considered in this study (*N* = 8967 pairs). Pairs above the dotted threshold are considered sympatric for the main analyses of this study. (b) Points denote the same dataset, decomposed into binary sympatry or allopatry states. The curve is the posterior mean PLMM estimate of the relationship between pairwise ecomorphological distance and the probability of sympatry. Progressively darker polygons highlight the 90%, 75%, 50%, 25%, and 10% credibility intervals around the mean. (c) The same relationship as (b), but fitting the model only to species pairs with morphological distances less than 6.0, which accounts for 95.8% of all species pairs. This analysis was performed to ensure that the overall negative relationship was not driven by outliers.

Table S3.1 Sympatry and range overlap data for all realms
Patterns of sympatry and range overlap for pairs of bats within each WWF biogeographic realm, with the Afrotropics (excluding Madagascar, Seychelles, and Comoros), and with Oceania and Australasia combined (Olson *et al*. 2001).

WWF biogeographic realm	Species with spatial data	Percentage of sympatric pairs (20% threshold)	Average pairwise range overlap
Afrotropics	78	46.5% of pairs	31.3%
Indomalaya	175	38.7% of pairs	28.2%
Nearctic	40	56.4% of pairs	40.9%
Neotropics	235	48.2% of pairs	38.2%
Oceania & Australasia	82	29.2% of pairs	22.3%
Palearctic	70	25.3% of pairs	16.0%

Table S3.2 Maximum-likelihood model descriptions
Model numbers and descriptions for our maximum-likelihood modeling of the probability of sympatry, given different models of how this probability could change with divergence (Figure 3.2). These models were used for analysis of bat sister species pairs.

Model	***Sympatry-divergence relationship***
M1	NA (H_0)
M2a	exponential age
M2b	exponential morphology
M2c	exponential age*morphology
M3a	logistic age
M3b	logistic morphology
M3c	logistic age*morphology

Table S3.3 Likelihood-ratio tests for maximum-likelihood models

Likelihood-ratio tests for models of the probability of secondary sympatry, fitted first (left) to sister species of all extant bat sister species with spatial and morphological data, and then (right) to New World (Nearctic and Neotropical) sister species only. In each case, M1 represents the null hypothesis (H_0) of no relationship between the probability of sympatry and divergence, which both M2 and M3 are tested against. Note that we cannot reject H_0 in any case. All models are detailed in Figure 3.2 and Table S3.2. For our χ^2 tests, *df* is 1 for M2 and 2 for M3.

Global bats			**New World bats**		
Model	***χ^2***	***Pr (> χ^2)***	***Model***	***χ^2***	***Pr (> χ^2)***
M1 (H_0)	-	-	M1 (H_0)	-	-
M2a	2.3770	0.1231	M2a	3.0347	0.0815
M3a	1.2229	0.2688	M3a	1.4205	0.2333
Model	***χ^2***	***Pr (> χ^2)***	***Model***	***χ^2***	***Pr (> χ^2)***
M1 (H_0)	-	-	M1 (H_0)	-	-
M2b	0.0001	0.9912	M2b	0.0001	0.9997
M3b	1.2123	0.2709	M3b	0.9281	0.3354
Model	***χ^2***	***Pr (> χ^2)***	***Model***	***χ^2***	***Pr (> χ^2)***
M1 (H_0)	-	-	M1 (H_0)	-	-
M2c	0.8017	0.3706	M2c	0.8574	0.3545
M3c	0.4916	0.4832	M3c	0.4930	0.4826

Table S3.4 Maximum-likelihood parameter estimates
ML parameter estimates for each of our approach #3 models (see Methods), untransformed (*i.e.* α can be greater than 1 due to the logit transformation of sympatry state). Note that morphology models (*b*) both imply declining probabilities of sympatry given higher divergence in M3b, as we suggest in our PLMMs, though this is not the case for M2b. This may reflect very different processes that occur at the short timescale of sister species.

Global bats

Model	***ML parameter estimates***
M1	*theta* = 0.57
M2a	α = 0.64, *k* = -0.91
M2b	α = 0.27, *k* = 4.7
M2c	α = 0.37, *k* = 0.55
M3a	α = 0.69, *k* = -0.89, *w* = 0.40
M3b	α = 13.28, *k* = -9.75, *w* = -16.6
M3c	α = 0.38, *k* = 0.77, *w* = -0.82

New World bats

Model	***ML parameter estimates***
M1	*theta* = 0.57
M2a	α = 0.89, *k* = -1.11
M2b	α = 0.27, *k* = 5.27
M2c	α = 0.41, *k* = 0.49
M3a	α = 0.99, *k* = -1.12, *w* = 0.67
M3b	α = 10.03, *k* = -7.33, *w* = -13.1
M3c	α = 0.42, *k* = 0.72, *w* = -0.80

Table S3.5 Furnariid ecomorphology-sympatry relationships
PLMM results for the effects of age (β_1), ecomorphological divergence (β_2), and combined age and ecomorphological divergence (β_3) on pairwise patterns of sympatry (at a 20% overlap threshold) for 94 sister species pairs of the bird family Furnariidae. Separate analyses for datasets of just bill ecomorphology (bMorph) and total ecomorphology (tMorph) are reported. Posterior means and pMCMC-values are included, and bolded with asterisks when considered "significant" (*pMCMC* < 0.05, though note that this is *not* a frequentist approach). Note that divergence *strongly* predicts sympatry in furnariids, in contrast with most bats (though the directionality of effects for combined age and ecomorphology).

Dataset	**β_1 posterior mean**	**β_1 pMCMC**	**β_2 posterior mean**	**β_2 pMCMC**	**β_3 posterior mean**	**β_3 pMCMC**
bMorph	**0.333**	**0.00333***	**4.282**	**0.0289***	**-0.520**	**0.04333***
tMorph	**0.355**	**0.0333***	**3.976**	**0.0322***	-0.503	0.0544

Table S3.6 Furnariid maximum-likelihood model descriptions
For our ML model-fitting, we expanded both M2 and M3 (prefixed with F for Furnariidae here) to include separate fits for bill and total morphology.

Model	*Sympatry-divergence relationship*
FM1	NA
FM2a	exponential age
FM2b	exponential bill morphology
FM2c	exponential total morphology
FM2d	exponential age*bill morphology
FM2e	exponential age*total morphology
FM3a	logistic age
FM3b	logistic bill morphology
FM3c	logistic total morphology
FM3d	logistic age*bill morphology
FM3e	logistic age*total morphology

Table S3.7 Furnariid ΔAICc scores and likelihood-ratio tests

ΔAICc scores and likelihood-ratio tests for all models of the probability of secondary sympatry, fitted to sister species of the bird family Furnariidae. In each case, FM1 represents the null hypothesis (H_0) of no relationship between the probability of sympatry and divergence, which both FM2 and FM3 are tested against. Note that we reject null hypotheses in favor of alternative hypotheses invoking divergence for furnariids, in contrast with extant bats.

Model	***χ^2 (df = 1)***	***Pr (> χ^2)***
FM1 (H_0)	-	-
FM2a	**13.1600**	**< 0.0001***
FM3a	0.3712	0.5424

Model	***χ^2 (df = 1)***	***Pr (> χ^2)***
FM1 (H_0)	-	-
FM2b	0.2223	0.6373
FM3b	**6.2837**	**0.0122***

Model	***χ^2 (df =1)***	***Pr (> χ^2)***
FM1 (H_0)	-	-
FM2c	1.3961	0.2374
FM3c	**4.7573**	**0.0292***

Model	***χ^2 (df =1)***	***Pr (> χ^2)***
FM1 (H_0)	-	-
FM2d	**8.4358**	**0.0004***
FM3d	0.5522	0.4574

Model	***χ^2 (df =1)***	***Pr (> χ^2)***
FM1 (H_0)	-	-
FM2e	**9.8527**	**0.0002***
FM3e	0.3894	0.5326

Table S3.8 Neotropical ecomorphology-sympatry relationships at finer scales
An additional PLMM analysis conducted analogously to our main analysis, focused on the Neotropical species for which we have morphological data (see Figure 3.4c for more details). Here, we reduced the dataset even further to just those pairs within 6 Euclidean distance of each other in morphospace, where the vast majority of our data lie. We recover negative results concordant with our main analysis for morphology, but an additional, significant interaction component. We discuss potential reasons for interactions between age and morphology in our main text.

Realm (*N*)	**β_1 posterior mean**	**β_1 pMCMC**	**β_2 posterior mean**	**β_2 pMCMC**	**β_3 posterior mean**	**β_3 pMCMC**
Neotropics	-0.0024	0.07	**-0.260**	**0.00111***	**0.0043**	**0.0033***

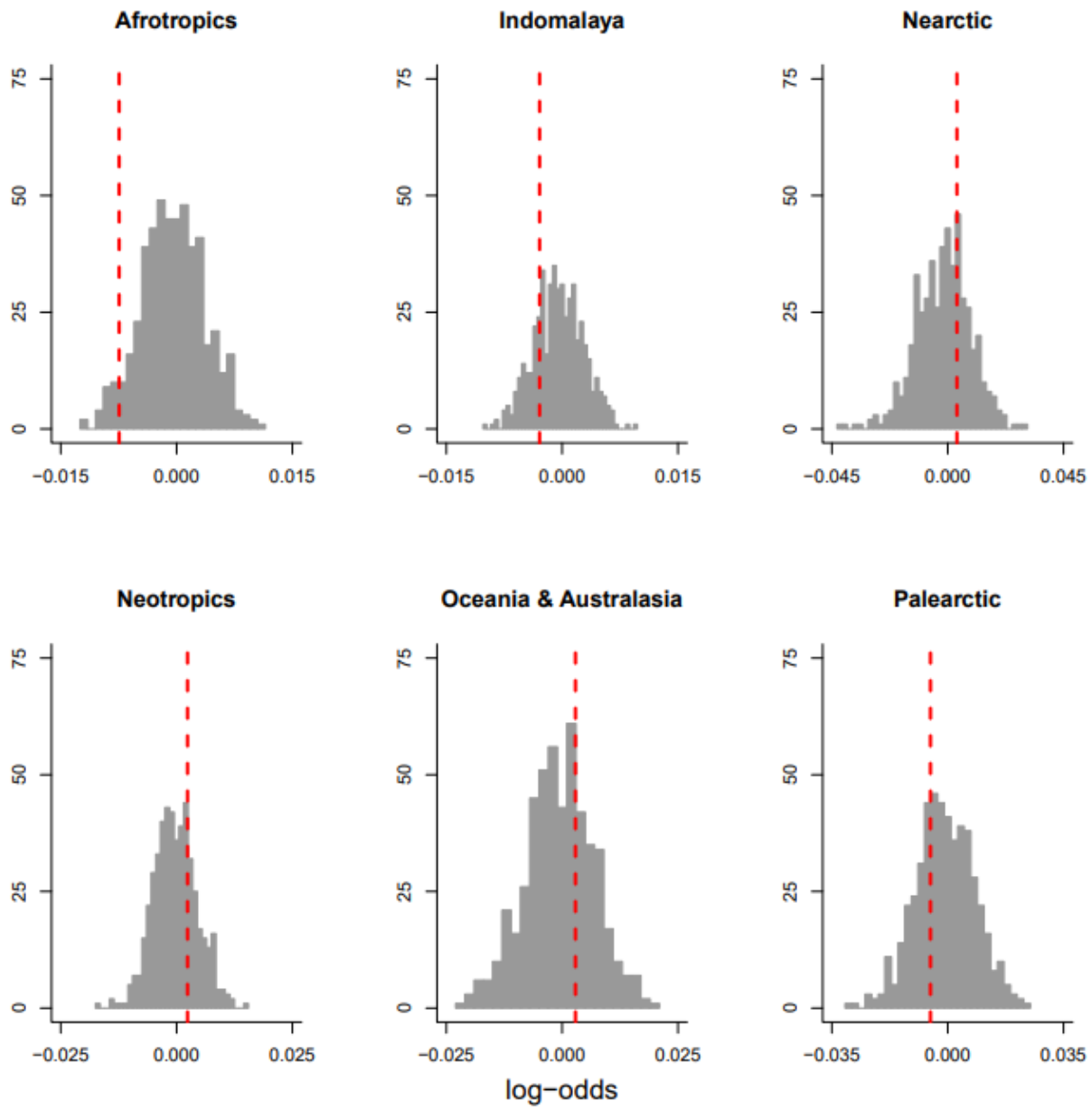

Figure S3.1 Null distributions of age-sympatry relationships across realms
The expected distribution of the age-sympatry relationship for 6 biogeographic realms, calculated by randomizing species range assignments 500 times per realm. Vertical lines depict the empirical log-odds calculated from a logistic regression of age and binary sympatry state. A positive log-odds, for example, suggests a scenario where sympatry is more likely as time since divergence increases. See Methods and Figure 3.3 for more details on methodology.

CHAPTER 4

Digitizing extant bat diversity: an open-access repository of 3D μCT-scanned skulls for research and education[5]

ABSTRACT

Biological specimens are primary records of organismal ecology and history. As such, museum collections are invaluable repositories for testing ecological and evolutionary hypotheses across the tree of life. Digitizing and broadly sharing the phenotypic data from these collections serves to expand the traditional reach of museums, enabling widespread data sharing, collaboration, and education at an unprecedented scale. In recent years, μCT-scanning has been adopted as one way for precisely digitizing museum specimens. Here, we describe a large repository of 3D, μCT-scanned images and surfaces of skulls from 359 extant species of bats, a highly diverse clade of modern vertebrates. This digital repository spans much of the taxonomic, biogeographic, and morphological diversity present across bats. All data have been published to the MorphoSource platform, an online database explicitly designed for the archiving of 3D morphological data. Beyond its intrinsic utility to bat biologists, our digital specimens represent

[5] Shi, J.J., Westeen, E.P., & Rabosky, D.L. *In review*. Digitizing extant bat diversity: an open-access repository of μCT-scanned skulls for research and education. *PLOS ONE*.

a resource for educators and for any researchers seeking to broadly test theories of trait evolution, functional ecology, and community assembly.

INTRODUCTION

Organismal morphology is key to our conception of how species interact with one another and with their environments (Galis 1996, Koehl 1996, Wainwright 2007). Furthermore, morphology often reflects and represents some of the clearest examples of natural selection and adaptation, both over evolutionary timescales and in response to global change. Given these considerations, physical repositories of specimens, like museums of natural history, are invaluable resources for ecologists and evolutionary biologists (Graham *et al.* 2004, Pyke & Ehrlich 2010). Analyzing the morphology of specimens collected for and preserved within these repositories can reveal the tempo and mode of morphological evolution (Foote 1997), species' responses to external change (Gardner *et al.* 2011, Sheridan & Bickford 2011, DuBay & Fuldner 2017), and can be a window into the scale and diversity of biological innovation (Thompson & Timmermans 2014, Curtis & Simmons 2017). By integrating data across these various collections, researchers can highlight broad ecological and evolutionary trends throughout branches of the tree of life and over multiple biogeographic realms.

The creation and curation of digital specimens - electronic records, visualizations, and reproductions of physical specimens - can improve accessibility and collaboration across institutions, especially when they are open-access to the research community. Some aspects of morphology that are difficult to investigate with fragile and rare physical specimens can be studied using digital specimens. For instance, some internal morphological traits cannot be

measured or otherwise studied without damaging or destroying samples (Ziegler *et al.* 2010). Digital specimens can also facilitate analysis of particularly small or cryptic aspects of morphology (Green *et al.* 2012, Gunz *et al.* 2012, Mason *et al.* 2015, Curtis & Simmons 2017). Rote tasks, including measurements and character scoring, can also be automated and scripted when digital specimens are used, streamlining data collection and accelerating the pace of museums-based research.

In recent years, researchers have harnessed X-ray computed microtomography (μCT) scanning as an approach for digitally capturing and visualizing morphology in three-dimensional space. μCT scans are particularly useful for digitally preserving hard tissue from specimens, though considerable advances have been made to extend the method to soft tissue scanning (Metscher 2009, Gignac *et al.* 2016). Generalized μCT scanning methods produce high-resolution images and 3D volumes and surfaces that can be used for a variety of derived analyses, ranging from finite element analysis (Santana *et al.* 2012) to both traditional linear and geometric morphometrics (van der Niet *et al.* 2011, Tokita *et al.* 2016).

Here, we describe a digital 3D, open-access repository of extant bat skull diversity that spans much of the phylogenetic and ecological breadth of the clade. We detail its assembly and accessibility, and discuss some of its potential uses for the general community. Bats (Mammalia: Chiroptera) are both ecologically and morphologically heterogeneous, with clear links between both axes of diversity (Simmons & Conway 2003, Simmons 2005). The close synergy between form and function in this clade also spans multiple facets of their ecology and behavior. For instance, measurements of wing shape have been linked to dispersal ability (Norberg & Rayner 1987), nasal and auricular geometry to echolocation broadcasting (Santana & Lofgren 2013, Curtis & Simmons 2017), and jaw morphology to trophic ecology (Santana *et al.* 2010, Dumont

et al. 2012). The bat skull and face, in particular, are bridges between physical performance and ecology, both externally (*e.g.* capturing and processing food) and internally (*e.g.* modulating and emitting echolocation calls). Our repository captures much of the skull diversity of extant bats, as it is designed to maximize sampling across both the bat phylogeny and their biogeographic distribution. Our goals are to provide a solid foundation for any researchers interested in bat morphology, its ecological consequences, and its evolutionary drivers.

MATERIALS AND METHODS

Specimen and collection details

We scanned adult skulls of bat specimens from the University of Michigan Museum of Zoology (UMMZ) and the American Museum of Natural History (AMNH). Sexual selection may occur in some bat species (*e.g.* Myers 1978, Willig & Hollander 1995); as such, we generally measured females, but maximized species-level taxonomic diversity whenever possible. We separated mandibles and crania for most specimens, though a small fraction were articulated enough to make this unfeasible. We mounted all specimens in foam to prevent movement in preparation for μCT-scanning.

For this database, we first prioritized scanning across all families present in the UMMZ collections, where scans were performed. We then expanded on the species scanned per family through the AMNH collections. Our database also predominantly prioritized specimens represented in the species-level phylogeny of Shi & Rabosky (2015). We μCT-scanned 435 total skulls across the two museums: 230 skulls of specimens from the UMMZ collections and 205 skulls of specimens from the AMNH.

μCT-scanning, image processing, and validation

All specimens were scanned and reconstructed using a μCT scanner (μCT100 Scanco Medical, Bassersdorf, Switzerland) associated with the University of Michigan School of Dentistry. We performed nearly all scans and reconstructions at a voxel size between 12 and 30 μm (with the vast majority of scans at 20 μm), with a peak kilovoltage of 70V across the X-ray tube and a current of 114 μA (Table S4.1). Each scan was filtered with a 0.5 mm aluminum filter, and scanning proceeded for 750 projections with an integration time of 750 ms. Only the disproportionately large skulls of the flying fox family Pteropodidae were scanned with significantly different voxel sizes of 30-60 μm. Full scan details are available in the Table S4.1.

We imported the resulting 16-bit DICOM stacks for each cranium and mandible into the program ImageJ (Schneider *et al.* 2012), where they were cropped and edited to minimize scanning artifacts and to enhance contrast between bone and negative space. In general, editing was restricted to minimal adjustments of brightness and contrast. We then converted all images into 8-bit TIFF stacks for further processing and digital storage.

To generate 3D surfaces for all of the UMMZ specimens, we imported the specimen-specific TIFF stacks into the program Avizo 9.2.0 (FEI, Hillsboro, USA) for reconstruction and segmentation. We segmented bone from other material, such as the mountain foam, using built-in multi-thresholding and segmentation editors, and then generated three-dimensional surfaces. All thresholded and segmented surfaces were exported as PLY files for storage and broad compatibility with widely-used morphometric software.

As our goal is for digital specimens to be comparable with and used alongside physical specimens, there may be concern about how the scanning and reconstruction process may make digital measurements differ significantly from physical measurements. As one estimate of how a

simple analysis may differ based on using digital specimens or their original physical specimens, we compared linear caliper measurements taken from the original, physical specimens with electronic measurements processed in Avizo 9.2.0.

MorphoSource storage

We archived all data on MorphoSource (http://www.morphosource.org/), an online data archive that sorts 3D datasets into individual projects for rapid dissemination and ease of sharing with collaborators and practitioners. These data were all archived under a Creative Commons license (CC-BY-NC), making them open-access to the community. Each specimen was vouchered and represented by a compressed folder of TIFF images and, for the UMMZ specimens, an associated PLY surface file.

RESULTS

Repository details

Our database includes species from 14 of the 20 extant families of bats (Simmons 2005; Figure 4.1). Five of the missing families are either currently monotypic (Craseonycteridae, Mystacinidae) or monogeneric with low and particularly undersampled diversity in our source collections (Myzopodidae, Furipteridae, Rhinopomatidae). The fifth missing family, Cistugidae, is not included to avoid misidentification: this family's species are included in the genus *Myotis* (Family Vespertilionidae) on many databases, including iDigBio, despite recent elevation to family status (Lack *et al.* 2010). Due to the potential for these species to both be mislabeled and misidentified as extremely similar *Myotis* conspecifics, we have avoided including this family until we can validate them with more specimens.

Most species are represented by a single digital specimen, though some have multiple digital specimens in the database due to physical damage, or for testing intraspecific variability (see Table S4.1). In total, we have 359 unique species in our repository, spanning roughly 30% of extant diversity (Figure 4.1; Simmons 2005, Shi & Rabosky 2015). We note that bat taxonomy, as is true of many clades, has constantly evolved over the course of specimen collection at both institutions. As such, species names for some specimens are not always consistent across databases. The hierarchy of genera, species, and subspecies is notably in flux for many of the bat taxa we include here. Our count of 359 species reflects taxonomy as defined by our species-level molecular phylogeny (Shi & Rabosky 2015). However, if we use iDigBio taxonomy, which is automatically associated with MorphoSource, we count 344 species, as many putative species are considered subspecies according to this taxonomy. We make note of these discrepancies and changes to taxonomy in Table S4.1.

These species span all biogeographic realms as defined by Olson *et al.* (2001), and also cover all major trophic classifications of extant bats, including insectivory, nectarivory, frugivory, sanguivory, carnivory, and piscivory (Nowak 1994, Simmons & Conway 2003). Skulls of bats with different trophic behavior are notably distinct, and are unevenly distributed across the phylogeny (Figure 4.2).

Image file and surface use

File size and image count vary depending on length of an individual cranium or mandible and voxel size, but most surfaces are approximately 500MB with between 400-1000 individual images in their associated TIFF stack. Some representative surfaces are depicted in Figure 4.2, showcasing some of the ecomorphological disparity of extant bat skulls.

The images in the TIFF stack can be used to reconstruct volumetric data, which are appropriate for functional studies of bone density, or comparative studies on the evolution of internal cavities related to sensory behavior. By contrast, researchers can use the included example PLY surface files for morphometric work, as they can easily be imported into software designed for linear morphometrics or geometric morphometrics (*e.g.* the R package *geomorph*; Adams *et al.* 2017). Researchers can also create their own surface files in other formats from the original TIFF stack, especially if they desire higher resolution or surface fidelity than is feasible for bulk online storage.

We estimate how a basic morphometric analysis may differ based on usage of digital or physical specimens by comparing a set of nine linear measurements (as described by Dumont *et al.*, 2012) taken using caliper measurements on physical specimens with those taken in digital space using Avizo 9.2.0. Across 20 different specimens, all of different species, we find physical and digital measurements differ by less than 2% for all measurements, on average (Figure 4.3, Table S4.2).

DISCUSSION

We created and shared a digital repository of 3D μCT morphological data for 359 species of extant bats. The data are publicly and freely available through the MorphoSource portal (Project #386), for immediate use or collaboration by any researchers. Several limitations of our repository should be acknowledged. While we only include skeletal data at this time, diffusible iodine-based contrast-enhanced μCT (diceCT) scans have highlighted the functional diversity of soft tissue like muscle and cartilage in bats (Santana 2018), and can be integrated into this repository. Higher-resolution scanning, in general, in conjunction with soft tissue data can

illuminate aspects of morphology that are not as clear at our current resolution, such as the turbinates (Gunz *et al.* 2012). Our database is also disproportionately biased towards noctilionoid bats, which have historically been the focus of much research on bat form and function (Dumont *et al.* 2012). This fact alone has likely driven research questions and specimen collectors; phyllostomid bats, for instance, are among the most well-studied bats for ecologists and evolutionary biologists alike. Old World rhinolophoids and the cosmopolitan, insectivorous vespertilionoids, which together comprise the vast majority of unsampled species (Figure 4.1), are a natural target for future sampling.

We emphasize that digital databases should not be viewed as permanent replacement for primary, vouchered materials. Museum collections, despite often being critically underfunded and underappreciated, play important roles in society, policy, and education (Suarez & Tsutsui 2004, Rocha *et al.* 2014, Cook *et al.* 2016). Digital specimens will not replace museums and their collections. Instead, we believe that digital repositories can actually highlight the extent to which museums are critical to modern research, and thus should be viewed as natural extensions of an institution's mission of promoting specimen collection. For example, digital specimens can be used to pilot initial studies, before undertaking a more expansive project housed within the physical collections or with long-term loans. Accessibility to museum collections is also only improved by digitization of specimens. Groups and individuals at institutions without affiliated museums, or who lack resources to travel can also benefit from access to a freely available database like ours. The carbon footprint of specimens-based research can even be reduced across the board by minimizing the travel and transport costs associated with physical specimens.

Digital specimens also have clear utility as teaching tools that can promote discussions about a variety of ecological and evolutionary processes to students of all levels. With freely

available specimens, instructors can design curricula around specimens that are fragile, rare, or otherwise unavailable for use in physical form. Finally, we emphasize that all repositories, including ours, can only be improved through collaboration with other researchers and institutions. Unlike with genetic data and GenBank, high-resolution morphological data are not currently widely archived and shared online. Just as the availability of genetic data through GenBank catalyzed rapid innovation in phylogenetic research, we believe that widespread community adoption of an open-access model for sharing digital specimens will lead to similar advances in morphological research (Strasser 2011). Our hope is that by building a digital library of phenotypes, we will facilitate increased cooperation among researchers and collections around the world, and expand the scope of possible research on form and function across the tree of life.

ACKNOWLEDGEMENTS

The authors would like to thank NT Katlein, MA Lynch, NB Simmons, CW Thompson, and HL Williams for their support in data management and collection. JJS would also like to thank DM Boyer and J Winchester for assistance with digital repository management, and CV Avena, AA Curtis, M Kirijo, KA Speer, and LR Yohe for numerous helpful discussions about bats and their diversity, and GE Gerstner for helpful comments on earlier versions of this manuscript.

DATA ARCHIVING

All 3D data referenced in this study (and more) will be archived on and freely available from the MorphoSource database (Project ID 386).

REFERENCES

Adams, D.C., Collyer, M.L., Kaliontzopoulou, A., Sherratt, E. (2017) Geomorph: Software for geometric morphometric analyses. *R package*, **version 3.0.5**.

Cook, J.A., Lacey, E.A., Ickert-Bond, S.M., Hoberg, E.P., Galbreath, K.E., Bell, K.C., Greiman, S.E., McLean, B.S., & Edwards, S. (2016) From museum cases to the classroom: emerging opportunities for specimen-based education. *Aspects of Biodiversity II Archives of the Zoological Museum of Moscow State University*, **54**, 787–799.

Curtis, A.A. & Simmons, N.B. (2017) Unique turbinal morphology in horseshoe bats (Chiroptera: Rhinolophidae). *The Anatomical Record*, **300**, 309–325.

DuBay, S.G. & Fuldner, C.C. (2017) Bird specimens track 135 years of atmospheric black carbon and environmental policy. *Proceedings of the National Academy of Sciences of the United States of America*.

Dumont, E.R., Dávalos, L.M., Goldberg, A., Santana, S.E., Rex, K., & Voigt, C.C. (2012) Morphological innovation, diversification and invasion of a new adaptive zone. *Proceedings of the Royal Society B: Biological Sciences*, **279**, 1797–1805.

Foote, M. (1997) The evolution of morphological diversity. *Annual Review of Ecology and Systematics*, **28**, 129–152.

Galis, F. (1996) The application of functional morphology to evolutionary studies. *Trends in Ecology and Evolution*, **11**, 124–129.

Gardner, J.L., Peters, A., Kearney, M.R., Joseph, L., & Heinsohn, R. (2011) Declining body size: A third universal response to warming? *Trends in Ecology and Evolution*, **26**, 285–291.

Gignac, P.M., Kley, N.J., Clarke, J.A., *et al*. (2016) Diffusible iodine-based contrast-enhanced computed tomography (diceCT): An emerging tool for rapid, high-resolution, 3-D imaging of metazoan soft tissues. *Journal of Anatomy*, **228**, 889–909.

Graham, C.H., Ferrier, S., Huettman, F., Moritz, C., & Peterson, A.T. (2004) New developments in museum-based informatics and applications in biodiversity analysis. *Trends in Ecology and Evolution*, **19**, 497–503.

Green, P.A., Van Valkenburgh, B., Pang, B., Bird, D., Rowe, T., & Curtis, A. (2012) Respiratory and olfactory turbinal size in canid and arctoid carnivorans. *Journal of Anatomy*, **221**, 609–621.

Gunz, P., Ramsier, M., Kuhrig, M., Hublin, J.-J., & Spoor, F. (2012) The mammalian bony labyrinth reconsidered, introducing a comprehensive geometric morphometric approach. *Journal of Anatomy*, **220**, 529–543.

Koehl, M.A.R. (1996) When does morphology matter? *Annual Review of Ecology and Systematics*, **27**, 501–542.

Lack, J.B., Roehrs, Z.P., Stanley, C.E., Ruedi, M., & Van Den Bussche, R.A. (2010) Molecular phylogenetics of Myotis indicate familial-level divergence for the genus Cistugo (Chiroptera). *Journal of Mammalogy*, **91**, 976–992.

Mason, M.J., Segenhout, J.M., Cobo-Cuan, A., Quiñones, P.M., & van Dijk, P. (2015) The frog inner ear: picture perfect? *Journal of the Association for Research in Otolaryngology*, **16**, 171–188.

Metscher, B.D. (2009) MicroCT for comparative morphology: simple staining methods allow high-contrast 3D imaging of diverse non-mineralized animal tissues. *BMC Physiology*, **9**, 11.

Myers, P. (1978) Sexual dimorphism in size of vespertilionid bats. *The American Naturalist*, **112**, 701–711.
Norberg, U.M. & Rayner, J.M. V (1987) Ecological morphology and flight in bats (Mammalia; Chiroptera): wing adaptations, flight performance, foraging strategy and echolocation. *Philosophical Transactions of the Royal Society B: Biological Sciences*, **316**, 335–427.
Nowak, M.D. (1994) *Walker's bats of the world.* Johns Hopkins University Press, Baltimore.
Olson, D.M., Dinerstein, E., Wikramanayake, E.D., Burgess, N.D., Powell, G.V.N., Underwood, E.C., D'amico, J. A., Itoua, I., Strand, H.E., Morrison, J.C., Loucks, C.J., Allnutt, T.F., Ricketts, T.H., Kura, Y., Lamoreux, J.F., Wettengel, W.W., Hedao, P., & Kassem, K.R. (2001) Terrestrial ecoregions of the world: a new map of life on Earth. *BioScience*, **51**, 933–938.
Pyke, G.H. & Ehrlich, P.R. (2010) Biological collections and ecological/environmental research: A review, some observations and a look to the future. *Biological Reviews*, **85**, 247–266.
Rocha, L.A., Aleixo, A., Allen, G., Almeda, F., Baldwin, C.C., Barclay, M.V. *et al.* (2014) Specimen collection: An essential tool. *Science*, **344**, 814-815.
Santana, S.E. (2018) Comparative anatomy of bat jaw musculature via diffusible iodine-based contrast-enhanced computed tomography. *The Anatomical Record*, **301**, 267–278.
Santana, S.E., Grosse, I.R., & Dumont, E.R. (2012) Dietary hardness, loading behavior, and the evolution of skull form in bats. *Evolution*, **66**, 2587–2598.
Santana, S.E. & Lofgren, S.E. (2013) Does nasal echolocation influence the modularity of the mammal skull? *Journal of Evolutionary Biology*, **26**, 2520–2526.
Santana, S.E., Dumont, E.R., & Davis, J.L. (2010) Mechanics of bite force production and its relationship to diet in bats. *Functional Ecology*, **24**, 776–784.
Schneider, C.A., Rasband, W.S., & Eliceiri, K.W. (2012) NIH Image to ImageJ: 25 years of image analysis. *Nature Methods*, **9**, 671–675.
Sheridan, J.A. & Bickford, D. (2011) Shrinking body size as an ecological response to climate change. *Nature Climate Change*, **1**, 401–406.
Shi, J.J. & Rabosky, D.L. (2015) Speciation dynamics during the global radiation of extant bats. *Evolution*, **69**, 1528–1545.
Simmons, N.B. & Conway, T.M. (2003) Evolution of ecological diversity in bats. *Bat ecology* (ed. by T.H. Kunz and M.B. Fenton), pp. 493–535. University of Chicago Press, Chicago.
Simmons, N.B. (2005) An Eocene big bang for bats. *Science*, **307**, 527–528.
Strasser, B.J. (2011) The experimenter's museum: GenBank, natural history, and the moral economies of biomedicine. *Isis*, **102**, 60-96.
Suarez, A. V. & Tsutsui, N.D. (2004) The value of museum collections for research and society. *BioScience*, **54**, 66–74.
Thompson, M.J. & Timmermans, M.J.T.N. (2014) Characterising the phenotypic diversity of Papilio dardanus wing patterns using an extensive museum collection. *PLoS One*, **9**, e96815.
Tokita, M., Abzhanov, A., Yano, W., & James, H.F. (2016) Cranial shape evolution in adaptive radiations of birds: comparative morphometrics of Darwin's finches and Hawaiian honeycreepers. *Philosophical Transactions of the Royal Society B: Biological Sciences*, **372**, 20150418.
van der Niet, T., Zollikofer, C.P.E., León, M.S.P. De, Johnson, S.D., & Linder, H.P. (2010) Three-dimensional geometric morphometrics for studying floral shape variation. *Trends in Plant Science*, **15**, 423–6.

Wainwright, P.C. (2007) Functional versus morphological diversity in macroevolution. *Annual Review of Ecology, Evolution, and Systematics*, **38**, 381–401.
Willig, M.R. & Hollander, R.R. (1995) Secondary sexual dimorphism and phylogenetic constraints in bats: a multivariate approach. *Journal of Mammalogy*, **76**, 981–992.
Ziegler, A., Ogurreck, M., Steinke, T., Beckmann, F., Prohaska, S., & Ziegler, A. (2010) Opportunities and challenges for digital morphology. *Biology Direct*, **5**, 45.

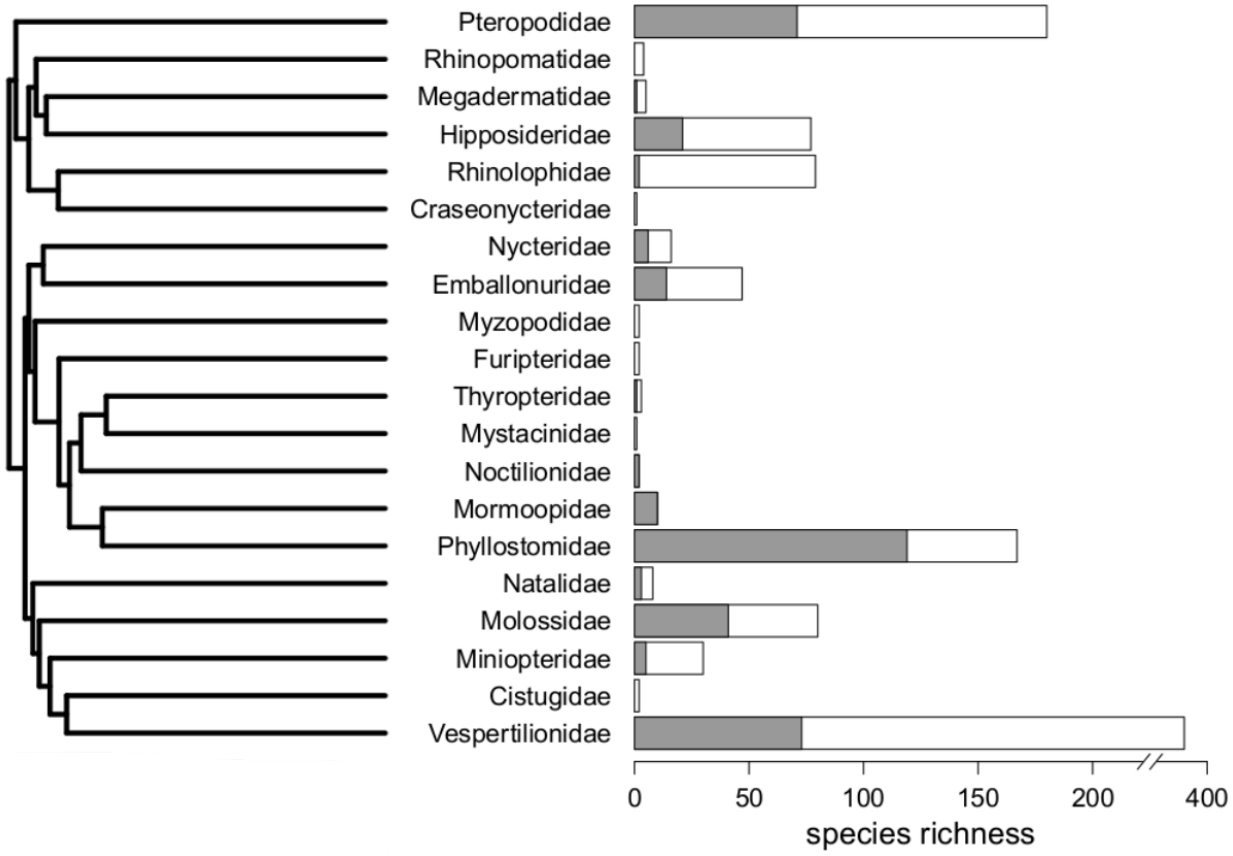

Figure 4.1 Sampling of each extant bat family within this repository
On the left, all twenty extant families of bats (Simmons 2005) and their phylogenetic structure, from Shi & Rabosky (2015). On the right, estimated total richness (background, white bars), and the repository richness (filled, dark grey sections) for each family. Note that the axis for species richness is broken between 200 and 400 due to the high richness of extant vespertilionids.

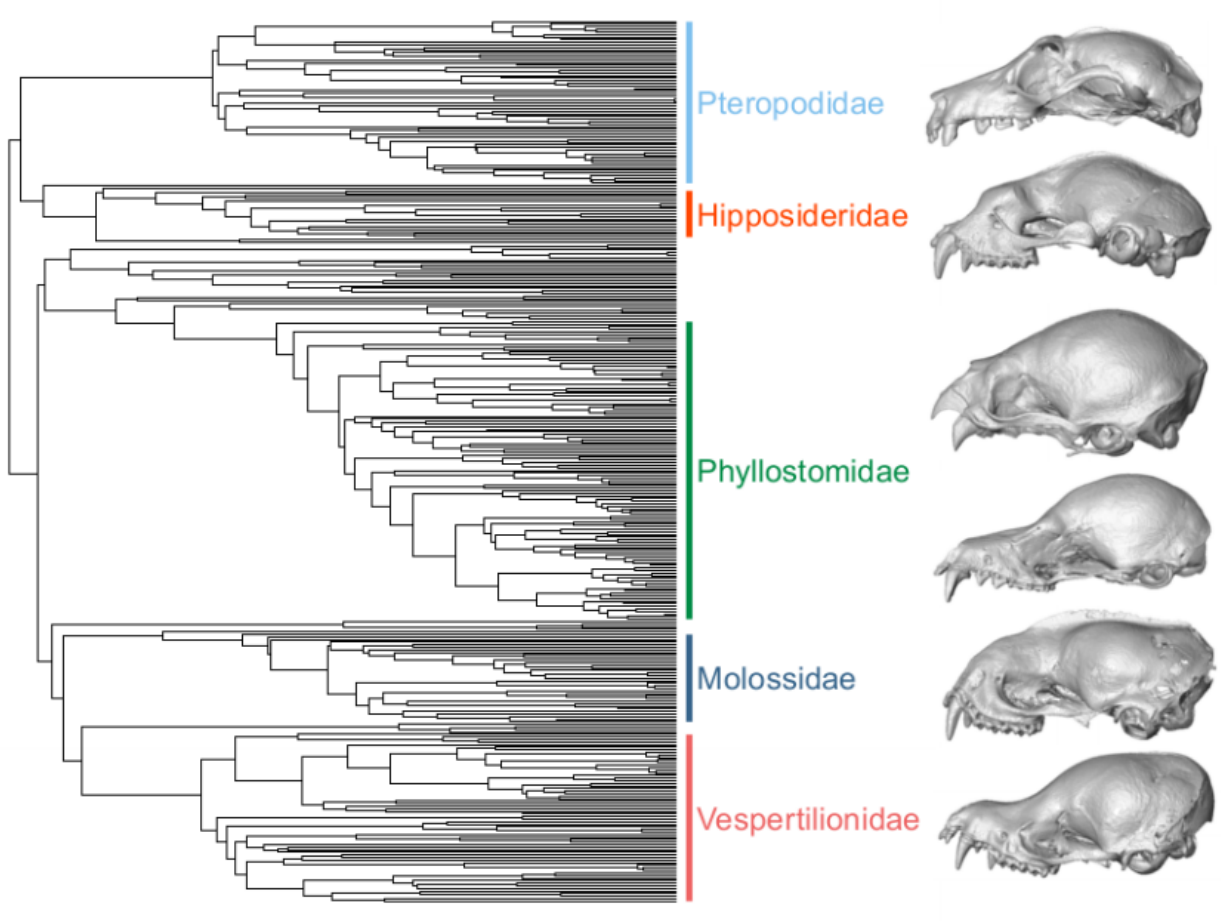

Figure 4.2 Species and skull disparity included in this repository
The phylogeny of bats included in this repository, with the most well-sampled families labeled. We include some examples of cranial surfaces from this repository for these labeled clades, to showcase the breadth of morphological disparity contained in this database, and its link to trophic diversity. Skulls are scaled to be of comparable lengths. Genera from top to bottom: *Pteropus* (frugivore), *Hipposideros* (insectivore), *Desmodus* (sanguivore), *Glossophaga* (nectarivore), *Molossus* (insectivore), *Myotis* (insectivore).

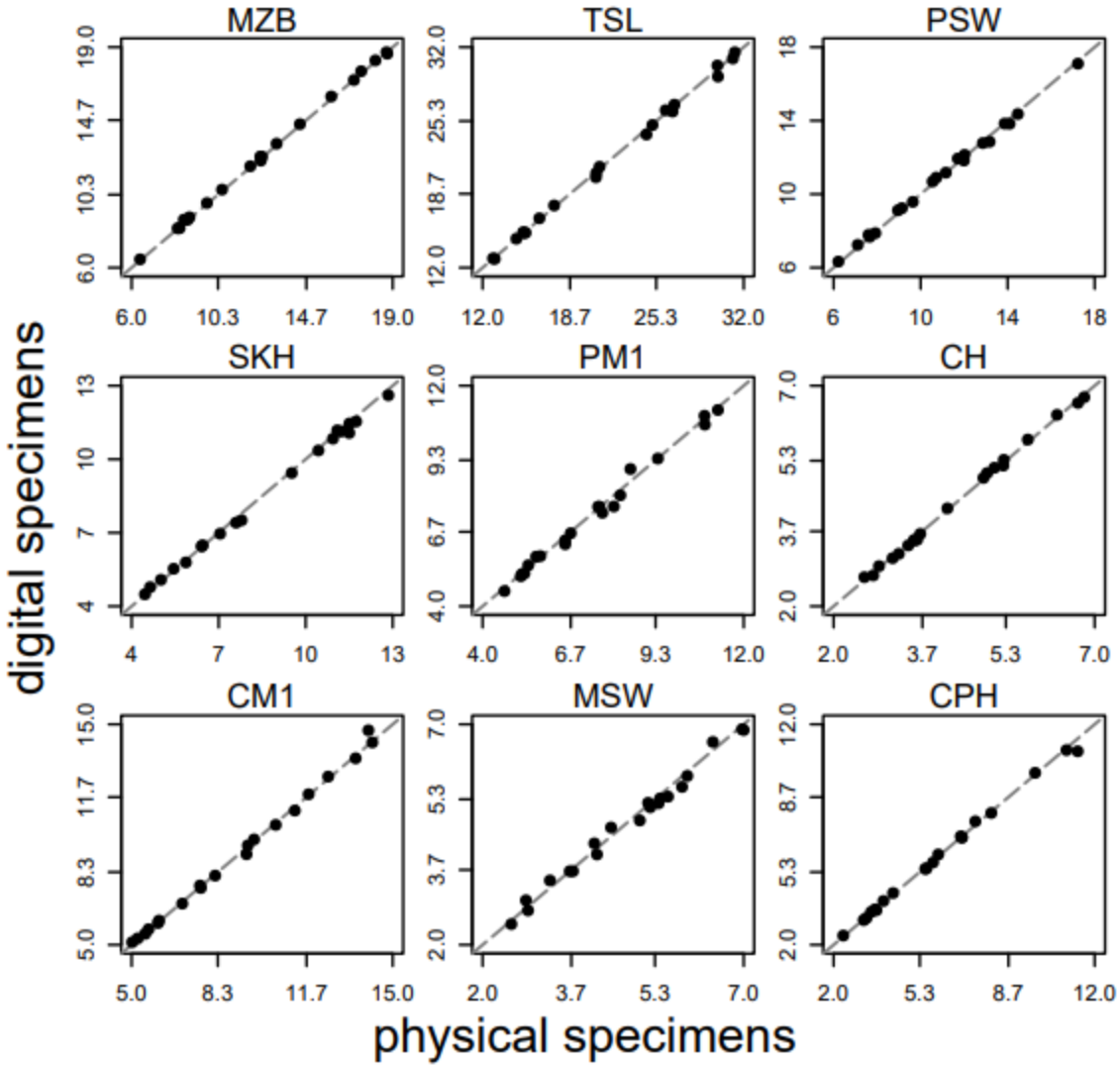

Figure 4.3 Relationships between measurements taken from digital and physical specimens For each of 9 linear measurements, we present the relationship between measurements taken using calipers on physical measurements versus measurements taken on the surface of digital specimens, across 20 different bat species. A dashed 1:1 line is included for each measurement. The measurements are described in full by Dumont *et al.* (2012), and are abbreviated MZB (maximum zygomatic breadth), TSL (total skull length), PSW (posterior skull width or mastoid breadth), SKH (skull height), PM1 (palate width at molar 1), CH (condyle height), CM1 (mandibular length from condyle to molar 1), MSW (minimum skull width), and CPH (coronoid process height). Differences between the two methods are minimal and appear random with respect to species.

Table S4.1 Specimen details

A full table describing the 435 specimens contained in this repository at the time of manuscript submission, taxonomy information, sex, and associated identifiers from their parent institutions. We also note where GenBank taxonomy (our primary classification system) diverges from that of iDigBio, which is automatically associated with all MorphoSource data. Finally, we note the cases where scans were not performed at our standard 20 μm voxel size.

species	subspecies	family	sex	museum number	taxonomy notes	scan size
Balantiopteryx plicata		Emballonuridae	F	UMMZ102659		12 μm
Centronycteris maximiliani		Emballonuridae	M	AMNH267397		
Chaerephon pumilus		Emballonuridae	F	AMNH184402		
Diclidurus albus	*virgo*	Emballonuridae	U	AMNH99478		
Emballonura alecto		Emballonuridae	F	UMMZ156848		
Emballonura raffrayana	*cor*	Emballonuridae	M	AMNH99487		
Emballonura raffrayana	*raffrayana*	Emballonuridae	M	AMNH101939		
Emballonura semicaudata	*semicaudata*	Emballonuridae	F	AMNH68724		
Peropteryx kappleri		Emballonuridae	F	UMMZ105776		
Peropteryx macrotis		Emballonuridae	F	UMMZ156592		
Saccolaimus saccolaimus	*saccolaimus*	Emballonuridae	M	AMNH101604		
Saccolaimus saccolaimus	*saccolaimus*	Emballonuridae	M	AMNH101605		
Saccopteryx canescens	*canescens*	Emballonuridae	U	AMNH23642		
Taphozous longimanus	*albipinnis*	Emballonuridae	M	AMNH103824		
Taphozous mauritianus		Emballonuridae	F	AMNH179287		
Taphozous melanopogon		Emballonuridae	F	UMMZ156810	iDigBio: *Taphozous philippinensis*	
Taphozous nudiventris	*nudiventris*	Emballonuridae	M	AMNH27391		
Aselliscus stoliczkanus		Hipposideridae	M	AMNH115576		
Aselliscus tricuspidatus	*koopmani*	Hipposideridae	M	AMNH159388		
Cloeotis percivali	*australis*	Hipposideridae	F	AMNH168162		
Hipposideros abae		Hipposideridae	F	AMNH49120		
Hipposideros ater	*saevus*	Hipposideridae	M	AMNH107819		

Hipposideros caffer	*caffer*	Hipposideridae	F	AMNH161913		
Hipposideros calcaratus	*calcaratus*	Hipposideridae	M	AMNH194346		
Hipposideros cervinus	*cervinus*	Hipposideridae	F	AMNH102250		
Hipposideros cervinus	*cervinus*	Hipposideridae	F	AMNH159351		
Hipposideros cervinus	*cervinus*	Hipposideridae	F	AMNH194862		
Hipposideros cervinus	*cervinus*	Hipposideridae	M	AMNH221992		
Hipposideros cyclops		Hipposideridae	F	AMNH239401		
Hipposideros diadema	*speculator*	Hipposideridae	M	AMNH102302		
Hipposideros diadema		Hipposideridae	F	UMMZ157092		
Hipposideros dyacorum		Hipposideridae	M	AMNH106953		
Hipposideros fuliginosus		Hipposideridae	M	AMNH241043		
Hipposideros gigas		Hipposideridae	M	AMNH236305		
Hipposideros grandis		Hipposideridae	M	AMNH112943		
Hipposideros larvatus	*neglectus*	Hipposideridae	F	AMNH103231		
Hipposideros larvatus	*poutensis*	Hipposideridae	M	AMNH26704		
Hipposideros lylei		Hipposideridae	F	AMNH235581		
Hipposideros obscurus		Hipposideridae	F	AMNH241832		
Hipposideros pelingensis		Hipposideridae	M	AMNH102291		
Hipposideros pomona	*sinensis*	Hipposideridae	F	AMNH57166		
Hipposideros ruber	*guineensis*	Hipposideridae	M	AMNH241034		
Hipposideros turpis	*turpis*	Hipposideridae	M	AMNH244345		
Megaderma lyra	*lyra*	Megadermatidae	M	AMNH208822		
Miniopterus natalensis		Miniopteridae	F	UMMZ103548	iDigBio: *Miniopterus schreibersii natalensis*	
Miniopterus paululus		Miniopteridae	F	UMMZ157118	iDigBio: *Miniopterus australis paululus*	
Miniopterus pusillus		Miniopteridae	F	UMMZ172243		
Miniopterus schreibersii		Miniopteridae	F	UMMZ156998		
Miniopterus tristis		Miniopteridae	F	UMMZ160305		
Chaerephon ansorgei		Molossidae	M	AMNH257449		
Chaerephon chapini	*chapini*	Molossidae	U	AMNH49209		
Chaerephon jobensis		Molossidae	F	UMMZ81125		
Chaerephon nigeriae	*spillmani*	Molossidae	M	AMNH89187		

Chaerephon nigeriae	*spillmani*	Molossidae	M	AMNH89193		
Chaerephon nigeriae	*spillmani*	Molossidae	U	AMNH89200		
Chaerephon plicatus		Molossidae	F	UMMZ163623	iDigBio: *Chaerephon plicata (deprecated)*	
Chaerephon pumilus		Molossidae	F	AMNH168211		
Chaerephon pumilus		Molossidae	F	AMNH168216		
Cheiromeles parvidens		Molossidae	M	AMNH241941		
Cheiromeles torquatus	*torquatus*	Molossidae	F	AMNH247585		
Cynomops abrasus	*cerastes*	Molossidae	F	AMNH236220		
Cynomops abrasus		Molossidae	F	UMMZ124418		
Cynomops paranus		Molossidae	M	AMNH94639		
Cynomops planirostris		Molossidae	M	AMNH236221		
Eumops bonariensis	*bonariensis*	Molossidae	F	AMNH235961		
Eumops dabbenei		Molossidae	F	UMMZ146477		
Eumops glaucinus	*glaucinus*	Molossidae	F	AMNH93859		
Eumops patagonicus	*beckeri*	Molossidae	F	AMNH234702		
Eumops patagonicus		Molossidae	F	UMMZ125387	iDigBio: *Eumops patagonicus beckeri*	
Eumops perotis		Molossidae	F	UMMZ77780		
Eumops underwoodi		Molossidae	F	UMMZ89461		
Molossops temminckii	*temminckii*	Molossidae	F	AMNH260262		
Molossops temminckii	*temminckii*	Molossidae	F	AMNH264110		
Molossops temminckii		Molossidae	F	UMMZ125373	iDigBio: *Molossops temminckii temminckii*	
Molossus coibensis		Molossidae	F	UMMZ105734	iDigBio: *Molossus molossus coibensis*	
Molossus molossus	*fortis*	Molossidae	F	AMNH234923		
Molossus molossus	*molossus*	Molossidae	F	AMNH178664		
Molossus molossus	*molossus*	Molossidae	F	AMNH205675		
Molossus molossus	*molossus*	Molossidae	F	AMNH211304		
Molossus molossus	*molossus*	Molossidae	F	AMNH211380		
Molossus molossus	*molossus*	Molossidae	F	AMNH40723		
Molossus molossus	*molossus*	Molossidae	F	AMNH78443		
Molossus molossus	*molossus*	Molossidae	M	AMNH78895		
Molossus molossus	*molossus*	Molossidae	M	AMNH94694		
Molossus molossus	*molossus*	Molossidae	F	AMNH97080		
Molossus molossus	*tropidorhynchus*	Molossidae	U	AMNH176099		
Molossus rufus		Molossidae	F	UMMZ124432		
Molossus sinaloae		Molossidae	F	UMMZ76728		

Mops condylurus	*osborni*	Molossidae	M	AMNH115937		
Mops leucostigma		Molossidae	M	AMNH170639		
Mops midas	*midas*	Molossidae	F	AMNH218980		
Mops mops		Molossidae	M	AMNH233589		
Mormopterus acetabulosus		Molossidae	F	UMMZ115817		
Myopterus daubentonii	*albatus*	Molossidae	F	AMNH48855		
Nyctinomops aurispinosus		Molossidae	U	AMNH178100		
Nyctinomops femorosaccus		Molossidae	F	UMMZ111017	iDigBio: *Tadarida fulminans*	
Nyctinomops laticaudatus		Molossidae	F	UMMZ91175		
Nyctinomops macrotis		Molossidae	F	UMMZ113271		
Otomops martiensseni	*icarus*	Molossidae	M	AMNH172858		
Promops centralis		Molossidae	F	UMMZ124419		
Promops nasutus		Molossidae	F	UMMZ125377		
Tadarida aegyptiaca		Molossidae	F	UMMZ114851		
Tadarida brasiliensis		Molossidae	F	UMMZ90485		
Tadarida brasiliensis		Molossidae	F	UMMZ90486		
Tadarida brasiliensis		Molossidae	F	UMMZ90487		
Tadarida brasiliensis		Molossidae	F	UMMZ90494		
Tadarida brasiliensis		Molossidae	F	UMMZ90495		
Tadarida brasiliensis		Molossidae	F	UMMZ98525		
Tadarida teniotis	*teniotis*	Molossidae	U	AMNH235609		
Mormoops blainvillii	*blainvillii*	Mormoopidae	F	AMNH271513		
Mormoops megalophylla		Mormoopidae	F	UMMZ109749		
Mormopterus beccarii		Mormoopidae	F	AMNH197749		
Mormopterus planiceps		Mormoopidae	F	AMNH220094		
Pteronotus davyi		Mormoopidae	F	UMMZ81050		
Pteronotus gymnonotus		Mormoopidae	F	UMMZ105780		
Pteronotus macleayii	*griseus*	Mormoopidae	M	AMNH60897		
Pteronotus parnellii		Mormoopidae	F	UMMZ105664		
Pteronotus parnellii		Mormoopidae	F	UMMZ99273		
Pteronotus personatus	*personatus*	Mormoopidae	F	AMNH32129		
Pteronotus personatus	*psilotis*	Mormoopidae	M	AMNH177725		
Pteronotus quadridens		Mormoopidae	F	UMMZ68173	iDigBio: *Pteronotus personatus fuliginosus*	
Natalus jamaicensis		Natalidae	M	AMNH271576		
Natalus stramineus		Natalidae	F	UMMZ98847		

Natalus tumidirostris	*haymani*	Natalidae	M	AMNH178687		
Nyctiellus lepidus		Natalidae	F	UMMZ105767	iDigBio: *Natalus lepidus*	
Noctilio albiventris		Noctilionidae	F	UMMZ105827		
Noctilio leporinus		Noctilionidae	F	UMMZ68190		
Nycteris arge		Nycteridae	F	AMNH86770		
Nycteris grandis		Nycteridae	F	AMNH265825		
Nycteris hispida	*hispida*	Nycteridae	M	AMNH184475		
Nycteris javanica		Nycteridae	M	AMNH102372		
Nycteris javanica		Nycteridae	F	AMNH102378		
Nycteris macrotis	*luteola*	Nycteridae	F	AMNH187705		
Nycteris thebaica	*damarensis*	Nycteridae	M	AMNH168133		
Ametrida centurio		Phyllostomidae	F	UMMZ53108		
Anoura caudifer		Phyllostomidae	F	UMMZ168864		
Anoura cultrata		Phyllostomidae	F	AMNH233253		
Anoura geoffroyi		Phyllostomidae	F	UMMZ108647		
Anoura latidens		Phyllostomidae	F	AMNH261230		
Ardops nichollsi	*koopmani*	Phyllostomidae	M	AMNH213954		
Ariteus flavescens		Phyllostomidae	U	AMNH265169		
Ariteus flavescens		Phyllostomidae	U	AMNH265176		
Ariteus flavescens		Phyllostomidae	U	AMNH265255		
Ariteus flavescens		Phyllostomidae	U	AMNH265311		
Artibeus anderseni		Phyllostomidae	F	UMMZ160648	iDigBio: *Dermanura anderseni*	
Artibeus aztecus		Phyllostomidae	F	UMMZ110526	iDigBio: *Dermanura azteca aztecus*	
Artibeus concolor		Phyllostomidae	F	AMNH267476		
Artibeus concolor		Phyllostomidae	F	AMNH267983		
Artibeus fimbriatus		Phyllostomidae	F	UMMZ125943		
Artibeus fraterculus		Phyllostomidae	F	AMNH62939		
Artibeus glaucus		Phyllostomidae	F	UMMZ126742	iDigBio: *Artibeus hirsutus glaucus*	
Artibeus intermedius		Phyllostomidae	U	AMNH212280		
Artibeus jamaicensis	*fuliginosus*	Phyllostomidae	F	UMMZ156077		
Artibeus jamaicensis	*jamaicensis*	Phyllostomidae	F	UMMZ123275		
Artibeus jamaicensis		Phyllostomidae	F	UMMZ108493		
Artibeus jamaicensis		Phyllostomidae	F	UMMZ93300		
Artibeus jamaicensis		Phyllostomidae	F	UMMZ93566		
Artibeus jamaicensis		Phyllostomidae	F	UMMZ93574		

Artibeus lituratus		Phyllostomidae	F	UMMZ169102		
Artibeus obscurus		Phyllostomidae	U	AMNH260234		
Artibeus obscurus		Phyllostomidae	M	AMNH266288		
Artibeus obscurus		Phyllostomidae	F	AMNH268966		
Artibeus phaeotis		Phyllostomidae	F	UMMZ65093	iDigBio: *Dermanura phaeotis palantinus*	
Artibeus planirostris		Phyllostomidae	F	UMMZ126736		
Artibeus toltecus		Phyllostomidae	F	UMMZ108586	iDigBio: *Dermanura tolteca*	
Brachyphylla cavernarum		Phyllostomidae	F	UMMZ68201		
Brachyphylla nana		Phyllostomidae	U	AMNH175982		
Carollia brevicauda		Phyllostomidae	F	UMMZ126789		
Carollia castanea		Phyllostomidae	F	UMMZ164872		
Carollia perspicillata		Phyllostomidae	F	UMMZ126791		
Carollia sowelli		Phyllostomidae	F	UMMZ126717	iDigBio: *Carollia brevicauda*	
Carollia subrufa		Phyllostomidae	F	UMMZ113603		
Centurio senex		Phyllostomidae	F	UMMZ117852		
Chilonatalus micropus	*macer*	Phyllostomidae	M	AMNH216125		
Chiroderma salvini		Phyllostomidae	F	UMMZ165308		
Chiroderma trinitatum		Phyllostomidae	F	UMMZ158061		
Chiroderma villosum		Phyllostomidae	F	UMMZ168882		
Choeroniscus godmani		Phyllostomidae	F	UMMZ83316		
Choeroniscus minor		Phyllostomidae	M	AMNH267152		
Choeronycteris mexicana		Phyllostomidae	F	UMMZ77764		
Chrotopterus auritus		Phyllostomidae	F	UMMZ125902		
Desmodus rotundus		Phyllostomidae	F	UMMZ116246		
Desmodus rotundus		Phyllostomidae	F	UMMZ116247		
Desmodus rotundus		Phyllostomidae	F	UMMZ116249		
Desmodus rotundus		Phyllostomidae	F	UMMZ116250		
Desmodus rotundus		Phyllostomidae	F	UMMZ116251		
Desmodus rotundus		Phyllostomidae	F	UMMZ116252		
Desmodus rotundus		Phyllostomidae	F	UMMZ116253		
Desmodus rotundus		Phyllostomidae	F	UMMZ116255		
Desmodus rotundus		Phyllostomidae	F	UMMZ116266		
Desmodus rotundus		Phyllostomidae	F	UMMZ99345		
Diaemus youngi		Phyllostomidae	F	AMNH257104		
Diphylla ecaudata		Phyllostomidae	F	UMMZ99089		

Erophylla bombifrons		Phyllostomidae	F	UMMZ68205	iDigBio: *Erophylla sezekorni*	
Erophylla sezekorni		Phyllostomidae	F	UMMZ97624	iDigBio: *Erophylla sezekorni planifrons*	
Glossophaga commissarisi		Phyllostomidae	F	UMMZ108497		
Glossophaga leachii		Phyllostomidae	F	AMNH136085		
Glossophaga leachii		Phyllostomidae	F	AMNH185964		
Glossophaga leachii		Phyllostomidae	M	AMNH185970		
Glossophaga longirostris	*longirostris*	Phyllostomidae	F	AMNH130668		
Glossophaga longirostris	*longirostris*	Phyllostomidae	F	AMNH182725		
Glossophaga morenoi	*mexicana*	Phyllostomidae	M	AMNH189645		
Glossophaga soricina		Phyllostomidae	F	UMMZ126822		
Glyphonycteris sylvestris		Phyllostomidae	M	AMNH183846		
Hylonycteris underwoodi		Phyllostomidae	F	UMMZ113582		
Leptonycteris curasoae		Phyllostomidae	M	AMNH149387		
Leptonycteris yerbabuenae		Phyllostomidae	F	UMMZ77740		
Lichonycteris obscura		Phyllostomidae	F	AMNH95118		
Lionycteris spurrelli		Phyllostomidae	F	UMMZ160712		
Lonchophylla handleyi		Phyllostomidae	M	AMNH230214		
Lonchophylla mordax	*concava*	Phyllostomidae	U	AMNH269452		
Lonchophylla robusta		Phyllostomidae	F	UMMZ112036		
Lonchophylla thomasi		Phyllostomidae	F	UMMZ160708	iDigBio: *Hsunycteris thomasi*	
Lonchorhina aurita	*aurita*	Phyllostomidae	M	AMNH269496		
Lophostoma brasiliense		Phyllostomidae	F	AMNH71626		
Lophostoma carrikeri		Phyllostomidae	F	AMNH30180		
Lophostoma schulzi		Phyllostomidae	F	AMNH267421		
Lophostoma silvicolum	*laephotis*	Phyllostomidae	M	AMNH95454		
Lophostoma silvicolum	*laephotis*	Phyllostomidae	F	AMNH97011		
Macrophyllum macrophyllum		Phyllostomidae	M	AMNH78416		
Macrotus californicus		Phyllostomidae	F	AMNH139571		
Macrotus waterhousii		Phyllostomidae	F	UMMZ95718		
Mesophylla macconnelli	*macconnelli*	Phyllostomidae	M	AMNH76569		
Micronycteris brosseti		Phyllostomidae	M	AMNH266032		
Micronycteris hirsuta		Phyllostomidae	F	UMMZ125174		
Micronycteris matses		Phyllostomidae	F	AMNH273044		
Micronycteris megalotis		Phyllostomidae	F	UMMZ95660		
Micronycteris microtis	*microtis*	Phyllostomidae	M	AMNH14581		

Micronycteris microtis		Phyllostomidae	F	AMNH267872		
Micronycteris minuta		Phyllostomidae	F	UMMZ126729		
Micronycteris schmidtorum		Phyllostomidae	F	AMNH130719		
Mimon cozumelae		Phyllostomidae	F	UMMZ103428		60 µm
Mimon crenulatum	*keenani*	Phyllostomidae	M	AMNH64541		
Mimon crenulatum	*longifolium*	Phyllostomidae	F	AMNH236001		
Monophyllus redmani		Phyllostomidae	F	UMMZ123278		
Musonycteris harrisoni		Phyllostomidae	F	UMMZ110524		
Phylloderma stenops		Phyllostomidae	F	AMNH267441		
Phyllonycteris aphylla		Phyllostomidae	F	AMNH186967		
Phyllonycteris aphylla		Phyllostomidae	M	AMNH214130		
Phyllonycteris poeyi	*obtusa*	Phyllostomidae	F	AMNH236697		
Phyllonycteris poeyi	*poeyi*	Phyllostomidae	U	AMNH176194		
Phyllops falcatus		Phyllostomidae	F	UMMZ123279		
Phyllostomus discolor		Phyllostomidae	F	UMMZ59984		
Phyllostomus elongatus		Phyllostomidae	F	UMMZ168806		
Phyllostomus hastatus		Phyllostomidae	F	UMMZ65078		
Platalina genovensium		Phyllostomidae	M	AMNH257108		
Platyrrhinus brachycephalus		Phyllostomidae	F	UMMZ160636		
Platyrrhinus dorsalis		Phyllostomidae	F	UMMZ169060		
Platyrrhinus helleri		Phyllostomidae	F	UMMZ168983		
Platyrrhinus infuscus		Phyllostomidae	F	UMMZ160631		
Platyrrhinus lineatus		Phyllostomidae	F	UMMZ124331		
Platyrrhinus masu		Phyllostomidae	F	UMMZ158068	iDigBio: *Platyrrhinus brachycephalus*	
Platyrrhinus vittatus		Phyllostomidae	F	UMMZ116681		
Pygoderma bilabiatum		Phyllostomidae	F	UMMZ124377		60 µm
Rhinophylla fischerae		Phyllostomidae	F	AMNH230485		
Rhinophylla pumilio		Phyllostomidae	F	UMMZ158063		
Sphaeronycteris toxophyllum		Phyllostomidae	F	AMNH21344		
Stenoderma rufum		Phyllostomidae	F	UMMZ156615		
Sturnira bidens		Phyllostomidae	M	AMNH214349		
Sturnira bogotensis		Phyllostomidae	F	AMNH207851		
Sturnira lilium	*lilium*	Phyllostomidae	F	AMNH248873		
Sturnira ludovici		Phyllostomidae	F	UMMZ95704		
Sturnira magna		Phyllostomidae	F	UMMZ160654		

Sturnira mordax		Phyllostomidae	F	UMMZ112038		
Sturnira nana		Phyllostomidae	F	AMNH219138		
Sturnira oporaphilum		Phyllostomidae	F	UMMZ126751		
Sturnira tildae		Phyllostomidae	F	AMNH209408		
Tonatia saurophila	*bakeri*	Phyllostomidae	F	AMNH139443		
Tonatia saurophila	*melosi*	Phyllostomidae	F	AMNH180263		
Trachops cirrhosus		Phyllostomidae	F	UMMZ103421		
Uroderma bilobatum		Phyllostomidae	F	UMMZ114483		
Uroderma magnirostrum		Phyllostomidae	F	UMMZ156056		
Vampyressa bidens		Phyllostomidae	F	AMNH261626	iDigBio: *Vampyressa pusilla pusilla*	
Vampyressa brocki		Phyllostomidae	F	AMNH268566	iDigBio: *Vampyriscus brocki*	
Vampyressa melissa		Phyllostomidae	F	AMNH233761		
Vampyressa nymphaea		Phyllostomidae	F	UMMZ168944	iDigBio: *Vampyriscus nymphaea*	
Vampyressa pusilla		Phyllostomidae	F	UMMZ133730		
Vampyressa thyone		Phyllostomidae	F	UMMZ122267	iDigBio: *Vampyressa pusilla thyone*	
Vampyrodes caraccioli		Phyllostomidae	F	UMMZ160626		
Acerodon celebensis		Pteropodidae	F	AMNH153137		30 µm
Acerodon jubatus		Pteropodidae	F	UMMZ161197		60 µm
Aethalops alecto	*alecto*	Pteropodidae	F	AMNH247163		
Balionycteris maculata	*seimundi*	Pteropodidae	F	AMNH233970		
Cynopterus brachyotis		Pteropodidae	F	UMMZ117123		
Cynopterus horsfieldii		Pteropodidae	F	UMMZ117125		
Cynopterus sphinx		Pteropodidae	F	UMMZ172227		
Cynopterus titthaecheilus	*terminus*	Pteropodidae	M	AMNH235612		
Cynopterus titthaecheilus	*titthaecheilus*	Pteropodidae	F	AMNH107921		
Dobsonia minor		Pteropodidae	M	AMNH105177		
Dobsonia pannietensis	*pannietensis*	Pteropodidae	M	AMNH157368		30 µm
Eidolon helvum	*helvum*	Pteropodidae	F	AMNH48701		
Eonycteris robusta		Pteropodidae	F	UMMZ160278		
Eonycteris spelaea		Pteropodidae	F	UMMZ156952		
Epomophorus gambianus	*gambianus*	Pteropodidae	M	AMNH239361		30 µm
Epomophorus labiatus		Pteropodidae	F	AMNH48742		
Epomophorus minor		Pteropodidae	F	AMNH161858		
Epomophorus wahlbergi		Pteropodidae	F	AMNH187275		
Epomops franqueti		Pteropodidae	F	UMMZ124059		

Haplonycteris fischeri		Pteropodidae	F	UMMZ162225		
Harpyionycteris celebensis		Pteropodidae	M	AMNH153590		
Harpyionycteris whiteheadi		Pteropodidae	F	UMMZ158715		
Hypsignathus monstrosus		Pteropodidae	F	AMNH86764		30 µm
Macroglossus minimus		Pteropodidae	F	UMMZ161346		
Macroglossus sobrinus	*sobrinus*	Pteropodidae	M	AMNH107480		
Megaerops ecaudatus		Pteropodidae	F	AMNH216753		
Megaerops niphanae		Pteropodidae	M	AMNH87290		
Megaloglossus woermanni		Pteropodidae	M	AMNH236289		
Myonycteris torquata		Pteropodidae	F	AMNH236256		
Nanonycteris veldkampii		Pteropodidae	M	AMNH241024		
Nyctimene aello		Pteropodidae	F	AMNH105102		
Nyctimene albiventer	*papuanus*	Pteropodidae	U	AMNH237058		
Nyctimene albiventer	*papuanus*	Pteropodidae	U	AMNH237065		
Nyctimene cephalotes	*aplini*	Pteropodidae	F	AMNH109030		
Nyctimene certans		Pteropodidae	F	AMNH279187		
Nyctimene major	*geminus*	Pteropodidae	F	AMNH159262		
Nyctimene major		Pteropodidae	U	AMNH221419		
Nyctimene robinsoni		Pteropodidae	F	AMNH196644		
Nyctimene vizcaccia	*vizcaccia*	Pteropodidae	M	AMNH222641		
Otopteropus cartilagonodus		Pteropodidae	F	UMMZ156972		
Paranyctimene raptor		Pteropodidae	F	AMNH194853		
Penthetor lucasi		Pteropodidae	F	UMMZ159632		
Ptenochirus jagori		Pteropodidae	F	UMMZ162262		
Ptenochirus minor		Pteropodidae	F	UMMZ160287		
Pteropus admiralitatum	*solomonis*	Pteropodidae	F	AMNH99959		30 µm
Pteropus alecto	*alecto*	Pteropodidae	F	AMNH153534		30 µm
Pteropus alecto		Pteropodidae	F	AMNH153171		30 µm
Pteropus anetianus	*eotinus*	Pteropodidae	F	AMNH79962		
Pteropus capistratus	*capistratus*	Pteropodidae	M	AMNH194275		30 µm
Pteropus conspicillatus	*conspicillatus*	Pteropodidae	F	AMNH66154		30 µm
Pteropus giganteus		Pteropodidae	F	UMMZ91079	iDigBio: *Pteropus vampyrus giganteus*	60 µm
Pteropus hypomelanus		Pteropodidae	F	UMMZ130417		60 µm
Pteropus livingstonii		Pteropodidae	U	AMNH274500		30 µm
Pteropus lylei		Pteropodidae	F	AMNH240006		30 µm

Pteropus mariannus	*mariannus*	Pteropodidae	M	AMNH249983		30 µm
Pteropus molossinus		Pteropodidae	F	AMNH87168		
Pteropus neohibernicus	*neohibernicus*	Pteropodidae	M	AMNH105251		30 µm
Pteropus neohibernicus	*neohibernicus*	Pteropodidae	M	AMNH105285		60 µm
Pteropus neohibernicus	*neohibernicus*	Pteropodidae	M	AMNH157324		60 µm
Pteropus ornatus	*auratus*	Pteropodidae	F	AMNH130313		30 µm
Pteropus poliocephalus		Pteropodidae	M	AMNH274435		30 µm
Pteropus pumilus		Pteropodidae	F	UMMZ162253		
Pteropus rufus		Pteropodidae	F	AMNH100492		30 µm
Pteropus samoensis	*samoensis*	Pteropodidae	F	AMNH256968		30 µm
Pteropus scapulatus		Pteropodidae	M	AMNH154582		30 µm
Pteropus tonganus	*basiliscus*	Pteropodidae	U	AMNH221146		30 µm
Rousettus aegyptiacus		Pteropodidae	F	UMMZ161026		
Rousettus amplexicaudatus		Pteropodidae	F	UMMZ162316		
Rousettus leschenaultii		Pteropodidae	M	AMNH208123		
Scotonycteris ophiodon		Pteropodidae	F	AMNH256534	iDigBio: *Casinycteris ophiodon*	
Scotonycteris zenkeri	*occidentalis*	Pteropodidae	F	AMNH239380		
Sphaerias blanfordi		Pteropodidae	M	AMNH274330		
Thoopterus nigrescens		Pteropodidae	M	AMNH196444		
Rhinolophus arcuatus		Rhinolophidae	F	UMMZ162885		
Rhinolophus cornutus		Rhinolophidae	F	UMMZ165617		
Thyroptera tricolor		Thyropteridae	F	UMMZ53240		
Antrozous pallidus		Vespertilionidae	F	UMMZ86542		
Corynorhinus rafinesquii		Vespertilionidae	F	UMMZ115745		
Corynorhinus townsendii		Vespertilionidae	F	UMMZ105878		
Eptesicus andinus		Vespertilionidae	F	UMMZ116679		
Eptesicus brasiliensis		Vespertilionidae	F	UMMZ125740		
Eptesicus diminutus		Vespertilionidae	F	UMMZ125748		
Eptesicus furinalis		Vespertilionidae	F	UMMZ124387		
Eptesicus fuscus		Vespertilionidae	F	UMMZ77842		
Hesperoptenus tickelli		Vespertilionidae	F	UMMZ172254		
Hypsugo savii		Vespertilionidae	F	UMMZ117578		
Idionycteris phyllotis		Vespertilionidae	F	UMMZ111018		
Kerivoula pellucida		Vespertilionidae	F	UMMZ161396		
Kerivoula pellucida		Vespertilionidae	F	UMMZ161396		

Lasionycteris noctivagans		Vespertilionidae	F	UMMZ76424		
Lasiurus blossevilli		Vespertilionidae	F	UMMZ125725	iDigBio: *Lasiurus borealis blossevillii*	
Lasiurus borealis		Vespertilionidae	F	UMMZ89680		
Lasiurus cinereus		Vespertilionidae	F	UMMZ51379		
Lasiurus ega		Vespertilionidae	F	UMMZ125726		
Lasiurus intermedius		Vespertilionidae	F	UMMZ110529		
Lasiurus seminolus		Vespertilionidae	F	UMMZ123983		
Murina aurata		Vespertilionidae	F	UMMZ112549		
Murina cyclotis		Vespertilionidae	F	UMMZ112542		
Murina huttonii		Vespertilionidae	F	UMMZ75150		
Myotis albescens		Vespertilionidae	F	UMMZ125732		
Myotis auriculus		Vespertilionidae	F	UMMZ113204		
Myotis austroriparius		Vespertilionidae	F	UMMZ58824		
Myotis californicus		Vespertilionidae	F	UMMZ98964		
Myotis chiloensis		Vespertilionidae	F	UMMZ156356		
Myotis ciliolabrum		Vespertilionidae	F	UMMZ175836		
Myotis elegans		Vespertilionidae	F	UMMZ116274		
Myotis emarginatus		Vespertilionidae	F	UMMZ146940		
Myotis evotis		Vespertilionidae	F	UMMZ66051		
Myotis formosus		Vespertilionidae	F	UMMZ53119		
Myotis grisescens		Vespertilionidae	F	UMMZ76874		
Myotis horsfieldii		Vespertilionidae	F	UMMZ157003		
Myotis keenii		Vespertilionidae	F	UMMZ175831		
Myotis leibii		Vespertilionidae	F	UMMZ90146	iDigBio: *Myotis subulatus subulatus*	
Myotis lucifugus		Vespertilionidae	F	UMMZ122615		
Myotis macrotarsus		Vespertilionidae	F	UMMZ160308		
Myotis melanorhinus		Vespertilionidae	F	UMMZ105939	iDigBio: *Myotis subulatus melanorhinus*	
Myotis muricola		Vespertilionidae	F	UMMZ160381		
Myotis myotis		Vespertilionidae	F	UMMZ123522	iDigBio: *Myotis austroriparius austroriparius*	
Myotis mystacinus		Vespertilionidae	F	UMMZ88614		
Myotis nigricans		Vespertilionidae	F	UMMZ160598		
Myotis riparius		Vespertilionidae	F	UMMZ126242		
Myotis ruber		Vespertilionidae	F	UMMZ125729		
Myotis septentrionalis		Vespertilionidae	F	UMMZ106030	iDigBio: *Myotis keenii septentrionalis*	

Myotis sodalis		Vespertilionidae	F	UMMZ83587		
Myotis thysanodes		Vespertilionidae	F	UMMZ81965		
Myotis velifer		Vespertilionidae	F	UMMZ100817		
Myotis velifer		Vespertilionidae	F	UMMZ61438		
Myotis velifer		Vespertilionidae	F	UMMZ61439		
Myotis velifer		Vespertilionidae	F	UMMZ61440		
Myotis velifer		Vespertilionidae	F	UMMZ61441		
Myotis velifer		Vespertilionidae	F	UMMZ61444		
Myotis velifer		Vespertilionidae	F	UMMZ61445		
Myotis vivesi		Vespertilionidae	F	UMMZ115551		
Myotis volans		Vespertilionidae	F	UMMZ106018		
Myotis yumanensis		Vespertilionidae	F	UMMZ105958		
Neoromicia capensis		Vespertilionidae	F	UMMZ59013		
Nyctalus leisleri		Vespertilionidae	F	UMMZ167693		
Nyctalus plancyi		Vespertilionidae	F	UMMZ55831	iDigBio: *Nyctalus noctula plancei*	
Nycticeius humeralis		Vespertilionidae	F	UMMZ123988		
Philetor brachypterus		Vespertilionidae	F	UMMZ156906		
Pipistrellus coromandra		Vespertilionidae	F	UMMZ172276		
Pipistrellus hesperidus	*hesperus*	Vespertilionidae	F	UMMZ87877		
Pipistrellus javanicus		Vespertilionidae	F	UMMZ172303		
Pipistrellus nathusii		Vespertilionidae	F	UMMZ123232		
Pipistrellus pipistrellus		Vespertilionidae	F	UMMZ146941	iDigBio: *Pipistrellus coromandra*	
Pipistrellus subflavus		Vespertilionidae	F	UMMZ98947	iDigBio: *Perimyotis subflavus subflavus*	
Pipistrellus tenuis		Vespertilionidae	F	UMMZ160299		
Plecotus auritus		Vespertilionidae	F	UMMZ111012		
Rhogeessa aeneus		Vespertilionidae	F	UMMZ79938	iDigBio: *Rhogeessa tumida aenus*	
Rhogeessa parvula		Vespertilionidae	F	UMMZ83314	iDigBio: *Rhogeessa tumida major*	
Rhogeessa tumida		Vespertilionidae	F	UMMZ116286		
Scotophilus heathii		Vespertilionidae	F	UMMZ172261		
Scotophilus kuhlii		Vespertilionidae	F	UMMZ157013		
Tylonycteris pachypus		Vespertilionidae	F	UMMZ158856		
Tylonycteris robustula		Vespertilionidae	F	UMMZ158855		

Table S4.2 Percentage difference between physical and digital measurements

20 UMMZ specimens of bats, their taxonomic and museum identification information, and differences in 9 linear measurements taken from physical and digital specimens. The measurements are described in full by Dumont *et al.* (2012). For each specimen and measurement, we calculated the percentage that digital measurements in Avizo differ from physical measurements taken using calipers. These data are also displayed in Figure 4.3.

Species	Subspecies	Family	UMMZ ID	MZB	TSL	PSW	SKH	PM1	CH	CM1	MSW	CPH
Cynopterus sphinx		Pteropodidae	172227	18.22	30.97	12.14	11.54	7.61	5.32	14.18	5.22	10.83
Ptenochirus minor		Pteropodidae	160287	18.61	30.33	11.94	12.61	8.03	5.78	14.73	5.58	10.78
Hipposideros diadema	*griseus*	Hipposideridae	157092	17.58	29.33	13.83	11.18	9.36	5.14	12.63	3.46	7.98
Taphozous melanopogon	*philippinensis*	Emballonuridae	156810	12.55	21.15	11.17	7.51	7.61	4.91	8.14	4.82	6.92
Emballonura alecto	*alecto*	Emballonuridae	156848	8.83	15.21	7.79	5.79	5.49	3.19	6.1	2.78	3.49
Peropteryx macrotis		Emballonuridae	156592	8.82	15.15	7.88	5.53	5.82	3.09	5.71	3.01	3.22
Desmodus rotundus	*murinus*	Phyllostomidae	99345	12.31	24.94	12.78	11.23	6.25	6.74	9.51	5.36	6.87
Brachyphylla cavernarum	*intermedia*	Phyllostomidae	68201	17.06	31.53	14.36	11.46	10.59	6.34	13.46	6.87	9.8
Leptonycteris yerbabuenae	*sanborni*	Phyllostomidae	77740	10.6	26.16	10.69	7.41	5.17	3.51	11.09	4.66	4.35
Artibeus toltecus		Phyllostomidae	108586	12.54	20.58	10.9	9.44	7.62	3.5	7.58	5.12	5.47
Sturnira mordax		Phyllostomidae	112038	13.31	24.08	11.83	10.36	7.39	3.64	9.11	5.83	5.44
Platyrrhinus masu		Phyllostomidae	158068	16.09	26.78	12.85	10.84	11.12	3.5	10.44	6.6	6.87
Mormoops megalophylla	*megalophylla*	Mormoopidae	109749	9.81	15.17	9.24	11.13	6.65	5.19	6.87	5.21	3.99
Noctilio leporinus	*mastivus*	Noctilionidae	68190	18.7	26.28	17.1	11.07	10.91	6.61	11.83	6.89	7.6
Nyctiellus lepidus		Natalidae	105767	6.49	12.8	6.33	4.49	4.55	2.66	5.12	2.47	2.42
Cynomops abrasus	*cerastes*	Molossidae	124418	14.46	20.2	13.84	6.96	8.98	5.02	9.78	5.32	6.1
Eptesicus brasiliensis	*argentinus*	Vespertilionidae	125740	11.98	17.64	9.12	6.49	6.39	4.22	7.69	4.05	5.74
Pipistrellus coromandra		Vespertilionidae	172276	8.32	12.84	7.24	4.78	5.09	2.7	5.29	3.67	3.12
Corynorhinus rafinesquii	*macrotis*	Vespertilionidae	115745	8.33	16.48	9.58	6.44	5.8	2.91	5.99	3.67	3.61
Myotis lucifugus	*lucifugus*	Vespertilionidae	122615	8.97	14.63	7.68	5.08	5.19	3.38	5.5	4.3	3.57

CHAPTER 5

The omnivores' dilemma: decoupling of ecological and morphological evolution across New World bats[6]

ABSTRACT

Coupled rates of speciation and morphological evolution have been identified by numerous studies throughout the tree of life. By contrast, morphological evolution is typically assumed to be correlated with underlying patterns of ecological evolution, yet fewer studies have documented this relationship. This study explicitly tests for where rates of ecological, trophic innovation and morphological evolution are coupled in New World bats. We infer major dynamics of both trophic and morphological evolution by using species-level diet data and multivariate cranial shape to fit models of species belonging to discrete, rate-varying partitions. Instead of relying on stepwise model selection or maximum-likelihood fitting, we summarize across all inferred models of discrete partition membership. Surprisingly, we find that while the dynamics of trophic evolution are heterogeneous across New World bats, they are largely decoupled from those of shape evolution. This finding is particularly surprising given well-established functional links between the skull morphologies and trophic ecologies of extant bats. We hypothesize that this discordance could be driven by high lability of bat crania, and a higher prevalence of omnivory than is often assumed.

[6] Shi, J.J., Westeen, E.P., & Rabosky, D.L. *Manuscript in preparation for submission to Ecol. Lett.*

INTRODUCTION

Ecological diversity and morphological disparity are closely linked throughout the tree of life. For example, phenotypic traits are tied to mechanical performance (Arnold 1983, Kingsolver & Huey 2003), which governs many aspects of organismal ecology. These include locomotion, the processing of food, and how interactions occur with other species (Norberg & Rayner 1987, Losos 1990, Berwaerts *et al.* 2002, Calsbeek & Irschick 2007, Langerhans 2009). The assumption that ecomorphological relationships are prevalent is so entrenched that one component of diversity is often used as a proxy for the other (Dawideit *et al.* 2008, Zanno & Makovicky 2011). Furthermore, many clades that are characterized by high ecological diversity also seem to be morphologically disparate.

The evolutionary dynamics of ecology and morphology also often appear tied to one another. Adaptive radiations, for example, are characterized by the rapid accumulation of both ecological and morphological diversity alongside heightened diversification (Stebbins 1970, Sturmbauer 1998, Schluter 2000, Losos & Mahler 2010). Ecological opportunity and divergence can promote the process of speciation itself, by driving adaptation and reinforcing isolation among lineages (Schluter 1996, Rundell & Price 2009). Morphological divergence could also facilitate this process, leading us to predict that species richness, ecological innovation, and disparity should all covary during an adaptive radiation. Numerous clades are characterized by patterns of diversity consistent with this conceptual, coupled model (*e.g.* Gillespie 2004, Cozzolino & Widmer 2005, Wagner *et al.* 2012). However, while many studies test whether speciation and morphological evolution covary across radiations (Gould & Eldredge 1993, Yang 2001, Ricklefs 2004, Rabosky 2012), fewer test explicitly for relationships between ecological and morphological evolution.

The evolution of ecology and morphology is also linked through convergence, where similar, derived morphologies and ecologies arise independently across lineages (Blackburn 1992, Rosenblum 2006, terHorst *et al.* 2010, Muschick *et al.* 2012). Convergence could thus also reinforce a strong relationship between the evolutionary dynamics of both ecology and morphology. However, convergence can also be morphologically imperfect, potentially leading to high disparity even among functionally similar lineages (Collar *et al.* 2014). In these cases, we might not expect morphological and ecological evolution to be strongly correlated, with the possibility that morphological disparity accumulates without ecological divergence.

Previous researchers have suggested that one example of a classic adaptive radiation is that of extant bats. The order is characterized by high variation in species richness, ecological diversity, and morphological disparity across its subclades (Simmons & Conway 2003, Jones *et al.* 2005). The predominantly Neotropical superfamily Noctilionoidea, for example, is by far the most ecologically diverse clade of bats, and has also been characterized as an adaptive radiation (Dumont *et al.* 2012). By contrast, the superfamily Vespertilionoidea is relatively homogeneous in both ecology and morphology, and is predominantly comprised of obligate insectivores like the large, cosmopolitan genus *Myotis* (Nowak 1994, Simmons 2005). Across many clades of bats, there are biomechanical links between skull morphology and trophic ecology (Dumont *et al.* 2009, Santana & Dumont 2009). The shapes of bat crania are predictive of bite force and the ability to process foods with different material properties (Santana *et al.* 2010, 2012). Previous researchers have also inferred fast rates of trait evolution and speciation among noctilionoids, which are characterized by high ecological diversity and species richness (Monteiro & Nogueira 2011, Dumont *et al.* 2012, Rojas *et al.* 2018). However, no study has yet tested whether morphological lability of the cranium itself is coupled with trophic evolution.

In this study, we test for the relationship between ecological, trophic evolution and morphological evolution across New World bats. Within the New World, the temperate Nearctic is characterized by low bat richness, with insectivorous vespertilionoids comprising the clear majority of the realm's extant species (Nowak 1994, Simmons 2005). By contrast, the Neotropics are extremely species-rich, with noctilionoids being among the most abundant mammals in the realm (Fleming & Kress 2013). Noctilionoid bats are known for the breadth of their trophic ecology, and especially for their many interactions with Neotropical plants as frugivores, nectarivores, and omnivores (Monteiro & Nogueira 2011, Dumont *et al.* 2012, Simmons 2005). The independent origins of nectarivory, and associated specializations in cranial morphology, may also be products of convergence (Griffiths 1983, Datzmann *et al.* 2010, Rojas *et al.* 2016). The New World bat radiation thus provides an excellent opportunity for testing the relationships between trophic and morphological evolution within an adaptive radiation.

A simple explanation for the patterns of diversity among New World bats is that groups with low trophic diversity are also characterized by low rates of trophic and morphological evolution. By contrast, we would expect to find rapid evolutionary rates and lability of both trophic ecology and morphology among the most trophically diverse clades. We would thus find an overall coupling of both trophic innovation and morphological evolution across this radiation. High morphological convergence among the most specialized noctilionoids could reinforce these dynamics, with unique ecologies and morphologies evolving independently at similar rates. However, it is also possible that more imperfect degrees of convergence could lead to a disconnect between ecology and morphology. Here, we quantify these evolutionary dynamics using diet data and a high-dimensional morphological dataset of bat crania, and infer whether they covary across New World bats.

METHODS

Phylogeny and ecology

We used the phylogeny of Shi & Rabosky (2015), as updated by Shi *et al.* (2018), for our study. We classified each New World species to WWF biogeographic realms as described by Olson *et al.* (2001) and Shi *et al.* (2018). We further classified each species according to superfamily, family, and subfamily as described by Simmons (2005), Teeling *et al.* (2005), Shi & Rabosky (2015), and Rojas *et al.* (2016).

We then assigned each species to an ecological guild, based on preferred diet(s), if known. Diet data were compiled from a review of the literature (Table S5.1). We compared and corroborated our literature review with the recently published diet data and guild classifications of Rojas *et al.* (2018). These researchers used a 60% dietary cutoff for assigning a single ecological guild, like nectarivory or insectivory. We classified bats that consume both animals and plants regularly according to this threshold as omnivores. Similarly, we classified bats that consume both nectar and fruit regularly as herbivores. We used these trophic guilds as ecological character states for our subsequent analyses. The overall phylogenetic framework of our study is depicted in Figure 5.1.

Trophic evolution

To infer dynamics of ecological, trophic evolution, we fitted a set of phenotypic evolutionary models that allowed rates of character evolution to vary across the phylogeny (*sensu* Davis Rabosky *et al.* 2016). We constructed these multi-rate models by constraining split-MuSSE (multistate speciation and extinction) models to split-Mk (character-independent) models using the R package *diversitree* (FitzJohn 2012). As there is currently no implementation

of partitioned Mk models in *diversitree*, we necessarily had to create these models by constraining split-MuSSE models. We set speciation and extinction rates to their maximum likelihood (ML) tree-wide estimates under a constant-rate birth-death process. However, the relative likelihood of the data with respect to character evolutionary rates is mathematically independent of the diversification rates used to constrain the models; hence, this approach simply creates split-Mk models that characterized rates of trophic evolution for New World bats.

With these models, we calculated the likelihood that individual partitions of the phylogeny had different transition rates $q_{i,j}$ between any character (trophic guild) states *i* and *j*. We first fit a model with only a *single*, global partition across the phylogeny, and then fit all possible *two*-partition models where every internal node partitioned the phylogeny into two groups. We then defined all possible *three*-partition models for our dataset by identifying all unique node *pairs*, which partitioned the phylogeny into three groups. For all partitioned models, we set equal transition rates $q_{i,j}$ between trophic states *within* partitions, but allowed these rates to vary *across* partitions. Using this overall methodology, we calculated the ML fit and parameter estimates for every possible one-, two-, and three-partition models across the phylogeny. It was computationally infeasible to add additional partitions throughout our methods, given non-linear increases in *k*-combinations and the large total number of nodes.

Instead of relying on either a global ML split-Mk model, or stepwise model selection, we used model averaging to infer macroevolutionary "cohorts," or sets of taxa that have evolved under a shared evolutionary rate regime (Rabosky *et al.* 2014a; Figure S5.1). Operationally, the pairwise cohort probability is the probability that two taxa belong to the same evolutionary rate partition across all possible one-, two-, or three-partition split-Mk models. To infer cohorts, we created pairwise matrices of partition membership for every split-Mk model as follows. In a Mk

model with no splits, there is only a single background partition across the tree that contains all taxa. Our initial assumption of the pairwise probability of any two species belonging to the same cohort is thus 100%; we then weighted this matrix by multiplying it by the Akaike weight of an unsplit Mk model among all our possible models. The weighted transition rate for this single partition $q_{i,j}$, among any two diet states *i* and *j*, was similarly the fitted estimate of $q_{i,j}$ multiplied by the Akaike weight of the generating unsplit model.

For a split-Mk model with an added partition *k*, we still assumed all species of the background partition, but were not within *k*, were characterized by a pairwise cohort probability of 100%. This is also true of all pairs of species within *k*. However, all pairwise probabilities between species within partition *k* and the background partition were 0%. We then weighted the resulting binary state matrix, and the transition rates $q_{i,j}$ for each partition, by the Akaike weight of the generating split-Mk model, as before. This overall procedure was analogous for three partition models. After inferring these weighted pairwise probability matrices for every split-Mk model, we calculated their grand sum as the *overall* pairwise cohort probability. This cohort matrix thus depicted overall patterns of trophic evolution across New World bats.

We used the weighted character transition rates from the above procedure to visualize trophic evolution, as transition rates among states, along branches (*sensu* Rabosky *et al.* 2014b). We emphasize that because our analyses infer rates at internal nodes, we do not have information to calculate how rates may change through time between nodes and along branches. In this overall framework, we considered cohorts with relatively high within-partition transition rates $q_{i,j}$ to be trophically labile. By contrast, we considered cohorts with low transition rates to be trophically static. We highlighted these ecological cohorts for downstream analyses of disparity

and shape evolution, to test if trophic evolution is coupled with morphological diversification and convergence.

Specimens and shape quantification

For our morphological analyses, we collected data from 167 crania of New World bat specimens from the University of Michigan's Museum of Zoology and the American Museum of Natural History. We digitized each cranium using X-ray computed microtomography (μCT) scanning. These data are fully described and publicly available as presented in Chapter 4.

For each cranium, we quantified shape using 3D landmark-based geometric morphometrics, given connections between cranial shape and the feeding biomechanics (Santana *et al.* 2010, 2012). We performed all landmarking in the program Checkpoint (Stratovan, Davis, USA). Each cranium was represented by a set of 18 unique, homologous landmarks. As 11 of these are symmetrical points, we digitized a total of 29 fixed landmarks per cranium. We additionally placed 15 equidistant semilandmarks along the midline of the cranium (Figure S5.2). This set of 44 total points was adapted from Santana & Lofgren (2013).

After landmarking each specimen, we assembled a species-level dataset of 3D coordinates, and performed most subsequent shape analyses using the R package *geomorph* v3.0.6 (Adams *et al.* 2017). We first estimated the coordinates of missing landmarks (*e.g.* on damaged crania) by identifying the specimens with complete coordinates, aligning target specimens with missing landmarks, and using a thin-plate spline to estimate their locations based on the complete data (Gunz *et al.* 2009).

We transformed the raw shape data using a generalized Procrustes analysis that aligned the dataset in a common coordinate system, scaled by centroid size (Rohlf & Slice 1990). During the alignment, we allowed semilandmarks to slide along the specified curves using the Procrustes

distance criterion (Rohlf 2010). The resulting superimposed coordinates served as our shape variable for each specimen. While superimposing the coordinates, we also calculated centroid sizes; these are often used as a proxy for total size in shape analyses (Kosnik *et al.* 2006, McGuire 2010, Zelditch *et al.* 2017).

Cranial shape variation

Using our aligned coordinates, we first inferred how clade age might predict disparity. To do this, we tested for the linear relationship between clade age and clade disparity, as calculated by the within-clade median interspecific Euclidean distance between crania, for each New World subfamily. We also calculated what has been termed phylogenetic disparity by generalizing the methods of Serb *et al.* (2017) to account for nonindependence, as follows. We first calculated the multivariate *K* statistic (K_{mult}) for assessing phylogenetic signal of cranial shape on our phylogeny (Blomberg *et al.* 2003, Adams 2014a). After using a permutation test to confirm significant phylogenetic signal, we inferred the relationship between shape and potential predictors by using phylogenetic generalized least squares (PGLS) (Adams 2014b, Adams & Collyer 2015). We then calculated phylogenetic disparity, as currently implemented in *geomorph*, by using the PGLS residuals, thus conditioning our disparity calculations with the phylogeny. Significance was assessed using 1000 permutations of the observed data. We tested for how phylogenetic, cranial disparity is predicted by our previously identified ecological cohorts, family, or trophic guild.

To visualize how cranial shape varies with ecology, and to reduce the dimensionality of our dataset for some subsequent analyses, we re-ordinated our data using a principal components (PC) analysis. To focus on the effects of shape alone, we also tested for and removed potential

effects of allometry from our PC data. We first confirmed significant allometric effects using a PGLS of shape on centroid size. We then added the residuals from this PGLS to the phylogenetic mean of our aligned coordinates, and performed a PC analysis on these transformed data (Klingenberg & Marugán-Lobón 2013, Sherratt *et al.* 2014, Santana & Cheung 2016). We used these allometry-free PC scores for some downstream analyses. However, we emphasize that the original PC scores and these allometry-free scores are well-correlated ($p < 0.001$, mean $r = 0.78$), especially among the first 3 PC axes (mean $r = 0.94$).

Cranial shape evolution

We calculated multivariate rates of shape evolution using two different classes of methods (*sensu* Adams 2014c). The first, an **R**-mode method, utilized phylogenetic variance-covariance matrices to estimate rates. In these methods, diagonals of evolutionary rate matrices represent rates (σ^2), and off-diagonals represent covariances among traits (Revell & Harmon 2008, Revell & Collar 2009, Adams 2014c). There are two major limitations of **R**-mode methods that informed our approach. First, data matrices where the dimensionality of the traits equals or exceeds the number of taxa are singular, making likelihood calculations impossible for some implementations. Second, reducing dimensionality (*e.g.* using a subset of PC axes) can potentially result in high Type 1 error rates when selecting and fitting non-Brownian motion (BM) models of trait evolution (Adams 2014c, Adams & Collyer 2018).

We performed these **R**-mode analyses using the R package *mvMORPH* (Clavel *et al.* 2015). For this study, we only used BM models of trait evolution, given the aforementioned issues with reduced dimensionality (though see Supporting Information of forthcoming paper). Specifically, we fit multivariate BM models of shape evolution to the first 3 PC axes, which

explained 64% of the total shape variance. Constraints on the phylogenetic variance-covariance matrix, both across the tree and within individual partitions, can be specified with *mvMORPH*. We initially parameterized six nested, three-rate BM models using the three partitions of our ML split-Mk model of trophic evolution. These six models had different potential constraints on the rate matrices (Table S5.3). We then selected the best-fitting constraint model for all subsequent analyses.

To match our split-Mk analyses of trophic evolution, we adapted a similar partitioned framework and cohort inference approach. We first fit a one-rate (BM1) model to the entire tree. Then, we fit two-rate and three-rate (BMM) models to every node, and every unique pair of nodes, respectively. In these BMM models, partitions of the phylogeny were characterized by distinct evolutionary rate matrices (Revell & Harmon 2008, Revell & Collar 2009). With three PC axes, we could not allow partitions with fewer than four taxa. For each fit, we calculated the model likelihood and inferred rate matrices for each partition. We then identified cranial shape cohorts, using Akaike weights for each BM model, as previously described. By multiplying each evolutionary rate matrix by the Akaike weight of its generating BM model, and summing the diagonals of each rate matrix as the overall rate for that partition, we also visualized rates (σ^2) of shape evolution on the phylogeny (Rabosky *et al.* 2014b).

Our second approach for calculating rates of shape evolution was a **Q**-mode method implemented in *geomorph* (Adams 2014c). These rates (σ^2_{mult}) are net estimates of rates for *a priori* defined groups, under a BM model of trait evolution, calculated using a centered distance matrix between shapes (Adams 2014c, Adams & Collyer 2018). With this method, we were able to calculate σ^2_{mult} as a rate estimate for the *entire* cranium, as opposed to a subset of PC axes. We assessed statistical significance using both simulations and permutations of the observed data

(Denton & Adams 2015, Adams & Collyer 2018). We calculated σ^2_{mult} for all families and subfamilies of New World bats, and also for both ecological and the (**R**-mode) morphological cohorts described above, to assess if trophic evolution is coupled with shape evolution.

Convergence

We tested for shape convergence by calculating the C1 statistic (Stayton 2015). This statistic estimated the proportion of maximum, ancestral distance that was subsequently closed by potentially convergent evolution among a specified set of taxa. We assessed significance by simulating trait datasets under BM, estimating C1, and recording when it exceeded the observed estimate. We used code from Zelditch *et al.* (2017) to calculate C1 for non-monophyletic trophic guilds using the first 20 PC axes of our shape data, which explained 95% of the variance in shape.

RESULTS

Species characteristics

We present data for 167 species of extant New World bats (Table S5.1). This comprises about 75% (31 species) of estimated Nearctic diversity, and 60% (144 species) of estimated Neotropical diversity, with 8 species present in both realms (Figure 5.1; Simmons 2005, Shi *et al.* 2018).

Among noctilionoids, 54% appear omnivorous to some degree - that is, they include more than a single type of food in their diet (Table S5.1). However, using the 60% threshold of Rojas *et al.* (2018), most noctilionoids are classified according to a single diet item, with only 13% of species being omnivores or generalist herbivores by this metric (Figure 5.2).

Trophic evolution

Out of 13696 possible one-, two-, and three-partition split-Mk models (where each species is assigned a discrete trophic guild as a state, *sensu* Rojas *et al.* 2018), only 14 contribute more than 1% to the overall Akaike weight. These 14 models only contribute a total of 54.5% of the sum Akaike weight, with the ML fit accounting for 26.2% of the total weight. This means that the vast majority of models, despite each being individually poor fits, still sum to nearly half of the total Akaike weight. The ML fit is a three-partition model that includes a background partition, a partition at the base of the subfamily Stenodermatinae, and another at the base of a clade including most other phyllostomids. However, the next-best fitting model only differs from the ML model by adding a single branch (*Rhinophylla*) to the stenodermatine partition.

The general uncertainty around model-fitting highlights a strength of our cohort-based approach for working with coarse data, where assignment of discrete states could make it difficult to identify the "best" partitions. Cohort analyses summarize broad patterns of shared evolutionary rate dynamics across taxa, and allow general patterns to emerge even when many models have broadly equivalent support. Our cohorts highlight the probability with which taxa belong to the same partition across all possible models of up to three partitions. We highlight clear ecological cohorts across the New World bat phylogeny (Figure 5.2a). All vespertilionoids (Figure 5.1) belong to a distinct, independent ecological cohort (median pairwise probability *mpp* = 99%). The other major clades of insectivores, however, including the families Emballonuridae, Mormoopidae, and Noctilionidae, and the earliest diverging phyllostomid subfamilies (Macrotinae and Micronycterinae) have lower probabilities of belonging to this cohort (*mpp* = 70-90%). To be conservative, we assigned these to separate cohorts: one of tMacrotinae and Micronycterinae (*mpp* = 100%), and one of Emballonuridae, Mormoopidae, and Noctilionidae

(*mpp* = 96%). These insectivorous cohorts are characterized by the slowest weighted transition rates across the phylogeny (Figure 5.2b, Table 5.1).

Phyllostomids are heterogeneous in dynamics of trophic evolution (Figure 5.2a). All species of the predominantly frugivorous subfamily Stenodermatinae clearly belong to an ecological cohort (*mpp* = 95%) that is distinct from the rest of the family (*mpp* < 54%) with relatively slow transition rates (Figure 5.2b). There is also evidence for a rapidly evolving, paraphyletic cohort that includes the trophically diverse phyllostomid subfamilies Lonchorhininae, Rhinophyllinae, Glyphonycterinae, Phyllostominae, Lonchophyllinae, and Carolliinae (*mpp* = 98%). For brevity, we will refer to this cohort as the Lonchophyllinae cohort. We also find clear support for fast rates within a cohort of the nectarivorous subfamily Glossophaginae (*mpp* = 95%), and a separate cohort for the vampire subfamily Desmodontinae (*mpp* = 100%). It is more equivocal whether there is a clear delineation between vampires and glossophagines (*mpp* = 76%), or between glossophagines and the Lonchophyllinae cohort (*mpp* = 81%).

Shape variation and disparity

There is a significant, positive relationship between disparity and clade age among all 14 non-monotypic subfamilies (Figure 5.3: $R^2 = 0.534$, $p < 0.01$). We also find significant phylogenetic signal in cranial shape among New World bats ($K_{mult} = 0.581$, $p < 0.01$). After accounting for phylogenetic structure (Serb *et al.* 2017), the only significant differences in shape (Procrustes variance) we find among our ecological cohorts is higher disparity of the Stenodermatinae and Lonchophyllinae cohorts than of the Mormoopidae cohort. For trophic guilds, we only find that frugivores have higher disparity than insectivores, and vampires have

lower disparity than frugivores, nectarivores, and herbivores (Table S5.2). Finally, among families, we find that phyllostomids have significantly higher disparity than all other families but Mormoopidae. Vespertilionids have significantly higher disparity than the family Molossidae (Table S5.2).

Our taxa, when ordinated in PC space, can be qualitatively grouped into the three major trophic guilds (Figure 5.4) with the highest sample sizes. If we visualize our ecological cohorts (Table 5.1) in this morphospace, we find that omnivores and herbivores are generally found overlapping these major groups. The first 20 PC axes explain 95% of the variance in our shape data; however, after the first 3 axes, each subsequent axis only explains 5% or less of the total variance.

Variation in PC1 is primarily aligned with the relative length of the snout in relation with the braincase, with short-nosed frugivores having low scores and long-nosed nectarivores having high scores. PC2 is aligned with both the width of the snout and its position relative to the rest of the cranium. Insectivorous species (*e.g. Lasiurus*, *Myotis*) with wider and/or more sloped snouts have low PC2 scores, and nectarivorous and frugivorous species with narrow and/or relatively straight snouts have the highest scores. Finally, PC3 is best aligned with the height of the cranial vault in relation to the slope and shape of the snout. Frugivorous species with larger snouts and pronounced cranial vaults, and a clear angle between the two, like *Platyrrhinus*, have low PC3 scores; nectarivores and vampires both have generally high scores.

Cranial shape evolution

For our **R**-mode analyses, our initial three-rate BMM model fit with the partitions of our ML split-Mk model strongly supports a model with no constraints on the rate matrices (Table S5.3). We used these parameters to fit a total of 2391 single-rate BM1 or two/three-rate BMM

models to our shape data, once we constrained the possible partitions to containing at least 4 species. Unlike with our split-Mk models, only 3 models contribute even 1% to the total Akaike weight, with the ML model accounting for a substantial 91.6% of the total weight. This ML BMM model is one with separate rate matrices for Glossophaginae and a small clade of frugivorous stenodermatines (*Ametrida*, *Pygoderma*, *Sphaeronycteris*, and *Centurio*), in addition to the background partition of all other species.

We find evidence for few clearly-delineated morphological cohorts (Figure 5.5a). All the predominantly insectivorous clades - Vespertilionoidea, Emballonuridae, Mormoopidae, and Noctilionidae (piscivorous/insectivorous) - are clearly united into one morphological cohort that includes the many phyllostomid subfamilies of our Lonchophyllinae ecological cohort (*mpp* = 100%). Surprisingly, we find that most stenodermatines are also likely part of the same general, background cohort (*mpp* = 91.8%). The strongest evidence for truly differentiated cohorts follows the ML model, with a clear Glossophaginae (*mpp* = 100%) cohort and the aforementioned *Ametrida* complex of frugivores (*mpp* = 100%). It is very unlikely that either of these are part of the same morphological cohort as the rest of phyllostomids, despite shared ancestry (*mpp* < 10%). We summarize these cohort inferences in Table 5.2.

We infer generally homogeneous rates (σ^2) of trait evolution among New World bats with our **R**-mode analyses (Figure 5.5), with two exceptions. We infer elevated rates of morphological evolution among the Glossophaginae and *Ametrida* cohorts, as might be expected from the divergent snout shapes of these nectarivores and frugivores (Figure 5.5b).

With our **Q**-mode analyses of rates (σ^2_{mult}) of overall cranial shape evolution, we find no significant differences among families, subfamilies, ecological cohorts, or guilds. We do find, however, that the three morphological cohorts defined by our *mvMORPH* analyses differ

significantly in σ^2_{mult}, with faster rates of shape evolution among glossophagines and the *Ametrida* complex (Table 5.2).

Convergence

Omnivory, herbivory, nectarivory, frugivory, and insectivory all define paraphyletic groups in New World bats; as such, species that converge on these trophic ecologies may also converge morphologically. We find, however, that only nectarivores are significantly convergent based on the C1 statistic (Table S5.4).

DISCUSSION

Trophic lability of New World bats

We find that dynamics of trophic evolution are heterogeneous within phyllostomid bats. Within phyllostomids, the subfamily Glossophaginae is characterized by the fastest rates of transitions among trophic guilds (Figure 5.2). Fast rates within glossophagines represent transitions between highly specialized, obligate nectarivores and species that are facultatively omnivorous depending on seasonality (Valiente-Banuet *et al.* 1996, Zortéa 2003, Tschapka 2005). The complex of phyllostomid subfamilies within our Lonchophyllinae cohort (Table 5.1) is also characterized by high transition rates and ecological diversity. This group contains the lonchophyllines, which include most of the other nectarivores, as well as the insectivores, carnivores, and omnivores of the extremely ecologically diverse subfamily Phyllostominae (Hoffmann *et al.* 2008). The subfamily Carolliinae is also included in this cohort, though it is characterized by its slowest rates. While most *Carollia* species are considered frugivores, it is also clear that they often consume other resources like nectar (Winter *et al.* 2003).

The stenodermatines are a well-discriminated ecological cohort with relatively slow rates of character evolution (Figure 5.2b). Even though stenodermatines have speciated rapidly (Shi & Rabosky 2015, Rojas *et al.* 2016), this appears to have occurred with relatively little ecological divergence, as most stenodermatines strongly prefer hard fruits (Table S5.1, Rojas *et al.* 2018). The ability to process hard fruits has been considered a key innovation that precipitated their rapid speciation (Dumont *et al.* 2012). However, these increased speciation rates are not coupled with increased rates of trophic evolution.

Vespertilionoids and other insectivores, including the earliest diverging phyllostomid subfamilies, have the slowest rates of trophic evolution (Figure 5.2, Table 5.1). This is unsurprising, as their static trophic states across large portions of the phylogeny reflect a slowly evolving ecological process. This is also true of the small cohort of vampire bats, all three of which are obligate sanguivores (Table S5.1). Within both insectivores (Bell 1982, Lenhart *et al.* 2008) and vampires (Delpietro & Russo 2002, Carter *et al.* 2005, Voigt & Kelm 2006) there is evidence for fine-scaled divergence in feeding behavior and diet based on prey size and host specialization. This may mean that trophic categories could be expanded for these bats beyond general insectivory or sanguivory. At the same time, it is also possible that their trophic ecologies are dynamic, and that these species may be flexible based on prey and host availability.

Disparity and cranial shape evolution

Cranial shape evolution across New World bats is relatively homogeneous, especially compared with trophic evolution. Most species are united into a single morphological cohort, which spans every trophic guild and almost every subfamily (Table 5.2, Figure 5.5a). Furthermore, disparity is generally not predicted by our ecological cohorts, and only by a small subset of family or guild comparisons (Table S5.2). We only find significantly elevated rates of

shape evolution for two groups: glossophagines and a clade of four of the most morphologically derived stenodermatine genera (*Ametrida, Centurio, Pygoderma,* and *Sphaeronycteris*).

The *Ametrida* complex belongs to a small clade (subtribe Stenodermatina) of strictly frugivorous stenodermatines with notably short faces (Dávalos 2006). They are known for high degrees of morphological divergence among the stenodermatine radiation (*i.e.* Rubi Angulo *et al.* 2008). These four taxa, and other unsampled close relatives, could be an intriguing example of rapidly accumulating morphological divergence despite static frugivory across most stenodermatines (Table S5.1). While there may be other examples of small cohorts (< 4 taxa) that are masked from our **R**-mode analyses, this seems unlikely given that even the highly derived vampire bats (3 species) do not significantly differ in σ^2_{mult} (see Supporting Information of forthcoming paper).

Our **R**- and **Q**-mode analyses both recover the fastest shape evolution rates for glossophagines; this is the only cohort identified with consistently high rates of evolution for both trophic ecology and morphology (Figure 5.2, 5.5). Though we find strong evidence of morphological convergence among nectarivores (Table S5.4), only the glossophagines have high rates of cranial shape evolution. However, novel morphological characteristics of the other major clade of nectarivores, the lonchophyllines, may be undetectable with our landmark scheme (Dávalos 2004, Dias *et al.* 2013). Trajectory-based methods (*e.g.* Sherratt *et al.* 2016) that consider the orientation of ancestor-descendant vectors in morphospace may reveal more divergence among nectarivores. While being restricted to one specimen per species may potentially bias our shape results, it is unclear if increased sampling would reveal intraspecific variation that strongly overturns the signal of interspecific variation. Even given these caveats, however, New World bat crania are still strikingly homogeneous in dynamics of shape evolution.

Decoupling of trophic and shape evolution

What causes trophic evolution to be decoupled from cranial shape evolution in New World bats? One possibility is that phyllostomids are more plastic in their trophic ecology than is often assumed, and that much of the clade could be characterized by varying degrees of opportunism and generalist omnivory. Even the most morphologically specialized nectarivores regularly supplement their diets with insects and fruits, despite the disparate mechanical requirements for processing these resources, and vice versa (Winter *et al.* 2003, Barros *et al.* 2012). While cranial shapes in bat skulls appear to predict trophic ecology (Figure 5.4; Santana *et al.* 2010, 2012), the degree to which many species exclusively feed on one diet could be overstated. Generalist behavior despite ecomorphological specialization, or functional versatility, can potentially explain high species richness among many radiations (Robinson & Wilson 1998, Bellwood *et al.* 2006).

Field studies have consistently emphasized that many phyllostomid diets are more omnivorous and plastic than previously expected, even across foods of very different material properties (Rex *et al.* 2009). This may also explain the imperfect morphological convergence we find among many trophic guilds (Table S5.4). If omnivory is more common than is often assumed, we may be overestimating heterogeneity in our ecological analyses. Dynamics of trophic and morphological evolution would thus be reconciled, and would both be relatively homogenous, by recognizing more species as generalists than disparate morphology or limited diet sampling might imply.

Cranial morphology could also be more labile than soft tissue or mandibular morphology. Our analyses only highlight *relative* rates of shape evolution, and do not imply that cranial evolution is *absolutely* slow across bats. Considering extant morphological diversity, the rates we

infer could be rapid in comparison to other phenotypic traits. Mammal crania in general may be particularly labile and evolvable at macroevolutionary timescales (Linde-Medina *et al.* 2016). The cranium is highly modular, and linked to other aspects of ecology beyond the capturing and processing of food, including echolocation, smell, and eyesight (Goswami 2006, Machado *et al.* 2007, Curtis & Simmons 2017). The mandible and its associated muscles, on the other hand, are more integrated and functionally constrained by bite force and mastication (Santana *et al.* 2010, López-Aguirre *et al.* 2015). Mandibular shape evolution may thus be better coupled with patterns of trophic evolution.

While we removed allometric effects in our analyses to focus on shape disparity, cranium size is adaptive in other clades (Marroig & Cheverud 2005), and should be explicitly integrated into future research; however, we re-emphasize that there is an extremely high correlation between raw and allometry-corrected data in this study. Phenotypic evolution of many parts of the skull could also be best explained by non-BM models of trait evolution, like an Ornstein-Uhlenbeck model (Dumont *et al.* 2014, Cressler *et al.* 2015; though note that support for OU models is equivocal for our data). Successfully adapting these models for high-dimensional data will be paramount for assessing shape evolution across many clades, despite the known statistical challenges in doing so (Adams & Collyer 2018).

These general possibilities are not mutually exclusive. Heightened omnivory across noctilionoids may also mean that competition for resources among bats is dampened, potentially leading to high morphological lability of crania. These hypotheses could anchor the strong, positive relationship between within-clade cranial disparity and crown age (Figure 5.3) across all New World bats. This disparity-age relationship could be one indicator that bat diversity is unsaturated and expanding (McPeek & Brown 2007, Shi & Rabosky 2015), unlike many other

radiations (Rabosky 2009). While omnivory is a macroevolutionary dead-end in other major vertebrate clades (Burin *et al.* 2016), this would not appear to be the case with noctilionoids (Rojas *et al.* 2018). Overall, any future research on noctilionoids will face a difficult dilemma. Thresholds for classifying a species as one discrete state over another are unavoidably arbitrary at some level, and are highly dependent on sampling, or seasonal and temporal variation. Yet the degree to which many noctilionoids can be considered omnivorous has major repercussions for how we interpret the entire New World bat radiation.

The relationship between morphology and ecology has consistently been of interest to ecologists and evolutionary biologists. Links between morphological evolution and diversification are often used to test for adaptive radiations, and rapid trait evolution is often associated with ecological divergence (Schluter 2000, Losos & Mahler 2010, Rabosky *et al.* 2013). Yet in some cases, like we find here with New World bats, ecology and morphology appear decoupled even amidst rapid diversification (Rundell & Price 2009, Blankers *et al.* 2012). We suggest that New World bats may represent a particular paradigm for how diversification intersects with ecology and morphology to produce a radiation best characterized by general opportunism and plasticity.

ACKNOWLEDGEMENTS

The authors would like to thank A.A. Curtis, N.T. Katlein, M.A. Lynch, N.B. Simmons, K.A. Speer, C.W. Thompson, and H.L. Williams for specimen and scanning support, and D.C. Adams, J. Clavel, M.C. Grundler, T.Y. Moore, and M.L. Zelditch for guidance and suggestions on analyses. J.J.S. would also like to thank C. Badgley, G.E. Gerstner, D.W. McShea, V.L. Roth,

and S. Tigh for insights and inspiration. This project was supported by a National Science Foundation Doctoral Dissertation Improvement Grant (NSF DEB 1501304) to J.J.S. and D.L.R.

REFERENCES

Adams, D.C. (2014a) A generalized K statistic for estimating phylogenetic signal from shape and other high-dimensional multivariate data. *Systematic Biology*, **63**, 685–697.

Adams, D.C. (2014b) A method for assessing phylogenetic least squares models for shape and other high-dimensional multivariate data. *Evolution*, **68**, 2675–2688.

Adams, D.C. (2014c) Quantifying and comparing phylogenetic evolutionary rates for shape and other high-dimensional phenotypic data. *Systematic Biology*, **63**, 166–177.

Adams, D.C. & Collyer, M.L. (2018) Multivariate phylogenetic comparative methods: evaluations, comparisons, and recommendations. *Systematic Biology*, **67**, 14–31.

Adams, D.C. & Collyer, M.L. (2015) Permutation tests for phylogenetic comparative analyses of high-dimensional shape data: what you shuffle matters. *Evolution*, **69**, 823–829.

Adams, D.C., Collyer, M.L., Kaliontzopoulou, A., & Sherratt, E. (2017) Geomorph: software for geometric morphometric analyses. **Version 3.0.6**.

Angulo, S.R., Ríos, J.A., & Díaz, M.M. (2008) *Sphaeronycteris toxophyllum* (Chiroptera: Phyllostomidae). *Mammalian Species*, **814**, 1.

Arnold, S.J. (1983) Morphology, performance, and fitness. *American Zoologist*, **23**, 347–361.

Barros, M.A.S., Rui, A.M., & Fabian, M.E. (2013) Seasonal variation in the diet of the bat *Anoura caudifer* (Phyllostomidae: Glossophaginae) at the southern limit of its geographic range. *Acta Chiropterologica*, **15**, 77–84.

Bell, G.P. (1982) Behavioral and ecological aspects of gleaning by a desert insectivorous bat *Antrozous pallidus* (Chiroptera: Vespertilionidae). *Behavioral Ecology and Sociobiology*, **10**, 217–223.

Bellwood, D.R., Wainwright, P.C., Fulton, C.J., & Hoey, A.S. (2006) Functional versatility supports coral reef biodiversity. *Proceedings of the Royal Society B: Biological Sciences*, **273**, 101-107.

Berwaerts, K., Van Dyck, H., & Aerts, P. (2002) Does flight morphology relate to flight performance? An experimental test with the butterfly *Pararge aegeria*. *Functional Ecology*, **16**, 484–491.

Blackburn, D.G. (1992) Convergent evolution of viviparity, matrotrophy, and specializations for fetal nutrition in reptiles and other vertebrates. *American Zoologist*, **32**, 313–321.

Blankers, T., Adams, D.C., & Wiens, J.J. (2012) Ecological radiation with limited morphological diversification in salamanders. *Journal of Evolutionary Biology*, **25**, 634–646.

Blomberg, S.P., Garland Jr., T, & Ives, A.R. (2003) Testing for phylogenetic signal in comparative data: behavioral traits are more labile. *Evolution*, **57**, 717–745.

Burin, G., Kissling, W.D., Guimarães, P.R., Şekercioğlu, Ç.H., & Quental, T.B. (2016) Omnivory in birds is a macroevolutionary sink. *Nature Communications*, **7**, 11250.

Calsbeek, R. & Irschick, D.J. (2007) The quick and the dead: correlational selection on morphology, performance, and habitat use in island lizards. *Evolution*, **61**, 2493–2503.

Carter, G.G., Coen, C.E., Stenzler, L.M., & Lovette, I.J. (2006) Avian host DNA isolated from the feces of white-winged vampire bats (*Diaemus youngi*). *Acta Chiropterologica*, **8**, 255–258.

Clavel, J., Escarguel, G., & Merceron, G. (2015) mvMORPH: an R package for fitting multivariate evolutionary models to morphometric data. *Methods in Ecology and Evolution*, **6**, 1311–1319.

Collar, D.C., Reece, J.S., Alfaro, M.E., Wainwright, P.C., & Mehta, R.S. (2014) Imperfect morphological convergence: variable changes in cranial structures underlie transitions to durophagy in moray eels. *The American Naturalist*, **183**, E168-E184.

Cozzolino, S. & Widmer, A. (2005) Orchid diversity: an evolutionary consequence of deception? *Trends in Ecology & Evolution*, **20**, 487-494.

Cressler, C.E., Butler, M.A., & King, A.A. (2015) Detecting adaptive evolution in phylogenetic comparative analysis using the Ornstein-Uhlenbeck model. *Systematic Biology*, **64**, 953–968.

Curtis, A.A. & Simmons, N.B. (2017) Unique turbinal morphology in horseshoe bats (Chiroptera: Rhinolophidae). *The Anatomical Record*, **300**, 309–325.

Datzmann, T., von Helversen, O., & Mayer, F. (2010) Evolution of nectarivory in phyllostomid bats (Phyllostomidae Gray, 1825, Chiroptera: Mammalia). *BMC Evolutionary Biology*, **10**, 165.

Dávalos, L.M. (2004) A new Chocoan species of Lonchophylla (Chiroptera: Phyllostomidae). *American Museum Novitates*, **3426**, 1–14.

Dávalos, L.M. (2007) Short-faced bats (Phyllostomidae: Stenodermatina): a Caribbean radiation of strict frugivores. *Journal of Biogeography*, **34**, 364–375.

Davis Rabosky, A.R., Cox, C.L., Rabosky, D.L., Title, P.O., Holmes, I.A., Feldman, A., & McGuire, J.A. (2016) Coral snakes predict the evolution of mimicry across New World snakes. *Nature Communications*, **7**, 11484.

Dawideit, B.A., Phillimore, A.B., Laube, I., Leisler, B., & Böhning-Gaese, K. (2009) Ecomorphological predictors of natal dispersal distances in birds. *Journal of Animal Ecology*, **78**, 388–395.

Delpietro, H.A. & Russo, R.G. (2002) Observations of the common vampire bat (*Desmodus rotundus*) and the hairy-legged vampire bat (*Diphylla ecaudata*) in captivity. *Mammalian Biology*, **67**, 65–78.

Denton, J.S.S. & Adams, D.C. (2015) A new phylogenetic test for comparing multiple high-dimensional evolutionary rates suggests interplay of evolutionary rates and modularity in lanternfishes (Myctophiformes; Myctophidae). *Evolution*, **69**, 2425–2440.

Dias, D., Eduardo Esbérard, C.L., & Moratelli, R. (2013) A new species of *Lonchophylla* (Chiroptera, Phyllostomidae) from the Atlantic Forest of southeastern Brazil, with comments on L. bokermanni. *Zootaxa*, **3722**, 347–360.

Dumont, E.R., Grosse, I.R., & Slater, G.J. (2009) Requirements for comparing the performance of finite element models of biological structures. *Journal of Theoretical Biology*, **256**, 96–103.

Dumont, E.R., Samadevam, K., Grosse, I., Warsi, O.M., Baird, B., & Dávalos, L.M. (2014) Selection for mechanical advantage underlies multiple cranial optima in New World leaf-nosed bats. *Evolution*, **68**, 1436–1449.

Dumont, E.R., Dávalos, L.M., Goldberg, A., Santana, S.E., Rex, K., & Voigt, C.C. (2012) Morphological innovation, diversification and invasion of a new adaptive zone. *Proceedings of the Royal Society B: Biological Sciences*, **279**, 1797–1805.
FitzJohn, R.G. (2012) Diversitree : comparative phylogenetic analyses of diversification in R. *Methods in Ecology and Evolution*, **3**, 1084–1092.
Fleming, T. & Kress, W. (2013) *The ornaments of life: coevolution and conservation in the tropics.* University of Chicago Press, Chicago.
Gillespie, R. (2004) Community assembly through adaptive radiation in Hawaiian spiders. *Science*, **303**, 356–359.
Goswami, A. (2006) Cranial modularity shifts during mammalian evolution. *The American Naturalist*, **168**, 270–280.
Gould, S.J. & Eldredge, N. (1993) Punctuated equilibrium comes of age. *Nature*, **366**, 223.
Griffiths, T.A. (1983) On the phylogeny of the Glossophaginae and the proper use of outgroup analysis. *Systematic Zoology*, **32**, 283–285.
Gunz, P., Mitteroecker, P., Neubauer, S., Weber, G.W., & Bookstein, F.L. (2009) Principles for the virtual reconstruction of hominin crania. *Journal of Human Evolution*, **57**, 48–62.
Hoffmann, F.G., Hoofer, S.R., & Baker, R.J. (2008) Molecular dating of the diversification of Phyllostominae bats based on nuclear and mitochondrial DNA sequences. *Molecular Phylogenetics and Evolution*, **49**, 653–658.
Jones, K.E., Bininda-Emonds, O.R.P., & Gittleman, J.L. (2005) Bats, clocks, and rocks: diversification patterns in Chiroptera. *Evolution*, **59**, 2243–2255.
Kingsolver, J.G. & Huey, R.B. (2003) Introduction: the evolution of morphology, performance, and fitness. *Integrative and Comparative Biology*, **43**, 361–366.
Klingenberg, C.P. & Marugán-Lobón, J. (2013) Evolutionary covariation in geometric morphometric data: analyzing integration, modularity, and allometry in a phylogenetic context. *Systematic Biology*, **62**, 591–610.
Kosnik, M.A., Jablonski, D., Lockwood, R., & Novack-Gottshall, P.M. (2006) Quantifying molluscan body size in evolutionary and ecological analyses: maximizing the return on data-collection efforts. *Palaios*, **21**, 588–597.
Langerhans, R.B. (2009) Morphology, performance, fitness: functional insight into a post-Pleistocene radiation of mosquitofish. *Biology Letters*, **5**, 488–91.
Lenhart, P.A., Mata-Silva, V., & Johnson, J.D. (2010) Foods of the pallid bat, *Antrozous pallidus* (Chiroptera: Vespertilionidae), in the Chihuahuan desert of western Texas. *The Southwestern Naturalist*, **55**, 110–115.
Linde-Medina, M., Boughner, J.C., Santana, S.E., & Diogo, R. (2016) Are more diverse parts of the mammalian skull more labile? *Ecology and Evolution*, **6**, 2318–2324.
López-Aguirre, C., Pérez-Torres, J., & Wilson, L.A.B. (2015) Cranial and mandibular shape variation in the genus *Carollia* (Mammalia: Chiroptera) from Colombia: biogeographic patterns and morphological modularity. *PeerJ*, **3**, e1197.
Losos, J.B. & Mahler, D.L. (2010) Adaptive radiation: the interaction of ecological opportunity, adaptation, and speciation. *Evolution Since Darwin: The First 150 Years* (ed. by M. Bell, D. Futuyma, W. Eanes, and J. Levinton), pp. 381–420. Sinauer Associates, Sunderland.
Losos, J.B. (1990) The evolution of form and function: morphology and locomotor performance in West Indian *Anolis* lizards. *Evolution*, **44**, 1189–1203.

Machado, M., dos Santos Schmidt, E.M., Margarido, T.C., & Montiani-Ferreira, F. (2007) A unique intraorbital osseous structure in the large fruit-eating bat (*Artibeus lituratus*). *Veterinary Ophthalmology*, **10**, 100–105.

Marroig, G. & Cheverud, J.M. (2005) Size as a line of least evolutionary resistance: diet and adaptive morphological radiation in New World monkeys. *Evolution*, **59**, 1128-1142.

McGuire, J.L. (2010) Geometric morphometrics of vole (*Microtus californicus*) dentition as a new paleoclimate proxy: Shape change along geographic and climatic clines. *Quaternary International*, **212**, 198–205.

McPeek, M.A. & Brown, J.M. (2007) Clade age and not diversification rate explains species richness among animal taxa. *The American Naturalist*, **169**, E97-106.

Monteiro, L.R. & Nogueira, M.R. (2011) Evolutionary patterns and processes in the radiation of phyllostomid bats. *BMC Evolutionary Biology*, **11**, 137.

Muschick, M., Indermaur, A., & Salzburger, W. (2012) Convergent evolution within an adaptive radiation of cichlid fishes. *Current Biology*, **22**, 2362–2368.

Norberg, U.M. & Rayner, J.M. V (1987) Ecological morphology and flight in bats (Mammalia; Chiroptera): wing adaptations, flight performance, foraging strategy and echolocation. *Philosophical Transactions of the Royal Society B: Biological Sciences*, **316**, 335–427.

Nowak, M.D. (1994) *Walker's bats of the world.* Johns Hopkins University Press, Baltimore.

Olson, D.M., Dinerstein, E., Wikramanayake, E.D., Burgess, N.D., Powell, G.V.N., Underwood, E.C., D'amico, J. A., Itoua, I., Strand, H.E., Morrison, J.C., Loucks, C.J., Allnutt, T.F., Ricketts, T.H., Kura, Y., Lamoreux, J.F., Wettengel, W.W., Hedao, P., & Kassem, K.R. (2001) Terrestrial ecoregions of the world: a new map of life on Earth. *BioScience*, **51**, 933–938.

Rabosky, D.L. (2009) Ecological limits on clade diversification in higher taxa. *The American Naturalist*, **173**, 662–674.

Rabosky, D.L. (2012) Positive correlation between diversification rates and phenotypic evolvability can mimic punctuated equilibrium on molecular phylogenies. *Evolution*, **66**, 2622-2627.

Rabosky, D.L., Donellan, S.C., Grundler, M.C., & Lovette, I.J. (2014a) Analysis and visualization of complex macroevolutionary dynamics: an example from Australian scincid lizards. *Systematic Biology*, **63**, 610–627.

Rabosky, D.L., Grundler, M.C., Anderson, C.J.R., Title, P.O., Shi, J.J., Brown, J.W., Huang, H., & Larson, J.G. (2014b) BAMMtools: an R package for the analysis of evolutionary dynamics on phylogenetic trees. *Methods in Ecology and Evolution*, **5**, 701–707.

Rabosky, D.L., Santini, F., Eastman, J., Smith, S.A., Sidlauskas, B., Chang, J., & Alfaro, M.E. (2013) Rates of speciation and morphological evolution are correlated across the largest vertebrate radiation. *Nature Communications*, **4**, 1958.

Revell, L.J. & Harmon, L.J. (2008) Testing quantitative genetic hypotheses about the evolutionary rate matrix for continuous characters. *Evolutionary Ecology Research*, **10**, 311–331.

Revell, L.J. & Collar, D.C. (2009) Phylogenetic of the evolutionary correlation using likelihood. *Evolution*, **63**, 1090–1100.

Rex, K., Czaczkes, B.I., Michener, R., Kunz, T.H., & Voigt, C.C. (2010) Specialization and omnivory in diverse mammalian assemblages. *Ecoscience*, **17**, 37–46.

Ricklefs, R.E. (2004) Cladogenesis and morphological diversification in passerine birds. *Nature*, **430**, 338.

Robinson, B.W. & Wilson, D.S. (1998) Optimal foraging, specialization, and a solution to Liem's paradox. *The American Naturalist*, **151**, 223-235.
Rohlf, F.J. (2010) tpsRelw: relative warps analysis. **Version 1.49**.
Rohlf, F.J. & Slice, D. (1990) Extensions of the Procrustes method for the optimal superimposition of landmarks. *Systematic Zoology*, **39**, 40–59.
Rojas, D., Ramos Pereira, M.J., Fonseca, C., & Dávalos, L.M. (2018) Eating down the food chain: generalism is not an evolutionary dead end for herbivores. *Ecology Letters*, **21**, 402–410.
Rojas, D., Warsi, O. M., & Dávalos, L. M. (2016) Bats (Chiroptera: Noctilionoidea) challenge a recent origin of extant Neotropical diversity. *Systematic Biology*, **65**, 432-448.
Rosenblum, E.B. (2006) Convergent evolution and divergent selection: lizards at the White Sands ecotone. *The American Naturalist*, **167**, 1–15.
Rundell, R.J. & Price, T.D. (2009) Adaptive radiation, nonadaptive radiation, ecological speciation and nonecological speciation. *Trends in Ecology & Evolution*, **24**, 394–399.
Santana, S.E. & Cheung, E. (2016) Go big or go fish: morphological specializations in carnivorous bats. *Proceedings of the Royal Society B: Biological Sciences*, **283**, 20160615.
Santana, S.E. & Dumont, E.R. (2009) Connecting behaviour and performance: the evolution of biting behaviour and bite performance in bats. *Journal of Evolutionary Biology*, **22**, 2131–2145.
Santana, S.E. & Lofgren, S.E. (2013) Does nasal echolocation influence the modularity of the mammal skull? *Journal of Evolutionary Biology*, **26**, 2520–2526.
Santana, S.E., Dumont, E.R., & Davis, J.L. (2010) Mechanics of bite force production and its relationship to diet in bats. *Functional Ecology*, **24**, 776–784.
Santana, S.E., Grosse, I.R., & Dumont, E.R. (2012) Dietary hardness, loading behavior, and the evolution of skull form in bats. *Evolution*, **66**, 2587-2598.
Schluter, D. (1996) Ecological causes of adaptive radiation. *The American Naturalist*, **148**, S40–S64.
Schluter, D. (2000) *The ecology of adaptive radiation.* Oxford University Press, Oxford.
Serb, J.M., Sherratt, E., Alejandrino, A., & Adams, D.C. (2017) Phylogenetic convergence and multiple shell shape optima for gliding scallops (Bivalvia: Pectinidae). *Journal of Evolutionary Biology*, **30**, 1736–1747.
Sherratt, E., Alejandrino, A., Kraemer, A.C., Serb, J.M., & Adams, D.C. (2016) Trends in the sand: Directional evolution in the shell shape of recessing scallops (Bivalvia: Pectinidae). *Evolution*, **70**, 2061–2073.
Sherratt, E., Gower, D.J., Klingenberg, C.P., & Wilkinson, M. (2014) Evolution of cranial shape in caecilians (Amphibia: Gymnophiona). *Evolutionary Biology*, **41**, 528–545.
Shi, J.J. & Rabosky, D.L. (2015) Speciation dynamics during the global radiation of extant bats. *Evolution*, **69**, 1528–1545.
Shi, J.J., Westeen, E.P., Katlein, N.T., Dumont, E.R., & Rabosky, D.L. (2018) Ecomorphological and phylogenetic controls on sympatry across extant bats. *Journal of Biogeography*.
Simmons, N.B. (2005) Order Chiroptera. *Mammal species of the world: a taxonomic and geographic reference* (ed. by D.E. Wilson and D.M. Reeder), pp. 312–529. Johns Hopkins University Press, Baltimore.
Simmons, N.B. & Conway, T.M. (2003) Evolution of ecological diversity in bats. *Bat ecology* (ed. by T.H. Kunz and M.B. Fenton), pp. 493–535. University of Chicago Press, Chicago.

Stayton, C.T. (2015) The definition, recognition, and interpretation of convergent evolution, and two new measures for quantifying and assessing the significance of convergence. *Evolution*, **69**, 2140–2153.
Stebbins, G.L. (1970) Adaptive radiation of reproductive characteristics in angiosperms, I: pollination mechanisms. *Annual Review of Ecology and Systematics*, **1**, 307–326.
Sturmbauer, C. (1998) Explosive speciation in cichlid fishes of the African Great Lakes: a dynamic model of adaptive radiation. *Journal of Fish Biology*, **53**, 18–36.
Teeling, E.C., Springer, M.S., Madsen, O., Bates, P., O'Brien, S.J., & Murphy, W.J. (2005) A molecular phylogeny for bats illuminates biogeography and the fossil record. *Science*, **307**, 580–584.
terHorst, C.P., Miller, T.E., & Powell, E. (2010) When can competition for resources lead to ecological equivalence? *Evolutionary Ecology Research*, **12**, 843–854.
Tschapka, M. (2005) Reproduction of the bat *Glossophaga commissarisi* (Phyllostomidae: Glossophaginae) in the Costsa Rican rain forest during frugivorous and nectarivorous periods. *Biotropica*, **37**, 409–415.
Valiente-Banuet, A., Arizmendi, M.D.C., Rojas-Martínez, A., & Domínguez-Canseco, L. (1996) Ecological relationships between columnar cacti and nectar-feeding bats in Mexico. *Journal of Tropical Ecology*, **12**, 103–119.
Voigt, C.C. & Kelm, D.H. (2006) Host preference of the common vampire bat (*Desmodus rotundus*; Chiroptera) assessed by stable isotopes. *Journal of Mammalogy*, **87**, 1–6.
Wagner, C.E., Harmon, L.J., & Seehausen, O. (2012) Ecological opportunity and sexual selection together predict adaptive radiation. *Nature*, **487**, 366–369.
Winter, Y. & von Helversen, O. (2003) Operational tongue length in phyllostomid nectar-feeding bats. *Journal of Mammalogy*, **84**, 886–896.
Yang, A.S. (2001) Modularity, evolvability, and adaptive radiations: a comparison of the hemi- and holometabolous insects. *Evolution & Development*, **3**, 59-72.
Zanno, L.E. & Makovicky, P.J. (2011) Herbivorous ecomorphology and specialization patterns in theropod dinosaur evolution. *Proceedings of the National Academy of Sciences of the United States of America*, **108**, 232–237.
Zelditch, M.L., Ye, J., Mitchell, J.S., & Swiderski, D.L. (2017) Rare ecomorphological convergence on a complex adaptive landscape: Body size and diet mediate evolution of jaw shape in squirrels (Sciuridae). *Evolution*, **71**, 633–649.
Zortéa, M. (2003) Reproductive patterns and feeding habits of three nectarivorous bats (Phyllostomidae: Glossophaginae) from the Brazilian Cerrado. *Brazilian Journal of Biology*, **63**, 159–168.

Table 5.1 Ecological trophic cohorts
The ecological, trophic cohorts identified by our partitioned analyses of character evolution. We include the name and abbreviation of each cohort used within the text and figures (generally the largest or most distinctive member clade), clades included in each cohort, and the guilds represented by each cohort. We also include the median pairwise membership of taxa in each cohort, which is calculated from the weighted likelihoods of all models where they are members of the same partition. Finally, we include each cohort's median, weighted character transition rate $q_{i,j}$.

cohort name	**cohort members**	**ecological guilds**	**median pairwise membership**	**median cohort $q_{i,j}$**
Stenodermatinae	Phyllostomidae: subfamily Stenodermatinae	primarily frugivores	95%	2.31e-3
Lonchophyllinae (Lonch.)	Phyllostomidae: subfamilies Lonchophyllinae, Carolliinae, Glyphonycterinae, Lonchorhininae, Rhinophyllinae, Phyllostominae	insectivores, carnivores, frugivores, nectarivores, omnivores	98%	4.33e-3
Glossophaginae (Gloss.)	Phyllostomidae: subfamily Glossophaginae	primarily nectarivores	95%	6.27e-3
Desmodontinae	Phyllostomidae: subfamily Desmodontinae	all obligate sanguivores	100%	3.92e-3
Micronycterinae	Phyllostomidae: subfamilies Micronycterinae, Macrotinae	primarily insectivores	100%	6.01e-4
Mormoopidae	Mormoopidae, Emballonuridae, Noctilionidae	primarily insectivores, one piscivore	96%	3.16e-4
Vespertilionoidea	Vespertilionidae, Molossidae, Natalidae	all obligate insectivores in this dataset	99%	1.01e-4

Table 5.2 Morphological shape cohorts
The morphological, cranial shape cohorts identified by our multirate BM analyses on PC axes 1-3. Interpretation of this table is similar to that of Table 5.2. Median σ^2 refers to rates calculated from the evolutionary rate matrix, per PC axis, across our **R**-mode models. σ^2_{mult} refers to clade multivariate shape evolution rates calculated using our **Q**-mode analyses; these significantly differ based on both permutations ($p = 0.021$) and simulations ($p < 0.01$).

cohort name	**cohort members**	**ecological guilds**	**median pairwise membership**	**median cohort σ^2**	**cohort σ^2_{mult}**
Ametrida complex	Phyllostomidae: subfamily Stenodermatinae: *Ametrida, Centurio, Pygoderma, Sphaeronycteris*	all obligate frugivores	100%	PC1: 6.13e-4 PC2: 1.20e-4 PC3: 3.38e-5	2.70e-5
Glossophaginae	Phyllostomidae: subfamily Glossophaginae	primarily nectarivores	100%	PC1: 4.68e-4 PC2: 1.46e-4 PC3: 4.87e-5	7.78e-6
background radiation	all other bats	all New World ecological guilds	91.8%	PC1: 7.74e-5 PC2: 4.96e-5 PC3: 4.67e-5	4.41e-6

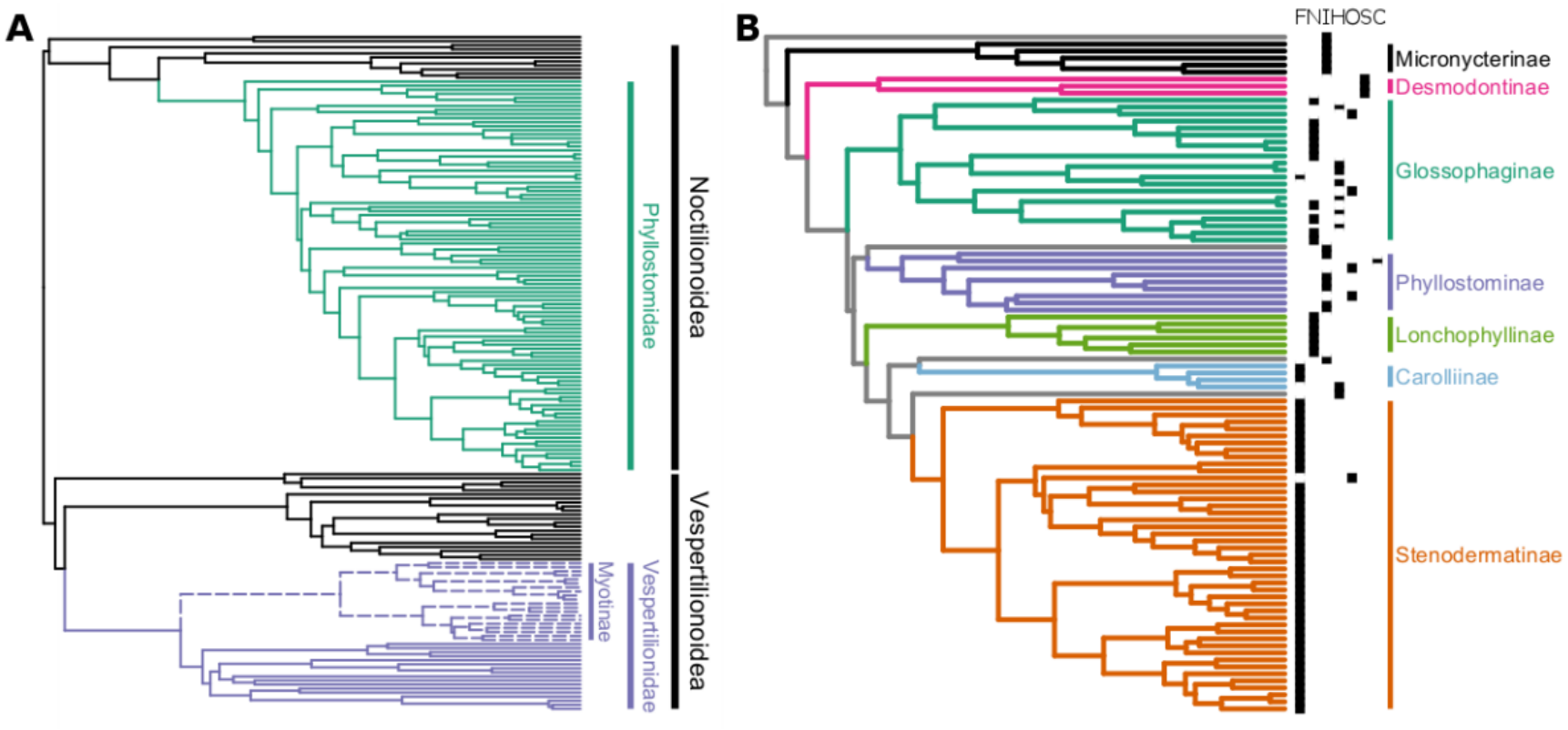

Figure 5.1 Phylogeny of New World bats
(a) The full species-level phylogeny of New World bats, with the clades Noctilionoidea, Phyllostomidae, Vespertilionoidea, and Myotinae (*Myotis*) labeled. (b) The Phyllostomidae phylogeny with all non-monotypic subfamilies labeled. Unlabeled taxa, from top to bottom, are the genera *Macrotus* (sister to all other phyllostomids), *Lonchorhina* (sister to Phyllostominae), *Glyphonycteris* (sister to Carolliinae), and *Rhinophylla* (sister to Stenodermatinae). Black rectangles indicate dietary ecology, as specified for this study, abbreviated as follows: (f)rugivory, (n)ectarivory, (i)nsectivory, (h)erbivory, (o)mnivory, (s)anguivory, and (c)arnivory. All non-phyllostomids included in this study are insectivorous at this scale, with one piscivorous exception (*Noctilio leporinus*).

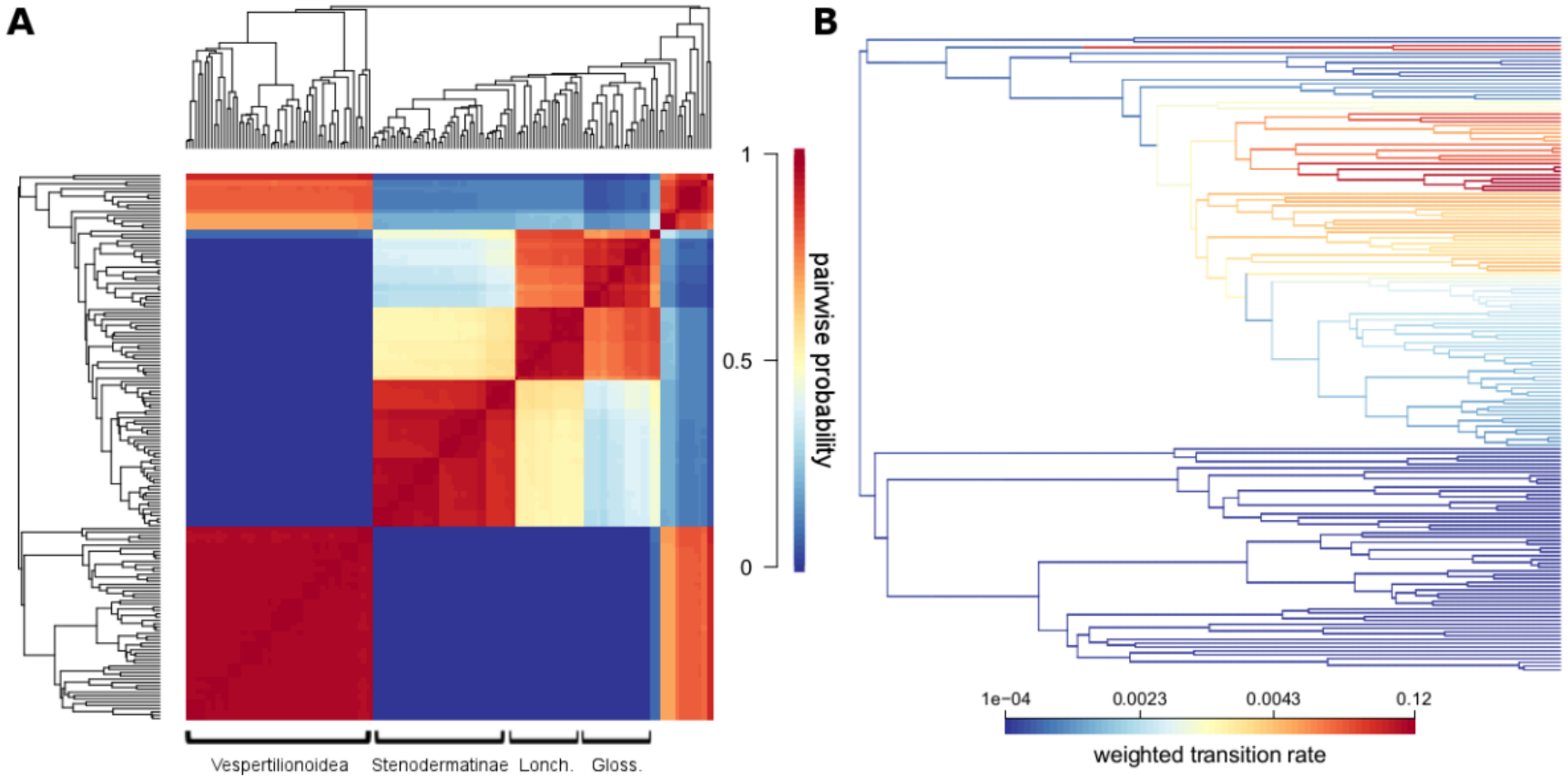

Figure 5.2 Ecological cohort matrix
(a) Ecological cohorts as inferred by our models of character evolution. The phylogeny is projected on the left and right sides of the matrix. Colors represent weighted pairwise probabilities of belonging to the same partition across all models. See Table 5.1 for cohort details and abbreviations. (b) Weighted transition rates among ecological states on the phylogeny, which we considered a measure of the rate of trophic evolution. We highlight heterogeneity in both ecological cohorts and rates of trophic evolution across New World bats.

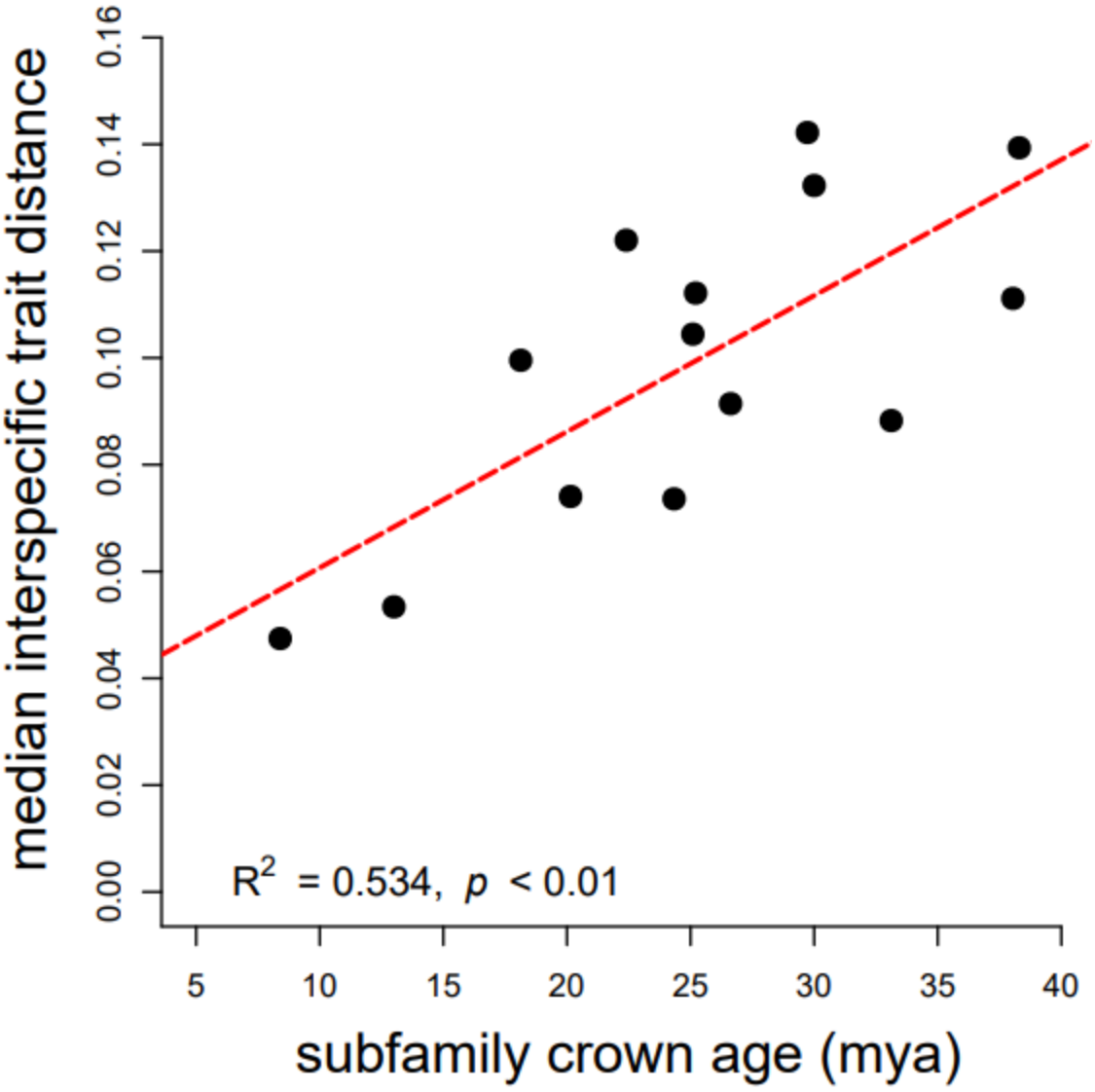

Figure 5.3 Disparity-age relationship
The significant and positive, linear relationship between the median interspecific Euclidean distance among skulls within clades, and the crown age of the clade (in millions of years). In this case, clades were represented by non-monotypic subfamilies from our New World phylogeny.

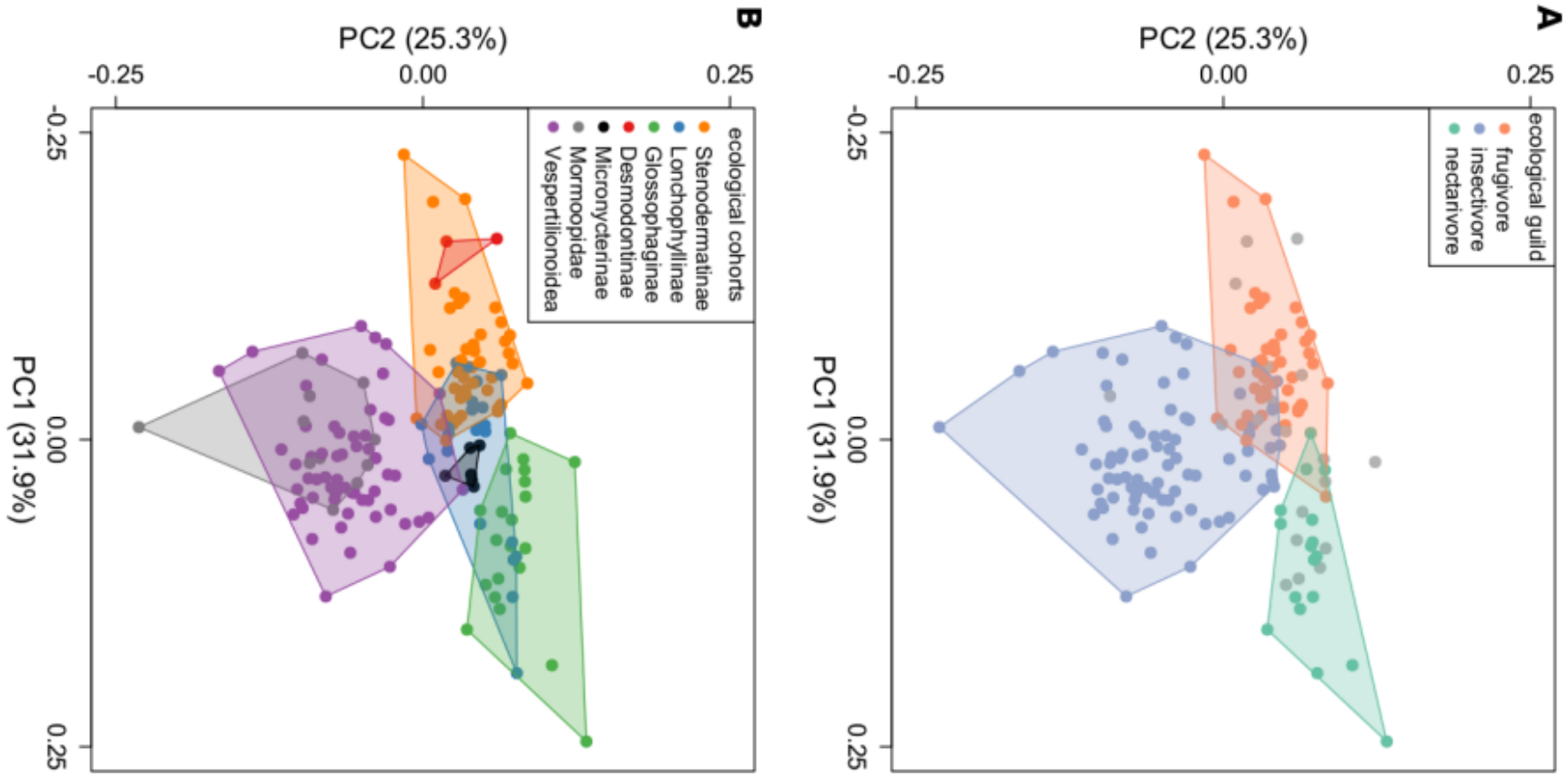

Figure 5.4 Principal component analysis of New World bat crania
(a) Our shape dataset as ordinated by its first two principal component axes. We highlight the three most species-rich ecological guilds in our dataset. (b) The same dataset, now colored by the ecological cohorts identified in our character analyses (Table 5.1).

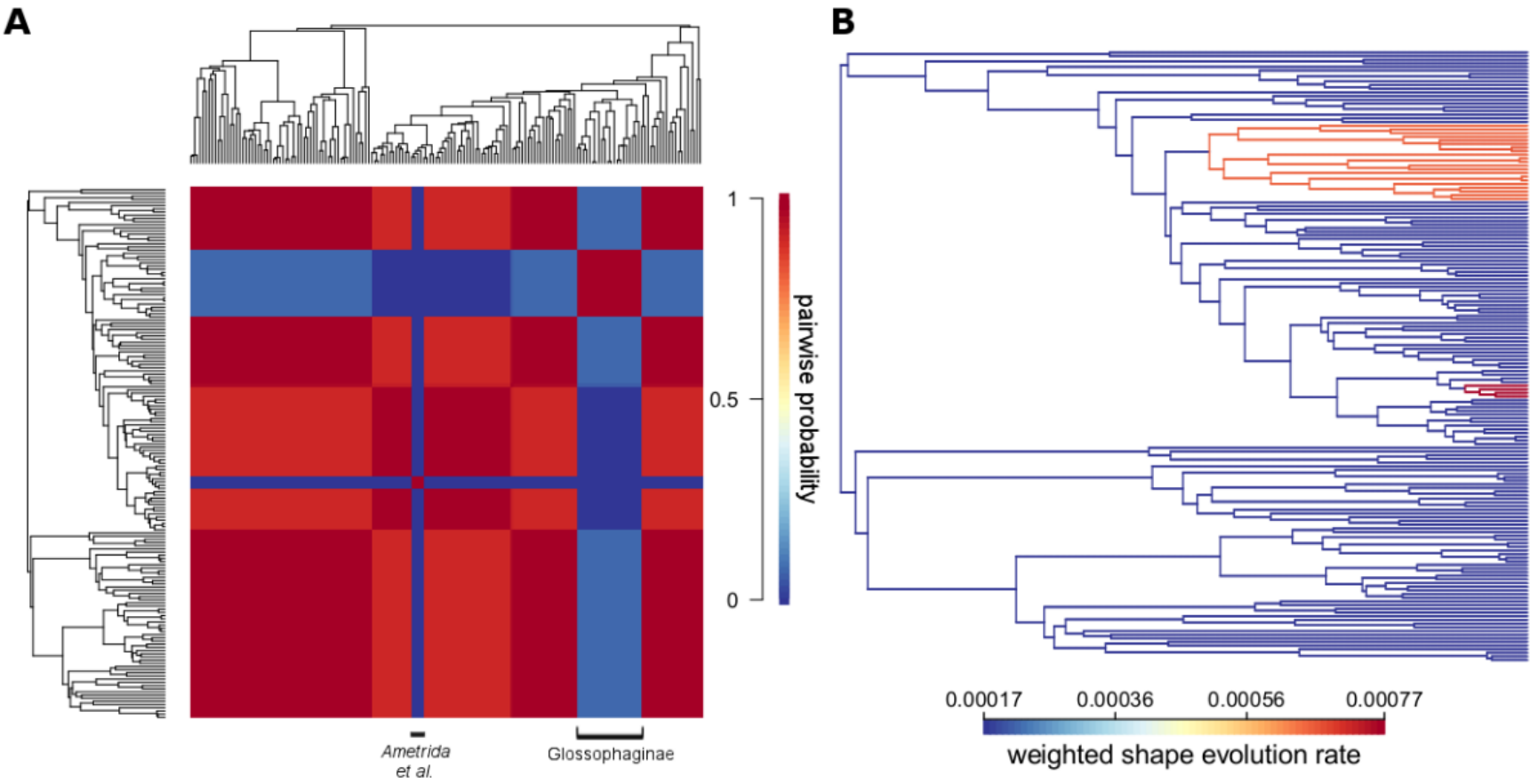

Figure 5.5 Morphological shape cohort matrix
(a) Morphological cohorts as inferred by our multirate BMM models of multivariate trait evolution, using PC axes 1-3. Our phylogeny is projected on the left and right sides of the matrix. Colors represent weighted pairwise probabilities of belonging to the same partition across all models. See Table 5.2 for cohort details. (b) Weighted rates of cranial shape evolution, from the evolutionary rate matrices of our multirate BMM models

Table S5.1 Phylogenetic, ecological, and morphological metadata

A summary of all metadata associated with the 167 cranial specimens used for this study. Each species is classified by superfamily, family, and subfamily as described by Simmons (2005), Shi & Rabosky (2015), and Rojas *et al.* (2016). They are further assigned trophic ecology states ("ecology") as in Rojas *et al.* (2018) and corroborated by our literature review; these states are used for the main analyses of this study. They are also classified according to a second trophic ecology classification scheme ("double_ecology") which is assigned based on the top two food items preferred by each species. Cohorts are assigned according to the main text; numbers follow the order (top to bottom) of the Tables 5.1 and 5.2. Literature information is detailed in the forthcoming paper.

species	superfamily	family	subfamily	realm	ecology	double_ecology	ecol. cohort	morph. cohort
Balantiopteryx plicata	Emballonuroidea	Emballonuridae	Emballonurinae	Neotropics	insectivore	InsIns	6	3
Centronycteris maximiliani	Emballonuroidea	Emballonuridae	Emballonurinae	Neotropics	insectivore	InsIns	6	3
Ametrida centurio	Noctilionoidea	Phyllostomidae	Stenodermatinae	Neotropics	frugivore	FruFru	1	1
Anoura cultrata	Noctilionoidea	Phyllostomidae	Glossophaginae	Neotropics	nectarivore	NecFru	3	2
Anoura geoffroyi	Noctilionoidea	Phyllostomidae	Glossophaginae	Neotropics	omnivore	InsNec	3	2
Anoura latidens	Noctilionoidea	Phyllostomidae	Glossophaginae	Neotropics	herbivore	NecFru	3	2
Ardops nichollsi	Noctilionoidea	Phyllostomidae	Stenodermatinae	Neotropics	frugivore	FruFru	1	3
Ariteus flavescens	Noctilionoidea	Phyllostomidae	Stenodermatinae	Neotropics	frugivore	FruFru	1	3
Artibeus anderseni	Noctilionoidea	Phyllostomidae	Stenodermatinae	Neotropics	frugivore	FruFru	1	3
Artibeus aztecus	Noctilionoidea	Phyllostomidae	Stenodermatinae	Neotropics	frugivore	FruIns	1	3
Artibeus concolor	Noctilionoidea	Phyllostomidae	Stenodermatinae	Neotropics	frugivore	FruNec	1	3
Artibeus fimbriatus	Noctilionoidea	Phyllostomidae	Stenodermatinae	Neotropics	frugivore	FruFru	1	3
Artibeus fraterculus	Noctilionoidea	Phyllostomidae	Stenodermatinae	Neotropics	frugivore	FruIns	1	3
Artibeus glaucus	Noctilionoidea	Phyllostomidae	Stenodermatinae	Neotropics	frugivore	FruIns	1	3
Artibeus intermedius	Noctilionoidea	Phyllostomidae	Stenodermatinae	Neotropics	frugivore	FruIns	1	3
Artibeus jamaicensis	Noctilionoidea	Phyllostomidae	Stenodermatinae	Neotropics	frugivore	FruNec	1	3
Artibeus lituratus	Noctilionoidea	Phyllostomidae	Stenodermatinae	Neotropics	frugivore	FruIns	1	3
Artibeus obscurus	Noctilionoidea	Phyllostomidae	Stenodermatinae	Neotropics	frugivore	FruFru	1	3

Artibeus phaeotis	Noctilionoidea	Phyllostomidae	Stenodermatinae	Neotropics	frugivore	FruIns	1	3
Artibeus planirostris	Noctilionoidea	Phyllostomidae	Stenodermatinae	Neotropics	frugivore	FruFru	1	3
Artibeus toltecus	Noctilionoidea	Phyllostomidae	Stenodermatinae	Neotropics	frugivore	FruFru	1	3
Brachyphylla nana	Noctilionoidea	Phyllostomidae	Glossophaginae	Neotropics	nectarivore	NecFru	3	2
Carollia brevicauda	Noctilionoidea	Phyllostomidae	Carolliinae	Neotropics	herbivore	FruNec	2	3
Carollia perspicillata	Noctilionoidea	Phyllostomidae	Carolliinae	Neotropics	frugivore	FruNec	2	3
Carollia sowelli	Noctilionoidea	Phyllostomidae	Carolliinae	Neotropics	frugivore	FruFru	2	3
Carollia subrufa	Noctilionoidea	Phyllostomidae	Carolliinae	Neotropics	frugivore	FruNec	2	3
Centurio senex	Noctilionoidea	Phyllostomidae	Stenodermatinae	Neotropics	frugivore	FruFru	1	1
Chiroderma salvini	Noctilionoidea	Phyllostomidae	Stenodermatinae	Neotropics	frugivore	FruNec	1	3
Chiroderma trinitatum	Noctilionoidea	Phyllostomidae	Stenodermatinae	Neotropics	frugivore	FruNec	1	3
Chiroderma villosum	Noctilionoidea	Phyllostomidae	Stenodermatinae	Neotropics	frugivore	FruNec	1	3
Choeroniscus godmani	Noctilionoidea	Phyllostomidae	Glossophaginae	Neotropics	nectarivore	NecFru	3	2
Choeronycteris mexicana	Noctilionoidea	Phyllostomidae	Glossophaginae	Neotropics_Nearctic	nectarivore	NecFru	3	2
Desmodus rotundus	Noctilionoidea	Phyllostomidae	Desmodontinae	Neotropics	sanguivore	Blood	4	3
Diaemus youngi	Noctilionoidea	Phyllostomidae	Desmodontinae	Neotropics	sanguivore	Blood	4	3
Diphylla ecaudata	Noctilionoidea	Phyllostomidae	Desmodontinae	Neotropics	sanguivore	Blood	4	3
Erophylla bombifrons	Noctilionoidea	Phyllostomidae	Glossophaginae	Neotropics	herbivore	FruNec	3	2
Erophylla sezekorni	Noctilionoidea	Phyllostomidae	Glossophaginae	Neotropics	herbivore	FruNec	3	2
Glossophaga commissarisi	Noctilionoidea	Phyllostomidae	Glossophaginae	Neotropics	nectarivore	NecFru	3	2
Glossophaga leachii	Noctilionoidea	Phyllostomidae	Glossophaginae	Neotropics	nectarivore	NecFru	3	2
Glossophaga longirostris	Noctilionoidea	Phyllostomidae	Glossophaginae	Neotropics	herbivore	NecFru	3	2

Glossophaga morenoi	Noctilionoidea	Phyllostomidae	Glossophaginae	Neotropics	nectarivore	NecFru	3	2
Glossophaga soricina	Noctilionoidea	Phyllostomidae	Glossophaginae	Neotropics	herbivore	NecFru	3	2
Glyphonycteris sylvestris	Noctilionoidea	Phyllostomidae	Glyphonycterinae	Neotropics	insectivore	InsFru	2	3
Hylonycteris underwoodi	Noctilionoidea	Phyllostomidae	Glossophaginae	Neotropics	nectarivore	NecFru	3	2
Leptonycteris curasoae	Noctilionoidea	Phyllostomidae	Glossophaginae	Neotropics	herbivore	NecFru	3	2
Leptonycteris yerbabuenae	Noctilionoidea	Phyllostomidae	Glossophaginae	Neotropics_Nearctic	nectarivore	NecFru	3	2
Lichonycteris obscura	Noctilionoidea	Phyllostomidae	Glossophaginae	Neotropics	nectarivore	NecFru	3	2
Lionycteris spurrelli	Noctilionoidea	Phyllostomidae	Lonchophyllinae	Neotropics	nectarivore	NecFru	2	3
Lonchophylla handleyi	Noctilionoidea	Phyllostomidae	Lonchophyllinae	Neotropics	nectarivore	NecFru	2	3
Lonchophylla mordax	Noctilionoidea	Phyllostomidae	Lonchophyllinae	Neotropics	nectarivore	NecFru	2	3
Lonchophylla robusta	Noctilionoidea	Phyllostomidae	Lonchophyllinae	Neotropics	nectarivore	NecFru	2	3
Lonchophylla thomasi	Noctilionoidea	Phyllostomidae	Lonchophyllinae	Neotropics	nectarivore	NecIns	2	3
Lonchorhina aurita	Noctilionoidea	Phyllostomidae	Lonchorhininae	Neotropics	insectivore	InsIns	2	3
Lophostoma brasiliense	Noctilionoidea	Phyllostomidae	Phyllostominae	Neotropics	insectivore	InsIns	2	3
Lophostoma schulzi	Noctilionoidea	Phyllostomidae	Phyllostominae	Neotropics	insectivore	InsIns	2	3
Lophostoma silvicolum	Noctilionoidea	Phyllostomidae	Phyllostominae	Neotropics	insectivore	InsFru	2	3
Macrophyllum macrophyllum	Noctilionoidea	Phyllostomidae	Phyllostominae	Neotropics	insectivore	InsIns	2	3
Macrotus waterhousii	Noctilionoidea	Phyllostomidae	Macrotinae	Neotropics	insectivore	InsFru	5	3
Micronycteris brosseti	Noctilionoidea	Phyllostomidae	Micronycterinae	Neotropics	insectivore	InsIns	5	3

Micronycteris hirsuta	Noctilionoidea	Phyllostomidae	Micronycterinae	Neotropics	insectivore	InsIns	5	3
Micronycteris matses	Noctilionoidea	Phyllostomidae	Micronycterinae	Neotropics	insectivore	InsIns	5	3
Micronycteris megalotis	Noctilionoidea	Phyllostomidae	Micronycterinae	Neotropics	insectivore	InsIns	5	3
Micronycteris schmidtorum	Noctilionoidea	Phyllostomidae	Micronycterinae	Neotropics	insectivore	InsIns	5	3
Mimon crenulatum	Noctilionoidea	Phyllostomidae	Phyllostominae	Neotropics	insectivore	InsIns	2	3
Monophyllus redmani	Noctilionoidea	Phyllostomidae	Glossophaginae	Neotropics	omnivore	NecIns	3	2
Mormoops megalophylla	Noctilionoidea	Mormoopidae	Mormoopinae	Neotropics_Nearctic	insectivore	InsIns	6	3
Musonycteris harrisoni	Noctilionoidea	Phyllostomidae	Glossophaginae	Neotropics	nectarivore	NecNec	3	2
Noctilio albiventris	Noctilionoidea	Noctilionidae	Noctilioninae	Neotropics	insectivore	InsIns	6	3
Noctilio leporinus	Noctilionoidea	Noctilionidae	Noctilioninae	Neotropics	piscivore	MeaIns	6	3
Phylloderma stenops	Noctilionoidea	Phyllostomidae	Phyllostominae	Neotropics	omnivore	FruIns	2	3
Phyllonycteris aphylla	Noctilionoidea	Phyllostomidae	Glossophaginae	Neotropics	frugivore	FruNec	3	2
Phyllonycteris poeyi	Noctilionoidea	Phyllostomidae	Glossophaginae	Neotropics	herbivore	FruNec	3	2
Phyllops falcatus	Noctilionoidea	Phyllostomidae	Stenodermatinae	Neotropics	frugivore	FruFru	1	3
Phyllostomus discolor	Noctilionoidea	Phyllostomidae	Phyllostominae	Neotropics	omnivore	FruNec	2	3
Phyllostomus elongatus	Noctilionoidea	Phyllostomidae	Phyllostominae	Neotropics	insectivore	InsFru	2	3
Platalina genovensium	Noctilionoidea	Phyllostomidae	Lonchophyllinae	Neotropics	nectarivore	NecFru	2	3
Platyrrhinus brachycephalus	Noctilionoidea	Phyllostomidae	Stenodermatinae	Neotropics	frugivore	FruNec	1	3
Platyrrhinus dorsalis	Noctilionoidea	Phyllostomidae	Stenodermatinae	Neotropics	frugivore	FruFru	1	3
Platyrrhinus helleri	Noctilionoidea	Phyllostomidae	Stenodermatinae	Neotropics	frugivore	FruFru	1	3
Platyrrhinus infuscus	Noctilionoidea	Phyllostomidae	Stenodermatinae	Neotropics	frugivore	FruNec	1	3

Platyrrhinus lineatus	Noctilionoidea	Phyllostomidae	Stenodermatinae	Neotropics	frugivore	FruNec	1	3
Platyrrhinus masu	Noctilionoidea	Phyllostomidae	Stenodermatinae	Neotropics	frugivore	FruFru	1	3
Platyrrhinus vittatus	Noctilionoidea	Phyllostomidae	Stenodermatinae	Neotropics	frugivore	FruFru	1	3
Pteronotus davyi	Noctilionoidea	Mormoopidae	Mormoopinae	Neotropics	insectivore	InsIns	6	3
Pteronotus gymnonotus	Noctilionoidea	Mormoopidae	Mormoopinae	Neotropics	insectivore	InsIns	6	3
Pteronotus macleayii	Noctilionoidea	Mormoopidae	Mormoopinae	Neotropics	insectivore	InsIns	6	3
Pteronotus parnellii	Noctilionoidea	Mormoopidae	Mormoopinae	Neotropics	insectivore	InsIns	6	3
Pteronotus personatus	Noctilionoidea	Mormoopidae	Mormoopinae	Neotropics	insectivore	InsIns	6	3
Pteronotus quadridens	Noctilionoidea	Mormoopidae	Mormoopinae	Neotropics	insectivore	InsIns	6	3
Pygoderma bilabiatum	Noctilionoidea	Phyllostomidae	Stenodermatinae	Neotropics	frugivore	FruFru	1	1
Rhinophylla fischerae	Noctilionoidea	Phyllostomidae	Rhinophyllinae	Neotropics	herbivore	FruNec	2	3
Sphaeronycteris toxophyllum	Noctilionoidea	Phyllostomidae	Stenodermatinae	Neotropics	frugivore	FruFru	1	1
Stenoderma rufum	Noctilionoidea	Phyllostomidae	Stenodermatinae	Neotropics	frugivore	FruFru	1	3
Sturnira bidens	Noctilionoidea	Phyllostomidae	Stenodermatinae	Neotropics	frugivore	FruFru	1	3
Sturnira bogotensis	Noctilionoidea	Phyllostomidae	Stenodermatinae	Neotropics	frugivore	FruFru	1	3
Sturnira lilium	Noctilionoidea	Phyllostomidae	Stenodermatinae	Neotropics	frugivore	FruFru	1	3
Sturnira ludovici	Noctilionoidea	Phyllostomidae	Stenodermatinae	Neotropics	frugivore	FruFru	1	3
Sturnira magna	Noctilionoidea	Phyllostomidae	Stenodermatinae	Neotropics	frugivore	FruFru	1	3
Sturnira mordax	Noctilionoidea	Phyllostomidae	Stenodermatinae	Neotropics	frugivore	FruNec	1	3
Sturnira nana	Noctilionoidea	Phyllostomidae	Stenodermatinae	Neotropics	frugivore	FruFru	1	3
Sturnira oporaphilum	Noctilionoidea	Phyllostomidae	Stenodermatinae	Neotropics	frugivore	FruFru	1	3
Sturnira tildae	Noctilionoidea	Phyllostomidae	Stenodermatinae	Neotropics	frugivore	FruNec	1	3
Trachops cirrhosus	Noctilionoidea	Phyllostomidae	Phyllostominae	Neotropics	carnivore	MeaIns	2	3
Uroderma bilobatum	Noctilionoidea	Phyllostomidae	Stenodermatinae	Neotropics	frugivore	FruIns	1	3

Uroderma magnirostrum	Noctilionoidea	Phyllostomidae	Stenodermatinae	Neotropics	frugivore	FruIns	1	3
Vampyressa bidens	Noctilionoidea	Phyllostomidae	Stenodermatinae	Neotropics	frugivore	FruFru	1	3
Vampyressa brocki	Noctilionoidea	Phyllostomidae	Stenodermatinae	Neotropics	frugivore	FruFru	1	3
Vampyressa melissa	Noctilionoidea	Phyllostomidae	Stenodermatinae	Neotropics	omnivore	InsFru	1	3
Antrozous pallidus	Vespertilionoidea	Vespertilionidae	Vespertilioninae	Nearctic	insectivore	InsIns	7	3
Chilonatalus micropus	Vespertilionoidea	Natalidae	Natalinae	Neotropics	insectivore	InsIns	7	3
Corynorhinus townsendii	Vespertilionoidea	Vespertilionidae	Vespertilioninae	Nearctic	insectivore	InsIns	7	3
Cynomops abrasus	Vespertilionoidea	Molossidae	Molossinae	Neotropics	insectivore	InsIns	7	3
Cynomops paranus	Vespertilionoidea	Molossidae	Molossinae	Neotropics	insectivore	InsIns	7	3
Cynomops planirostris	Vespertilionoidea	Molossidae	Molossinae	Neotropics	insectivore	InsIns	7	3
Eptesicus brasiliensis	Vespertilionoidea	Vespertilionidae	Vespertilioninae	Neotropics	insectivore	InsIns	7	3
Eptesicus diminutus	Vespertilionoidea	Vespertilionidae	Vespertilioninae	Neotropics	insectivore	InsIns	7	3
Eptesicus furinalis	Vespertilionoidea	Vespertilionidae	Vespertilioninae	Neotropics	insectivore	InsIns	7	3
Eptesicus fuscus	Vespertilionoidea	Vespertilionidae	Vespertilioninae	Nearctic	insectivore	InsIns	7	3
Eumops bonariensis	Vespertilionoidea	Molossidae	Molossinae	Neotropics	insectivore	InsIns	7	3
Eumops glaucinus	Vespertilionoidea	Molossidae	Molossinae	Neotropics	insectivore	InsIns	7	3
Eumops patagonicus	Vespertilionoidea	Molossidae	Molossinae	Neotropics	insectivore	InsIns	7	3
Eumops perotis	Vespertilionoidea	Molossidae	Molossinae	Neotropics	insectivore	InsIns	7	3
Eumops underwoodi	Vespertilionoidea	Molossidae	Molossinae	Neotropics_Nearctic	insectivore	InsIns	7	3
Idionycteris phyllotis	Vespertilionoidea	Vespertilionidae	Vespertilioninae	Nearctic	insectivore	InsIns	7	3
Lasionycteris noctivagans	Vespertilionoidea	Vespertilionidae	Vespertilioninae	Nearctic	insectivore	InsIns	7	3
Lasiurus borealis	Vespertilionoidea	Vespertilionidae	Vespertilioninae	Nearctic	insectivore	InsIns	7	3
Lasiurus cinereus	Vespertilionoidea	Vespertilionidae	Vespertilioninae	Neotropics_Nearctic	insectivore	InsIns	7	3
Lasiurus ega	Vespertilionoidea	Vespertilionidae	Vespertilioninae	Neotropics	insectivore	InsIns	7	3

Lasiurus intermedius	Vespertilionoidea	Vespertilionidae	Vespertilioninae	Neotropics_Nearctic	insectivore	InsIns	7	3
Molossus coibensis	Vespertilionoidea	Molossidae	Molossinae	Neotropics	insectivore	InsIns	7	3
Molossus molossus	Vespertilionoidea	Molossidae	Molossinae	Neotropics	insectivore	InsIns	7	3
Molossus rufus	Vespertilionoidea	Molossidae	Molossinae	Neotropics	insectivore	InsIns	7	3
Myotis albescens	Vespertilionoidea	Vespertilionidae	Myotinae	Neotropics	insectivore	InsIns	7	3
Myotis auriculus	Vespertilionoidea	Vespertilionidae	Myotinae	Nearctic	insectivore	InsIns	7	3
Myotis austroriparius	Vespertilionoidea	Vespertilionidae	Myotinae	Nearctic	insectivore	InsIns	7	3
Myotis californicus	Vespertilionoidea	Vespertilionidae	Myotinae	Nearctic	insectivore	InsIns	7	3
Myotis chiloensis	Vespertilionoidea	Vespertilionidae	Myotinae	Neotropics	insectivore	InsIns	7	3
Myotis ciliolabrum	Vespertilionoidea	Vespertilionidae	Myotinae	Nearctic	insectivore	InsIns	7	3
Myotis elegans	Vespertilionoidea	Vespertilionidae	Myotinae	Neotropics	insectivore	InsIns	7	3
Myotis evotis	Vespertilionoidea	Vespertilionidae	Myotinae	Nearctic	insectivore	InsIns	7	3
Myotis grisescens	Vespertilionoidea	Vespertilionidae	Myotinae	Nearctic	insectivore	InsIns	7	3
Myotis keenii	Vespertilionoidea	Vespertilionidae	Myotinae	Nearctic	insectivore	InsIns	7	3
Myotis lucifugus	Vespertilionoidea	Vespertilionidae	Myotinae	Nearctic	insectivore	InsIns	7	3
Myotis nigricans	Vespertilionoidea	Vespertilionidae	Myotinae	Neotropics	insectivore	InsIns	7	3
Myotis riparius	Vespertilionoidea	Vespertilionidae	Myotinae	Neotropics	insectivore	InsIns	7	3
Myotis ruber	Vespertilionoidea	Vespertilionidae	Myotinae	Neotropics	insectivore	InsIns	7	3
Myotis septentrionalis	Vespertilionoidea	Vespertilionidae	Myotinae	Nearctic	insectivore	InsIns	7	3
Myotis sodalis	Vespertilionoidea	Vespertilionidae	Myotinae	Nearctic	insectivore	InsIns	7	3
Myotis thysanodes	Vespertilionoidea	Vespertilionidae	Myotinae	Nearctic	insectivore	InsIns	7	3
Myotis velifer	Vespertilionoidea	Vespertilionidae	Myotinae	Nearctic	insectivore	InsIns	7	3
Myotis volans	Vespertilionoidea	Vespertilionidae	Myotinae	Nearctic	insectivore	InsIns	7	3
Myotis yumanensis	Vespertilionoidea	Vespertilionidae	Myotinae	Nearctic	insectivore	InsIns	7	3
Natalus jamaicensis	Vespertilionoidea	Natalidae	Natalinae	Neotropics	insectivore	InsIns	7	3
Natalus stramineus	Vespertilionoidea	Natalidae	Natalinae	Neotropics	insectivore	InsIns	7	3
Natalus tumidirostris	Vespertilionoidea	Natalidae	Natalinae	Neotropics	insectivore	InsIns	7	3
Nycticeius humeralis	Vespertilionoidea	Vespertilionidae	Vespertilioninae	Nearctic	insectivore	InsIns	7	3

Nyctiellus lepidus	Vespertilionoidea	Natalidae	Natalinae	Neotropics	insectivore	InsIns	7	3
Nyctinomops aurispinosus	Vespertilionoidea	Molossidae	Molossinae	Neotropics	insectivore	InsIns	7	3
Nyctinomops femorosaccus	Vespertilionoidea	Molossidae	Molossinae	Nearctic	insectivore	InsIns	7	3
Nyctinomops laticaudatus	Vespertilionoidea	Molossidae	Molossinae	Neotropics	insectivore	InsIns	7	3
Nyctinomops macrotis	Vespertilionoidea	Molossidae	Molossinae	Neotropics	insectivore	InsIns	7	3
Pipistrellus subflavus	Vespertilionoidea	Vespertilionidae	Vespertilioninae	Nearctic	insectivore	InsIns	7	3
Promops centralis	Vespertilionoidea	Molossidae	Molossinae	Neotropics	insectivore	InsIns	7	3
Rhogeessa aeneus	Vespertilionoidea	Vespertilionidae	Vespertilioninae	Neotropics	insectivore	InsIns	7	3
Rhogeessa parvula	Vespertilionoidea	Vespertilionidae	Vespertilioninae	Neotropics_Nearctic	insectivore	InsIns	7	3
Rhogeessa tumida	Vespertilionoidea	Vespertilionidae	Vespertilioninae	Neotropics	insectivore	InsIns	7	3
Tadarida brasiliensis	Vespertilionoidea	Molossidae	Molossinae	Neotropics_Nearctic	insectivore	InsIns	7	3

Table S5.2 Phylogenetic disparity
We calculated and assessed the significance of differences in Procrustes variances as predicted by three potential covariates: families, ecological guilds, and our ecological cohorts. We include most *significantly* different pairwise comparisons below. For the family comparisons, we only list two pairs, for clarity and given the small sample size of most other families. All pairwise comparisons between phyllostomids and other families are significant, however, besides with Mormoopidae. We conditioned all our calculations upon the phylogeny to account for nonindependence of data ("phylogenetic disparity"), as described by our Methods and Serb *et al.* (2017).

covariate class	**group 1**	**group 1 Procrustes variance**	**group 2**	**group 2 Procrustes variance**
family	Phyllostomidae	0.688	Vespertilionidae	0.266
family	Vespertilionidae	0.266	Molossidae	0.277
guild	frugivores	0.510	insectivores	0.370
guild	herbivores	0.492	sanguivores	0.362
guild	nectarivores	0.493	sanguivores	0.362
guild	frugivores	0.510	sanguivores	0.362
cohort	Stenodermatinae	0.494	Mormoopidae	0.212
cohort	Lonchophyllinae	0.439	Mormoopidae	0.212

Table S5.3 Constraints on evolutionary rate matrices
Constrained three-rate BMM fits, in *mvMORPH*, to PC axes 1-3 of our cranial shape data, ranked by Akaike weight. We specified the three partitions of our ML ecological lability analysis in MuSSE, which included an ancestral partition, a vespertilionoid partition, and a phyllostomid partition that spanned Lonchorhininae, Phyllostominae, Lochophyllinae, Glyphonycterinae, Carolliinae, Rhinophyllinae, and Stenodermatinae. For the unconstrained rate matrix model, we fit one version where there is a single multivariate trait mean at the root of the tree (*smean*), and one where each partition had its own multivariate trait mean at the crown node of the split. We used the model constraints with the highest AIC weight to parameterize the our fits to any potential BMM model of up to three rates across the tree. Names refer to constraint parameters as described in *mvMORPH* (Clavel *et al.* 2015).

model constraints	**Akaike weight**
unconstrained rate matrix, *smean*	**0.644***
shared eigenvectors across regimes (“shared”), *smean*	0.341
no covariance between traits (“diagonal”), *smean*	0.011
unconstrained rate matrix	0.004
proportional rate matrices among regimes (“proportional”), *smean*	0.000
equal variance of traits (“equal”), *smean*	0.000

Table S5.4 Convergence of trophic guilds
Stayton's (2015) C1 statistic for each non-monophyletic ecological guild across the New World phylogeny. The clades included in each guild are also included. Bolded and starred statistics are significantly convergent ($p < 0.05$) based on 100 simulations under a BM model of trait evolution. Higher and significant C1 statistics imply that descendants are more morphologically similar than expected based on the distances among their ancestors.

ecological guild	**clades**	**C1**
frugivores	Phyllostomidae: subfamilies Stenodermatinae, Carolliinae, Glossophaginae	0.0323
nectarivores	Phyllostomidae: subfamilies Lonchophyllinae, Glossophaginae	**0.1908***
insectivores	Vespertilionoidea, Emballonuridae, Mormoopidae, Noctilionidae, Phyllostomidae: subfamilies Macrotinae, Micronycterinae, Glyphonycterinae, Phyllostominae, Lonchorhininae	0.0387
herbivores	Phyllostomidae: subfamilies Rhinophyllinae, Carolliinae, Glossophaginae	0.0593
omnivores	Phyllostomidae: subfamilies Stenodermatinae, Phyllostominae, Glossophaginae	0.0512

Table S5.5 Convergence among vampires and other trophic guilds
In addition to testing for convergence within ecological guilds, we also tested for convergence between vampire bat crania and each of the major trophic categories within noctilionoids (insectivores, nectarivores, omnivores). Again, we use the first 20 PC axes to calculate the C1 statistic (95% of total shape variance). We find that vampires and nectarivores are significantly convergent (bolded/starred, $p < 0.001$) using the C1 statistic. The ancestral state of vampire bats is unclear and the subject of much debate - origins from nectarivory are sometimes hypothesized (Baker 1979, Straney *et al.* 1979), and may be corroborated by our results here. However, more recent analyses have disputed this ancestral state (Fenton 1992). In general, this bears further testing.

ecological guilds	**C1**
frugivores + sanguivores	0.0384
nectarivores + sanguivores	**0.1516***
insectivores + sanguivores	0.0379

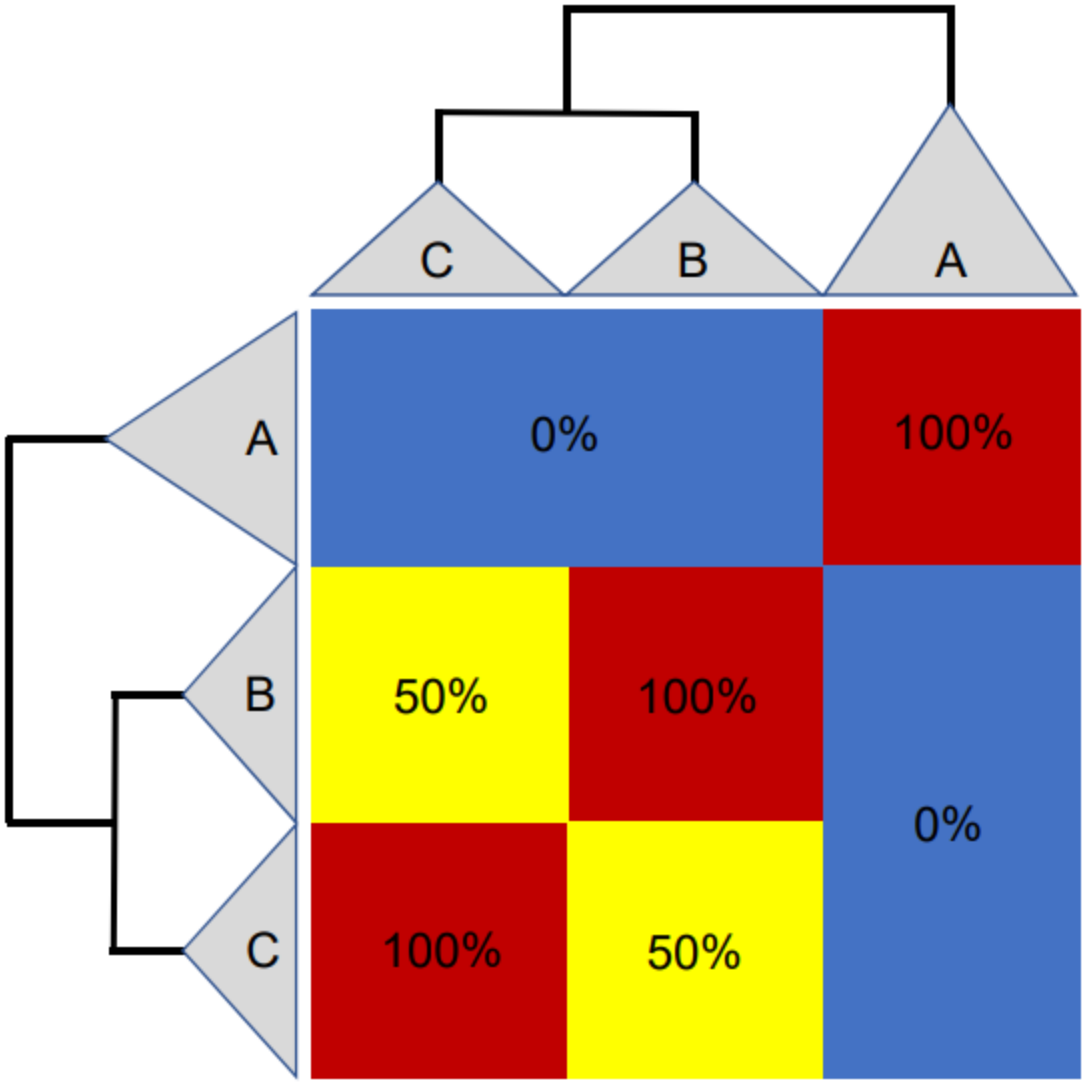

Figure S5.1 Cohort matrix illustration
An illustration of our cohort-based approach for this study, using a phylogeny with three clades *A*, *B*, and *C*. Species *within* each clade have 100% pairwise probability of belonging to the same cohort as each other, across all potential models (after factoring in the Akaike weight). Clade *A* is also clearly a cohort that is decoupled from the other two clades, as members of *B* and *C* have 0% weighted probability of belonging to the same partition as members of *A* across all models. It is more difficult to assign cohorts between *B* and *C*, however, with equivocal, weighted support across all models - thus, we might infer that *B* and *C* are one cohort to be conservative.

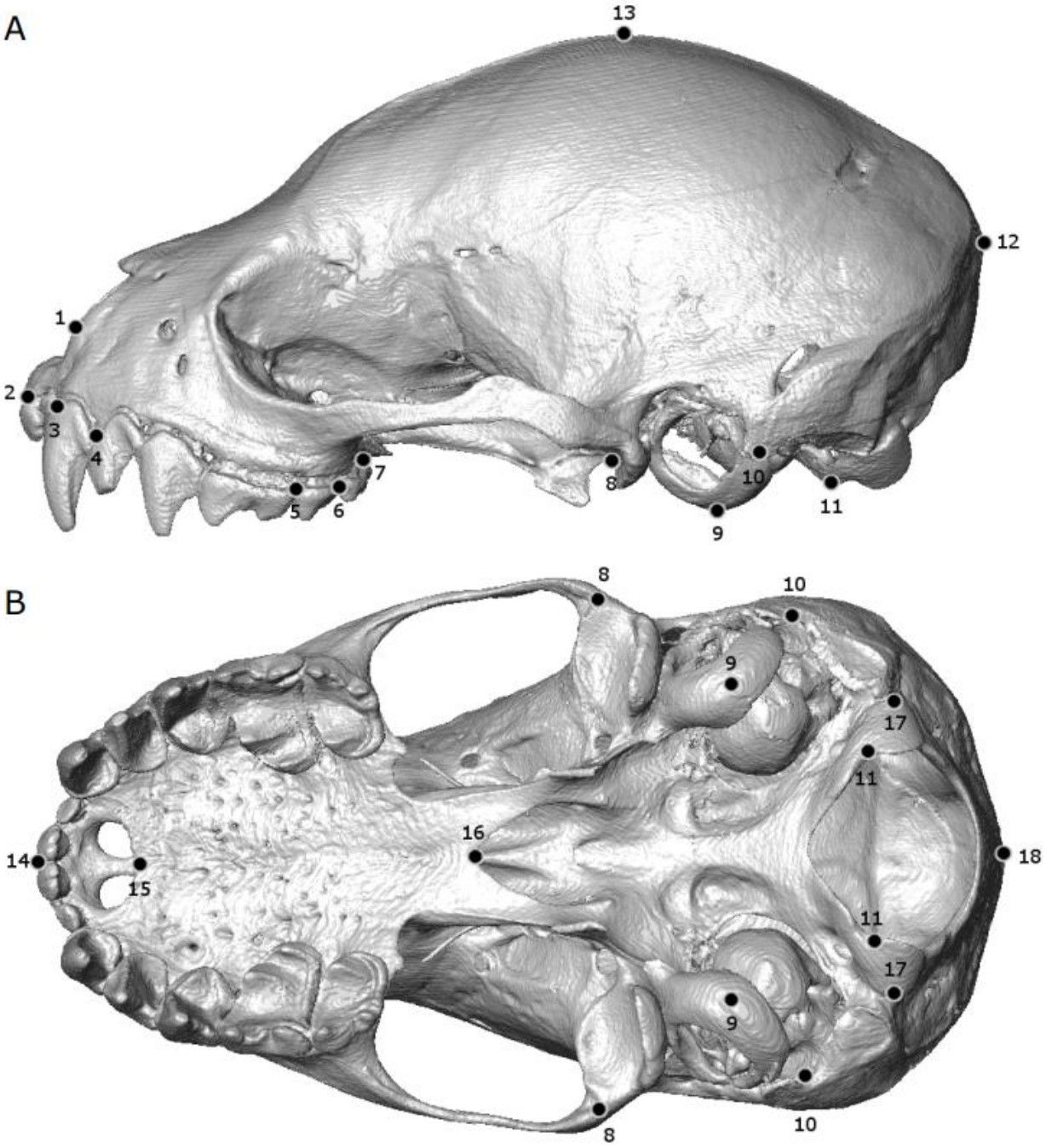

Figure S5.2 Landmarking details
Landmarking scheme used for digitizing shape data, on a specimen of *Artibeus aztecus* (Noctilionoidea: Phyllostomidae: Stenodermatinae). (a) Lateral and (b) ventral sides are shown, with numbered fixed landmarks. 15 sliding semilandmarks were also placed and allowed to slide along the curve, as detailed in the Methods, between landmarks 12 and 1.

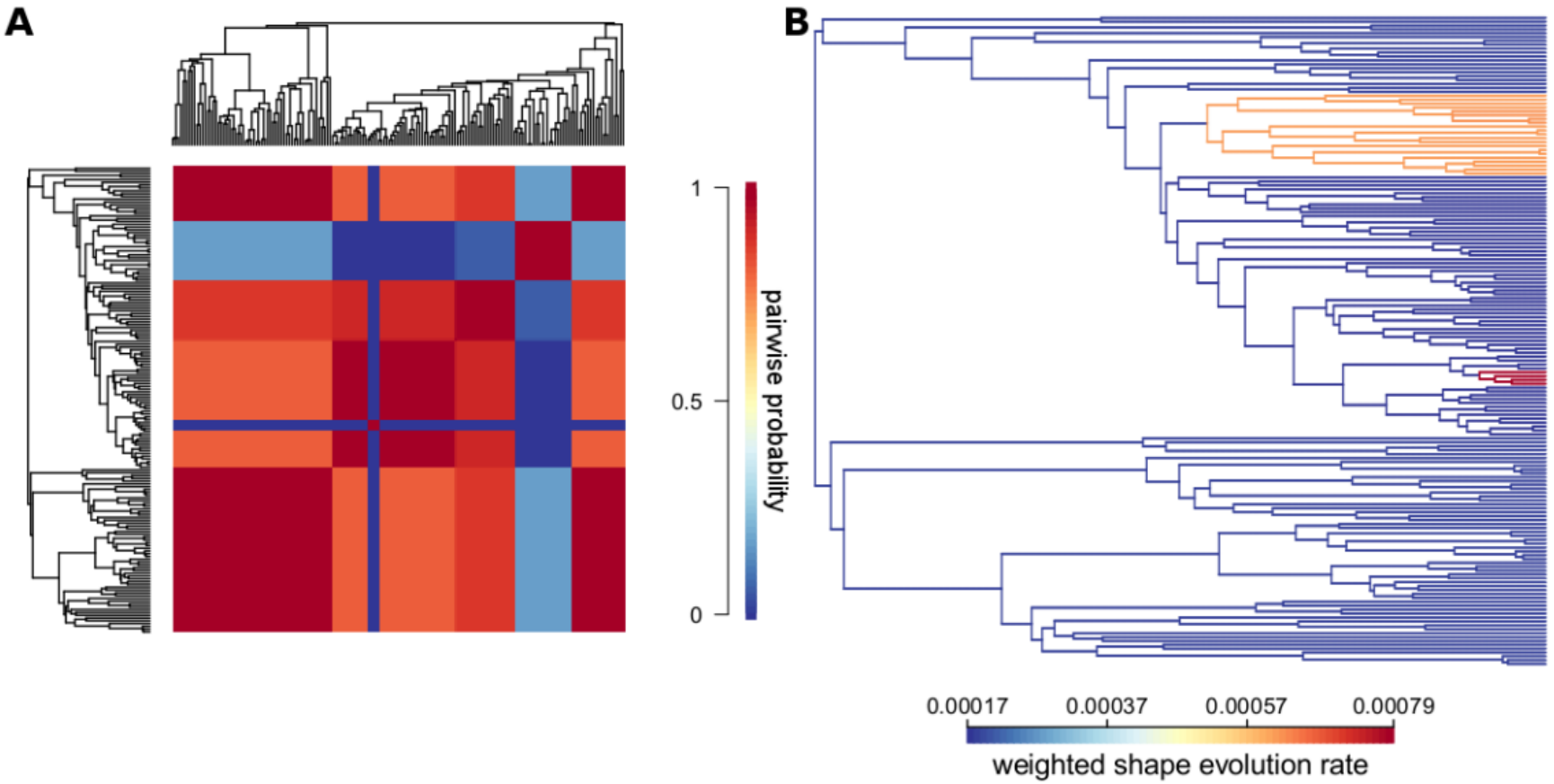

Figure S5.3 Results from all BMM models
After discarding all potential BMM models that had partitions with < 4 species, we fit a total of 3829 one-, two-, and three-rate models. However, some of these models did not converge and/or returned unreliable estimates, so were not presented in the main text. The main cause for failed model convergence and/or unreliable estimates for these models was that variances or covariances for small partitions were estimated - given computational precision - at 0. This issue is likely exacerbated when using a subset of the total PC data. We present a cohort analysis with these models included here, and note that qualitatively, there are few changes to our morphological cohorts. Intepretation is analogous to the cohort matrices and phylogenies of the main text.

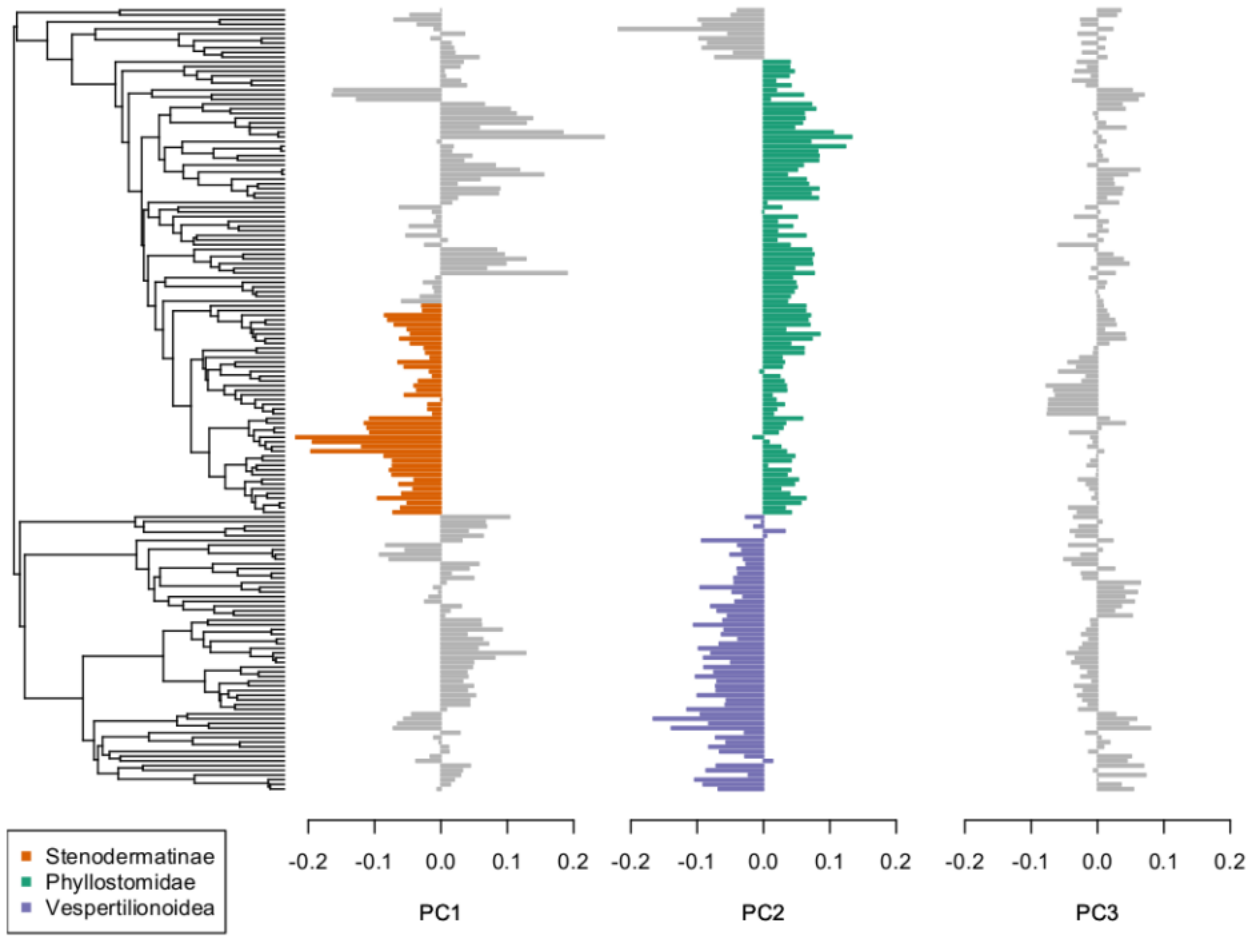

Figure S5.4 Principal components in a phylogenetic context
The species-level phylogeny of New World bats included in this study, and associated variation across the first two principal component (PC) axes. Negative PC1 scores are correlated with the subfamily Stenodermatinae, while positive and negative PC2 scores appear to discriminate between vespertilionoids (Vespertilionidae) and noctilionoids (Phyllostomidae). Patterns along PC3 are much less clear, though this explains much less of the overall shape variance than either PC1 or PC2.

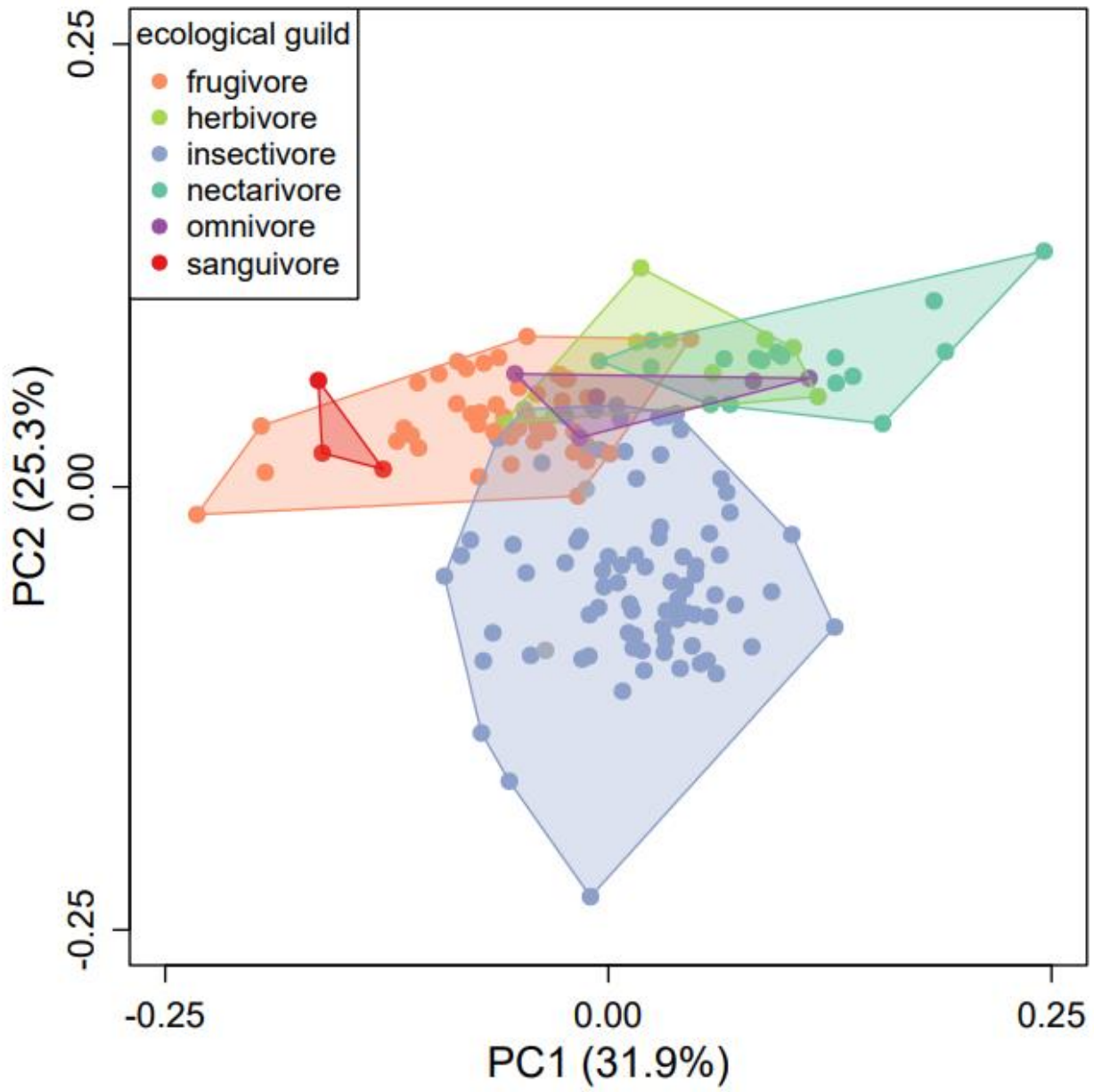

Figure S5.5 PCA with all trophic guilds
Our dataset in principal component space, as defined by the first two PC axes. All ecological guilds with more than two representative species are highlighted in this version of this figure. Note that omnivores and herbivores appear centered in the space among the main three cohorts (as described in our main text PCA figure), as expected. Curiously, vampire bats appear nested within frugivorous morphospace in these two axes, despite Figure S5.3. This is likely driven by the limited scope of this plot, which only encompasses about half of total shape variance.

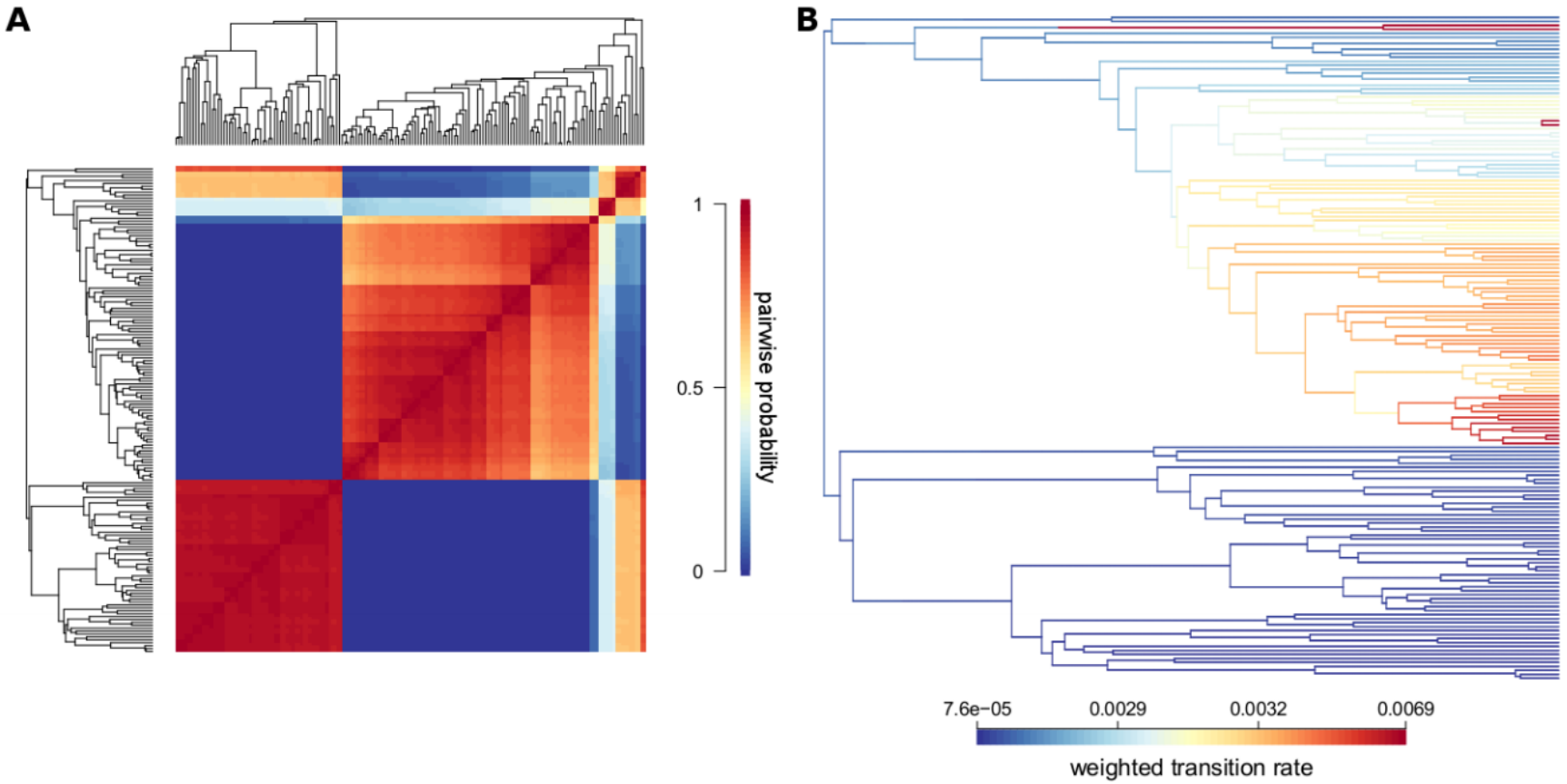

Figure S5.6 Results from more conservative ecological state assignments
In our main text, each species was assigned a discrete ecological state of a single, defined guild (*sensu* Rojas *et al.* 2018; *e.g.* herbivore, frugivore). Here, each bat is assigned its two top diet items as a discrete "double-character" state (*e.g.* fruit/insect, where obligate frugivores would be assigned a fruit/fruit state). In some ways, this is a more conservative analysis, as there is no minimum percentage threshold for when a bat is considered one guild over another. These states are listed as "double_ecology" in Table S5.1. Overall, we still find more heterogeneity among ecological cohorts than in our morphological analyses. However, there is much more uncertainty in exact cohort membership. Interpretation of these figures is analogous to the results of the main text.

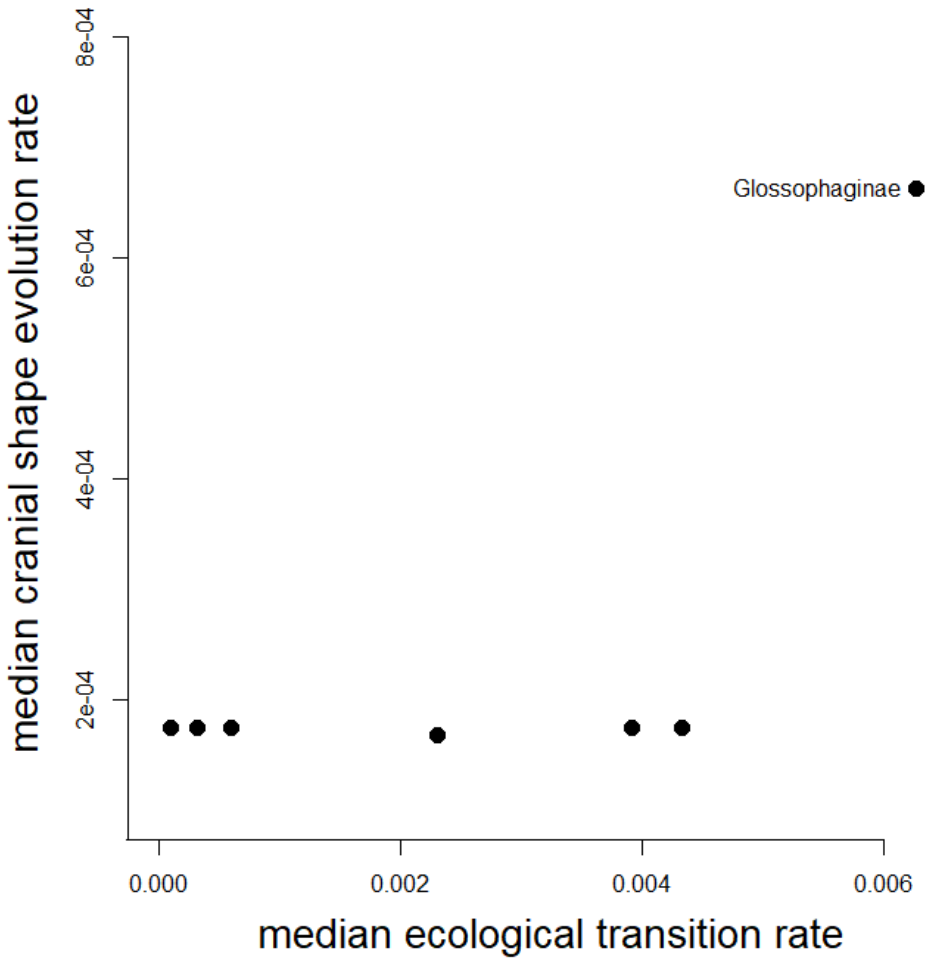

Figure S5.7 Ecological transition rates and cranial shape evolution rates
The relationship between median rates of morphological and ecological evolution for our 7 ecological cohorts identified in our main analyses and tables. Note that morphological rates are largely homogeneous across these groups, besides among glossophagines. We compared the model-averaged (weighted) rates of morphological and ecological evolution across all our split-Mk (ecology) and *mvMORPH* (**R**-mode morphology). The linear relationship between the two, for all species, is positive and significant (R^2 = 0.286, $p < 0.05$; PGLS $p < 0.05$), however, this is driven almost entirely by the extremely high rates, along both axes, of glossophagines. If we remove the 21 glossophagine species, this relationship entirely disappears (R^2 = 0.00192, p = 0.6; PGLS p = 0.94). The variance among morphological rates is overall extremely low (3.32e-8) compared to ecological rates (3.43e-4).

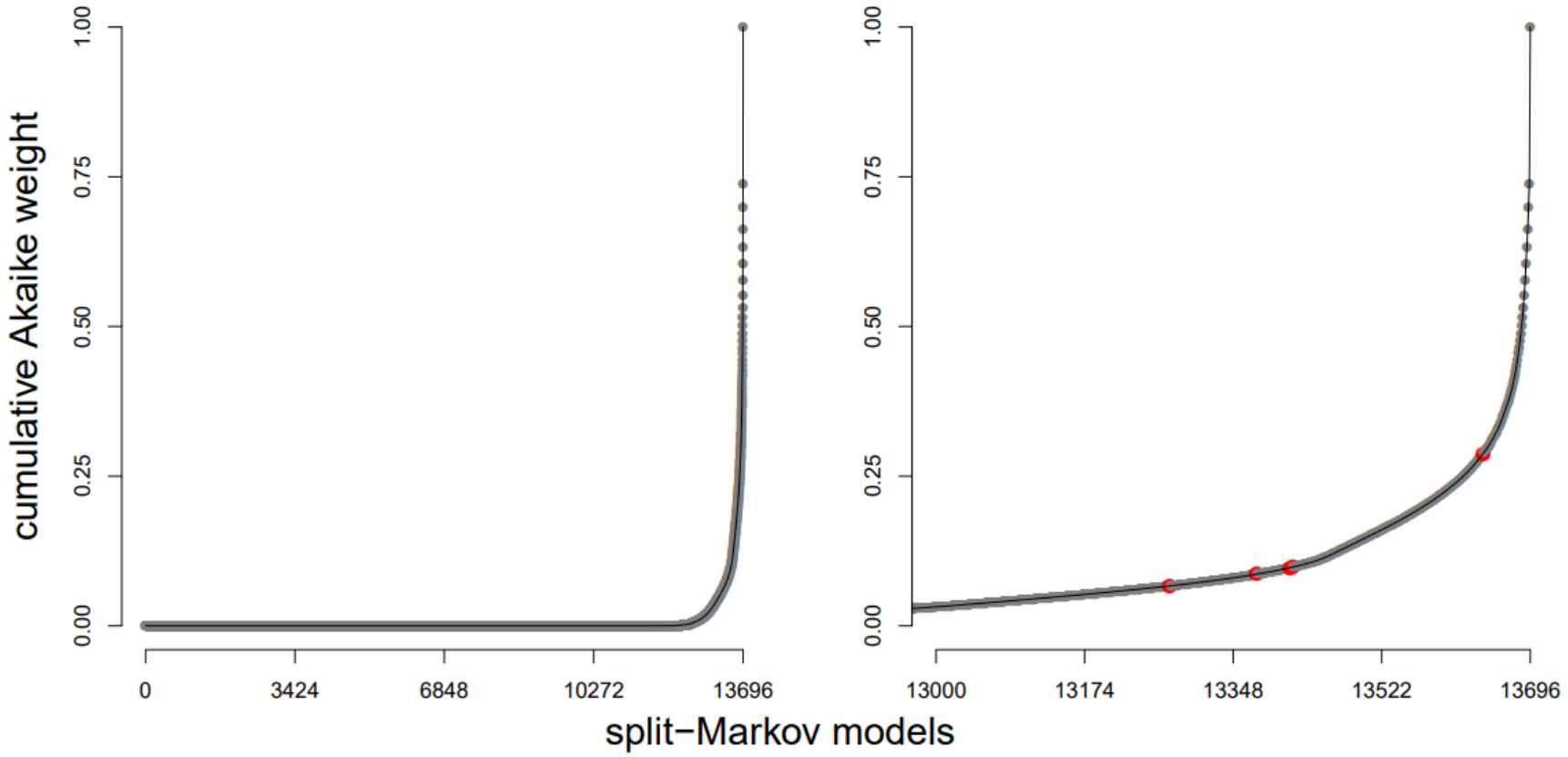

Figure S5.8 Cumulative Akaike weights
On the left, a plot of cumulative Akaike weights over all our split-Mk models of ecological evolution, similar to a scree plot for factor analyses. On the right, the same plot zoomed in over the 696 models with the highest Akaike weights. Enlarged, red points indicate those models that only have two partitions - all other (gray) points are three-partition models. We do not provide a similar figure for our partitioned **R**-mode analyses of morphological evolution because considerably fewer contribute substantially to the total weight, and the ML model contributes over 90% of the total weight.

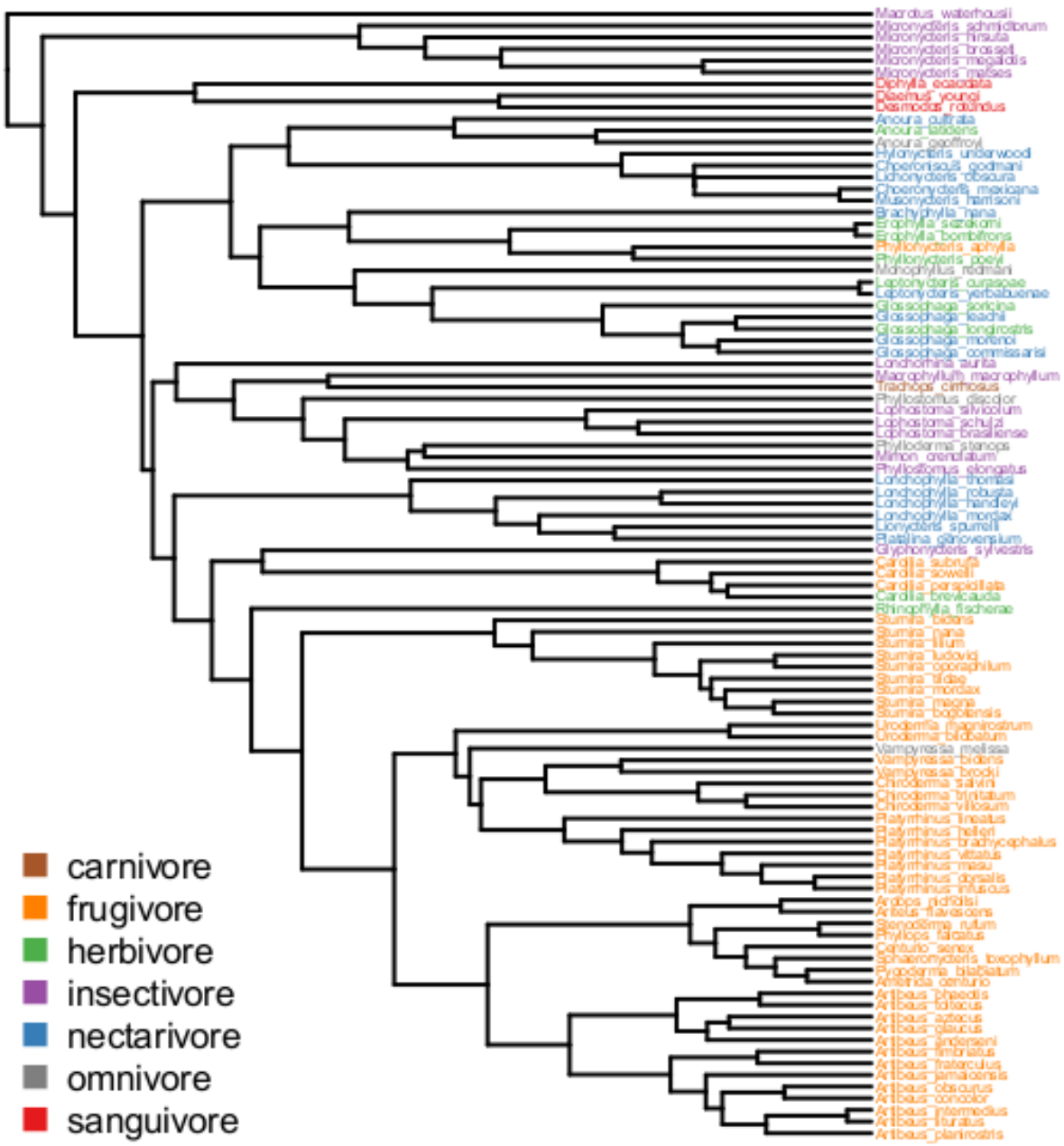

Figure S5.9 Diet states among phyllostomid species
A modified version of the right panel of the first figure in the main text. Each phyllostomid species' name is colored according to their dietary ecology, as specified for this study. This figure is best viewed online, in electronic form.

CHAPTER 6

Conclusion[7]

RECAPITULATION

With this dissertation, my co-authors and I highlighted the historical processes of diversification that have produced extant patterns of biodiversity among bats. Because biodiversity encompasses so many axes - behavior and ecological interactions with other organisms, the morphological traits that govern them, species richness and its distribution in space - the diversification processes that govern an entire, truly cosmopolitan radiation are equally diverse. As such, each of the chapters of this dissertation focused on and highlighted different aspects of the entire bat radiation.

The first chapter, the introduction, framed the rest of the dissertation in a global context by outlining how patterns of bat diversity vary across major biogeographic realms. This literature review highlighted disparate spatial patterns of diversity and richness at regional and continental scales, particularly focusing on differences among extant families. Among other aspects of bat diversity, I identified two major themes that continually reappear throughout the entire dissertation. First, bat behavior and ecology can often be highly opportunistic and plastic. Though this is most apparent in the tropics, temperate bats are also characterized by more

[7] or, if preferred, "***B***ayesian ***a***nalyses and ***t***ree/truth searching/***s***eeking"

flexible ecology and behavior than is often assumed. Second, the spatial distributions of temperate bats appear to be best predicted by abiotic characteristics of the environment, which govern the availability of water and suitable roosts or hibernacula. Tropical bat distributions, on the other hand, are better predicted by biotic factors, including the spatial distribution and seasonal abundance of different resources.

With the second chapter, I investigated how patterns of species richness vary across the order. Extant bat richness is unevenly distributed across the global radiation, and previous researchers have suggested that this unevenness may be related to speciation rate heterogeneity. First, we constructed a species-level molecular phylogeny for the order, which was critical for every subsequent analysis of the entire dissertation. We then inferred how speciation dynamics vary across extant bat clades, which are characterized by unequal species richnesses. We found that speciation rates across the order are surprisingly homogeneous, with little evidence that higher richness is associated with higher rates. The only evidence for decoupled, higher rates in the entire, global radiation is within the stenodermatines, a large subfamily of short-faced, predominantly frugivorous Neotropical phyllostomids.

The third chapter of this dissertation tested the relationship between spatial co-occurrence and divergence. In other major vertebrate clades, divergence - both in time and ecology - is positively related with the probability of sympatry, suggesting that species interactions like competition for resources may mediate broad-scale co-occurrence. While we expected that divergence would also predict range overlap in bats, we find no support for this hypothesis within any biogeographic realms. Instead, we find evidence that Neotropical bats are most likely to co-occur when ecomorphologically similar. We thus hypothesize that environmental filtering is the dominant mechanism of the sorting of Neotropical bat diversity at these broad, regional

scales. Because stenodermatines comprise a considerable percentage of endemic Neotropical bat diversity, it is also possible that their rapid speciation rates are related to low competition for resources.

In the fourth and fifth chapters of this dissertation, we describe and then harness a high-resolution, three-dimensional dataset of bat skulls to link organismal form and ecological function. Previous researchers have highlighted that bat skulls are predictive of feeding performance and trophic ecology. Disparity in skull shape and trophic diversity, like patterns of species richness, are also unevenly distributed across the order. To test whether the evolution of skull shape and trophic ecology are coupled, we first digitized a large collection of bat skulls using 3D X-ray computed microtomography. We then described making these data openly accessible to the wider scientific and educational community, and outlined avenues for contributing to and improving this repository.

We used the crania from that repository, alongside an ecological dataset of species diets, to infer dynamics of both ecological character evolution and cranial shape evolution across New World bats. Due to functional links between morphology and ecology, many researchers often predict and assume that morphology and ecology covary as part of diversification processes. We explicitly test for this relationship, and find that contrary to expectations, these two processes are largely decoupled from one another in this system. New World bats appear to be characterized by heterogeneous rates of ecological evolution in spite of homogeneous rates of shape evolution. Stenodermatines, in particular, are characterized by relatively slow rates of ecological, dietary evolution, despite their rapid speciation rates. Among other possibilities, we suggest that the overall discordance between morphology and ecology could be driven by underestimating the frequency of omnivory among many New World bats, particularly within noctilionoids. Trophic

plasticity and facultative omnivory could also contribute to the high degrees of co-occurrence among New World bats, in general, and also support the major themes of the initial literature review. Our results may also indicate that bat crania are more labile than other aspects of their morphologies, such as the mandible, dentition, or post-cranial elements.

SYNTHESIS: THE EVOLUTION OF CHIROPTERA

The exceptional diversity of bats has been highlighted for centuries, especially among biologists interested in ecological innovation and adaptive radiations. Their cranial and facial diversity is illustrated in the *Kunstformen der Natur* - one of only two mammalian prints in the collection - which has influenced designers, artists, and architects interested in the natural world since its publication (Figure 6.1). Leigh Van Valen dedicated an article in his personal *Evolutionary Theory* journal to understanding the evolution of the clade, which he clearly found vexing and inscrutable (Van Valen 1979). Fascination with bats has not been limited to just biologists, either. The philosopher Thomas Nagel, in his seminal treatise on consciousness, famously used bats - or rather, the experience of being a bat - as an example for something truly alien and incomprehensible to the human mind (Nagel 1974). My hope is that this dissertation, and the intervening decades of passionate work from other researchers, have at least moved us slightly beyond the dry wit of Nagel and Van Valen.

One theme that emerges from the major findings of this dissertation is that bat diversity appears unconstrained in many respects. Strong, positive relationships between crown clade age and species richness have sometimes been proposed to suggest non-equilibrial diversification, unlike in other major clades that display diversity dependence (Etienne *et al.* 2012). While in

many cases, this relationship is simply the product of sampling within large radiations, it may cast our other results in a different light. The phylogenetic imbalance we find in richness across clades can also largely be explained by time since diversification. This positive relationship extends to morphology as well, as we find that cranial disparity within clades is also positively linked with crown clade age.

Furthermore, bats species co-occur at high frequencies across the globe, throughout all its major biogeographic realms. This is especially true in the tropics, where species richness is the highest, but temperate bats also readily co-occur with high degrees of range overlap. Even more surprisingly, co-occurrence is frequent without evidence for strong controls of divergence. Divergence often limit range overlap, size, and expansion in other species, potentially due to interactions with other organisms (Jonathan Davies *et al.* 2007, Grossenbacher & Whittall 2011, Pigot & Tobias 2013). To the degree that these broad patterns of co-occurrence are linked with sympatry and local syntopy among bats, there are few constraints on which bats are sorted into communities from larger species pools. These major patterns can potentially be driven by the large, continental scales of many bat radiations, which can be truly cosmopolitan (Schweizer *et al.* 2014). Yet they are still strikingly different from patterns inferred in other clades at similarly broad scales, like with Neotropical passerines (Pigot & Tobias 2013).

The importance of flight to the radiation of bats cannot be overstated. This is not simply a trivial point - whether flight or echolocation evolved first, for example, was the central focus of macroevolutionary research on the order for many years. Fossil evidence generally indicates that powered flight predates echolocation, and that it is perhaps a key innovation that defines the order (Simmons *et al.* 2008). Flight has had enormous ramifications during the 50+ million year radiation of bats. Powered flight has evolved independently four times during the history of life:

once in insects, and three times in tetrapods - in two archosaur lineages (birds and pterosaurs), and in bats (Templin 2000). In each case, flight is often considered a classic example of a key innovation that precipitated radiation into unoccupied niches (Hunter 1998).

For bats, a common proposition is that it was the *combination* of nocturnality *and* flight that has driven their radiation (Hill & Smith 1984). Few other clades are as successful as *nocturnal* and aerial insectivores, frugivores, nectarivores, and the many other ecological guilds discussed in this dissertation. Bats are highly maneuverable in flight, and can also precisely navigate, forage, and hunt in cluttered environments by using echolocation (Schnitzler *et al.* 2003, Simmons 2005). Wing morphology and echolocation behavior may thus be two of the most critical aspects of bats to study in the context of the major questions raised by this dissertation.

Ecomorphological relationships between wing shape and flight behavior are established for some bats (Norberg 1986, Norberg & Rayner 1987), yet have not been pursued by large-scale macroecological and macroevolutionary research. High-resolution scanning of internal aspects of crania and faces can reveal the relationship between morphology and echolocation behavior in many species (Curtis & Simmons 2017). The continued development of scanning and digitization technology that preserves soft tissue will only further broaden the scope of possible research on the radiation of extant bats (Gignac *et al.* 2016). Furthermore, while the final chapters of this dissertation predominantly focused on cranial morphology, dentition and mandibular size and shape are also directly tied to functional ecology. Behavioral and performance studies on foraging and sensory ecology that move beyond morphology will also broaden our understanding of any potential constraints on bat diversity.

ECOLOGY & MACROEVOLUTION

A central goal of macroevolution is to understand the drivers of major patterns of biodiversity, including the unequal distribution of species richness across time and space, and the waxing and waning of clade diversity through geologic time (Gould 1980, Jablonski 1986, Gould 1994, Chown & Gaston 2000). At a simplified level, it is about inferring the most likely historical *causes* from a suite of observed *effects* in the present. This inverted, inference-based goal colors many of the building blocks of evolutionary research, from ancestral state reconstructions, to phylogeny building, to selection of appropriate trait evolution models. Yet we are faced with enormous obstacles at almost every step: from the phylogeny itself, which may always be incomplete, to testing for absolute model adequacy within a boundless sea of possibilities. If we can only peer through this very narrow keyhole of the present, how can we best understand the limitless possibilities of the past?

I know that my dissertation is simply this immense goal of macroevolution writ very, very small. Consider, for example, the marginal tips and leaves of the tree of life that all bats have ever represented (Hinchcliff *et al.* 2015; Figure 6.2). No one theory, or even a concerted assemblage of processes and hypotheses, can be responsible for all patterns of biodiversity across the myriad forms of life that have existed throughout Earth's history. One thing that *is* clear, however, is that given the computational and statistical tools at our disposal, we can and should continue to integrate complex ecological interactions and data into macroevolutionary inference (Rabosky 2013). Though these ecological data can be noisy and coarse, and though they require painstaking decades of field and lab studies to amass, they are the backbone for all

the research I have presented here. And in at least one case that I know very well, it is the ecological drama of organisms that fascinates and draws prospective scientists to understand the natural world; and what is evolution, then, if not a script for all these stories of life (Hutchinson 1965)?

+++++++

"There isn't any particular relationship between the messages,
except that the author has chosen them carefully, so that, when seen all at once,
they produce an image of life that is beautiful and surprising and deep.
There is no beginning, no middle, no end, no suspense, no moral, no causes, no effects.
What we love in our books are the depths of many marvelous moments seen all at one time."
Kurt Vonnegut; *Slaughterhouse-Five* (1969)

REFERENCES

Chown, S.L. & Gaston, K.J. (2000) Areas, cradles and museums: the latitudinal gradient in species richness. *Trends in Ecology & Evolution*, **15**, 311–315.

Curtis, A.A. & Simmons, N.B. (2017) Unique turbinal morphology in horseshoe bats (Chiroptera: Rhinolophidae). *The Anatomical Record*, **300**, 309–325.

Etienne, R.S., Haegeman, B., Stadler, T., Aze, T., Pearson, P.N., Purvis, A., & Phillimore, A.B. (2012) Diversity-dependence brings molecular phylogenies closer to agreement with the fossil record. *Proceedings of the Royal Society B: Biological Sciences*, **279**, 1300–1309.

Gignac, P.M., Kley, N.J., Clarke, J.A., *et al*. (2016) Diffusible iodine-based contrast-enhanced computed tomography (diceCT): An emerging tool for rapid, high-resolution, 3-D imaging of metazoan soft tissues. *Journal of Anatomy*, **228**, 889–909.

Gould, S.J. (1994) Tempo and mode in the macroevolutionary reconstruction of Darwinism. *Proceedings of the National Academy of Sciences of the United States of America*, **91**, 6764–6771.

Gould, S.J. (1980) Is a new and general theory of evolution emerging? *Paleobiology*, **6**, 119–130.

Grossenbacher, D.L. & Whittall, J.B. (2011) Increased floral divergence in sympatric monkeyflowers. *Evolution*, **65**, 2712–2718.

Hill, J.E. & Smith, J.D. (1984) *Bats: a natural history.* British Museum of Natural History, London.

Hinchliff, C.E., Smith, S.A., Allman, J.F., *et al*. (2015) Synthesis of phylogeny and taxonomy into a comprehensive tree of life. *Proceedings of the National Academy of Sciences of the United States of America*, **112**, 12764–12769.

Hunter, J.P. (1998) Key innovations and the ecology of macroevolution. *Trends in Ecology & Evolution*, **13**, 31–36.

Hutchinson, G.E. (1965) *The ecological theater and the evolutionary play.* Yale University Press, New Haven.

Jablonski, D. (1986) Background and mass extinctions: the alternation of macroevolutionary regimes. *Science*, **231**, 129–133.
Jonathan Davies, T., Meiri, S., Barraclough, T.G., & Gittleman, J.L. (2007) Species co-existence and character divergence across carnivores. *Ecology Letters*, **10**, 146–152.
Nagel, T. (1974) What is it like to be a bat? *The Philosophical Review*, **83**, 435–450.
Norberg, U.M. (1986) Evolutionary convergence in foraging niche and flight morphology in insectivorous aerial-hawking birds and bats. *Ornis Scandinavica*, **17**, 253–260.
Norberg, U.M. & Rayner, J.M. V (1987) Ecological morphology and flight in bats (Mammalia; Chiroptera): wing adaptations, flight performance, foraging strategy and echolocation. *Philosophical Transactions of the Royal Society B: Biological Sciences*, **316**, 335–427.
Pigot, A.L. & Tobias, J.A. (2013) Species interactions constrain geographic range expansion over evolutionary time. *Ecology Letters*, **16**, 330–338.
Rabosky, D.L. (2013) Diversity-dependence, ecological speciation, and the role of competition in macroevolution. *Annual Review of Ecology, Evolution, and Systematics*, **44**, 481–502.
Schnitzler, H.-U., Moss, C.F., & Denzinger, A. (2003) From spatial orientation to food acquisition in echolocating bats. *Trends in Ecology & Evolution*, **18**, 386–394.
Schweizer, M., Hertwig, S.T., & Seehausen, O. (2014) Diversity versus disparity and the role of ecological opportunity in a continental bird radiation. *Journal of Biogeography*, **41**, 1301–1312.
Simmons, N.B. (2005) An Eocene big bang for bats. *Science*, **307**, 527–528.
Simmons, N.B., Seymour, K.L., Habersetzer, J., & Gunnell, G.F. (2008) Primitive early Eocene bat from Wyoming and the evolution of flight and echolocation. *Nature*, **451**, 818–821.
Templin, R.J. (2000) The spectrum of animal flight: insects to pterosaurs. *Progress in Aerospace Sciences*, **36**, 393–436.
Van Valen, L. (1979) The evolution of bats. *Evolutionary Theory*, **4**, 103–121.

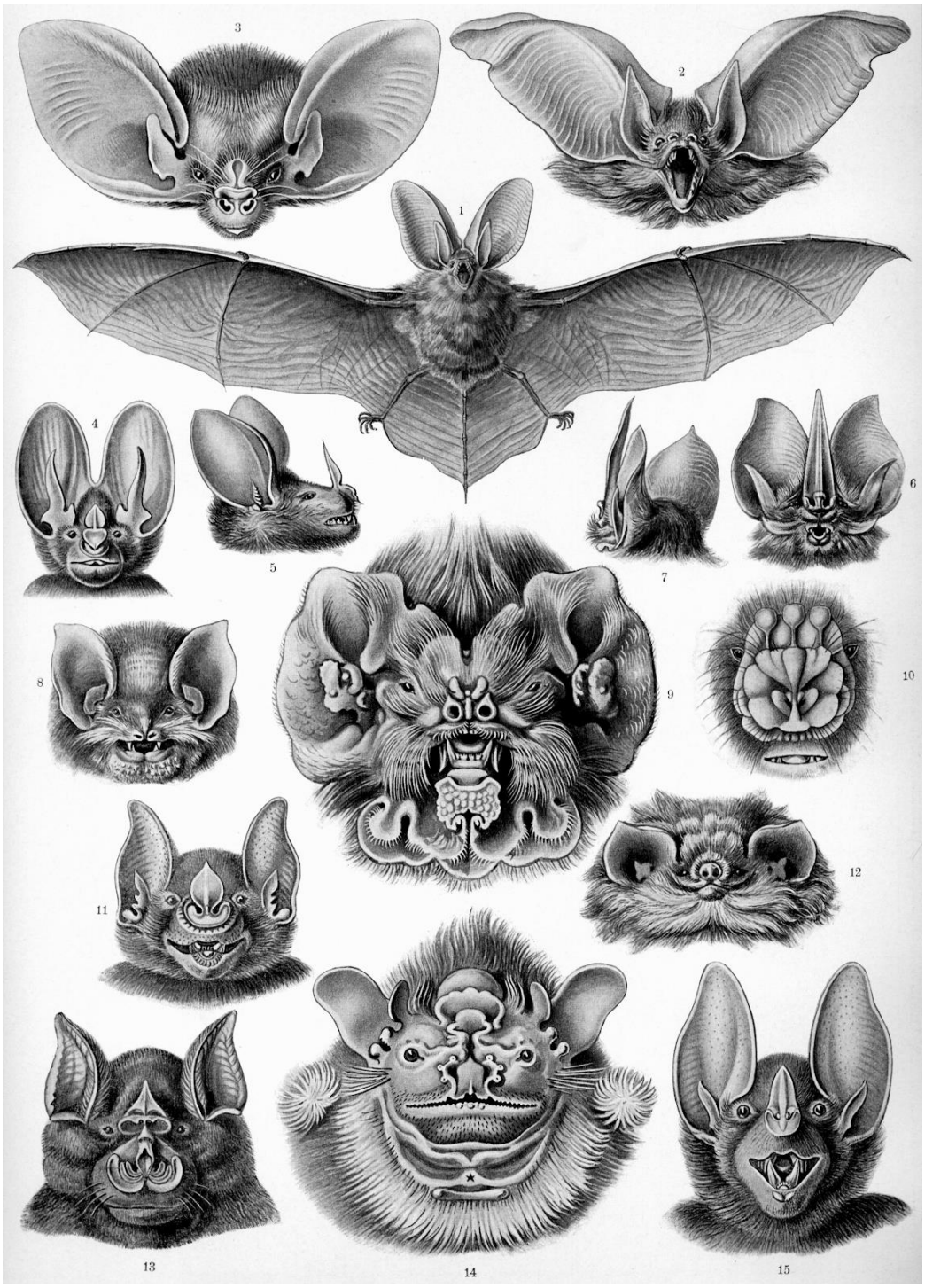

Figure 6.1 *Kunstformen der Natur*, plate 67: Chiroptera (1904)
This plate illustrates facial diversity across numerous bat clades, including the families Vespertilionidae, Mormoopidae, Phyllostomidae, Natalidae, Furipteridae, and Rhinolophidae. Reproduced as a work in the public domain of the United States of America; accessible via the Wikimedia Commons repository.

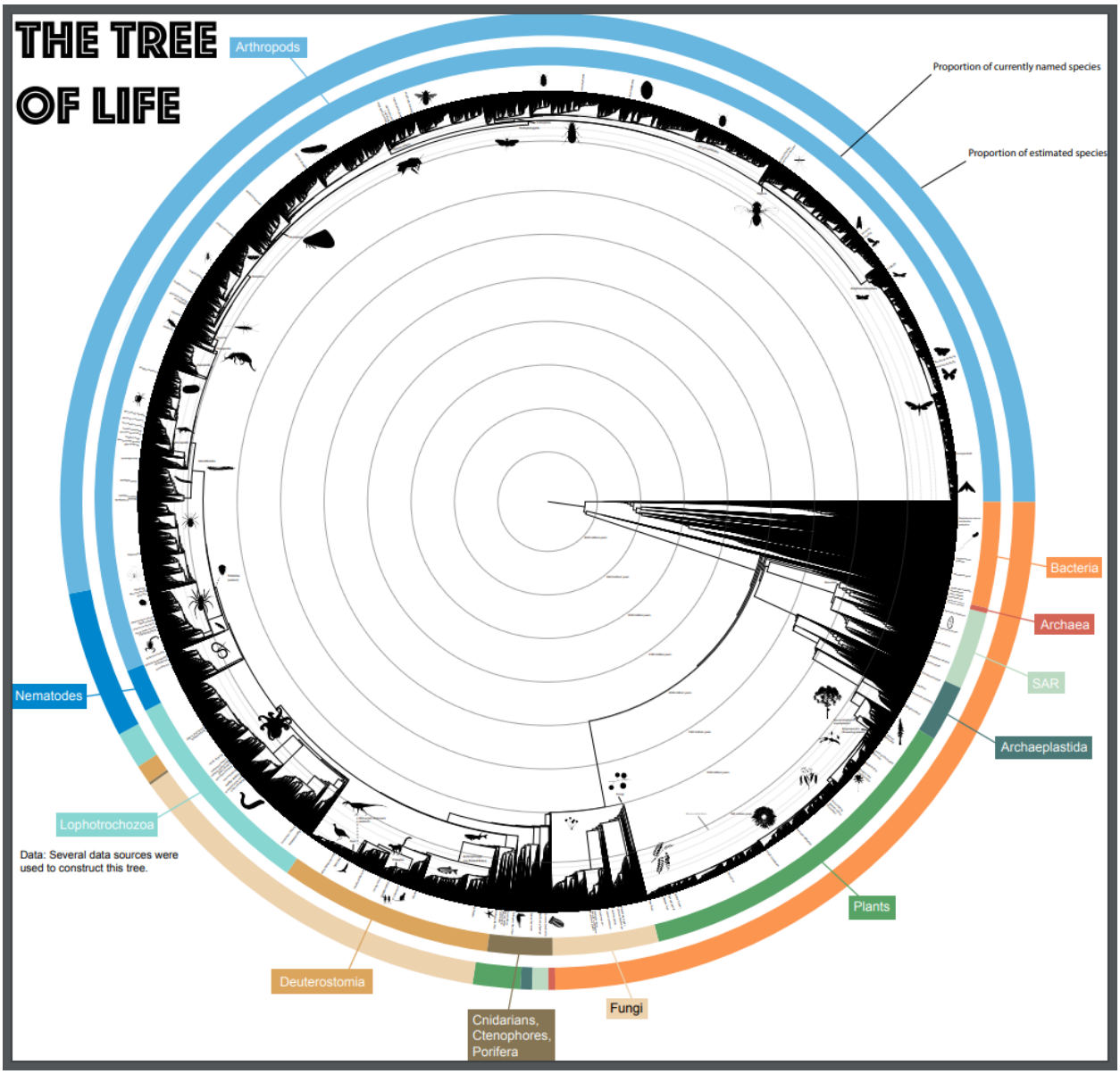

Figure 6.2 Insights from the tree of life
A recent estimate of the distribution of diversity across the tree of life, using data from Hinchcliff *et al.* (2015). The outermost circle represents estimated diversity, while the inner circle represents named diversity. This tree is noticeably imbalanced in species richness, with arthropods and bacteria most likely representing the vast majority of life on Earth. Deuterostomes, by contrast, occupy a relatively small portion of described species richness, and even less of estimated total biodiversity. Reproduced here with the permission of Stephen A. Smith, one of the original authors.